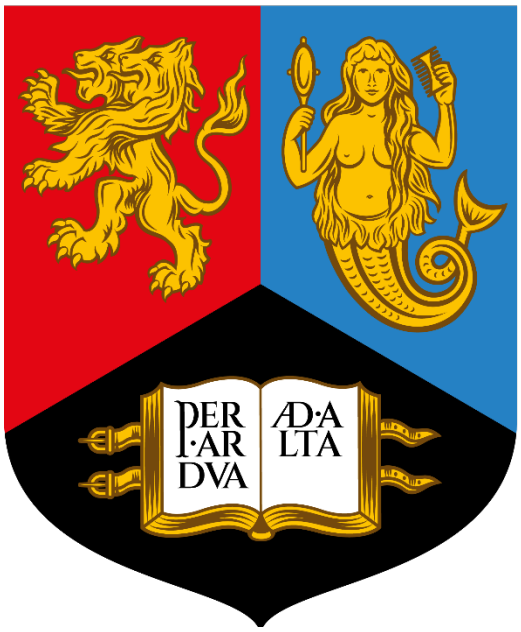

Dynamic Tracing of T Cell Receptor Signalling

by

Thomas Ashton Emmerson Elliot

A thesis submitted to the University of Birmingham for the degree of DOCTOR OF PHILOSOPHY

Institute of Immunology and Immunotherapy
College of Medical and Dental Sciences
University of Birmingham
March 2024

Abstract

The T cell receptor (TCR) determines the antigen-specificity of T cells and tightly controls T cell activation status. The TCR can be ligated by binding to peptide loaded MHC, initiating a complex set of downstream signalling pathways, that result in nuclear entry of transcription factors that regulate the expression of genes involved in T cell function. TCR signalling can lead to proliferation, migration, cytokine production, metabolic re-programming, and killing of target cells. The TCR is co-regulated by a number of co-stimulatory and co-inhibitory receptors; expression of TCR co-receptors changes dramatically upon T cell activation. TCR signalling is therefore a very dynamic process regulated by a number of context dependent factors. To study dynamic control of TCR signalling we generated Nur77 Tempo mice, that express a Fluorescent Timer protein under the control of the regulatory regions of *Nr4a1,* the expression of which is dependent on TCR signalling. Fluorescent Timer protein matures over time, shifting its emission spectrum from blue to red. This allows for distal reporting of TCR signalling events with high time sensitivity. We validated the utility of Nur77 Tempo to track TCR signalling events and compared it to a similar reporter, Nr4a3 Tocky, that reports Fluorescent Timer under the regulation of related gene *Nr4a3*. We highlight key differences in the expression patterns of Nur77 Tempo and Nr4a3 Tocky, notably that Nr4a3 Tocky requires a higher strength of TCR signal and is absolutely dependent on Calcineurin-NFAT signalling. In contrast, Nur77 Tempo can detect weaker signals such as those involved in thymic positive selection and is dependent on NFAT independent signalling pathways. Using a tumour model and an in vitro model of T cell exhaustion, we show that chronic TCR stimulation of $CD8^+$ T cells results in sustained NFAT signalling but shutting down of NFAT independent signalling in a way that is not reversible with immunotherapy. We go on to show that transient inhibition of NFAT signalling is sufficient to partially reverse some phenotypic features of $CD8^+$ T cell exhaustion.

In a separate body of work, we investigate the drivers of intra-tumoural immunity in human colorectal cancer (CRC) patients. A small subset of CRC patients have an aggressive $CD8^+$ T cell mediated immune response due to a high neo-antigen burden as a result of microsatellite instability and abundant frameshift and missense mutations. However, some patients without microsatellite instability have transcriptional scores of anti-tumour immunity that are equivalent to those that do. We use CD39, a biomarker of tumour antigen reactive T cells, to evaluate the role of antigen recognition in driving high immune scores, finding a redundant role among microsatellite stable patients. We went on to investigate the potential role of microbial adjuvantisation. Meta-genome sequencing was not able to identify differences in relative bacterial abundance between low and high immunity microsatellite stable patients. However, many genes involved in innate immune response to bacteria were elevated in high immunity patients, particularly some transcripts encoding guanylate binding proteins. We confirmed protein expression of GBP5, a necessary component of NLRP3 inflammasome assembly. We confirmed that human intestinal epithelial cells can clave NLP3 executor Caspase-1 and posit a GBP5-NLRP3-IL-18 pathway as a key regulator of immunity in low mutational burden CRC

Acknowledgements

I would first like to thank my primary funder, the MRC, who have facilitated this work through the AIM/iCASE doctoral training programme. I would like to thank those who have administrated the programme Vikki Harrison, Dan Tennant, David Bending, and Sarah Dimeloe, all of whom supported my transition to working across two labs. I would like to thank my funders at AstraZeneca, particularly Jim Eyles and Robert Wilkinson who provided feedback, advice, and reagents. I would like to thank my supervisors David Bending and Ben Willcox who have both mentored me as I have developed as a scientist over the last 4-5 years. I'd like to thank those who have been part of the Bending group during my tenure, particularly Lozan Sheriff, Ally Copland, David Lecky, Emma Jennings, Lizzie Jinks, Lorna George, Sophie Rouvray, and Natasha Thawait all of whom have provided invaluable help with my experiments. I'd also like to thank those from the Willcox group who have supported me, including Carrie Willcox, Taher Taher, Mab Salim, Juliet Gunn, Charlotte Begley, and Maria Sharif. An additional thank you to Neeraj Lal for his advice during supervisory meetings with Ben.

I'd like to thank Guillaume Desanti, Adriana Flores-Langarcia, and Ferdus Sheik for their flow cytometry technical support. Thank you to Michael Russel from HBRC for providing FFPE samples, Ana Teodosio, Joe Flint, Kelly Hunter, and Triin Major from the BTA for providing staining and imaging services. A thanks to Ash Renelt, Alastair Tew, and Kevin Hardware who run the stores facilities I have used. I'd like to say a particular thank you to Jack McMurray who started the CIRC project, curated the CIRC patient transcriptional databases, processed the metagenome sequencing dataset, and provided valuable advice both technical and strategic when I first started as a PhD student. I'd like to thank my friends at the University and my wider support network in Birmingham including Lisa Scarfe, Poppy Nathan, Abbey Lightfoot, Ladi Abudu, Sofia Hain, Tristan Kennedy, Peter Smith, Leanne Chapman, Kendle Maslowski, and

Rebecca Drummond. I'd also like to thank my friends from my time in Sheffield who got me through my bachelor's degree: Sam, Sean, Max, Jake, Nat, Lucy, Jordan, Hannah, Katie, and Ben.

I'd like to thank my Dad Stuart and my Mum Gwen, who have always encouraged my academic endeavours since primary school and have always been ready to provide emotional and logistical support. I'd like to thank my sister Grace and my brother George for their love and support. Lastly, I would like to thank my partner/proof-reader Gillian who has been supporting me since we started revising for our exams together almost a decade ago. I feel privileged to work in research and I am grateful to those around me who have facilitated my doing so.

TABLE OF CONTENTS

Figures

Tables

ABBREVIATIONS

4-1BB	Tumour Necrosis Receptor Superfamily 9
AKT	Protein Kinase B
AP1	Activator Protein 1
APC	Antigen Presenting Cell
ATP	Adenosine Tri-Phosphate
BCL6	B Cell Lymphoma b
CARMA1	Caspase recruitment domain-containing-associated guanylate kinase protein 1
CDR	Complementarity Determining Region
CIMP	CpG Island Methylator Phenotype
CIRC	Co-ordinated Immune Response Cluster
CTLA4	Cytotoxic T-Lymphocyte Associated Protein 4
DAG	diacylglycerol
DAMP	Damage Associated Molecular Pattern
dMMR	Defective Mismatch Repair
DNA	Deoxy-Ribonucleic Acid
DP	Double Positive
ELK1	ETS Like-1 Protein
ERK	Extracellular Regulated Kinase
FMO	Fluorescence Minus One
FT	Fluorescent Timer
GBP	Guanylate-Binding Protein
GDP	Guanine Di-Phosphate
GEF	Guanine Nucleotide Exchange factor
GITR	Tumour Necrosis Receptor Superfamily 18
GRB2	Growth Factor receptor-bound protein 2
GTP	Guanine Tri-Phosphate
ICOS	Inducible T cell Co-stimulator
IEC	Intestinal Epithelial Cell
IFNγ	Interferon gamma
IL	Interleukin
ILC	Innate Lymphoid Cell
IP3	inositol 1,4,5-trisphosphate
ITAM	Immuno Tyrosine-based Activation Motif
ITIM	Immuno Tyrosine-based Inhibitory Motif
JNK	c-Jun N-terminal Kinase
KLRG1	Killer Cell Lectin-Like Receptor Subfamily G Member 1
LAG-3	Lymphocyte-Activation Protein 3
LAT	Linker for Activation of T Cells
LCK	Lymphocyte-Specific Protein Tyrosine Kinase
LCMV	Lymphocytic Choriomeningitis Virus

LPS	Lipopolysaccharide
MALT1	Mucosa-Associated Lymphoid Tissue Lymphoma Translocation Protein 1
MAPK	Mitogen Activated Protein Kinase
MEK	Mitogen Activated Protein Kinase
MHC	Major Histocompatibility Complex
MMR	Mismatch Repair
MPEC	Memory Precursor Effector Cell
MSI	Microsatellite Instable
MSS	Microsatellite Stable
mTORC1	Mammalian Target of Rapamycin Complex 1
MyD88	Myeloid differentiation primary response 88
NFAT	Nuclear Factor of Activated T cells
NFκB	Nuclear factor kappa-light-chain-enhancer of activated B cells
NK	Natural Killer
NKG2D	Killer Cell Lectin-Like Receptor Subfamily C Member 1
NR4A1	Nuclear Receptor Subfamily 4 Group A member 1
NR4A2	Nuclear Receptor Subfamily 4 Group A member 2
NR4A3	Nuclear Receptor Subfamily 4 Group A member 3
OT-I	Ovalbumin-Specific TCR
OUT	Operational Taxonomic Unit
OVA	Ovalbumin
OX40	Tumour Necrosis Receptor Superfamily 4
PAMP	Pathogen Associated Molecular Pattern
PCA	Principal Component Analysis
PD-1	Programmed Death 1
PDK1	Pyruvate Dehydrogenase Kinase 1
PD-L1	Programmed Death Ligand 1
PIP2	phosphatidylinositol-4,5-bisphosphate
PKC	Protein Kinase C
PLCγ1	Phospho-lipase Cγ1
pMHC	Peptide Loaded Major Histocompatibility Complex
RAC1	Ras-related C3 botulinum toxin substrate 1
RAF1	Rapidly Accelerated Fibrosarcoma 1
RASGRP1	Ras Guanyl-Release Protein 1
RNA	Ribonucleic Acid
SH2	Spectrin Homology Domain 2
SHP1	Src homology region 2 domain-containing phosphatase-1
SHP2	Src homology region 2 domain-containing phosphatase-2
SLEC	Short-Lived Effector Cell
SOS	Son-of-Sevenless
SP	Single Positive
TBI	Total Body Irradiation
TCF1	T Cell Factor 1

TCGA-COADREAD	The Cancer Genome Atlas Colon Adenocarcinoma Rectal Adenocarcinoma
TCR	T Cell Receptor
Tempo	Timer rapidly expressed in lymphocytes
T_{EX}	Exhausted T cell
TGFβ	Transforming Growth Factor Beta
Th1	T Helper 1
TIGIT	T Cell Immunoreceptor with Ig and ITIM domains
TIL	Tumour Infiltrating Lymphocyte
TIM-3	T Cell Immunoglobulin and Mucin-Domain Containing 3
TNFα	Tumour Necrosis Factor α
Tocky	Timer of cell kinetics and activity
T_{PEX}	Pre-cursor Exhausted T Cell
T_{REG}	Regulatory T Cell
ZAP70	Zeta-Chain-Associated Protein Kinase 70

1 MATERIALS AND METHODS

1.1 KEY MATERIALS TABLE

Flow Cytometry Antibodies (mouse reactive)

Product	Supplier	Catalogue ID
CD4 (GK1.5) BUV737	BD Biosciences	564298; RRID: AB_2738734
CD8α (53-6.7) BUV395	BD Biosciences	563786; RRID: AB_2732919
CD8α (53-6.7) FITC	BioLegend	100706; RRID: AB_312744
CD8β (53-5.8) PerCP-Cy5.5	BioLegend	140417; RRID: AB_2800650
TCRβ (H57-597) AF700	BioLegend	109224; RRID: AB_1027648
TCRγδ (GL3) APC	BioLegend	118116; RRID: AB_1731813
CD25 (PC61) PE-Cy7	BioLegend	102016; RRID: AB_312865
CD69 (H1.2F3) FITC	BioLegend	104506; RRID: AB_313109
CD69 (H1.2F3) AF700	BioLegend	104539; RRID: AB_2566304
PD-1 FITC (29F.1A12)	BioLegend	135213; RRID: AB_10689633
PD-1 AF488 (29F.1A12)	BD Biosciences	568577; RRID: N/A
LAG-3 PerCP-Cy5.5 (C9B7W)	BioLegend	125211; RRID: AB_2561516
TIGIT APC (1G9)	BioLegend	142105; RRID: AB_10960139
TIM-3 PE-Cy7 (RMT3-23)	BioLegend	119715; RRID: AB_2571933
NKG2A PE-Cy7 (16A11)	BioLegend	142809; RRID: AB_2728160
CD39 BUV395 (Y23-1185)	BD Biosciences	567264; RRID: AB_2916524
SLAMF6 (13G3)	BD Biosciences	741893; RRID: AB_2871212
IL-2 APC (JES6-5H4)	BioLegend	503809; RRID: AB_315303
TNFα PerCP-Cy5.5 (MP6-XT22)	BioLegend	506321; RRID: AB_961434
IFNγ PE-Cy7 (XMG1.2)	BioLegend	505825; RRID: AB_2295770

Other Flow Cytometry Reagents

Product	Supplier	Catalogue ID
H2-Kb KSPWFTTL APC	ProImmune	828
CellTrace Blue	ThermoFisher	C345574
eFluor 780 Viability Dye	ThermoFisher	65-0865-14
24G2 Fc Block	Kind gift Prof. Anne Cooke	N/A
Golgi Plug	BD Biosciences	555029

Blocking/Stimulating Antibodies

Product	Supplier	Catalogue ID
αPD-L1 Clone 80	Kind gift from AstraZeneca	N/A
αCD3 Ultra-LEAF (17A2)	BioLegend	100239
F(ab')2 IgM μ chain (21571)	BioLegend	157102
CD3/CD28 beads	ThermoFisher	11456D

Cell Lines

Product	Supplier	Catalogue ID
MC38	Kind gift Prof. David Withers	N/A
HIEC-6	Kind gift Dr. Dave Boucher	N/A

Cell Culture

Product	Supplier	Catalogue ID
PBS	Sigma	10500064
RPMI	Gibco	11875093
Opti-MEM	Gibco	31985070
Trypsin-EDTA	Sigma	T4049
FBS (heat inactivated)	Gibco	A5256801
B-Mercaptoethanol	Gibco	31350010
Glutamax	Gibco	35050061
HEPES	Gibco	15630080
Penicillin/Streptomycin	Gibco	15140122
Human rEGF	BioLegend	585506
Mouse rIL-2	BioLegend	575406
Mouse rIL-7	BioLegend	577806
Mouse rIL-15	BioLegend	566304
Nigericin Sodium Salt	Merck	N7143-5MG

PCR

Product	Supplier	Catalogue ID
PowerUp SYBR Green	ThermoFisher	A25742
OneTaq 2X Mastermix	New England Biolabs	M0482
Genomic DNA mini kit	ThermoFisher	K182001
SYBR Safe DNA gel stain	ThermoFisher	S33102

Tissue Dissociation Reagents

Product	Supplier	Catalogue ID
DNAse I	Merck	10104159001
Collagenase D	Merck	11088858001
Dispase II	Sigma	102405030
EDTA	Invitrogen	15575020

IHC and Multispectral IF Reagents

Product	Supplier	Catalogue ID
αGBP5 Polyclonal	Protein tech	13220-1-AP; RRID: AB_2109348
αCD39 (EPR20627)	Abcam	Ab223842; RRID: AB_2889212
αCD4 (EPR6855)	Abcam	Ab133616; RRID:AB_2750883
αCD8 (4B11)	Leica	NCL-L-CD8-4B11
αFOXP3 (236A/E7)	Abcam	Ab20034; RRID: AB_445284
Bond Polymer Refine	Leica	102405030
Opal 520	Akoya Biosciences	FP1487001KT
Opal 570	Akoya Biosciences	FP1488001KT
Opal 620	Akoya Biosciences	FP1495001KT
Opal 690	Akoya Biosciences	FP1497001KT

Western Blotting

Product	Supplier	Catalogue ID
αGBP5 Polyclonal	Protein tech	13220-1-AP; RRID: AB_2109348
α β-Tublin	Abcam	Ab15568; RRID: AB_2210952

Small Molecule Inhibitors

Product	Supplier	Catalogue ID
PP2	Sigma	529573-1MG
Cyclosporine A	Cell Guidance Systems	SM43-50
PD0325901	Tocris	4192
GO 6983	Tocris	2285
SP600125	Tocris	1496
SB203580	Cell Guidance Systems	SM32-100
LY 294002	Sigma	440202
GDC-0941	Cell Guidance Systems	GDC-0941

1.2 MICE

Nr4a3 Tocky mice were generated in the Ono lab as previously described (Bending et al., 2018). Nur77 Tempo mice were generated by Taconic/Cyagen using their 'Piggybac-on-BAC' approach. Using bacterial artificial chromosome (BAC) RP24-366J14, which contains the entire Nr4a1 gene, a Fast-FT-rBG pA Zeomycin (Zao) cassette was inserted upstream of the Nr4a1 ATG start codon located in exon 2 (the first coding exon). The Zeo cassette was deleted by homologous recombination. A pair of piggyBac inverted terminal repeats (ITRs) flanking an ampicillin resistance cassette were introduced into the modified BAC vector backbone. The two ITR elements are recognition sequences of the piggyBac transposase (PBase), which facilitates integration into random TTAA sites by PBases, with one copy per integration site. The Modified BAC was injected into single-cell stage fertilized eggs. Pups were genotyped by PCR to screen for founder lines. A total of eight founder lines were generated, of which four had germline transmission. All animal experiments were approved by the local animal welfare and ethical review body and authorized under the authority of Home Office licenses P18A892E0A and PP3965017 (held by Dr. David Bending). Animals were housed in specific pathogen-free conditions.

1.3 MC38 TUMOUR MODEL

MC38 colorectal cell line was passaged in 10% FBS (v/v) RPMI containing 1% penicillin/streptomycin. On day of experiment, MC38 cells at the log stage of growth were harvested and resuspended in PBS at a concentration of 2.5 million/ mL and 0.25 million MC38 cells injected sub-cutaneously under the right flank of Nur77 Tempo or Nr4a3 Tocky mice in a final volume of 100 mL PBS. Tumours were excised and dissociated using scissors in 1.2 mL of

digestion media containing 1 mg/mL collagenase D and 0.1 mg/mL DNase I in RPMI. Samples were then incubated for 20-25 min at 37°C in

a thermoshaker. Digestion mixture was then passed through a 70 mm filter and washed with 30 mL ice cold media (10% FBS RPMI). Suspension was then centrifuged at 1500 rpm for 5 min at 4°C. Pellets were then re-suspended in FACS buffer (2% FBS PBS, 1 mM EDTA) for labelling with fluorescently conjugated antibodies.

1.4 TISSUE PREPARATIONS

Spleen and thymus were forced through a 70 µm filter and centrifuged at 1500 rpm for 5 mins. Red blood cells were lysed in RBC lysis buffer for 2 mins or ice before washing in PBS.

Lungs were perfused with PBS and minced using a scalpel before 40 mins digest in RPMI 10% FBS (v/v), 1% penicillin–streptomycin (v/v), 1 mg/mL collagenase D (w/v), 1 mg/mL dispase (w/v), 40 µg/mL DNase I (w/v). Digested lung tissue was passed through 100 µM filter and centrifuged at 1500 rpm for 5 mins. Red blood cells were lysed in RBC lysis buffer for 2 mins or ice before washing in PBS. Resulting sample was passed through a 40 µm filter, resuspended in FACS buffer, then analysed by flow cytometry.

Livers were perfused with PBS and forced through 70 µM cell strainers. Homogenate was topped up to 15 mL with ice-cold RPMI and centrifuged at 2000 rpm for 5 mins. Resulting pellet was resuspended in 10 mL ice-cold RPMI and layered over OptiPrep density gradient medium (Sigma), then centrifuged at 1000 g for 25 mins at deceleration setting 3. Leukocyte layer was aspirated, washed in RPMI, resuspended in FACS buffer, the analysed by flow cytometry.

Lymphocytes from small intestine epithelial layer were isolated as previously described (James et al., 2020).

1.5 GENOTYPING

Genomic DNA was extracted from ear punch biopsies using ThermoFisher genomic DNA mini kit. For endpoint PCR, Ft Fast genomic DNA was amplified using New England Biolabs OneTaq mastermix according to the manufacturer's instruction using an annealing temperature of 60°C. Samples were separated by gel electrophoresis and visualized using Invitrogen SYBR safe DNA gel stain. To determine copy number, RT–PCR of genomic DNA was performed using Applied Biosystems PowerUp SYBR green mastermix. Copy number was estimated by based on a presumption that the lowest delta cycle threshold (Ct) value represented a single copy transgenic, and a single copy $2^{\Delta CT}$ averaged ~0.7.

1.6 PRIMERS

Nr4a1-Ft Fast BAC (product size 362bp): For: GTGTACCCGTCCATGAAGGTGCT, Rev: CTGCTGTCCATTCCTTATTCCATAG

Il2ra: For: CAGGAGTTTCCTAAGCAACG Rev: CTGTGTCTGTATGACCCACC

Ft Fast: For: CGCGGAACTAACTTCCCCTC Rev: GTCTTGACCTCAGCGTCGTA

1.7 *IN VITRO* LYMPHOCYTE CULTURE AND SHORT-TERM STIMULATIONS

Single-cell suspensions of splenocytes were generated as described above and were cultured in RPMI containing 10% FBS (v/v) 1% penicillin/streptomycin (v/v) at 37°C 5% CO2. B cells were activated with 1 µg/mL anti-IgM (polyclonal). T cells were activated with 1 µg/mL anti-CD3ε (clone 145.2C11) stimulating antibody with or without small molecule inhibitors indicated in the resources table or DMSO vehicle control. Inhibitor concentrations are indicated in figure legends. Following in vitro activation, T cells or B cells were analysed by flow cytometry.

1.8 IN VIVO T CELL ACTIVATION

Mice were weighed and then injected intraperitoneally with 1 mg/kg anti-CD3ε (BioLegend, clone 145.2C11). Mice were culled 4 hours later, and spleens were removed for analysis.

1.9 $CD8^+$ T CELL EXHAUSTION ASSAY

Splenocytes and inguinal lymph nodes from Nur77 Tempo and Nr4a3 Tocky mice were processed as above, $CD8^+$ T cells were sorted using CD8 bead negative selection kit. Cells were counted and plated in 96 well plates at 1 density on 1*10^6 cells/ml in RPMI containing 10% FBS (v/v), 1% penicillin/streptomycin (v/v), 50 μM β-mercaptoethanol, and concentrations of IL-2, IL-7, and IL-15 indicated in figures. Sorted cells were the co-cultured with αCD3/αCD28 coated magnetic beads in a 1:1 ratio for 48 hours. A magnetic plate stand was used to remove beads, before resting in cytokine supplemented media (acute conditions) or further culture with αCD3/αCD28 coated magnetic beads or on plates coated with 1 μM αCD3 (chronic conditions). For re-stimulations, splenocytes from a wild-type mouse were processed enzymatically to preserve antigen myeloid cells. Spleens were excised and dissociated using scissors in 1.2 mL of digestion media containing 1 mg/mL collagenase D and 0.1 mg/mL DNase I in RPMI. Samples were then incubated for 20-25 min at 37°C in a thermoshaker. Digestion mixture was then passed through a 70 μm filter and washed with 30 mL ice cold media (10% FBS RPMI). Suspension was then centrifuged at 1500 rpm for 5 min at 4°C. T cells were depleted from wild type splenocytes using CD90.2 bead negative selection kit. Wild-type splenocytes were treated overnight with 10 ng/ml recombinant IFNγ in RPMI containing 10% FBS (v/v), 1% penicillin/streptomycin (v/v). Concurrently, sorted $CD8^+$ T cells were rested overnight in cytokine supplemented media. Sorted $CD8^+$ T cells were then co-cultured with IFNγ stimulated wild-type splenocytes at a 1:1 ratio for six hours in the

presence (intracellular cytokine staining) or absence (Fluorescent Timer analysis) of GolgiPlug (containing Brefeldin A).

1.10 FLOW CYTOMETRY

Samples were pelleted by centrifugation at 1500rpm for 3 minutes before re-suspension in FACS buffer containing fluorescently labelled antibodies and 24G2 αCD16/32 Fc block. Samples were incubated at 4°C protected from light for 30 minutes before being washed twice with FACS buffer. For intracellular cytokine staining, samples were then re-suspended in 200 µL fixation buffer (eBioscience) and incubated at RT protected from light for 30 minutes. Samples were then washed twice in 1X permeabilization buffer before incubation with fluorophore conjugated antibodies suspended in permeabilization buffer. Samples were then washed twice in FACS buffer. After staining samples were re-suspended in FACS buffer and analysed using a Sony ID7000 spectral cytometer (Figures 3.9, 3.10, 4.35-4.39, 4.41-4.44) or a BD-LSR Fortessa X20 (all other analyses).

1.11 ANALYSIS OF WITHER ET AL., 2023 DATASET

Transcript per million normalised read count data was accessed from (GSE242418) (Wither et al.,2023). Mean read counts from two biological repeats were plotted in a heatmap using GraphPad Prism software.

1.12 TCGA COHORT AND CIRC SCORE ANALYSIS

Development of a database of TCGA patients, CQN RNAseq data, and associated CIRC scores was performed by Dr. Jack McMurray (McMurray, 2021). Briefly, TCGA-COAD and TCGA-READ datasets were read into R and batch effects between Illumina Genoma Analyser and Illumina

HiSeq were removed using *sva* R package (Leek et al., 2012). Outliers were removed using *arrayQualityMetrics* (Guinney et al., 2015; Kauffmann et al., 2009). Count data was processed using *TCGAbiolinks* (Colaprico et al., 2016). Counts were normalised using conditional quartile normalisation procedure *cqn* (Hansen et al., 2012). CIRC enrichment score was calculated using geneset variation analysis *gsva* (Hänzelmann et al., 2013).

1.13 LOCAL COHORTS

Queen Elizabeth Birmingham local CRC cohorts were utilised for imaging analysis and metagenome analysis. MMR status had already been determined by IHC staining for MSH2, MSH6, MLH1, and PMS2; negative staining for all four proteins was classified as MSI-H. RNA sequencing data of local cohorts kindly provided by Dr. Toritseju Sillo and was used to calculate CIRC scores as described above.

1.14 IMMUNOHISTOCHEMISTRY

FFPE sections were analysed on a Leica Bondmax autostainer using the standard Bond Polymer Refine Detection (F) protocol. Briefly, sections were baked and dewaxed, heat-induced epitope retrieval was performed at 95°C for 20 minutes with pH9 TRIS-EDTA buffer. Samples underwent peroxide block for 5 minutes, were washed 3 times, then incubated with primary antibody for 30 minutes at RT. Samples were washed 3 times then incubated with secondary detection antibodies for 10 minutes at RT. Samples were washed 3 times then incubated with DAB refine solution for 10 minutes. Samples were washed 3 times then incubated with haematoxylin counter stain for 5 minutes. Samples were washed 3 times then scanned for analysis by Vectra 3.0 Automated Quantitative Pathology Imaging system.

1.15 MULTISPECTRAL IMMUNOFLUORESCENCE

Samples were stained using the automated Bond RX platform (Leica). Heat based removal was performed between each antibody incubation. Single stains were used for spectral deconvolution and an unstained slide was used for autofluorescence correction. Slides were scanned for analysis by Vectra 3.0 Automated Quantitative Pathology Imaging system.

1.16 IMAGING ANALYSIS

QuPath was used for analysis of Haematoxylin-DAB IHC scanned slides. Briefly, tissue detection was performed to remove empty space from the analysis. Selected regions were used to train a classifier for tumour epithelium, tumour stroma, and other (mucosa and smooth muscle areas). Tissue regions were classified before cell detection based on haematoxylin gamma values. Individual cells were thresholded based on cell mean DAB intensity (A) <0.15< (B) <0.25< (C) <0.4< (D). These values were used to calculate cell DAB H scoring for slide regions.

InForm was used for analysis of multispectral IF. Briefly, tissue detection was performed to remove empty space from the analysis. Selected regions were used to train a classifier for tumour epithelium, tumour stroma, and other (mucosa and smooth muscle areas). Tissue detection was based on DAPI station alone. Tissue regions were classified before cell detection based on DAPI gamma values. Cells representative of different cellular phenotypes were used to train a classifier, which was then applied to whole slide regions.

1.17 METAGENOME SEQUENCING ANALYSIS

Access to whole genome sequencing (WGS) data from the 100,000 genomes project was granted on 10/02/2021. Samples were sequenced by and sorted by Illumina, and subsequently aligned to GRch38. Sorted bam files were subjected to bacterial calling by Centrifuge (version 1.0.4) ((D. Kim

et al., 2016)). Default settings were used other than the minimum hit length (--min-hitlen) being increased to 35 (default = 22) and the host tax ID (--host-taxids) was set to 9606 (Homo sapiens). The reference database included: the human genome, prokaryotic genomes, and viral genomes. These initial analyses were performed by Boris Noyvert, and access was granted to output files on 06/05/2021 for downstream analyses.

Output files were annotated by NCBI taxonomic ID. These values were used as input to the *taxonomizr* R package (Sherrill-Mix, 2021) to gain taxonomy data for each of the microbes. 49 microbial species lacked taxonomy data and were discarded, leaving 5,753 species for investigation.

Differential microbe analysis utilised the *metagenomeSeq* R package for the fixed feature model they employ ((Paulson et al., 2013).

1.18 HIEC-6 STIMULATION AND CASPASE-1 WESTERN BLOT

HIEC-6 cells were culture in OptiMEM 1 reduced serum media containing 4% FBS (v/v), 20 mM HEPES, 10 ng/ml recombinant human Epidermal Growth Factor, 10 mM GlutaMax. Cells were grown to ~70% confluency and then stimulated with 10 µM nigericin sodium salt for time periods indicated in figure. Pellets were then lysed with RIPA buffer (150mM NaCl, 1% IGEPAL CA-630, 0.5% sodium deoxycholate (w/v), 0.1% SDS (w/v), 50mM Tris-HCl pH 8.0, protease inhibitor) on ice for 30 minutes. Samples were then centrifuged at 13,000g for 10 minutes, cell debris pellet was discarded. Samples were diluted 1:1 with 2x lamelli running buffer, loaded into 10% polyacrylamide gels and separated by electrophoresis. Gels were transferred onto PVDF membranes and blocked with 5% BSA (w/v) TBS for 1 hour at RT. Membranes were incubated with αCASP1 primary antibody (1:1000) or α β-Tublin (1:1000) dilutied in 5% BSA (w/v) TBS overnight at 4°C with constant agitation. Membranes were washed for 5 minutes in 0.5% Triton-X (v/v) TBS for

a total of 3 times. Membranes were incubated with anti-rabbit HRP secondary antibody for 1 hour at RT and then washed 3 times. Membranes were detected using ECL detection kit and a Bio-Rad Chemidoc.

1.19 STATISTICS

All statistical analysis was performed using GraphPad Prism 10. As N<50 for all experiments (with the exception of the transcriptional analysis in Figure 5.1 and 5.10, where D'Agostino Pearson test was used) normality was determined using Shapiro-Wilk test. If datasets passed normality testing, parametric tests were used to determine p values. In experiments with two groups, paired or unpaired t-tests were used, in all tests Welch's correction for uneven standard deviations was applied. In experiments with more than two groups, one way or two way ANOVAs were performed using Tukey's or Šídák's multiple comparison tests respectively. In cases where normality testing was not passed, non-parametric rank sum tests were performed, these were Mann-Whitney in the case of two conditions or Kruskal-Wallis in the case of more than two conditions. Details of statistics testing and N are included in all figure legends.

2 INTRODUCTION

The primary function of the immune system is to detect and eliminate threats associated with damage or pathogen invasion. The two arms of the immune system, innate and adaptive, are broadly defined by how they detect threats. The innate immune system is non-specific; its simplest form is the physical barriers of mucous and epithelium that separate the host from its environment. The innate immune system can detect pathogen associated molecular patterns (PAMPs) via intracellular or cell surface receptors. Examples of these are lipopolysaccharide, an endotoxin found in the cell wall of bacteria (Poltorak et al., 1998), or double-stranded RNA, generated during viral genome replication (Nallagatla et al., 2007). The innate immune system can also detect damage associated molecular patterns (DAMPs) that arise during states of cell stress such as extracellular ATP (Mariathasan et al., 2006). Innate immune cells such as macrophages and neutrophils can target pathogens with mechanisms such as phagocytosis, production of reactive oxygen species, and production of antimicrobial peptides. The adaptive immune system, consisting of B cells and T cells, uses re-arranged antigen receptors to detect short peptide sequences that are specific to individual pathogens. B cells mediate the humoral response to infection; cytotoxic T cells largely mediate killing target cells whilst T helper cells are responsible for supporting cytotoxic and B cell responses, mostly via the production of cytokines.

2.1 SPECIFICITY AND DEVELOPMENT OF T CELLS

T cells can transition from quiescence into an activated state, characterised by proliferation, differentiation into memory and effector phenotypes, cytokine production, migration, metabolic re-programming, and killing of infected or malignant host cells. The activation of T cells is tightly controlled by the T cell receptor (TCR), a member of the immunoglobulin superfamily of cell surface proteins. Conventional TCRs consist of α and β chain heterodimers (Punt et al., 1994),

associated with CD3εγ and CD3δγ heterodimers and CD3ζζ homodimers that mediate signal transduction (Morath & Schamel, 2020). TCRs are ligated by peptide loaded major histocompatibility complex (MHC) molecules; the variable region of the α and β chains determine the peptide specificity of the TCR. Binding to MHC class I or class II requires the TCR co-receptor CD8 or CD4 respectively.

The specificity of the convention TCR is determined by six complementarity-determining regions (CDRs) which bind to pMHC (Rudolph et al., 2006). The T cell pool within an individual must be very diverse in order to recognise the wide variety of antigens humans encounter, the diversity of unique TCRs is estimated to be ~10^8 (Arstila et al., 1999). T cells develop in the thymus where the α and β chains undergo V(D)J gene recombination (Hozumi & Tonegawa, 1976) allowing formation of a heterodimer of two randomly rearranged gene segments, creating very high levels of diversity. The diversity of peptides that can be generated from the 20 amino acids that are translated into proteins is larger than that of the T cell pool. It has been estimated that an individual MHC II molecule could present up to 10^{17} peptides, far exceeding the TCR diversity in a human (Mason, 1998). Therefore, TCRs must be highly cross-reactive (Sewell, 2012); whilst a TCR may have a cognate peptide to which it binds with highest affinity it can also recognise other amino acid sequences with lower affinity (Wilson, 2004).

After V(D)J recombination in the thymus, T cells enter the double-positive (DP) stage where they express both CD4 and CD8. In the thymic cortex, DP thymocytes are presented with self-antigens by cortical thymic epithelial cells. Those T cells that have formed a functional TCR through V(D)J recombination will receive a survival signal and be positively selected whilst others will die by neglect. Depending on whether T cells bind MHC I or MHC II with higher affinity, they will downregulate CD4 or CD8 respectively to enter the single positive stage and migrate into the thymic medulla. Here, T cells are again presented with self-antigen by medullary thymic epithelial

cells and migratory dendritic cells. Those that bind with high affinity to self pMHC will enter an apoptosis programme or enter a regulatory differentiation programme. This process of negative selection and regulatory T cell (T_{REG}) development act to prevent T cell recognition of self and thus autoimmunity (Klein et al., 2014).

2.2 T CELL RECEPTOR SIGNALLING

TCR ligation triggers a set of downstream signalling pathways that are initiated by membrane proximal phosphorylation events. The TCR chains have no intrinsic kinase activity, instead recruiting Src family kinases to phosphorylate the immunotyrosine based activation motifs (ITAMs) on the intracellular regions of the TCR chains. The exact mechanism by which TCR binding to peptide loaded MHC (pMHC) triggers downstream signalling is not completely understood, however, it is unusual among signalling receptors in that it does not appear to undergo conformational change (Sušac et al., 2022). There are various proposed models for the initiation of TCR signalling. The co-receptor scanning model proposes that CD4 or CD8 proteins move freely within the membrane, initiating signalling when they encounter TCR bound to pMHC (Stepanek et al., 2014). The CD45 exclusion models proposes that TCR signalling is spontaneously activated at steady state but undergoes constitutive negative regulation by CD45 phosphatase (Courtney et al., 2019). Interaction with an APC and formation of an immune synapse drive exclusion of CD45, which has a large extracellular domain, allowing TCR triggering (Leupin et al., 2000). Finally, the mechanosensation model proposes that upon binding to pMHC, mechanical forces act upon the TCR to trigger its activation (Meng et al., 2020) all reviewed by (Courtney et al., 2018). There is evidence for all of these models and the proposed mechanisms are likely all involved in the initiation of TCR signalling.

T cells can sense antigen affinity (duration of TCR ligation), antigen abundance (density of TCR ligation), and antigen persistence (longevity of TCR ligation). Despite this relatively simple input,

T cells are able to encode antigen recognition signals into diverse functional outcomes through tightly controlled fate decisions. T cells are able to add complexity to this input signal using intricate and divergent signalling pathways downstream of the TCR.

TCR signalling is important for the recognition of foreign pathogens and cancers. Cancers are derived from self, making them difficult to detect for T cells that are self-tolerised during thymic development. Genetic instability of cancers can make them vulnerable to T cell recognition, mutations that change the amino acid sequence of a protein coding region can give rise to 'neo-antigens'. This process is critical to drive effective TCR signalling and sufficient T cell activation to mediate an anti-cancer immune response. Accordingly, patients with a high number of non-synonymous mutations tend to have an inflammatory response to their tumours (Schumacher & Schreiber, 2015). T cells can directly kill tumour cells by repeated delivery of cytotoxic granules (Weigelin et al., 2021), a process that is heavily reliant on TCR-pMHC interactions to guide directional granule release (Jenkins et al., 2009). Cytotoxic T cell can disengage from their target cells by ectocytosis of TCR molecules, this termination of TCR signalling to allow serial killing of multiple target cells (Stinchcombe et al., 2023). Abundance of cytotoxic T cells within a tumour is highly correlated with good clinical outcome (Galon et al., 2006), indicative of their potent anti-tumour activity.

TCR signalling is highly dynamic, regulated by a complex set of feedback pathways. Some cancer therapies aim to augment TCR signalling by blocking negative feedback pathways, yet many patients show primary or acquired resistance to these therapies. In order to target therapies at the right individuals and identify the optimal therapy combinations, we must gain a deeper understanding of the regulatory pathways that govern TCR signalling.

2.2.1 Proximal TCR Signalling

Signals are transduced form the TCR by a set of complex pathways (Figure 2.1). Following pMHC binding, phosphorylation events proximal to the TCR occur within seconds (Huse et al., 2007).

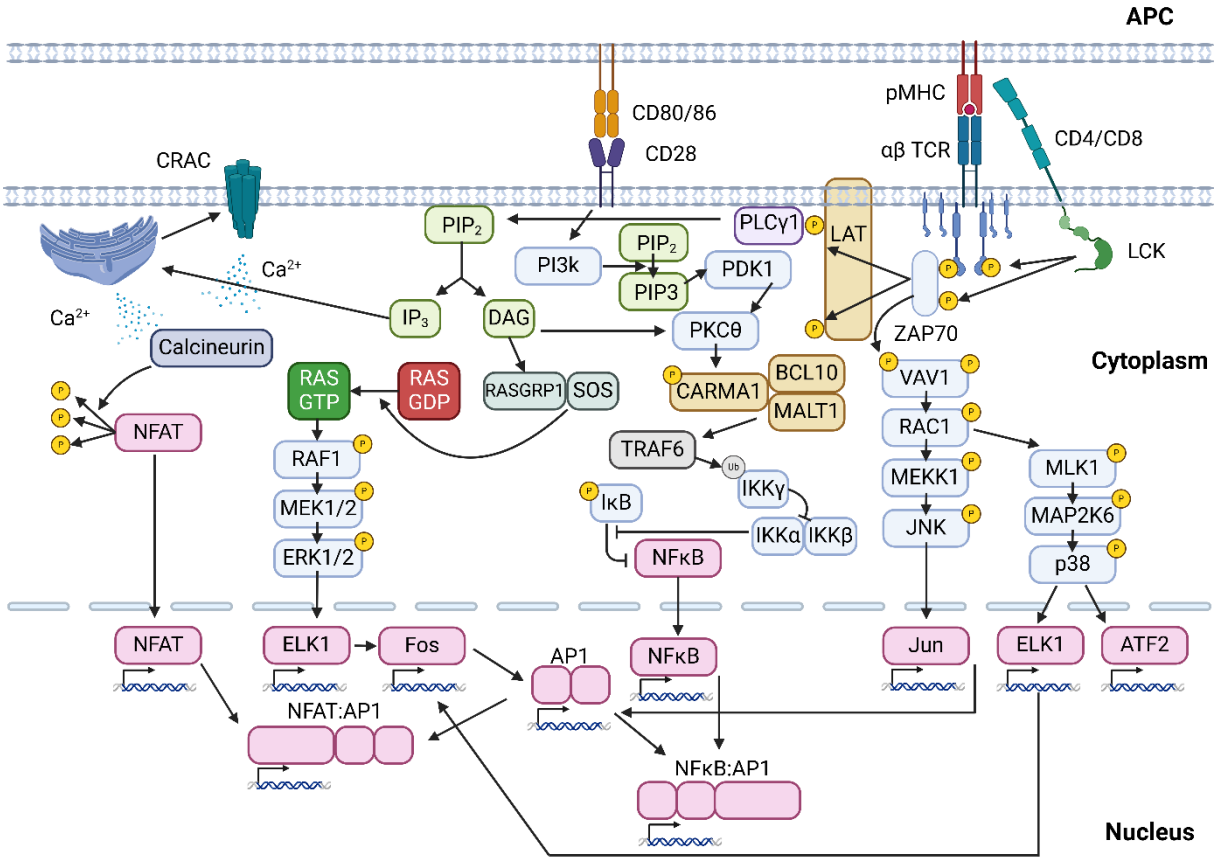

*Figure 2.**1 Schematic of signalling pathways downstream of the TCR and CD28.** Schematic is colour coded:light blue – kinases, yellow – scaffold proteins, pink – transcription factors, light green – lipid messengers, dark green – guanine nucleotide exchange factors, dark blue – phosphatases. Created using Biorender.com.*

The cytoplasmic tail of CD4 or CD8 interacts with SH4 domain of the tyrosine kinase LCK (Veillette et al., 1988), anchoring it at the membrane where it phosphorylates ITAMs of the CD3 chains (Kersh et al., 1998). Phosphorylated tyrosine residues within CD3ζ ITAMs create docking sites for SH2 domain containing proteins such as the ZAP70 kinase. ZAP70 tyrosine residues are phosphorylated by LCK, activating ZAP70 kinase activity (Williams et al., 1998). ZAP70

phosphorylates LAT, a large adaptor protein, creating docking sites for a number of secondary messengers (Finco et al., 1998). Phosphorylated LAT recruits PLCγ1, which acts as a key link between proximal and distal TCR signalling pathways (Beach et al., 2007).

2.2.2 RAS-MAPK-ERK-AP-1 Pathway

PLCγ1 hydrolyses PIP2, a lipid embedded in the cell membrane, into key secondary messengers IP3 and DAG (Rhee, 2001).

PIP2 derived DAG can bind to and recruit RASGRP1, a guanine nucleotide exchange factor (GEF) that co-operates with another GEF, SOS, to mediate release of GDP and binding of GTP to Ras (Ebinu et al., 1998). RAS intrinsic GTPase activity triggers serine/threonine kinase RAF1 to initiate the MAPK phosphorylation cascade, resulting in activation of ERK1/2. ERK1/2 play crucial roles in the development, (Fischer et al., 2005) differentiation, (Damasio et al., 2021) and activation (Houde et al., 2022) of T cells. Downstream of ERK1/2, transcription factor ELK is activated, driving expression of the transcription factor c-Fos (Cavigelli et al., 1995). The VAV-Rac1 pathway that acts via a MEK kinase cascade results in activation of JNK which facilitates nuclear entry of c-Jun by phosphorylation (Kaminuma et al., 2001). C-Fos and c-Jun form an AP1 heterodimer that plays a key role in T cell activation, regulating the transcription of many genes involved in proliferation (Foletta et al., 1998), cytokine production (Wagner & Eferl, 2005), and differentiation (Wagner & Eferl, 2005).

2.2.3 Ca^{2+}-Calcineurin-NFAT Pathway

IP3 derived from PIP2 can bind to the IP3 receptor located on the Ca^{2+} rich endoplasmic reticulum, triggering release of Ca^{2+} into the cytosol. The decrease in endoplasmic reticulum Ca^{2+} levels is detected by STIM proteins, driving tetramer formation of Orai1 subunits into calcium-release activated calcium (CRAC) channels (Penna et al., 2008). Influx of Ca^{2+} into the cytosol

drives activation of serine phosphatase Calcineurin, via its Ca^{2+} binding Calmodulin domain. Calcineurin can dephosphorylate members of NFAT transcription factor family (NFATc1-c5) allowing nuclear entry and transcriptional activity (Hogan et al., 2003).

NFAT works cooperatively with AP1 (Macián et al., 2001). In 1998 it was discovered that NFAT and AP1 bind composite sites in the regulatory regions of T cell activation associated genes (L. Chen et al., 1998), binding with high affinity as a complex compared to high dissociation rates when binding alone. Genes regulated by NFAT:AP1 complexes include those encoding cytokines such as IL2, IFNγ and TNFα, cell surface receptors such as CD40L and CD5, and chemokines MIP-1α (Rao et al., 1997).

NFAT can also bind as a dimer to NFκB-like sites on DNA. Studies involving a mutant of *NFATc1* that cannot bind to AP1 prevented transcription of some genes such as *IL2* but sustained transcription of *TNF* (Macian et al., 2000). However, it is important to note that ATF2-cFos dimers bind to a site upstream of the NFAT dimer binding site (Falvo et al., 2008), so although physical interaction is not necessary, AP1 transcription factor signalling is functionally required for *TNF* expression. NFAT signalling in the absence of RAS-ERK signalling has been shown to induce T cell functional anergy (Fields et al., 1996; Hogan, 2017; Macián et al., 2002; Martinez et al., 2015). Therefore, NFAT signalling may have antagonising roles, promoting T cell effector function or tolerance depending on cooperative signalling from the RAS-ERK-AP1 pathway.

2.2.4 PKC-IKK-NFκB Pathway

NFκB family of transcription factors include NF-κB1/p50, NF-κB2/p52, RelA (p65), RelB and Rel C that bind regulatory regions of DNA in a variety of homodimers and heterodimers (S.-C. Sun et al., 2013). NFκB transcription factors are sequestered in the cytosol by IκB family inhibitory proteins (S.-C. Sun, 2011), preventing their transcriptional activity. Activation of NFκB signalling is mediated by canonical and non-canonical PKC signalling. In T cells, canonical signalling via PKCθ

appears to be the key mediator of TCR signalling (Szamel & Resch, 1995). PKCθ is activated by DAG, allowing it to phosphorylate CARMA1, which can then oligomerise with BCL10 and MALT1 to from the CBM complex. The CBM complex recruits TRAF6, a polyubiquitinase that targets IKKγ, a regulatory subunit of the IKK complex. IKKα and IKKβ catalytic subunits are then free to phosphorylate IκB inhibitor proteins, freeing NFκB transcription factors to enter the nucleus and trigger transcription of target genes (Wertz et al., 2004) (L. Sun & Chen, 2004). Non-canonical PKC-NFκB signalling can occur in T cells, but this is associated with signalling from TNF receptors as opposed to the TCR (Daniels et al., 2023).

NFκB signalling plays a key role in CD4 T cell differentiation pathways (Aronica et al., 1999) (Das et al., 2001) and T cell activation status and memory (T. Liu et al., 2017), proliferation, cytokine production, and cytotoxicity (Gerondakis & Siebenlist, 2010).

2.3 DIGITAL VS GRADED RESPONSE TO TCR SIGNAL STRENGTH

T cells must be able to respond to different qualities of TCR signal. Discrimination between high and low affinity interactions with pMHC during thymic development dictates positive vs negative selection and natural T_{REG} differentiation (Gascoigne et al., 2016). Once T cells enter the periphery, they must be able to distinguish between low strength tonic self-antigen signalling (Elliot et al., 2022) (Moran et al., 2011) that promotes survival (Myers et al., 2017), and foreign antigen signals that necessitate an inflammatory response. During acute infection, higher strength of TCR signal favours short lived effector cell (SLEC) over memory precursor effector cell (MPEC) differentiation in both $CD4^+$ (Snook et al., 2018) and $CD8^+$ T cells (Solouki et al., 2020) (X. Huang & Yang, 2006) (King et al., 2012). Whilst signal strength during initial priming does not impact the fate of cytotoxic $CD8^+$ T cells (Richard et al., 2018), high signal strength upon target cell recognition is necessary for killing (Frazer et al., 2021). Additionally, chronic stimulation can

drive a state of T cell anergy (Shin & Wherry, 2007) (Fathman & Lineberry, 2007), where effector functions are shut down, to prevent lethal immunopathology (Barber et al., 2006).

The biochemical events that occur rapidly after TCR engagement are key decision making checkpoints that allow T cells to distinguish between low and high affinity peptide. At a population level, increasing TCR signal input by increased strength (Holler & Kranz, 2003) (S. Tian et al., 2007) or duration (Miskov-Zivanov et al., 2013) of antigenic stimulation drives a continuous increase in functional output such as cytokine secretion or surface expression of activation markers. However, studies of single cells have revealed 'digital' on/off behaviour, as opposed to continuous response (Au-Yeung et al., 2014).

Removal of clonal heterogeneity within a T cell population using a TCR transgenic model can lead to a binary output. Stimulation of thymocytes from OT-I mice (TCR transgenic specific for OVA peptide) with similar affinity variants of OVA peptide, caused 'all or nothing' positive (Daniels et al., 2006). A sharp threshold was observed where a slight increase in peptide strength dramatically increased the proportion of thymocytes that developed into CD8 SP cells. Western blot analysis did not reveal a significant difference in CD3ζ phosphorylation, but a significant effect on ERK phosphorylation. This highlights how T cells are able to convert an analogue input (e.g. number of phosphorylated CD3ζ ITAMs) into a digital output (e.g. selection of CD8 SP thymocytes). Accordingly, it has been well characterised that the signalling events following TCR engagement display switch like behaviour. Ras is activated by guanine nucleotide exchange factor SOS, and Ras can bind to SOS allosteric pocket to create a positive feedback loop. Therefore, the RAS-ERK-AP1 pathway experiences 'signalling hysteria' and a bimodal response to different input strengths (Das et al., 2009). Further downstream signalling events such as ERK phosphorylation (Altan-Bonnet & Germain, 2005) and nuclear entry of NFAT transcription factors (Conley et al., 2020; Dolmetsch et al., 1997; Gallagher et al., 2018; Podtschaske et al., 2007) are

also bimodal. Similar to Ras signalling, NFAT signalling is characterised by a positive feedback loop set at a certain threshold. At rest, cytosolic concentrations of Ca^{2+} are very low, maintaining constitutive phosphorylation of NFAT transcription factors. When TCR signalling crosses the threshold to induce release of Ca^{2+} from the endoplasmic reticulum, cytosolic Ca^{2+} increases. Concurrently, decreasing Ca^{2+} in the endoplasmic reticulum is detected, triggering Ca^{2+} flux across the plasma membrane, further increasing cytosolic Ca^{2+} (Srikanth et al., 2010); another example of signalling hysteria.

Digital behaviour of TCR signalling is governed by thresholds (Au-Yeung et al., 2014); thresholds are maintained by basal negative feedback pathways that require a certain level of positive signalling to be overcome. The 'kinetic proofreading' model, initially described in 1995 (McKeithan PNAS 1995), proposes that reversible phosphorylation events take place before an irreversible commitment to the TCR signalling cascade. Stronger pMHC-TCR interactions increase the 'dwell time' and decrease the 'proof-reading time delay', essentially decreasing the time to reach irreversible commitment and increasing the probability that a pMHC-TCR interaction will trigger downstream signalling. The kinetic proofreading model (McKeithan, 1995) is supported by recent experimental evidence (Tischer & Weiner, 2019).

Phosphatases such as CD45 can constitutively de-phosphorylate TCR signalling components such as LCK (Zamoyska, 2007) (McNeill et al., 2007), maintaining TCR signalling thresholds (Zikherman et al., 2010). In thymocytes, a key proximal regulator of digital signalling behaviour is Themis, a protein that binds to adaptor protein GRB2 at the TCR signalosome. Themis modulates the activity of phosphatases SHP-1 and SHP-2 to set digital TCR signalling threshold (Choi et al., 2017) facilitating sharp cut offs for positive and negative selection (Fu et al., 2013).

Phosphoproteome studies have been used to determine which phosphorylation events are sensitive to the affinity of pMHC-TCR interaction. Unlike CD3 ITAMs, phosphorylation of ZAP70

(Voisinne et al., 2022) and subsequent phosphorylation rate of LAT (Lo et al., 2023), are sensitive to antigen affinity. Therefore, activation of these two proteins may be the key bottleneck, determining whether the 'all or nothing' signalling threshold is crossed. The capability of a T cell to reach the activation threshold is highly dependent on the number of TCRs at the cell surface. Using TCR internalisation as a read-out of ligation, it has been estimated that ~8000 individual TCRs (or ~1500 with sufficient co-stimulation) must be ligated in order to reach activation threshold (Viola & Lanzavecchia, 1996).

Despite digital behaviour of RAS-ERK and Calcineurin-NFAT signalling pathways, different TCR regulated genes are differentially sensitive to TCR signal strength. *In vitro* stimulation of OVA peptide specific OTI TCR transgenic $CD8^+$ T cells with a dose titration of cognate peptide drives increasing expression of TCR regulated genes, with a sigmoidal dose response curve (Shimizu et al., 2020). This can be explained by conversion of a single cell digital signal to a population level analogue output. Although many TCRs must be ligated, a single pMHC molecule is in fact sufficient to drive T cell activation (J. Huang et al., 2013), highlighting the ability of pMHC to serially trigger many TCRs. Increasing peptide concentration increases the number of pMHC molecules, therefore increasing the likelihood that any given cell will cross the binary threshold for expression of any given gene. However, it was observed that different TCR regulated genes have different requirements for TCR signal strength(Shimizu et al., 2020). This qualitative change in the transcriptional profile in response to increasing TCR signal strength may be due to NFκB signalling. Unlike RAS-ERK and Calcineurin-NFAT signalling, NFκB signalling can be graded, via the activity of Tec kinase ITK (Conley et al., 2020). Unlike the bimodal distribution of NFAT nuclear entry and ERK phosphorylation, nuclear entry of NFκB p65 shows a graded increase in response to increasing doses of peptide. Accordingly, ATAC sequencing indicated that genes sensitive to TCR signal strength are enriched for NFκB binding motifs (Gallagher et al., 2021).

T cells are therefore able to enforce strict binary thresholds on some genes but graded expression of others via differential dynamics of signalling pathways downstream of the TCR. This allows T cells to exert threshold control over processes that require binary output such as positive vs. negative selection and the decision whether to divide or not. At the same time, T cells can exert tuneable control over biological processes where magnitude is important, such as the amount of cytokine to produce.

2.4 CO-REGULATION OF THE TCR

When an immune synapse is created between a T cell and an APC, a complex mix of co-stimulatory and co-inhibitory receptors co-localise with the TCR to fine tune the process of TCR activation (Saito et al., 2010). The makeup of these co-signalling receptors is dynamic, influenced strongly by T cell activation status and tissue environment. Co-signalling receptors are diverse, largely belonging to the immunoglobulin super family (IgSF) or tumour necrosis factor receptor super family (TNFRSF), reviewed by (L. Chen & Flies, 2013).

2.4.1 TCR Co-stimulation

CD28, of the IgSF, was the first discovered co-stimulatory receptor of the TCR (June et al., 1987), noted for its importance in T cell activation and IL-2 production. CD28 is ligated by CD80/86 proteins of the B7 family (van der Merwe et al., 1997), expressed on APCs. This gave rise to a 'two-step' model whereby stimulation of both the TCR and CD28 are required to promote full activation of T cells (Mueller et al., 1989). CD28 is expressed on naïve T cells and is involved in priming upon initial antigen encounter (Rudd et al., 2009). Like the CD3 chains, the intracellular region of CD28 has no intrinsic kinase activity but undergoes tyrosine phosphorylation by Src family kinases such as LCK and FYN. This mediates recruitment of GRB2 scaffold protein and PI3K (Raab et al., 1995). PI3K can phosphorylates PI into PIP2 and PIP3, which activates kinase PDK1, which in turn

activates PKB/AKT (Rudd & Schneider, 2003). Signalling via AKT has important roles in memory/effector differentiation via transcription factor FoxO, which regulates genes such as *IL7R* and *KLF2* (E. H. Kim & Suresh, 2013) (Weinreich et al., 2009). AKT can also act via mTORC1 to mediate metabolic reprogramming of T cells, to meet the energy demands of effector functions (Chi, 2012). Recruitment of GRB2 allows CD28 to activate many signalling pathways that are used to transduce TCR signals, such as RAS-ERK (Carey et al., 2000), PKC-NFκB (Thaker et al., 2015), and Calcineurin-NFAT (Boomer & Green, 2010).

ICOS is also an IgSF co-stimulatory receptor that works in a similar way to CD28, its intracellular domain recruits PI3K subunits and signals via AKT (Simpson et al., 2010). Signalling via ICOS is thought to be essential for the production of key cytokines such as IL-4, IL-21 and IL-10 (Gigoux et al., 2009), and transcription factor c-Maf (Bauquet et al., 2009) driving functional polarisation in $CD4^+$ T cells. ICOS does not have the same PYAP motif on its intracellular tail that CD28 has, meaning it cannot recruit LCK and GRB2, preventing signalling down canonical TCR pathways (Rudd & Schneider, 2003). ICOS is inducible upon TCR stimulation and therefore does not contribute to priming of naïve T cells, instead fine tuning signalling following initial activation.

Co-stimulatory receptors of the tumour necrosis factor superfamily are more diverse, including CD27, 4-1BB, OX40, GITR. They act to support proliferation, survival, and cytokine production (Croft, 2009). With the exception of CD27 (Hendriks et al., 2003), these co-stimulatory receptors are induced by TCR activation. Binding to ligand induced trimerization of TNFRSF co-stimulatory receptors, allowing them to recruit TRAF E3 ligases that mediate downstream signalling (King et al., 2006). Signalling pathways downstream of TRAF protein are not yet fully resolved, but can result in activation of NFκB, JNK, p38, and AKT (Ward-Kavanagh et al., 2016).

2.4.2 TCR Co-inhibition

There are several IgSF co-inhibitory receptors including CTLA-4, PD-1, LAG-3, TIGIT, and TIM-3 that use distinct mechanisms to negatively regulate TCR signalling. Unlike co-stimulatory receptors, which can be expressed at the cell surface constitutively, most co-inhibitory receptors are expressed in response to T cell activation.

CTLA-4 contains an intracellular YVKM motif that can recruit phosphatases such as SHP2 and PP2A. These can dephosphorylate proximal components of the TCR signalosome such as CD3ζ chains, LAT, and ZAP70 (Rudd et al., 2009). CTLA4 has also been shown to impact the kinase activity of JNK and ERK in the absence of any detectable changes to CD3ζ or ZAP70 phosphorylation (Calvo et al., 1997), however these observations are based on anti-pTyr western blots of co-immunoprecipitates so may not be as sensitive as more modern methods such as phosphoproteomics. However, other early studies have noted that CD28 and CTLA-4 appear to have antagonistic effects on TCR signalling (Krummel & Allison, 1995). CTLA-4 shares its ligand, CD80/86, with CD28 (Vandenborre et al., 1999) and in fact binds with much higher affinity than CD28 (Collins et al., 2002), effectively out competing CD28. Furthermore, CTLA-4 can mediate transendocytosis of CD80/86, removing the ligand for CD28 and targeting it for destruction in the lysosome (Qureshi et al., 2011). This can explain the phosphatase independent regulatory activity of CTLA-4, targeting both the TCR and co-stimulation pathways by distinct mechanisms.

PD-1 can also recruit phosphatases but does not contain YVKM motif like CTLA-4, instead contain an immunotyrosine based inhibitory motif (ITIM) and an immunotyrosine based switch motif (ITSM) (Riley, 2009). When bound to ligand (PD-L1 or PD-L2), tyrosine residues in ITIMs and ITSMs are phosphorylated, recruiting phosphatases such as SHP1 and SHP2 which mediate negative regulation of proximal signalling events (Sharpe & Pauken, 2018). Some have proposed that PD-1 acts primarily by inhibiting CD28 co-stimulatory pathways. In an *in vitro* system using human cell

lines, phosphorylation of CD28 is acutely sensitive to levels of PD-1 and super-resolution microscopy revealed PD-1 to be more closely associated with CD28 than the TCR (Hui et al., 2017). Furthermore, in *in vivo* models of infection and cancer, blockade of PD-1 signalling with a therapeutic anti-PD-L1 antibody is only effective if the CD28 co-stimulatory pathway is intact (Kamphorst et al., 2017). Other *in vitro* studies utilising primary mouse T cells have found that production of IL-2 can be attenuated by PD-1 signalling when antigen presenting cells do not express CD80/86, or T cells do not express CD28, suggesting a direct role in regulating TCR signalling (Mizuno et al., 2019; Sheppard et al., 2004) . PD-1 has also been shown to form clusters with TCR chains following PD-L1 binding in primary mice T cells, recruiting SHP2 and reducing the phosphorylation of PLCγ1 (Yokosuka et al., 2012). PD-1 can clearly target both the TCR and CD28, which target is more important for the regulatory role of PD-1 is likely context dependent on signalling pathway any given T cell is more reliant.

Suppressive activity of LAG-3 is dependent on an intracellular KIEELE motif, although the signalling pathways downstream are not understood (Workman & Vignali, 2003). Early reports of LAG-3 suppressive activity did suggest an effect on TCR signalling as cross-linking of LAG-3 lead to reduced Ca^{2+} flux and IL-2 production (Workman & Vignali, 2003). LAG-3 shares its ligand with CD4, MHC II. Studies that have utilised soluble LAG-3 tetramers have found that LAG-3 preferentially binds to stable pMHC complexes, suggesting LAG-3 targets T cell responses against high affinity antigens (Maruhashi Nature Immunology 2018). Unlike CTLA-4, where ligand competition appears to be a key regulatory mechanism, LAG-3 does not mediate transendocytosis of MHC II and allows CD4 to bind simultaneously (Maruhashi et al., 2018). As such, the as-not-yet characterised intracellular signalling must be key to suppressive activity (Graydon et al., 2021).

TIGIT also shares its ligands (CD155 and CD112) with a structurally related co-stimulatory receptor CD226. Ligation of TIGIT drives a T cell intrinsic negative regulation of T cell proliferation and cytokine production (Joller et al., 2011). TIGIT has an intracellular ITIM and also an ITT-like motif that recruits phosphatase SHIP1 via GRB2 adaptor protein, negatively regulating PI3K, MAPK, and non-canonical NFκB signalling (Johnston et al., 2014; S. Liu et al., 2013).

TIM-3 is an inhibitory receptor that forms a heterodimer with CEACAM1 (Y.-H. Huang et al., 2015), it is ligated primarily by Galectin 9 via interaction with its extracellular IgV domain (Sabatos et al., 2003). Intracellular signalling of TIM-3 is not well understood. Ligand binding leads to phosphorylated of tyrosine residues on the intracellular tail, this is necessary for direct binding to the p85 regulatory subunit of PI3K and negative regulation of T cell activation (J. Lee et al., 2011). TIM-3 can also function as a co-stimulatory receptor in the absence of ligand binding, via interaction with BAT3 and Src family kinases (Rangachari et al., 2012).

2.5 ACTIVATION INDUCED FEEDBACK CONTROL OF TCR SIGNALLING

Regulation of TCR signalling is highly dynamic and context dependent. The cell surface expression level of the TCR is a critical factor in determining a T cells ability to reach activation threshold to a given stimulus (Viola & Lanzavecchia, 1996). Yet, T cells respond to triggering of the TCR by internalising the TCR through phagocytic pathways within 10 minutes (Martínez-Martín et al., 2011), which is accompanied by a transcriptional downregulation of proximal components of the TCR signalling pathway (Elliot et al., 2021). T cells can respond to activation by changing the composition of co-stimulatory and co-inhibitory receptors at their cell surface, altering the signalling threshold for TCR regulated genes (Elliot et al., 2021) (Shimizu et al., 2020). Expression of co-stimulatory receptors is acutely sensitive to the strength (Elliot et al., 2021) (Trefzer et al., 2021) and duration (Wherry, 2011) of TCR signalling. Additionally, T cells can signal to APCs via pro-inflammatory cytokines such as IFNγ and TNFα or anti-inflammatory cytokines such as IL-10.

These can alter the antigen presentation machinery (Chadban et al., 1998; Mittal & Roche, 2015; Steimle et al., 1994) as well as the composition of ligands for co-stimulatory and co-inhibitory receptors (Garcia-Diaz et al., 2017). T cells can also facilitate an immunosuppressive local microenvironment, for example by upregulating CD39, an ectonucleotidase that is involved in the conversion of inflammatory extracellular ATP into immunosuppressive adenosine (Takenaka et al., 2016). In this way, T cells can set up positive and negative feedback pathway to fine tune TCR signalling following initial activation.

2.5.1 Regulation of the TCR Under Chronic Stimulation

Chronic stimulation of the TCR can lead to exhaustion - an alternative differentiation pathway, distinct from effector or memory phenotypes. T cell exhaustion is characterised by gradual loss of functions, such as proliferation and cytokine production, and high expression levels of multiple co-inhibitory receptors (Wherry, 2011). It has been noted as early as 1968 that tumours can progress despite immune recognition from lymphocytes (Hellström et al., 1968); we now know that this can be due to exhaustion of T cells that are specific for tumour antigens (Baitsch et al., 2011; Fourcade et al., 2010; Gros et al., 2014). Persistence of antigen due to a failure to clear the tumour is the primary driving factor in exhaustion of tumour specific T cells (Schietinger et al., 2016).

T cell exhaustion is best studied in $CD8^+$ T cells fighting chronic LCMV infection or cancer but $CD4^+$ T cells can also exhibit many of the hallmarks of exhaustion (Balança et al., 2021). During chronic LCMV infection, $CD8^+$ T cells lose the ability to respond to IL-7 and IL-15, the homeostatic cytokines that can sustain naïve and memory T cells long-term, downregulating respective receptors CD127 and CD122 (Shin & Wherry, 2007; Wherry et al., 2004). Although exhausted cells can display many features of effector cells, there are transcriptional (Singer et al., 2016) and epigenetic (Sen et al., 2016) features that are specific to exhaustion.

2.5.2 Progressive Nature of CD8$^+$ T Cell Exhaustion

T cell exhaustion is progressive. Studies have highlighted a difference between PD-1$^+$ TIM-3$^+$ CD39$^+$ TCF1$^-$ CD8$^+$ T cells that are terminally exhausted $T_{(EX)}$, and PD-1$^+$ TCF1$^+$ CD8$^+$ pre-cursor exhausted (T_{PEX}) cells. T_{PEX} are more proliferative than T_{EX} (S. J. Im et al., 2016) and they can sustain an ongoing response to chronic infection (Siddiqui et al., 2019; Utzschneider et al., 2016) and cancer (Connolly et al., 2021; Schenkel et al., 2021) due to their self-renewal capacity. T_{PEX} display epigenetic alterations (Abdel-Hakeem et al., 2021) that commit them to eventual exhaustion following a few days of chronic stimulation. This has been proven by generation of T_{PEX} by chronic LCMV infection and transfer of this population into a mouse harbouring an acute LCMV infection that drives typical effector/memory differentiation. Transferred T_{PEX} differentiated into T_{EX} despite withdrawal of chronic stimulation (Utzschneider et al., 2013). Conversion of T_{PEX} into T_{EX} is driven by TCR signalling (Miller et al., 2019) and IFNγ signalling (Mazet et al., 2023). In tumour models, T_{PEX} cells traffic between lymph nodes and the tumour site (Li JEM 2022); antigen recognition within the tumour site is a key driver for further differentiation (Prokhnevska et al., 2023).

A study using single cell RNA sequencing and tetramer staining of CD8$^+$ T cells during chronic LCMV infection has demonstrated multiple distinct states that T cells pass through during the trajectory of exhaustion differentiation (Daniel et al., 2022). For example, there are PD-1$^+$ TCF1$^-$ CX3CR1$^+$ CD8$^+$ T cells at an intermediate stage of exhaustion, retaining the ability to express KLRG1 and produce IFNγ, a key feature of effector CD8$^+$ T cells. In contrast there are PD-1$^+$ TIM-3$^+$ TCF1$^-$ CCR6$^+$ CD8$^+$ T cells that are at a terminal stage of exhaustion and cannot make IFNγ. Tetramer staining showed that very high affinity for LCMV antigen favoured CCR6$^+$ T_{EX} differentiation, suggesting that stronger TCR signalling is more effective in driving exhaustion. This is in agreement with studies performed in mouse models of cancer, where tumour cell lines

expressing variants of OVA peptide were used to show high affinity antigen recognition increases expression of co-inhibitory receptors whilst reducing proliferation and cytokine production (Shakiba et al., 2021). Similar studies have shown that strength of antigen recognition plays a key role in fate decisions that determine whether an antigen specific T cell will be effective at clearing cancer (Burger et al., 2021). There is also heterogeneity among PD-1$^+$ TCF1$^+$ CD8$^+$ T cells, with those expressing lymph node homing marker CD62L appearing to be at an earlier stage of differentiation and more proliferative (Q. Huang et al., 2022; Tsui et al., 2022).

2.5.3 Molecular Control of T Cell Exhaustion

Functional exhaustion of T cells is controlled by some transcription factors downstream of the TCR such as NFAT (Martinez et al., 2015), TOX (Khan et al., 2019; Scott et al., 2019; Sekine et al., 2020), NR4A1 (J. Chen et al., 2019; X. Liu et al., 2019), and NR4A3 (Jung et al., 2022) that drive expression of co-inhibitory receptors. There are also environmental factors that can contribute to T cell exhaustion. IL-27 signalling transcriptionally controls a module of co-inhibitory receptors through the activity of transcription factors c-Maf and BLIMP1 (Chihara et al., 2018). Inflammatory cytokines IL-12, IL-15 and IL-18 are sufficient to drive expression of TOX and PD-1 (Maurice et al., 2021). Retention in the T_{PEX} 'stem-like' state appears to be controlled by transcription factors TCF1 (Z. Chen et al., 2019) and MYB (Gautam et al., 2019; Tsui et al., 2022).

Much of what drives dysfunction in during chronic stimulation is epigenetic (Abdel-Hakeem et al., 2021; Bevington et al., 2020; Philip et al., 2017; Sen et al., 2016). In exhausted CD8$^+$ T cells this appears to be primarily mediated by TOX as its over-expression is sufficient to drive epigenetic dysfunction (Khan et al., 2019). Chromatin regions containing genes associated with key T cells functions, such as those encoding cytokines and mediators of cell cycle progression, are made inaccessible whilst those containing genes encoding co-inhibitory receptors are opened up. Increased expression of co-inhibitory receptors is sufficient to raise the threshold of TCR signal

strength that is required to drive expression of key T cell genes (Elliot et al., 2021). However, in exhausted T cells, chronic stimulation may have also made such genes epigenetically inaccessible, further repressing T cell functionality.

2.6 CO-INHIBITORY RECEPTOR BLOCKADE THERAPY

Blockade of co-inhibitory receptors or 'Immune Checkpoint Blockade' (ICB) therapy has revolutionised how some types of cancer are treated. The most successful targets to date are PD-1, PD-L1 and CTLA-4; antibodies targeting these proteins are used to treat a variety of cancers in the UK with perhaps most notable success in melanoma where PD-1 and CTLA-4 combinatorial blockade is standard of care. ICB aims to block the interaction between co-inhibitory receptors and their ligands, relieving negative co-regulation of TCR signalling. Early trials of PD-1 blockade in melanoma have noted that many TCR regulated functions such as proliferation, cytotoxic granule production and IFNγ signalling are increased in those patients that show pathological therapy response (Tumeh et al., 2014). ICB appears to primarily target tumour specific T cells (Gubin et al., 2014) but can also have an indirect effect on PD-1^{-} bystander CD8^{+} tumour infiltrating lymphocytes (TILs) (Kurtulus et al., 2019). T cells that recognise clonal neoantigens are the most effective responders to ICB, presumably due to decreased risk of evasion by immunoediting. The action of ICB therapy is not limited to interactions between T cells and tumour cells, PD-1 PD-L1 interactions involving professional APCs in the lymph node are also sensitive to ICB (Dammeijer et al., 2020). Furthermore, blocking the interaction between myeloid cell PD-1 and tumour cell PD-L1 can increase CXCL9 production and recruitment of cytotoxic T cells (Klement et al., 2023). Studies in mouse models of cancer have shown that the primary activity of TIM-3 blockade is regulation inflammasome activation and IL-18 production by dendritic cells (Dixon et al., 2021). These studies show that investigations into the anti-tumour effects of ICB therapy must carefully consider its impact on the immune microenvironment.

2.6.1 Cellular Targets of Co-inhibitory Receptor Blockade Therapy

Early studies of ICB from Rafi Ahmed's lab found that blockade of PD-L1 drove proliferation of antigen-specific T cells during chronic LCMV infection, apparently reversing exhaustion (Barber et al., 2006). This gave rise to the idea that T cell exhaustion is a reversible phenomenon, however more recent studies have shown that not all T cells are capable of responding to ICB. In 2016, Rafi Ahmed's lab characterised the sub-population of antigen-specific $CD8^+$ T cells that proliferate in response to ICB, comparing them to T follicular helper cells due to their co-expression of CXCR5 and PD-1 (S. J. Im et al., 2016). These cells were shown to express TCF1 but not CD39, resembling later descriptions of T_{PEX} cells. A month prior, a study published by Wener Held's lab reported similar findings of a specific response to ICB from PD-1^+ $TCF1^+$ T cells (Utzschneider et al., 2016). Therefore, ICB therapy may target only a small subset of exhausted T cells that are at an early stage of the exhaustion trajectory. Terminally exhausted cells may lose the ability to produce cytokines or proliferate in response to checkpoint blockade due to the epigenetic inaccessibility of the required genes.

Many of the exhaustion paradigms discovered in LCMV apply to the anti-tumour immune response. Single-cell RNA sequencing has revealed remarkable transcriptional similarity between exhausted $CD8^+$ T cells generated in LCMV infection and those generated in response to a sub-cutaneous tumour implant (Miller et al., 2019). Tumour progression drove the differentiation of distinct $TCF1^+$ TIM-3^- and $TCF1^-$ TIM-3^+ populations; upon transfer of purified population, the former underwent unidirectional differentiation into the latter. $TCF1^+$ cells selectively proliferated following PD-1 blockade, mirroring results of LCMV studies. Similar to models of chronic infection, T_{PEX} cells are essential for sustaining an anti-tumour response in mouse models of cancer, and drive the response to ICB therapy (Siddiqui et al., 2019). T_{PEX} have been identified in human lung cancer, re-capitulating many findings from mouse models such as

expression of CXCR5 and TCF1 and proliferative capacity (Brummelman et al., 2018). Disease progression was associated with a decrease in T_{PEX} numbers over time. $TCF1^+$ $CD8^+$ T cells with stem-like properties have also been identified in human melanoma, their abundance being correlated with good response to ICB therapy (Sade-Feldman et al., 2018).

Studies have utilised tetramer staining and single-cell RNAseq to identify the transcriptional profile of neo-antigen reactive $CD8^+$ T cells and compare them with those reactive for resolved infections like influenza. Neoantigen reactive cells expressed genes associated with terminal exhaustion, such as *ENDTP1* that encodes CD39, to a higher degree than influenza reactive cells (Caushi et al., 2021). However, it was the presence of atypical neoantigen reactive cells, that expressed genes associated with memory such as *IL7R* and *TCF7* that were correlated with effective response to ICB therapy. Tracking this population in the peripheral blood indicated a therapy induced terminal differentiation in a patient that underwent complete pathological response.

Similar to mice, terminally exhausted intratumoural T cells are likely not the critical responders to ICB therapy. Successful ICB therapy in melanoma patients causes a clonal replacement of $CD8^+$ T cells (Yost et al., 2019), suggesting a limited re-invigoration of existing exhausted T cells and instead an increase in the potency or duration of a new wave of T cell immunity. Analysis of the blood of melanoma patients receiving ICB therapy has shown that good response to ICB therapy is associated with greater expansions (Fairfax et al., 2020) and effector differentiation (Watson et al., 2021) of peripheral tumour-reactive $CD8^+$ T cells.

2.6.2 Acquired Resistance and Combination Co-inhibitory Receptor Blockade Therapy

Although co-inhibitory receptors can signal via distinct pathways, they may show some functional redundancy. For example, deletion of *Ptpn11* (encoding SHP-2, the primary phosphatase downstream of PD-1) does not prevent exhaustion during chronic infection or cancer (Rota et al., 2018). Expression of multiple co-inhibitory receptors is a key defining feature between T_{PEX} and T_{EX}. It may be that inhibitory signalling via PD-1 is the limiting factor for T_{PEX} reaching the signalling threshold to express genes involved in cytokine production and proliferation, but T_{EX} can compensate against the blockade of PD-1 via other inhibitory receptors.

The transcriptional response to PD-1 blockade in many ways mirrors the transcriptional response to increased TCR signal strength (Elliot et al., 2021). Expression of co-inhibitory receptors is TCR signal strength dependent (Elliot et al., 2021) and ICB therapy increases TCR signal strength, selectively driving the expression of genes dependent on strong TCR signalling (Shimizu molecular cell 2020). It then follows that T cells may respond to ICB therapy by compensatory upregulation of other inhibitory receptors. This is supported by experimental evidence in mice, where T cells bound by therapeutic PD-1 antibodies increase their expression of TIM-3 (S. Koyama et al., 2016). This may then represent a mechanism of acquired resistance to ICB therapy. In human cancer, upregulation of PD-1, LAG-3, (Gettinger et al., 2017) and VISTA (Kakavand et al., 2017) has been observed following ICB therapy.

A detailed single cell analysis of human renal cancer TILs found that ICB induced upregulation of co-inhibitory receptors was most pronounced in a '4-1BB-lo' population of $CD8^+$ T cells, that had relatively low expression of transcriptional signatures relating to exhaustion (Bi et al., 2021). It may therefore be precursor exhausted cells, the putative ICB responder population, that selectively mediate adaptive resistance to ICB therapy via other co-inhibitory receptors. $CD8^+$ cells with high expression of terminal exhaustion signatures were not transcriptionally inert in

response to ICB. They increased their expression of effector molecules such as *IFNG* and *GZMB*. However, upregulation of cytotoxic genes such as *GZMB* may have a limited effect on the cytolytic capacity of exhausted $CD8^+$ T cells. Effective killing is dependent on the formation of a 'cytolytic synapse' between $CD8^+$ T cells and their target (de la Roche et al., 2016). TCR signal strength is a key determinant of cytolytic synapse formation (Frazer et al., 2021); high levels of inhibitory signalling may reduce the ability of cytotoxic T cells to form cytolytic synapses. It has been demonstrated in natural killer cells that SHIP1 recruitment by TIGIT prevents polarisation of cytolytic granules and cytotoxic capacity (S. Liu et al., 2013).

How a T cell responds to ICB is dependent on context, TCR signalling history, and differentiation status. In patients where the antigen burden is low, ICB may be ineffective because the strength of TCR signalling is insufficient to reach activation threshold even when inhibitory receptors are blocked. In patients with an antigen driven anti-cancer T cell response, increasing the strength of TCR signalling via ICB therapy can drive proliferation and effector differentiation in cells at an earlier stage of differentiation, mediating a durable T cell response and tumour rejection. Cells at a later stage of differentiation may show an increase in cytotoxicity but not proliferation, or respond to therapy induced increase in TCR signal strength by upregulating alternative checkpoints as a mechanism of acquired resistance. Combatting this type of acquired resistance may require blocking multiple checkpoints with combinatorial therapy.

Different types of ICB therapy can target different cellular populations. Whilst αPD-1 and αCTLA-4 can both slow tumour progression in mouse models of cancer, they have distinct effects on TIL populations. Notably, CTLA-4 blockade reduces numbers of T_{REG} cells whilst increasing the number of Th1 $CD4^+$ effector cells. αPD-1 preferentially increased numbers of terminally differentiated $CD8^+$ T cells (Wei et al., 2017b). This differential activity on distinct inhibitory pathways may explain why combination of αPD-L1 and αCTLA-4 is more effective than single

agent in treating melanoma (Larkin et al., 2015). More recent trials have shown αLAG-3 and αPD-1 therapy has a similar benefit over PD-1 blockade alone (Tawbi et al., 2022). When designing therapy regiments, it is important to consider which immune cells will be affected. Blockade of PD-1 has a broad impact on T cells, as the majority of tumour specific TILs express PD-1 (Gros et al., 2014). In melanoma patients, NK cells express high levels of LAG-3 but almost no PD-1, as such combination of LAG-3 and PD-1 blockade causes distinct transcriptional changes in NK cells as compared to PD-1 alone (Huuhtanen et al., 2023). Similarly, inhibitory receptor NKG2A is expressed by both $CD8^+$ T cells and NK cells and its blockade invigorates both cell types in pre-clinical models (P. André et al., 2018). CTLA-4 is highly expressed on T_{REG} cells and activated $CD4^+$ T cells, hence its blockade has a significant impact on $CD4^+$ T cell differentiation in cancer patients (Wei et al., 2017a). Some inhibitory receptors such as TIGIT and TIM-3 are only expressed on T cells at the later stages of exhaustion (Wherry, 2011), thus their blockade is likely to only impact exhausted T cells. *In vitro* activation of TILs sorted from murine tumours show that co-blockade of PD-L1 and TIM-3 can restore cytokine production to exhausted $CD8^+$ T cells (Sakuishi et al., 2010). Similar studies in bladder cancer patients have shown increased cytokine expression following co-blockade of PD-1 and TIGIT.

2.7 FUTURE PROSPECTIVES AND PROJECT AIMS

In order to target the right therapies at the right patients, further work must be done to understand the mechanism of action of ICB therapies. Results from combinatorial blockade of PD-1 and CTLA-4 in melanoma patients show the importance of targeting non-redundant pathways. Pairing the right type of ICB to the right subset of patients will require careful consideration of the relevant subsets of immune cells. For example, some mismatch-repair deficient colorectal cancers mutate β2-microglobulin, a key component of the MHC I antigen processing pathway. Nevertheless, these patients can respond to PD-1 blockade, driven by a population of γδ T cells

that recognise stress ligands on tumour cells via NKG2D (de Vries et al., 2023). These patients may then benefit from a combinatorial approach that targets inhibitory receptors expressed by innate-like γδ TY cells such as NKG2A (Cazzetta et al., 2021). Cancers that we know contain high numbers of T_{REG} cells may be better served by combination with αCTLA-4, as we know this is a key suppressive mechanism of T_{REG} cells (Sobhani et al., 2021).

Obtaining this information pre-therapy will be critical to targeted ICB therapy, however we must also consider the dynamic changes in co-inhibitory receptor composition that occur following ICB therapy. Tracking the phenotype of T cells after they have responded to ICB will help us to understand the compensatory mechanisms that drive acquired resistance. Furthermore, we must understand how exactly the molecular pathways downstream of the TCR are affected by co-inhibitory receptor signalling and how this is modulated by therapy. This will involve complex mechanistic work, tracking how TCR signalling is affected by models of chronic stimulation, and how the TCR responds to ICB in different functional subsets of T cells.

Here we utilise transgenic mice that express dynamic, distal fluorescent reporters of TCR signalling to track downstream TCR pathway activity with high time resolution. We investigate the relative contribution of downstream pathways to reporter expression, highlighting differential pathway dependency between different reporters. We study the dynamics of TCR signalling during T cell development, steady state, acute stimulation, and tissue residency. Furthermore, we use sub-cutaneous implantation of tumour cells and chronic *in vitro* stimulation to model $CD8^+$ T cell exhaustion, discovering a rapid re-wiring of the different TCR signalling pathways that are active under chronic antigen exposure. Finally, in a distinct but related body of work, we investigate drivers of T cell immunity in low mutational burden human colorectal cancer. We imaged FFPE sections of human cancer and analysed transcriptional and metagenomic datasets

to investigate the relative contributions of antigen specific responses versus microbial adjuvantisation.

3 DEVELOPMENT AND VALIDATION OF NUR77 TEMPO

3.1 INTRODUCTION

In order to track TCR signalling in pre-clinical models, an effective biomarker of TCR signalling is required. Historically, cell surface markers of activation such as CD69 have been used as evidence of TCR signalling. Expression of CD69 is a good biomarker of TCR signalling; CD69 upregulation is very sensitive, and it is an effective read-out of TCR signalling in in vitro systems. However, CD69 can be expressed in response to type 1 interferons to promote retention in lymphoid organs (Shiow et al., 2006). Therefore, CD69 is not a specific biomarker of TCR signalling because its expression can be induced by an inflammatory environment. Experiments in 1994 aimed to identify genes that are associated with negative thymic selection by cloning DNA from apoptotic thymocytes (Z.-G. Liu et al., 1994). They identified a gene *Nr4a1* that encodes the Nur77 protein, its expression was inducible in vitro by ligation of the TCR alone and its loss prevented thymocyte apoptosis.

The Nr4a family are nuclear orphan receptors that play diverse roles in T cell development and function, particularly the induction of tolerance (Hiwa et al., 2022). Knockout studies have shown partial functional redundancy between Nr4a family members (Bending & Zikherman, 2023). TCR-induced expression of Nur77 appears to act as a negative feedback mechanism. For example, Nur77 can bind to AP1 consensus DNA binding sites to act as a competitive inhibitor of ERK:AP1 signalling (X. Liu et al., 2019). Nur77 can act to delay the metabolic switch associated with T cell activation (Liebmann et al., 2018). Activity of Nor1 (encoded by *Nr4a3*) restrains $CD8^+$ T cell cytokine production and memory formation during infection (Odagiu et al., 2020). Studies in chronically stimulated $CD8^+$ T cells have shown Nor1 antagonises the activity of BLIMP1 to promote exhaustion over stemness (Jung et al., 2022).

In 2007, microarray studies of thymocytes undergoing positive or negative selection found that Nr4a1 is upregulated ~2 fold during positive selection but ~10 fold during negative selection (Baldwin & Hogquist, 2007). This suggests that not only is Nr4a1 expression induced specifically by TCR signalling, but that its expression level may be related to TCR signal strength. In 2011, Kristin Hogquist's lab created a GFP reporter of Nr4a1 called Nur77 GFP, utilising a bacterial artificial chromosome strategy (Moran et al., 2011). GFP expression was inducible by stimulation with αCD3 or αIgM in lymph node $CD4^+$ T cells and B cells respectively. Nur77 GFP mice were crossed with OT-I TCR transgenics. Stimulation of thymocytes with different affinity variants of OVA peptide was related to brightness of GFP in a linear, graded fashion. This contrasts the previously observed functional outcome of OVA peptide variants and the resultant dogma of strictly thresholded binary selection (Daniels et al., 2006).

GFP expression was observed in thymocytes during positive selection and to a greater extent during negative selection. Furthermore, GFP expression was observed at a steady state in mature $CD4^+$ T cells demonstrating that Nr4a1 is induced by low strength recognition of self-antigen in the periphery, that is essential for T cell survival (Kirberg et al., 1997). Titrating the dose of αCD3 during in vitro stimulation has shown the threshold for Nur77 GFP expression to be lower than the threshold for proliferation (Au-Yeung et al., 2014).

Regulation of Nr4a1 was shown to be highly specific to the TCR; transfer of Nur77 GFP $CD4^+$ T cells into MHC-IINULL mice drove a loss of GFP expression. Induction of non-antigen specific inflammation by injection of LPS or pI:pC caused upregulation of CD69, but not GFP. Infection of Nur77 GFP OT-I mice with Listeria Monocytogenes only led to upregulated of GFP when the bacteria overexpressed OVA peptide, confirming peptide specificity. Expression of Nr4a1 was not related to IL-2 signalling, as a constitutively active mutant of STAT5 had no impact on GFP

expression. Thus, Nur77 GFP is a highly specific reporter of TCR signalling, that is graded in relation to TCR signal strength.

A significant drawback to the use of Nur77 GFP is its high background levels and lack of time resolution. GFP has a half-life of ~26 hours in mammalian cells (Corish & Tyler-Smith, 1999), subsequently GFP expression is detectable several days after TCR stimulation (Moran et al., 2011). To combat this limitation, the Nr4a3 Tocky mouse was generated in Masahiro Ono's lab at Imperial College London. It uses a BAC system to express FT Fast, that encodes a Fluorescent Timer protein, under the control of Nr4a3 regulatory regions. Fluorescent Timer is a mutant of mCherry that changes colour from blue to red over time (Subach et al., 2009); the in vivo half-life of FT Blue is approximately four hours (Bending et al., 2018). The shift in emission spectrum is driven by irreversible chromophore oxidation and double bond formation that is probabilistic and heavily dependent on temperature (Subach et al., 2009). Subach and colleagues made three Fluorescent Timer protein (FT Fast, FT Medium, FT Slow) that display different maturation rates from blue to red. FT Fast was selected to allow for a short time window of FT Blue detection, granting the system the sensitivity to distinguish between TCR signals that are only a few hours apart. Nr4a3 was selected through a multidimensional transcriptomic analysis (Ono et al., 2014). In short, transcriptional datasets representing in vivo TCR signalling (thymocytes undergoing selection) and in vitro signalling (αCD3 stimulation of peripheral $CD4^+$ T cells) were compared to transcriptome of resting T cells. Although Nr4a1 was highly correlated with in vivo and in vitro TCR signalling, the fold change of Nr4a3 was higher. This may be due to baseline levels of Nr4a1 expression in peripheral T cells at steady state due to tonic signalling. It was also noted that Nr4a3 may be an ideal target to trace the dynamics of TCR signalling because mRNA levels peak within two hours before returning almost to baseline by 24 hours (Bending et al., 2018).

The short-lived FT Blue form of the reporter provides finer temporal resolution than GFP reporters. FT Blue and FT Red have distinct excitation emission spectra (403/466 and 583/606 respectively). Using a BD LSR Fortessa X20 instrument, FT Blue can be excited by the 405nm laser and detected off the 450/50 filter, FT Red can be excited by the 561nm laser and detected off the 610/20 filter. This methodology allows single-cell discrimination between cells that have received a recent TCR signal (past few hours), a historic TCR signal (past few days), or both (persistent signalling). The Nr4a3 Tocky model has computational applications. The 'timer angle' can be calculated by plotting FT Red vs FT Blue and calculating the angle of the line between the origin of the graph and the data point against the FT Blue axis. Median timer angle can be used as an approximation of how frequently a population of T cells is receiving a TCR signal (Bending et al., 2018). Similar to Nur77 GFP, Nr4a3 Tocky was unaffected by IL-2. CD28 co-stimulation increased the brightness of the reporter in combination with TCR stimulation but was not able to induce reporter expression alone, confirming the absolute dependency on the TCR for reporter expression.

The Nr4a3 Tocky mice have been used to track the dynamics of TCR signalling events in models of multiple sclerosis (Bending et al., 2018), cancer, and tolerance (Elliot et al., 2021). We have previously used Nr4a3 Tocky mice to investigate dynamic tuning of TCR signalling thresholds, utilising the high time resolution to distinguish TCR responses to different immunisations only a day apart (Elliot et al., 2021).

We have previously compared the Nur77 GFP and Nr4a3 Tocky reporters. We have found that Nr4a3 Tocky, but not Nur77 GFP, is sensitive to inhibition of Calcineurin by Cyclosporine A (Jennings and Elliot et al., 2020). Accordingly, we found that endogenous transcripts of Nr4a2 and Nr4a3 were more sensitive than Nr4a1 to Cyclosporine A. In contrast, blockade of the ERK signalling pathway with a specific inhibitor of MEK reduced expression of all Nr4a family members to a similar extent. We mined a ChIP-seq dataset from a study conducted on a constitutively

active form of NFAT1 that cannot bind to AP1 (Martinez et al., 2015). We found that constitutively active NFAT1 increased mRNA expression of Nr4a2 and Nr4a3 but not Nr4a1, demonstrating that NFAT signalling alone is both necessary and sufficient for expression of Nr4a2/3 following TCR stimulation. By modulating the strength of TCR stimulation by titrating αCD3 or the length of TCR signalling by blocking kinase activity with an inhibitor, Nur77 GFP was more sensitive to lower strength and duration of TCR signal.

In order to utilise both the dynamic nature and time sensitivity of Fluorescent Timer and the likely increased sensitivity of Nr4a1 over Nr4a3 to TCR signals, the Nur77 Tempo mouse was developed using the 'piggybac-on-BAC' approach. Briefly, a cassette containing the FT Fast gene was inserted upstream of exon 2 of the Nr4a1 gene in the RP24-366J14 bacterial artificial chromosome (BAC) (Figure 3.1). The BAC used is identical to the one used by Kristin Hogquist's lab to develop Nur77 GFP mice. The construct was injected into single cell stage fertilised eggs, piggyBac Transposase facilitates random integration of the transgene into the chromosomal DNA. Assuming the transgene is located in an open chromatin site, this allows for expression of FT Fast under the control of Nr4a1 regulatory regions. This mirrors the development of the Nr4a3 Tocky mouse (Bending 2018).

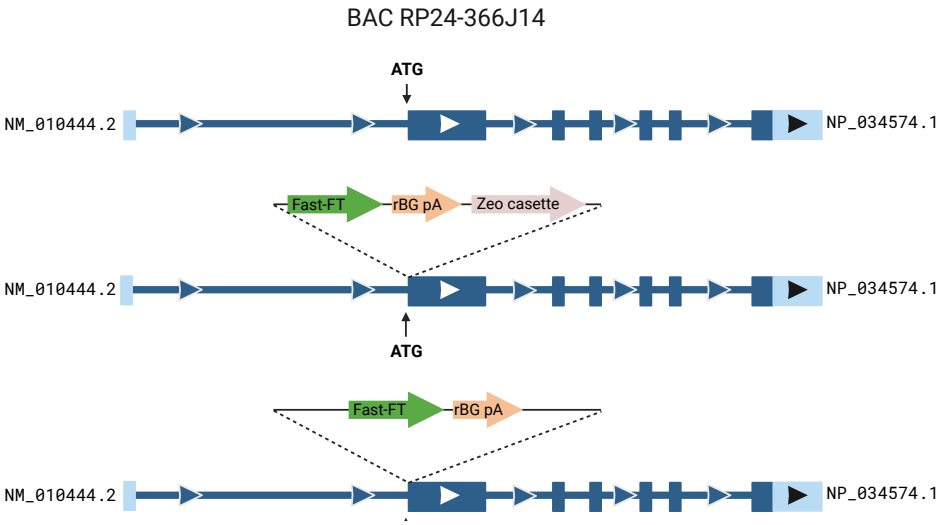

Figure 3.1. ***Schematic detailing the bacterial artificial chromosome strategy for generating Nur77 Tempo mice****. Further details in Materials and Methods.*

3.2 RESULTS

3.2.1 Development of Nur77 Tempo

Pups were screened by PCR for expression of FT Fast transgene to identify founder lines, 4 out of 8 founder lines were determined to carry germ line transmission and termed N7TA-D. Founder lines were mated to C57BL/6J mice and the progeny were genotyped by end point PCR and gel electrophoresis for expression of FT Fast. Bands of the expected 382bp size were identified in progeny of all 4 founder lines (Figure 3.2.A), these individuals were taken forward for phenotypic screening.

3.2.2 Validation of Nur77 Tempo

Splenocytes from the *FT Fast*$^{+}$ individuals were stimulated *in vitro* with 1 µg/ml αCD3 stimulating antibody for 4 hours before analysis by flow cytometry. Live single CD4^{+} TCRβ^{+} cells were gated on for quantification of FT Blue expression, excited by the 405nm laser and detected off the 450/50 filter nm (Figure 3.2.B). As compared to a wild-type control, we noted a bright signal off the 450/50 filter nm in *FT Fast*$^{+}$ individuals, indicative of high FT Blue expression. However, we also noted that the brightness was variable between individuals. It is possible that multiple copies of the transgene are inserted by transposase, we therefore hypothesised that the variable brightness may be due to variable copy number between individuals. We analysed genomic DNA by RT-PCR, using *Il2ra* as a double copy housekeeping gene. There was a cluster of individuals with a 2^ΔCT value of ~0.7 that are likely single-copy variants, whilst some individuals had higher 2^ΔCT values likely due to two or four copies of the transgene. Increased copy number was tightly correlated with FT Blue median fluorescent intensity (MFI) (Figure 3.2.C).

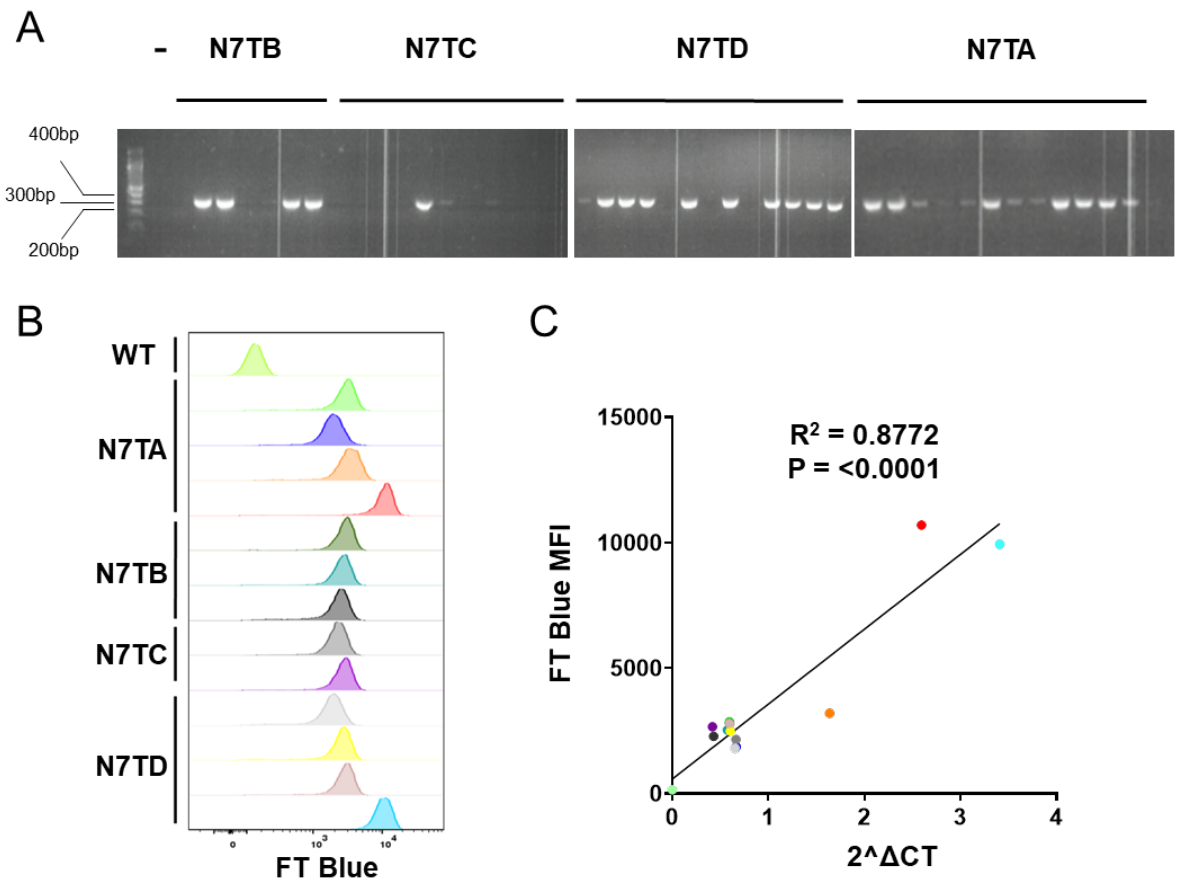

Figure 3.2. ***Screening of Nur77 Tempo founder lines for successful transgene insertion by PCR and flow cytometry.*** *A) Genomic DNA extracted from ear punch biopsies of progeny form indicated Nur77 Tempo founder lines. Product from end-point PCR amplification of genomic DNA with primers specific for FT Fast separated by DNA gel electrophoresis. B) Splenocytes of FT Fast+ progeny from Nur77 Tempo founder mice stimulated in vitro with 1µg/ml αCD3 for four hours and analysed by flow cytometry for expression of FT Blue. Population is gated on Live CD4+ TCRβ+ singlets. C) Genomic DNA extracted from ear punch biopsies of FT Fast+ mice amplified by RT-PCR. 2^ΔCT values are calculated and correlated with FT Blue MFI of CD4+ T cells as determined by flow cytometry. R2 value indicated is Pearsons's correlation coefficient P value is Pearson's correlation significance test.*

We compared the Fluorescent Timer profiles of a single-copy and a four-copy variant from the same litter. We noted that many splenic $CD4^+$ $TCR\beta^+$ cells, in agreement with work performed in Nur77 GFP mice (Moran et al., 2011), were FT Red^+ indicating a history of *Nr4a1* expression (Figure 3.3.A). This is likely reflective of the tonic signalling that T cells receive in the lymphoid environment to promote their survival and priming (Myers et al., 2017). The frequency and brightness of FT Red expression was higher in the four-copy variant and significant expression of FT Blue could be observed, which was absent in the single-copy variant (Figure 3.3.A). This suggests more frequent triggering of *FT Fast* expression in higher copy variants, likely due to decreased threshold of required TCR signal strength. We have previously observed that when Nur77 GFP and Nr4a3 Tocky are co-expressed, there is a partial quenching effect that causes a reduction in FT Blue MFI as the regulatory regions of both transgenes presumably compete for binding to a limited pool of nuclear transcription factors within each cell (Jennings and Elliot et al., 2020). Variance in copy number effects the stoichiometry of *FT Fast* transgene regulatory elements and regulatory elements of other genes controlled by the same transcription factors, thus impacting the likelihood that signal threshold for *FT Fast* expression will be crossed.

In splenic $TCR\beta^-$ $CD19^+$ B Cells, we saw a similar, but more pronounced, difference in Fluorescent Timer profile between the single-copy and four-copy variant (Figure 3.3.B). However, in contrast to what we observed in CD4 T cells, there was a significant proportion of cells that did not express FT Blue in response to stimulation, 1µg/ml αIgM, in the single-copy variant. These findings indicate that higher copy number may be more important for detecting B cell receptor (BCR) signals over TCR signals. In order to avoid variable brightness between individuals of experimental groups, going forward we genotyped mice by RT-PCR and selected only single-copy variants unless otherwise mentioned.

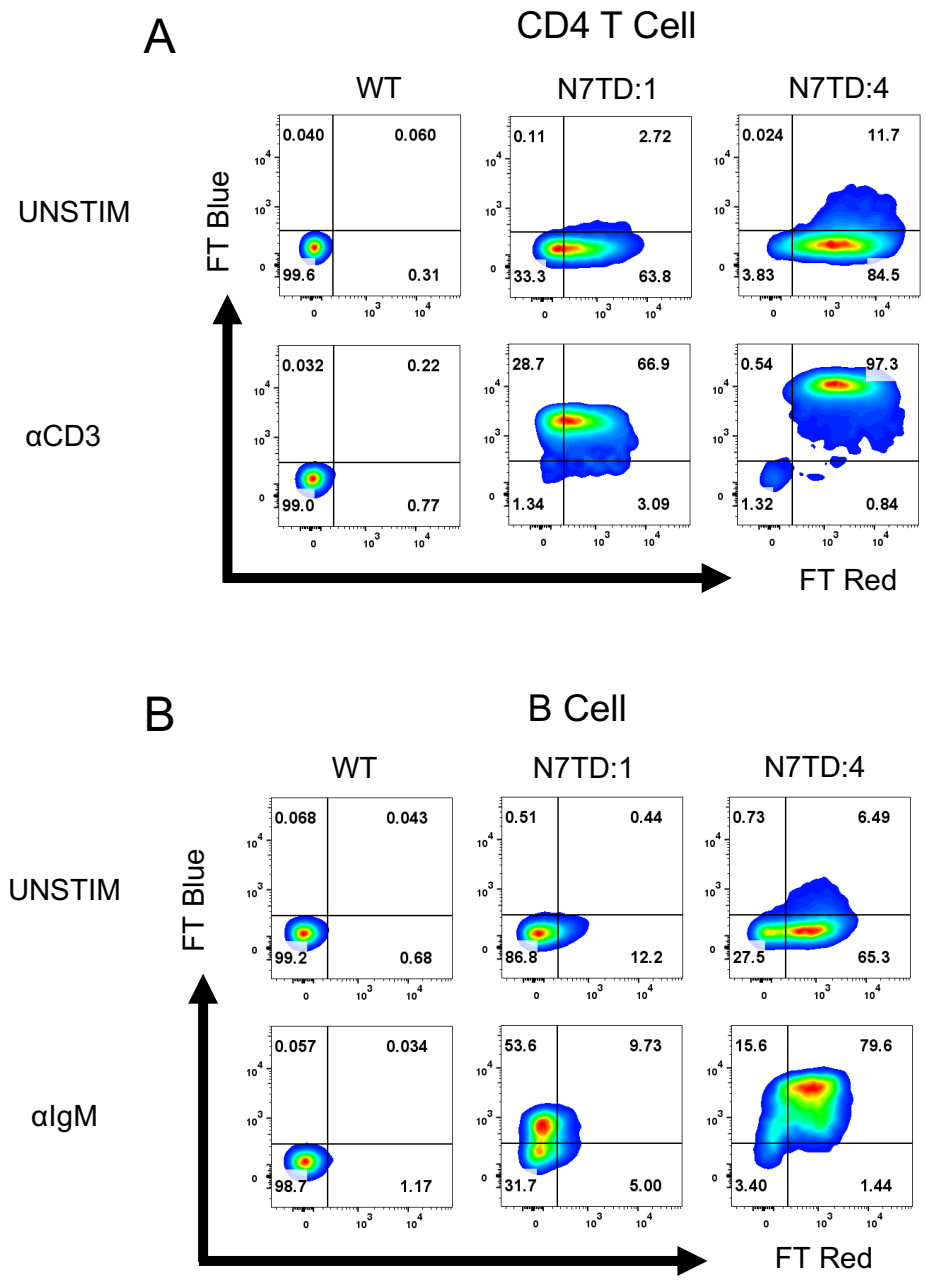

Figure 3.3 ***FT Blue and FT Red expression in steady state CD4 T cells and B cells in Nur77 Tempo single copy and four copy mice*** *A) Flow cytometry analysis of FT expression in the spleen gated on live CD4+ TCRβ+ singlets (A) or live CD19+ TCRβ- singlets (B) with or without four hour 1μg/ml αIgM stimulation in wild-type, single copy variant (N7TD:1), or four copy variant (N7TD:4).*

3.2.3 Comparison of Nur77 Tempo and Nr4a3 Tocky

Following our work validating that the Nur77 Tempo mouse expresses FT Fast protein in response to TCR stimulation we set out to characterise its sensitivity. Our previous work has shown that the Nur77 GFP mouse is more sensitive to lower strength or shorter duration TCR signals than the Nr4a3 Tocky mouse (Jennings and Elliot et al., 2020). However, these two lines were created using different BAC strategies, therefore it is not possible to determine whether this difference in sensitivity is due to BAC strategy or a true difference in the regulation of *Nr4a1* and *Nr4a3*. The design of Nur77 Tempo very closely mirrors that of Nr4a3 Tocky allowing for a more direct comparison. Developing thymocytes are subject to different strengths of TCR signals that mediate their progression to mature T cells (Gascoigne et al., 2016). $CD4^-$ $CD8^-$ double negative (DN) cells enter the thymic medulla and progress through 4 DN stages characterised by CD25 and CD44 expression. DN thymocytes then migrate to the subcapsular region and rearrange the TCRβ chain. This is followed by the double positive (DP) stage as cells upregulate CD4 and CD8 and re-arrange the TCRα chain. Here, cells that express a functional TCR will receive low strength positive selection signals and increase their surface TCR expression. Depending on whether developing cells bind peptide loaded MHC I or MHC II with higher affinity, thymocytes downregulate CD4 or CD8 respectively to enter the single positive (SP) stage and migrate to the medulla where negative selection takes place. Cells that bind with high affinity to self pMHC will enter an apoptotic programme to negatively select autoreactive T cells. In SP4 thymocytes, high affinity interaction with self pMHC, along with soluble factors such as IL-2 and TGFβ, can induce regulatory T cell development, marked by high expression of CD25.

We euthanised weaned mice and dissected the thymus for analysis by flow cytometry. Here, we can gate on different subsets (DP TCRβ low, DP TCRβ high, SP8, SP4 CD25 low, SP4 CD25 high) that represent developmental stages at which thymocytes receive increasing strengths of TCR

signal (Figure 3.4.A). We compared the Fluorescent Timer profiles of these subsets between Nur77 Tempo and Nr4a3 Tocky mice to determine the relative sensitivity of the two reporters to selection signals of varying strength (Figure 3.4.B). We observed significant FT expression in SP4 $CD25^+$ developing T_{REG} cells in both Nur77 Tempo and Nr4a3 Tocky mice, however FT expression was minimal in other subsets in Nr4a3 Tocky mice. In contrast, Nur77 Tempo mice demonstrated significant FT expression from the DP TCRβ high stage (Figure 3.4.B) (Figure 3.5.E). This highlights that expression of *Nr4a1* is more sensitive to weaker TCR signals than *Nr4a3*, such that the Nur77 Tempo reporter is able to detect low strength positive selection signals. Notably, expression of both FT Blue (Figure 3.5.A&C) and FT Red (Figure 3.5.B&D) was observed during positive selection of thymocytes. This contrasts the FT Red^+ FT $Blue^-$ profile of splenic $CD4^+$ T cells (Figure 3.3.A), highlighting a higher frequency of positive selection TCR signals over homeostatic TCR signals that occur peripherally.

We next sought to determine whether increased sensitivity to weak TCR signals was present in mature T cells, or whether this phenomenon was restricted to development. We stimulated bulk Nur77 Tempo and Nr4a3 Tocky splenocytes with a long dose titration of αCD3 for four hours and then analysed by flow cytometry to determine FT Blue expression in CD4 (Figure 3.6.A) and CD8 (Figure 3.6.B) T cells. We noted that Nur77 Tempo cells had a higher background expression of FT Blue, so we normalised the data (as described in the figure legend) to plot the dynamic range of FT $Blue^+$ frequency across the cell populations. We found a significantly higher frequency of FT Blue expression in response to lower concentrations of αCD3 in the Nur77 Tempo mice, confirming increased sensitivity to weaker signals.

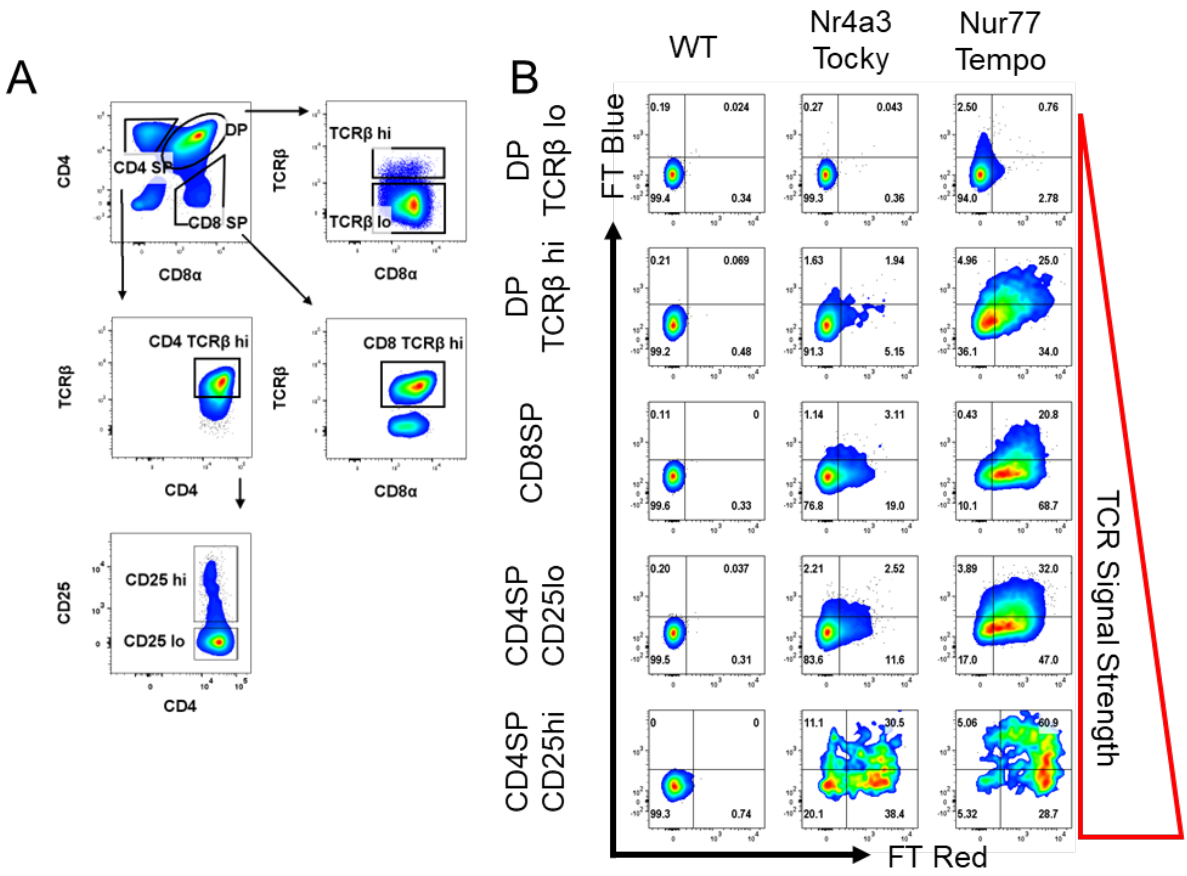

Figure 3.4. ***Expression of FT in developing thymocytes of Nur77 Tempo and Nr4a3 Tocky mice*** *A) Gating strategy for populations within the thymus that relate to different developmental stages. Pre-gated on live singlets. B) Flow cytometry analysis of FT expression in thymic populations of wild-type, Nur77 Tempo, or Nr4a3 Tocky mice.*

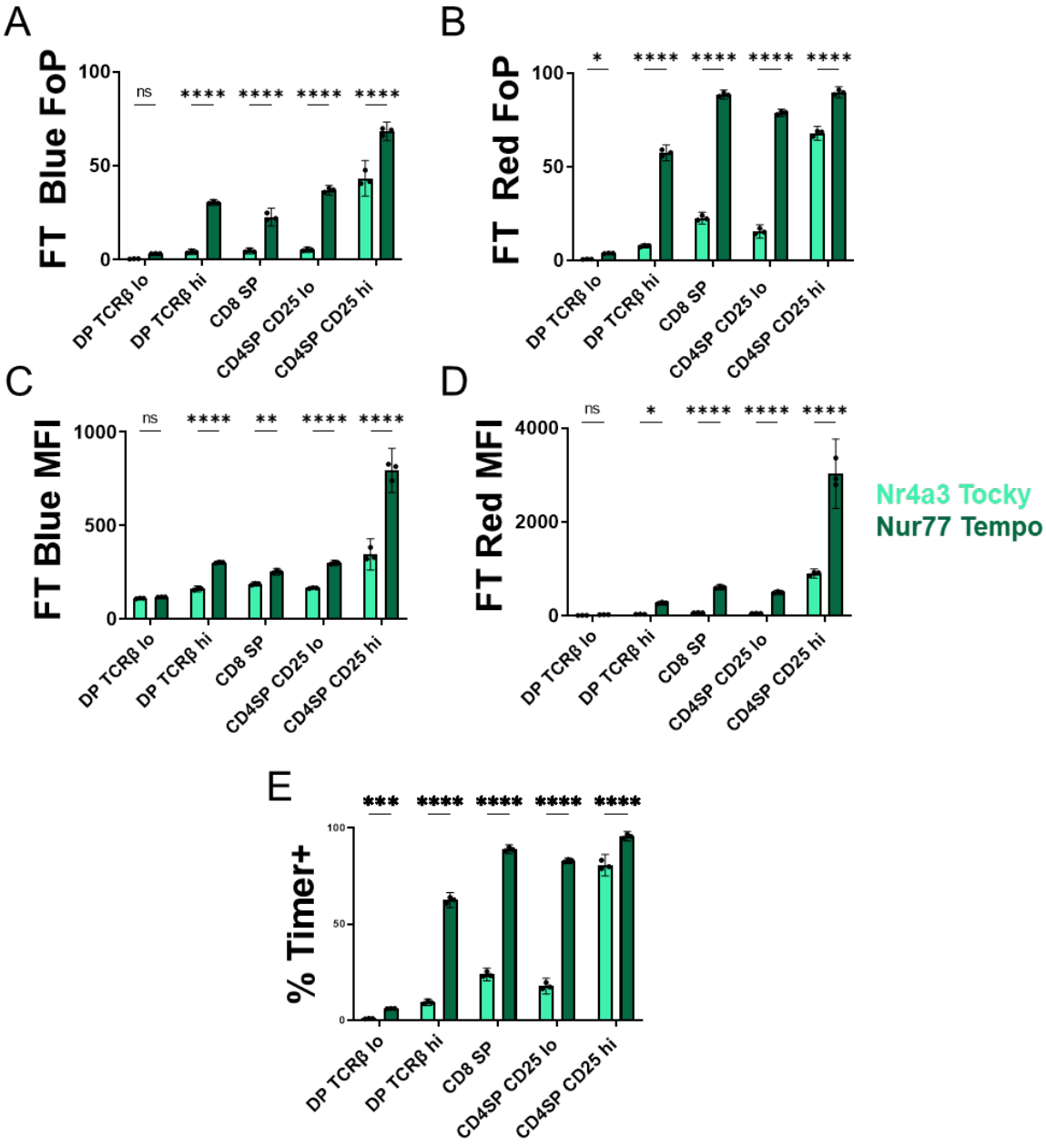

Figure 3.5. ***Expression of FT in developing thymocytes in Nur77 Tempo and Nr4a3 Tocky mice****. Quantification of analysis from figure 3.4B. Statistical test shown is ordinary two-way ANOVA, Šídák's multiple comparisons test with single pooled variance. *P ≤ 0.05, **P ≤ 0.01, ***P ≤ 0.001, ****P ≤ 0.0001. N=3. Error bars indicate mean and SEM.*

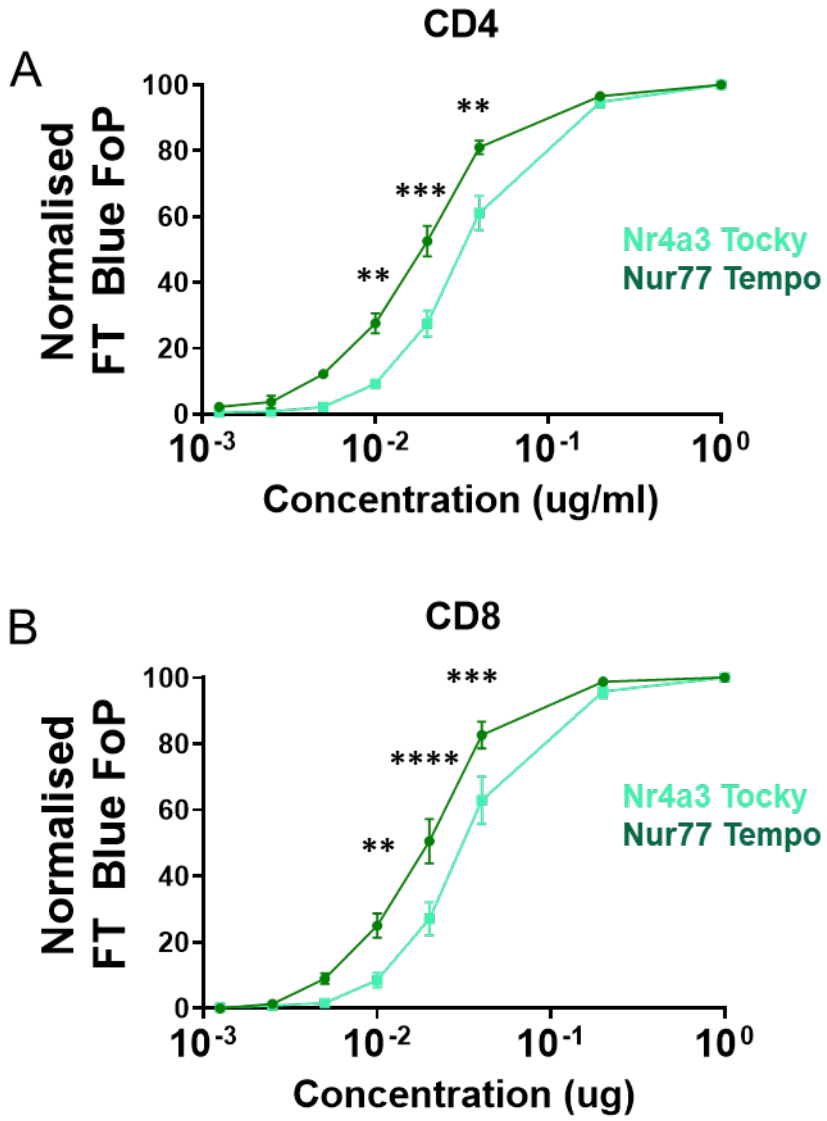

Figure 3.6. ***Expression of FT Blue following in vitro stimulation of splenocytes with a dose titration of αCD3 in Nur77 Tempo and Nr4a3 Tocky mice.*** *Flow cytometry analysis of FT Blue expression in splenic live CD4+ TCRβ+ singlets (A) or live CD8+ TCRβ+ singlets (B) stimulated with a dose titration of αCD3 for four hours. Data normalised as* $Normalised\ MFI = 100 * ((MFI(X) - MFI(minimum)) / (MFI(maximum) - MFI(minimum)))$. *Statistical test shown is ordinary two-way ANOVA, Šídák's multiple comparisons test with single pooled variance. *P ≤ 0.05, **P ≤ 0.01, ***P ≤ 0.001, ****P ≤ 0.0001. N=3. Error bars indicate mean and SEM.*

3.2.4 Differential Regulation of Nur77 Tempo and Nr4a3 Tocky

We hypothesised that the difference in sensitivity between the two reporters may be due to a difference in their regulation by different pathways that act downstream of the TCR. Indeed, our previous work has shown that Nr4a3 Tocky is sensitive to inhibition of the Calcineurin-NFAT pathway whilst the Nur77 GFP reporter is not (Jennings and Elliot et al., 2020). To interrogate differential pathway sensitivity, we stimulated bulk splenocytes from Nr4a3 Tocky and Nur7-Tempo mice with 1µg/ml of αCD3 for four hours following 30-minute pre-treatment with a panel of small molecule inhibitors (PP2 Src family kinase, Cyclosporin (CsA) Calcineurin-NFAT, PD 0325901 MEK-Fos, GO 6983 PKC-NFκB, SP600125 JNK-cJUN, Ly 294002-NFκB/mTORC1) or DMSO vehicle control (Figure 3.7) (Table 3.1). Following stimulation FT expression was analysed by flow cytometry in $CD4^+$ and $CD8^+$ T cells.

Name	**Target**
DMSO	Vehicle Control
PP2	Src family kinase
CsA	Calcineurin - NFAT
Ly 294002	PI3K - Akt
PD 0325901	MEK - ERK
SP 600125	JNK - cJun
GO 6983	PKC - NFκB

Figure 3.1. ***Table indicates small molecule inhibitors and their targets used in blocking experiments*** *(molecular target – primarily affected transcription factor).*

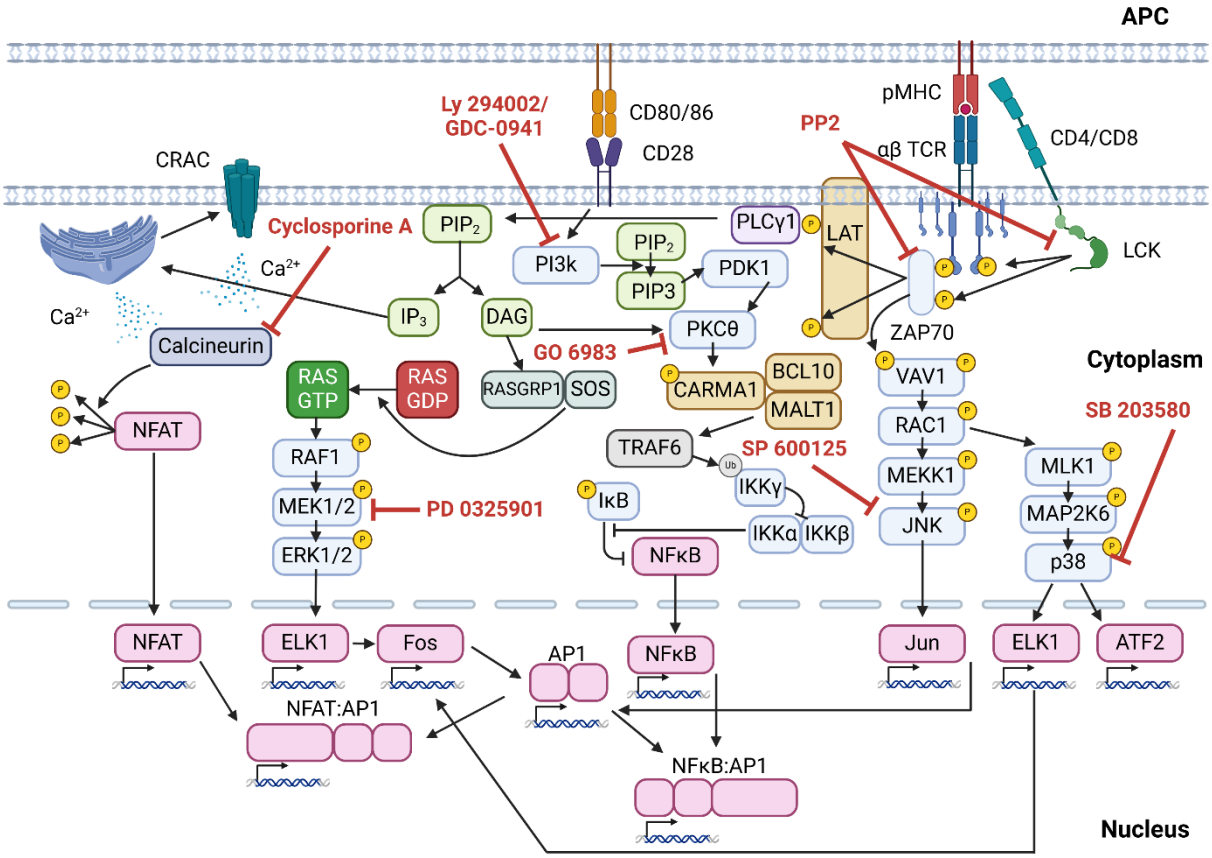

Figure 3.7. ***Schematic indicates molecular targets of small molecule inhibitors****. Created in www.biorender.com.*

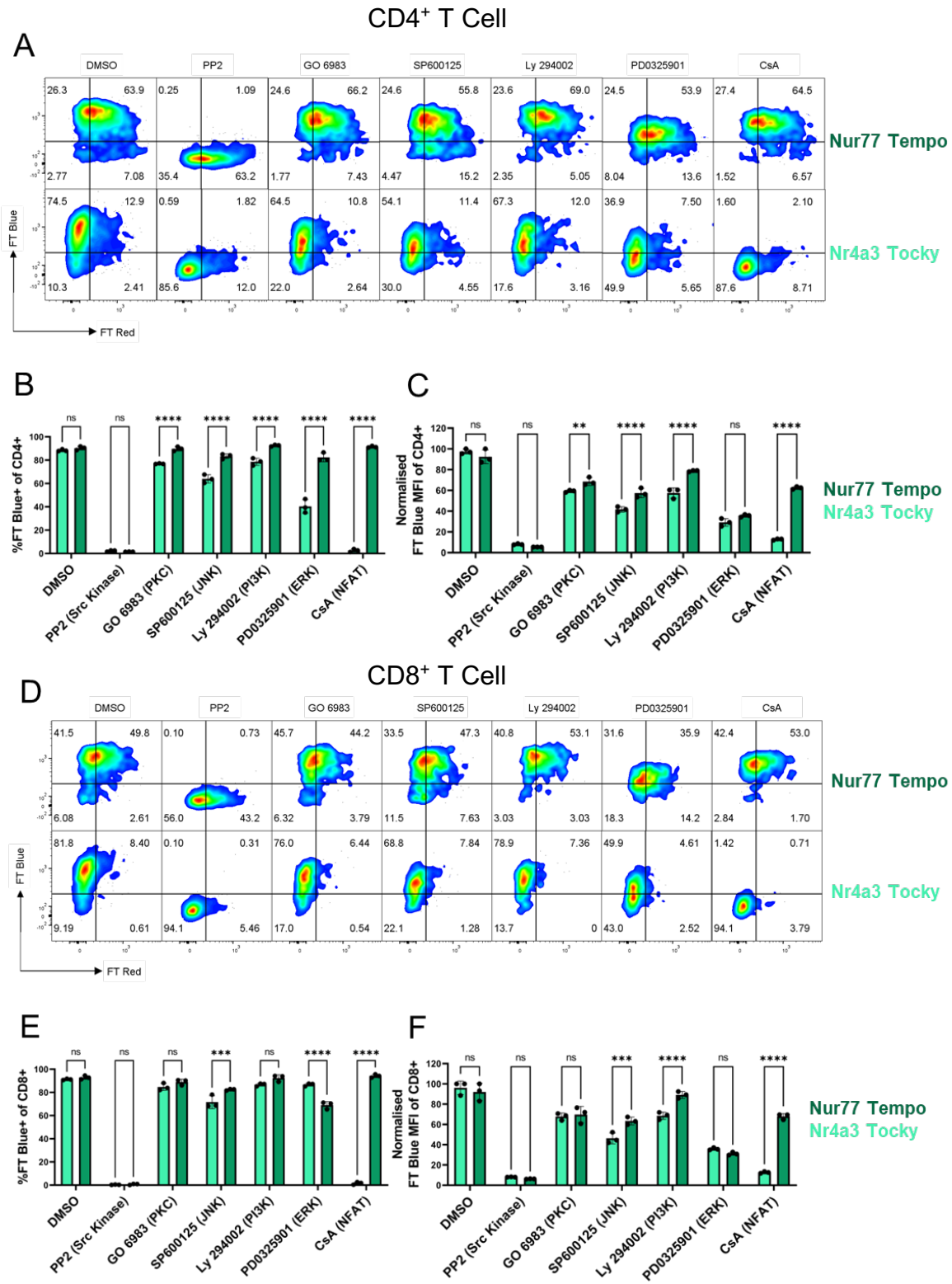

Figure 3.8 ***Contribution of TCR signalling pathways to Nur77 Tempo and Nr4a3 Tocky reporter expression investigated using small molecule inhibitors.*** *A&D) Splenocytes of Nur77 Tempo and Nr4a3 Tocky mice were stimulated in vitro with 1 µg/ml αCD3 for four hours in the presence of small molecule inhibitors (0.1% DMSO control, 20 µM PP2, 400 nM GO 6983, 10 µM SP600125, 200 nM Ly 294002, 5 µM PD0325901, 1 µM CsA). FT expression was analysed by flow cytometry, population gated on live CD4+ TCRβ+ singlets (A) or live CD8α+ TCRβ+ singlets. B&C) Quantification of (A) E&F) Quantification of (D). Data normalised in (C&F) as* $Normalised\ MFI = 100 * ((MFI(X) - MFI(minimum)) / (MFI(maximum) - MFI(minimum)))$. *Statistical test shown is ordinary two-way ANOVA, Šídák's multiple comparisons test with single pooled variance. *P ≤ 0.05, **P ≤ 0.01, ***P ≤ 0.001, ****P ≤ 0.0001. N=3/group. Error bars indicate mean and SEM.*

In $CD4^+$ T cells we recapitulated previous findings (Jennings and Elliot et al., 2020) showing that *Nr4a3* is much more sensitive to blockade of NFAT signalling than *Nr4a1* (Figure 3.8.A). Nr4a3 Tocky mice tended to show a much more significant decrease in the frequency of cells expressing FT Blue as compared to Nur77 Tempo (Figure 3.8.B), this is most notable with blockade of the ERK pathway by PD0325901, despite showing similar decreases in MFI (Figure 3.8.C). Therefore, blockade of NFAT-independent signalling pathways appears to drive a quantitative decrease in the proportion of cells that cross the signalling threshold to express *Nr4a3*. Comparatively, blockade of these pathways drives a qualitative decrease in *Nr4a1* expression levels. It has been previously noted that the Nr4a3 Tocky reporter displays digital, switch-like behaviour (Elliot et al., 2021), whilst the brightness of Nur77 GFP reporter is related to TCR signal strength (Moran et al., 2011). We observed similar findings in $CD8^+$ T cells (Figure 3.8.D-F), however the drop in FT $Blue^+$ frequency was less pronounced in Nr4a3 Tocky $CD8^+$ T cells compared to $CD4^+$ T cells. Surprisingly Nur77 Tempo showed a greater decrease in FT $Blue^+$ frequency than Nr4a3 Tocky following inhibition of the ERK pathway, highlighting slightly differential regulation between $CD4^+$ and $CD8^+$ T cells.

These results demonstrate that *Nr4a3* expression is partially sensitive to multiple pathways downstream of the TCR but absolute dependency on NFAT signalling. *Nr4a1* expression shows a similar partial sensitivity to multiple pathways, but without a complete sensitivity to any single pathway. Furthermore, particularly in $CD4^+$ T cells, FT brightness may be more graded in response to differences in TCR signal strength in Nur77 Tempo mice.

In order to fully utilise Nur77 Tempo mice for tracking TCR signalling in disease models, we thought it pertinent to understand the absolute dependencies for *Nr4a1* expression. We therefore designed a new screening panel of inhibitors, adding a p38 inhibitor SB 203580 and substituting Ly 294002 for a different PI3k inhibitor, GDC-0941, based on reports of an effect on *Nr4a1*

expression in human T cells (Ashouri & Weiss, 2017) (Table 3.2). Bulk splenocytes were pre-treated with single inhibitors, or in combinations scaling to all six, then stimulated with 1 µg/ml αCD3 for four hours before analysis of FT Blue and CD69 expression in $CD8^+$ T cells. The data is plotted as a 96 well plate-plan of the different inhibitor combinations, with relative frequencies of FT $Blue^+$ and $CD69^+$ CD8 T cells displayed as a heatmap (Figure 3.9).

Name	**Target**
DMSO	Vehicle Control
PP2	Src family kinase
CsA	Calcineurin - NFAT
GDC-0941	PI3K - Akt
PD 0325901	MEK - ERK
SP 600125	JNK - cJun
GO 6983	PKC - NFκB
SB 203580	P38 – cFos

Figure 3.2. ***Table indicates small molecule inhibitors and their targets used in blocking experiments*** *(molecular target – primarily affected transcription factor).*

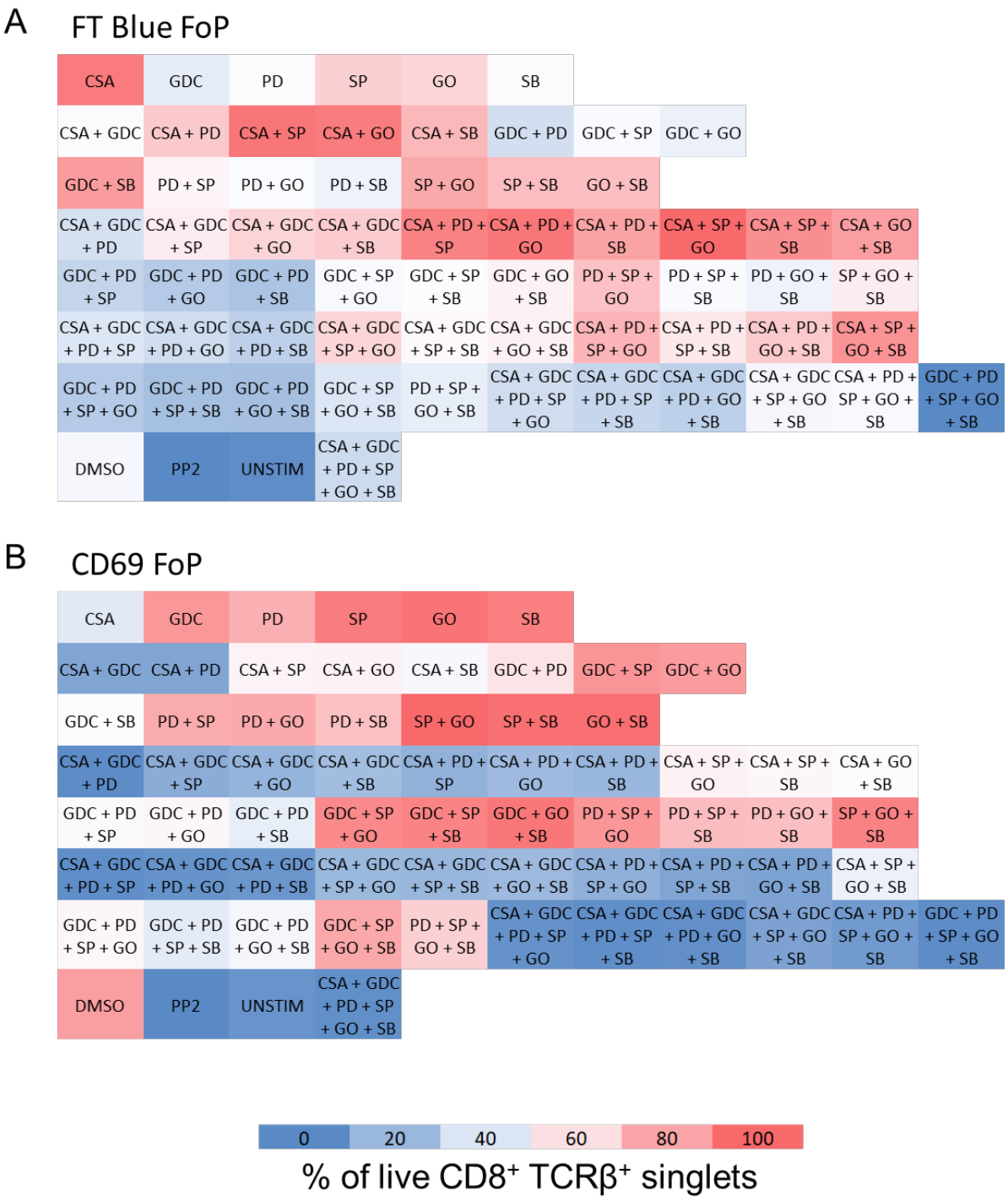

Figure 3.9. ***Nur77 Tempo FT expression is only abrogated by co-blockade of all NFAT independent signalling pathways.*** *Splenocytes of Nur77 Tempo mice were pre-treated with indicated combinations of small molecule inhibitors at the following concentrations (0.1% DMSO, 1 μM CsA, 0.1 μM PD 0325901, 1 μM SP 600125, 50 nM GO 6983, 1 μM SB 203580, 0.5 μM GDC 0941, 20 μM PP2). Flow cytometry analysis of FT Blue frequency (A) and CD69 frequency (B) gated on live CD8⁺ TCRβ⁺ singlets. Heatmap generated on median values from N=3(FT Blue)/4(CD69)*

Firstly, we noted that we did not achieve full activation of $CD8^+$ T cells (Figure 3.10.A). This is likely due to the comparatively lower cell number as compared to the previous inhibitor screen, owing to the larger number of experimental conditions. This may have reduced the probability that any given $CD8^+$ T cell was in contact with an APC necessary for activation of the TCR. We found a partial effect of inhibition of PI3K and ERK pathways on the frequency of FT $Blue^+$ cells and FT Blue brightness, which was compounded when both inhibitors were used (Figure 3.9.A) (Figure 3.10A-C). FT Blue expression was further decreased when inhibitors against PKC, JNK, p38 pathways were added, such that combination of all five mirrored complete blockade of TCR proximal kinase activity with PP2 (Figure 3.10.A-C). Surprisingly, blockade of the NFAT pathway slightly increased frequency (Figure 3.10.A) and brightness (Figure 3.10.B) of FT Blue. This is unlikely to be due to ineffective blockade of the NFAT pathway, because CD69 expression was markedly reduced (Figure 3.9.B) (Figure 3.10.A&D). Furthermore, when CsA was added to the other five inhibitors, FT Blue expression was increased such that treatment with all six inhibitors did not reduce FT Blue frequency enough to pass one way ANOVA statistical testing (Figure 3.10.B). In contrast CsA treatment does reduce CD69 expression when used in isolation or in combination with the other inhibitors (Figure 3.10.D). This finding contrasts our previous data that showed a small drop in FT Blue MFI followed NFAT pathway blockade (Figure 3.8). This discrepancy may be due to the large difference in cell density between experiments, possibly mediating its negative effect on FT Blue expression indirectly via APCs. A CsA mediated increase in $CD8^+$ T cell *Nr4a1* expression has been noted by others in a recent pre-print (Wither et al., 2023), where the authors suggest NFAT-AP:1 site re-direction as a possible mechanism.

Taken together, our small molecule inhibitor studies show that FT expression is dependent on NFAT signalling in Nr4a3 Tocky mice and NFAT-independent signalling in Nur77 Tempo mice.

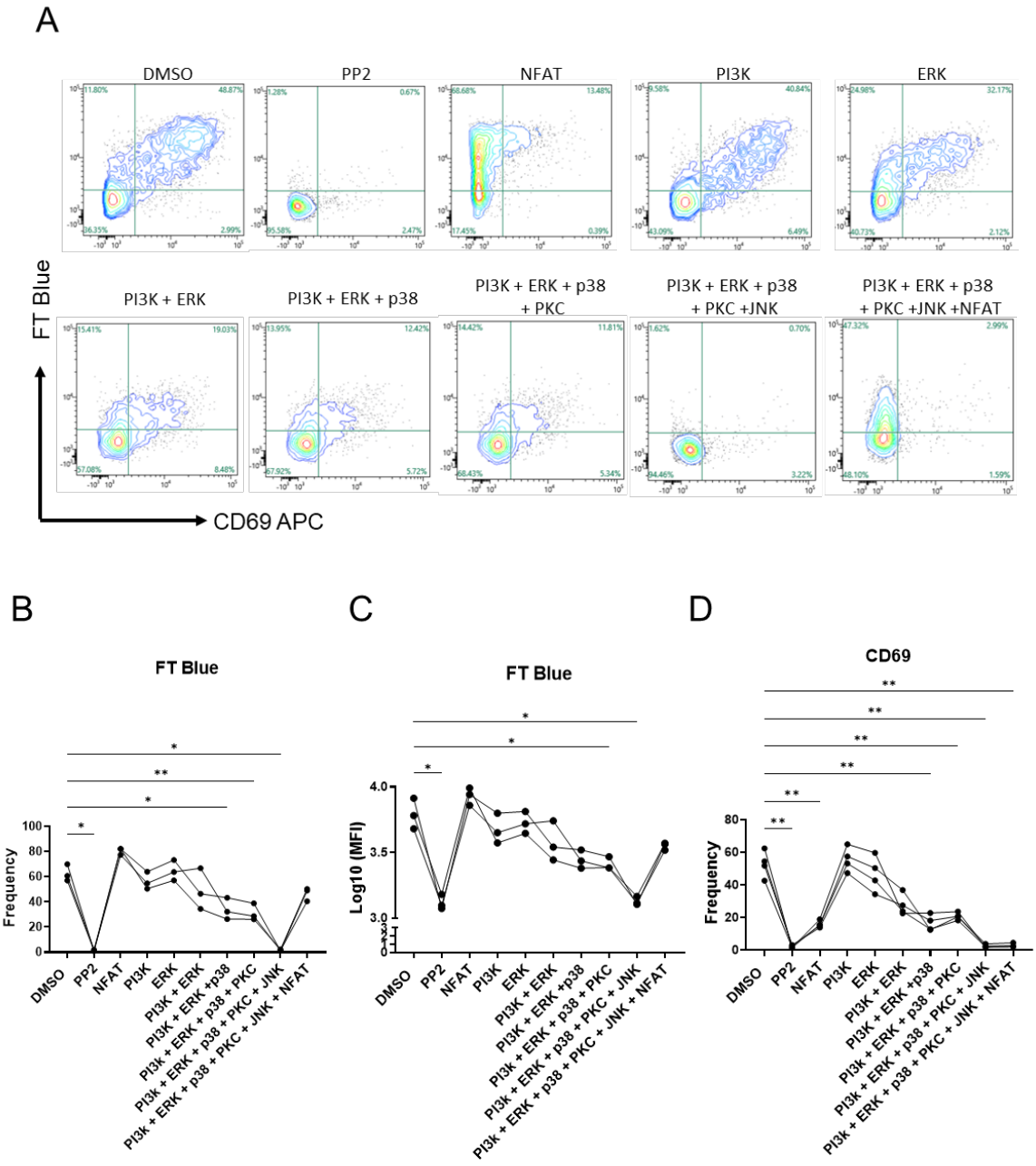

Figure 3.10. ***Response to in vitro stimulation in the presence of selected small molecule inhibitor combinations.*** *A) Splenocytes of Nur77 Tempo mice were pre-treated for thirty minutes with indicated combinations of small molecule inhibitors at the following concentrations (0.1% DMSO, 1 μM CsA, 0.1 μM PD 0325901, 1 μM SP 600125, 50 nM GO 6983, 1 μM SB 203580, 0.5 μM GDC 0941, 20 μM PP2). Splenocytes were stimulated with 1 μg/ml αCD3 for six hours before analysis by flow cytometry. Plots are annotated with pathways that are blocked by small molecule inhibitor combinations. Flow cytometry analysis of FT Blue and CD69 representative plots are shown. Gated on live CD8⁺ TCRβ⁺ singlets B) Quantification of FT Blue frequency. C) Quantification of CD69 frequency. D) Quantification of FT Blue Log10 MFI. Statistical test shown is one-way ANOVA with Geisser-Greenhouse correction. Dunnett's multiple comparison test, each group mean is compared to DMSO control. *P ≤ 0.05, **P ≤ 0.01, ***P ≤ 0.001, ****P ≤ 0.0001. N=3(FT Blue)/4(CD69).*

3.2.5 Characterisation of Steady State TCR Signalling in Peripheral Tissues of Nur77 Tempo Mice

We have shown that the Nur77 Tempo model is a highly sensitive reporter of TCR signalling *in vitro* (Figure 3.3) (Figure 3.6), during development (Figure 3.4), and steady state tonic signalling (Figure 3.3). We next sought to determine whether steady state signalling could be detected in peripheral tissues. We processed spleen, lung, and liver from Nur77 Tempo mice for analysis by flow

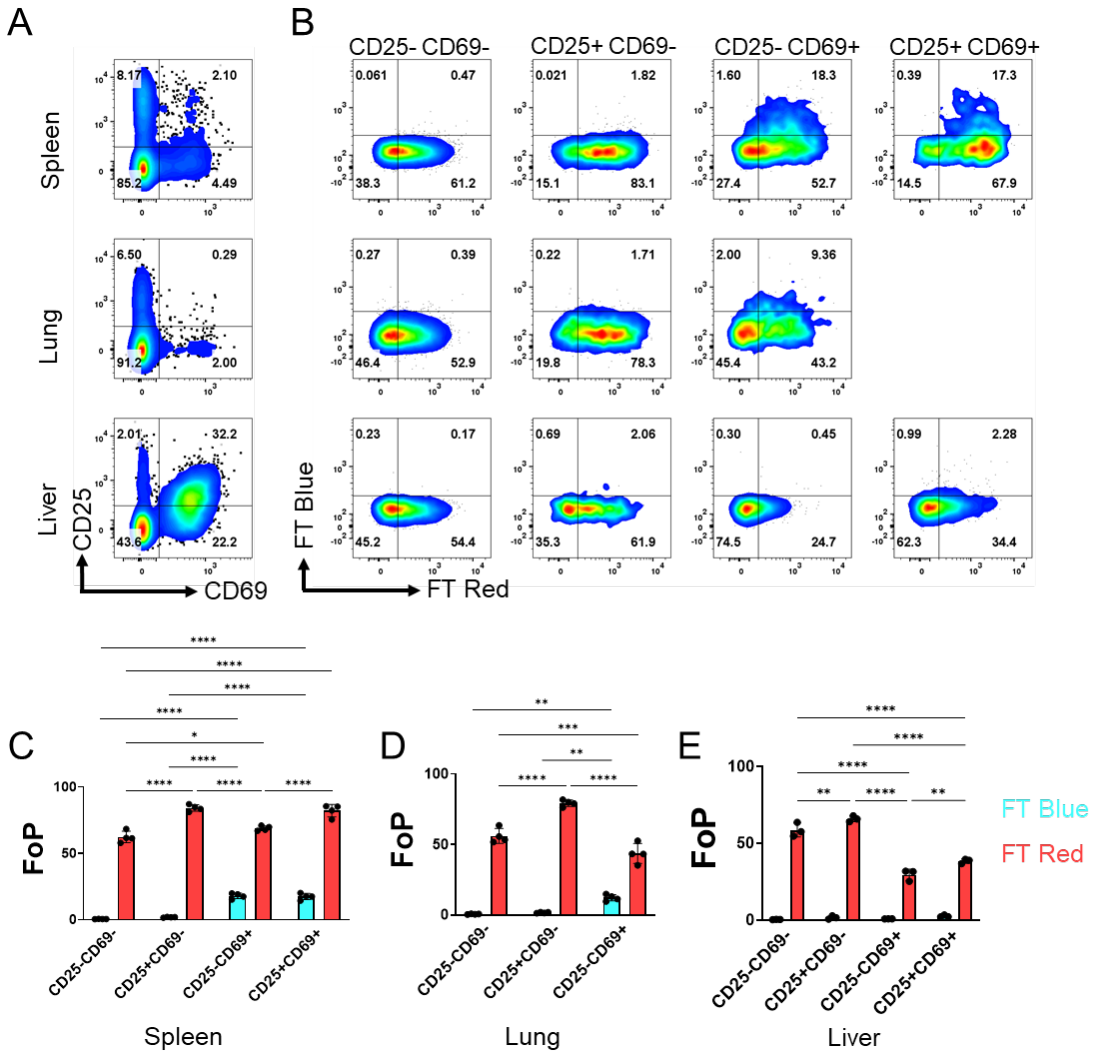

Figure 3.11. ***Analysis of how FT expression relates to expression of CD69 and CD25 in the spleen lung and liver of Nur77 Tempo mice.*** *A) Flow cytometry analysis of CD25 and CD69 in spleen lung and liver tissue of Nur77 Tempo mice gated on live CD4⁺ TCRβ⁺ singlets. B) Flow cytometry analysis of FT expression in populations gated in (A). C-E) Quantification of (B). Statistical test shown is ordinary two-way ANOVA, Šídák's multiple comparisons test with single pooled variance. *P ≤ 0.05, **P ≤ 0.01, ***P ≤ 0.001, ****P ≤ 0.0001. N=3. Error bars indicate mean and SEM. N=3*

cytometry. We stained for CD25 to identify T_{REG} cells and CD69 as a marker of early activation in the spleen and tissue residency in the lung and liver (Figure 3.11.A).

T_{REG} cells express TCRs that recognise self-antigen with high affinity, driving stronger affinity interactions with self-peptide MHC. Consequently, in all tissues, expression of CD25 was associated with brighter expression of FT Red (Figure 3.11.B&C). In lymphoid tissue, TCR ligation drives expression of CD69 to prevent egress into the circulation and promote retention. In the steady state spleen, CD69 expression is likely reflective of recent tonic signalling and was associated with increased expression of FT Blue (Figure 3.11.B&C) (Figure 3.12.A). In the liver, which contains a large number of $CD69^+$ resident T cells, CD69 was not associated with FT Blue expression, instead correlating with a decreased expression of FT Red (Figure 3.11.B&C) (Figure 3.12.B). These data again suggest that Nur77 Tempo can effectively detect steady-state tonic signalling in the lymphoid environment, but also that residency in non-lymphoid tissues prevents tonic signalling as cells are unable to re-circulate through the lymphoid environment.

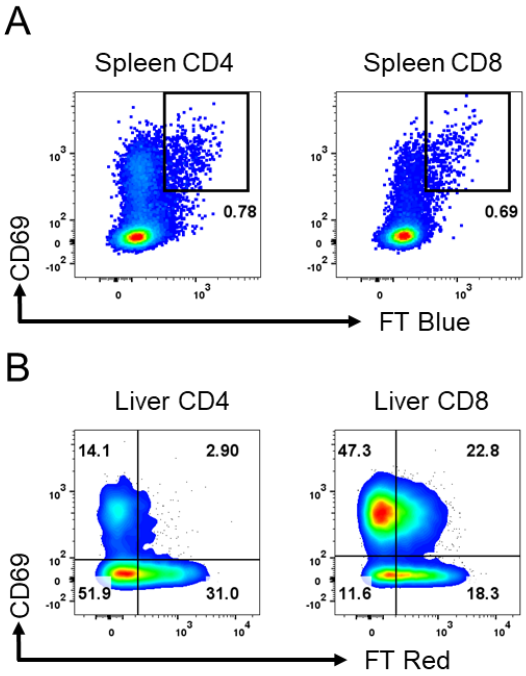

Figure 3.12. ***FT Blue is positively associated with CD69 expression in the spleen but negatively associated with CD69 expression in the liver.*** *A) Flow cytometry analysis of CD69 and FT Blue in the spleen of a representative Nur77 Tempo mouse. Gated on live $CD4^+$ $TCR\beta^+$ singlets and live $CD8^+$ $TCR\beta^+$ singlets. B) Flow cytometry analysis of CD69 and FT Red in the liver of a representative Nur77 Tempo mice. Gated on live $CD4^+$ $TCR\beta^+$ singlets and live $CD8^+$ $TCR\beta^+$ singlets.*

Murine intestinal intra-epithelial lymphocytes can be broadly categorised into natural or induced IELs. Natural IELs are predominantly CD8αα^{+} and express either TCRαβ or TCRγδ chains, they are thought to develop following self-antigen recognition in the thymus. Induced IELs are derived from circulating conventional T cells, they are predominantly TCRαβ^{+} CD8αβ^{+}, although some CD4^{+} induced IELs are present (Vandereyken et al., 2020). We processed IELs from the small intestines of Nur77 Tempo mice and analysed FT expression in natural and induced IELs (Figure 3.13.A).

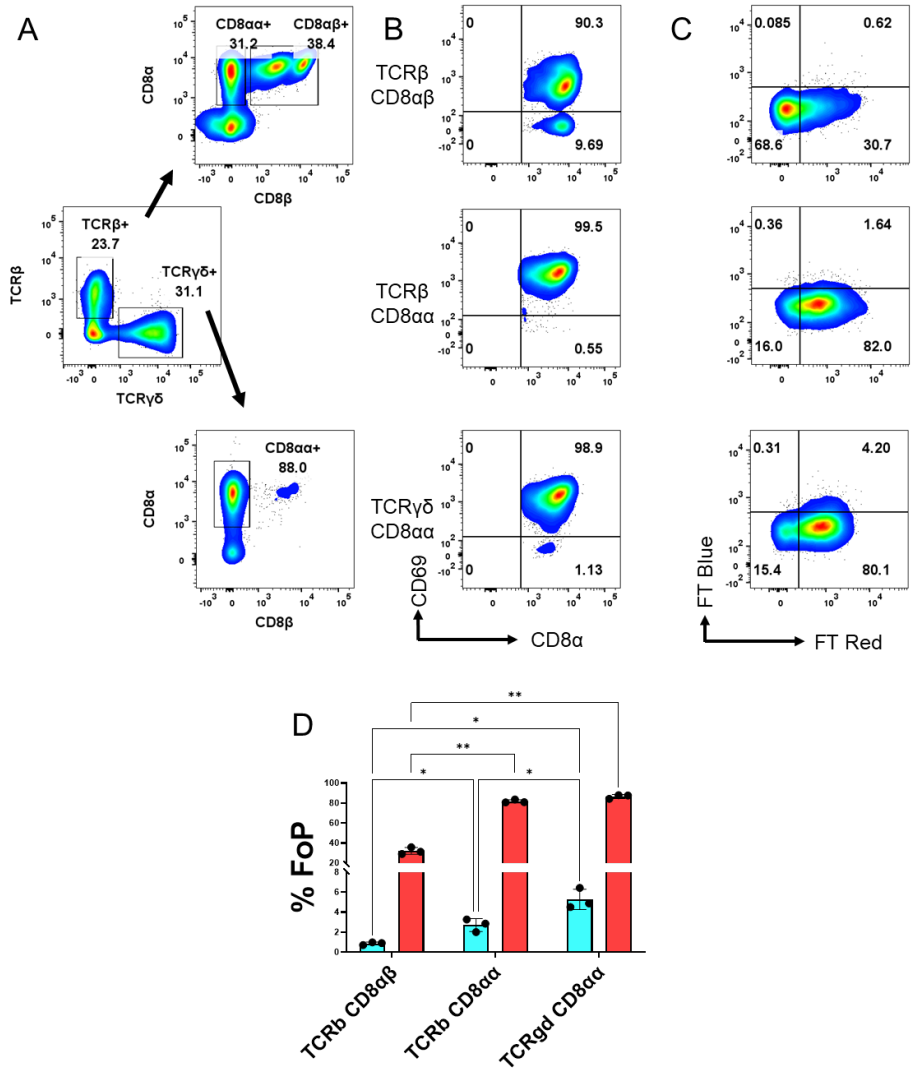

Figure 3.13. ***Intra-epithelial lymphocytes of Nur77 Tempo mice express high levels of FT*** *A) Gating strategy for small intestine intra-epithelial T cell subsets based on TCRβ, TCRγδ, CD8α, and CD8β expression. Pre-gated on live singlets. B) Expression of CD69 and CD8α in indicated subsets. C) Expression of FT Blue and FT Red in indicated subsets. D) Quantification of (C) displayed as FoP (% of subset positive for FT Blue and FT Red) n = 3. Statistical testing by two-way ANOVA with Sidak's multiple comparisons test. * P ≤ 0.05 **P ≤0 .01 ***P ≤ 0.001 ****P ≤ 0.0001.*

As expected, all IEL populations digested from the intestine were CD69$^+$ (Figure 3.13.B). CD8αβ$^+$ induced IELs showed a similar FT profile of CD69$^+$ T cells residing in the liver, with relatively low expression of FT Red suggesting that these cells do not receive a TCR signal in their local environment (Figure 3.13.C&D). In contrast, natural IELs expressed higher levels of FT Red and FT Blue (Figure 3.13.C&D), suggesting that these cells do receive TCR signals in their local environment, supporting the hypothesis that these cells arise due to self-antigen recognition in the thymus.

Finally, in order to validate the use of this model for tracking experimental induction of TCR signalling *in vivo*, we injected Nur77 Tempo mice with 1 mg/kg of αCD3 and culled four hours later. This resulted in dramatic increase in expression of CD69 and FT Blue (Figure 3.14), demonstrating the ability of Nur77 Tempo to detect recent TCR signals *in vivo*.

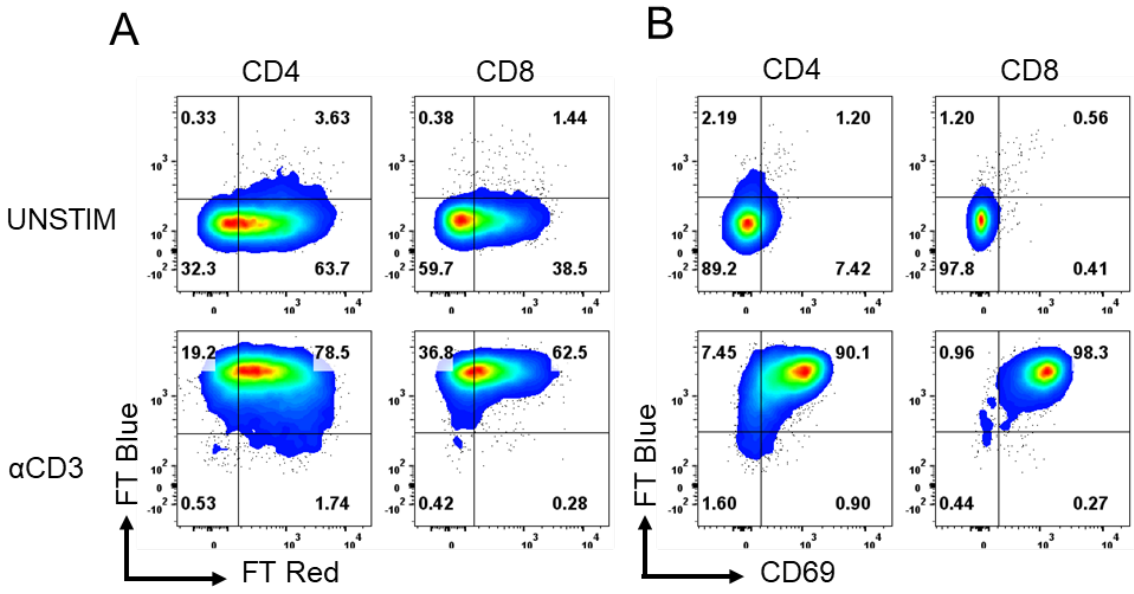

Figure 3.14. ***FT expression in the spleen of Nur77 Tempo mice following in vivo adminstration of αCD3 stimulating antibody.*** *Nur77 Tempo mice were injected with 1mg/kg αCD3. Four hours later mice were culled and splenocytes analysed for expression of FT Blue and FT Red (A) / CD69 (B) in CD4 and CD8 T cells. Pre-gated on live TCRβ$^+$ singlets.*

3.3 DISCUSSION

Here we have generated the Nur77 Tempo distal reporter of TCR signalling. As previously shown using the Nur77 GFP model, *Nr4a1* is expressed during positive selection of thymocytes and at steady state in the periphery. However, the Fluorescent Timer profiles of developing and steady state T cells are quite different. Thymocytes in the single positive stage of development show high levels of FT Blue expression but this is largely absent from T cells residing in the spleen at steady state. The half-life of FT Blue is around four hours, therefore TCR signalling events strong enough to cross the threshold for *Nr4a1* expression must happen on a frequent basis during positive selection, likely over the course of hours. Steady state splenic T cells express FT Red, evidence of a history of TCR signalling. This may be due to re-circulation into the thymus, or it may be due to low strength tonic self-antigen recognition in the splenic environment. Either way, these signalling events are infrequent as evidenced by the lack of FT Blue. Indeed, a significant proportion of splenic T cells are negative for FT Blue and FT Red, suggesting that the time between TCR signalling events that trigger *Nr4a1* expression can be as long as several days, the approximate half-life for mCherry to degradation.

Positive selection in the thymus and tonic signalling in the periphery are both required for survival of T cells at different stages of their development. Utilising the high time resolution of Nur77 Tempo we can demonstrate the different dependencies on the frequency of these signals. Whilst selection signals must be quite persistent in nature to prevent death by neglect, tonic signals in the spleen that happen approximately once a week may be sufficient.

When compared to the Nr4a3 Tocky model, we found very low signal in steady state splenic T cells and all thymic subsets except $CD25^+$ developing T_{REG} cells. Expression of *Nr4a3* is highly dependent on NFAT signalling, so we can determine that there are signals strong enough to induce expression of *Nr4a1*, but not strong enough to induce calcium flux and expression of

Nr4a3, that happen during positive selection and tonic signalling. The stronger self-antigen recognition that drives CD25 expression and T_{REG} development however is strong enough to induce NFAT signalling. Our findings that a single copy variant of Nur77 Tempo is more sensitive to low strength TCR signals than Nr4a3 Tocky particularly striking given that we estimate the Nr4a3 Tocky to carry 4-6 copies of the transgene (Jennings and Elliot et al., 2020).

To validate our findings that Nur77 Tempo is more sensitive than Nr4a3 Tocky, we stimulated splenocytes with a dose titration of αCD3. Since there was already a higher baseline expression of FT Blue in the Nur77 Tempo cells, we normalised this data across the dynamic range of FT Blue expression levels. We confirmed that Nur77 Tempo was more sensitive to lower doses of αCD3.

We next aimed to understand the signalling pathways downstream of the TCR that drives expression of the two reporter genes by stimulating splenocytes in the presence of a number of small molecule inhibitors. We re-capitulated previous findings that *Nr4a3* was acutely sensitive to inhibition of the NFAT pathway, whilst *Nr4a1* only showed partial sensitivity. Aside from inhibition of the NFAT pathway with Cyclosporine A, Nur77 Tempo and Nr4a3 Tocky showed similar drops in the median intensity of FT Blue expression in response to all the small molecule inhibitors we tested. This shows that both reporters are partially sensitive to all major signalling pathways downstream of the TCR. However, we did see a pronounced difference between the behaviour of the two reporters when we measured the frequency of FT Blue expression, particularly among $CD4^+$ splenic T cells. Nr4a3 Tocky showed a marked reduction in the proportion of cells that reached the threshold to express FT Blue above background detection levels, this was most pronounced by blockade of ERK and JNK pathways. In contrast, Nur77 Tempo showed only very slight decreases in the proportion of FT $Blue^+$ cells. Therefore, decreases in median intensity of FT Blue were largely driven by a graded decrease in brightness among Nur77 Tempo mice, but a reduction in proportion of cells crossing a digital threshold in Nr4a3 Tocky

mice. This phenomenon seemed limited to $CD4^+$ T cells; in $CD8^+$ T cells Nur77 Tempo showed a bigger decrease in FT $Blue^+$ frequency in response to an inhibitor of the ERK pathway. Unlike the relationship between Cyclosporine A and Nr4a3 Tocky, we were unable to identify a single pathway that was necessary for expression of Nur77 Tempo. A shared partial sensitivity to many of the pathways we tested is unsurprising as we have previously observed a 'quenching' effect by crossing Nr4a3 Tocky and Nur77 GFP mice (Jennings and Elliot et al., 2020), demonstrating that *Nr4a1* and *Nr4a3* to some extent compete for a limited pool of shared transcription factors.

In order to characterise the signalling dependency for *Nr4a1* expression, we designed a panel of small molecule inhibitor combinations. We swapped out our PI3K inhibitor from Ly 294002 to GDC 0941 due to reports that the latter can reduce expression of *Nr4a1* in human cells (Ashouri et al., 2017). We also included SB 203580, an inhibitor of p38, to allow blockade of both AP1 subunits Fos and Jun. Our large screen found that Nur77 Tempo reporter expression seemed to be most notably reduced by co-blockade of PI3K and ERK signalling pathways. This was then further reduced by adding inhibitors for p38, PKC, and JNK, such that a cocktail of all five inhibitors prevented reporter expression completely.

Unlike our previous experiment, blockade of NFAT signalling slightly increased reporter expression. It was also notable that FT Blue expression was higher with a combination of all six inhibitors compared to the cocktail that excluded just Cyclosporine A. This difference in results may be due to a slightly different experimental design. In the second experiment, cells were pre-treated with the small molecule inhibitor for 30 minutes prior to stimulation, whereas in the first experiment the inhibitors and stimulation were added at the same time. The second experiment also had a slightly longer stimulation duration of six hours compared to four hours in the first experiment. As the number of conditions was much higher in the second experiment, the splenocytes from each individual mouse were spread over a greater number of wells. The smaller

number of cells in each well impacted the quality of the *in vitro* stimulation. Even with only the DMSO control, ~50% of cells were FT Blue^{+} in the second experiment compared to ~95% in the first experiment. The lower number of cells may have reduced the probability that any given T cell was in contact with an APC and thus received a signal when αCD3 was added to the cultures.

The increase in FT Blue expression when cells were pre-treated with Cyclosporine A is likely a meaningful finding. Recent work performed on an *in vitro* reporter system of ERK and NFAT dependent signalling has revealed diverging dynamics of the two signalling pathways during the course of several hours after stimulation. RNA sequencing following stimulation in the presence of small molecule inhibitors of ERK or NFAT signalling pathways has revealed distinct transcriptional response to the activity of both pathways. Whilst some genes are reduced following blockade of either pathway, some are sensitive only to blockade of one of the pathways. Furthermore, some ERK regulated genes are increased following NFAT pathway blockade and vice versa (Wither et al., 2023). Genes can be activated or repressed by ERK and NFAT in isolation or by AP1 complexes, mediated by unique consensus binding motifs of the individual or dimerised transcription factors. However, the authors propose a model whereby NFAT can exert an influence over ERK signalling through the process of site re-direction. Binding to NFAT might impact the consensus binding sites for ERK regulated transcription factors. *Nr4a1* can be expressed in the absence of NFAT signalling as shown by our work with Cyclosporine. However, NFAT does bind to *Nr4a1* regulatory regions and in some circumstances loss of NFAT signalling may reduce *Nr4a1* expression. However, in other circumstances, perhaps during a longer-term stimulation, NFAT may reduce *Nr4a1* expression by re-directing AP1 transcription factors. Alterations to transcriptional regulation of T cells via site re-direction has been described between Runx1 and PU.1 transcription factors (Hosokawa et al., 2018). Additionally, since NFAT can form dimers with both AP-1 and NFκB, inhibition may prevent dimer formation and allow higher levels of NFAT independent AP-1 and NFκB signalling, increasing expression of *Nr4a1*.

The dependency of *Nr4a3* on NFAT signalling likely explains the differential expression patterns of Nr4a3 Tocky as compared to Nur77 Tempo. In the thymus we saw thresholded behaviour of Nr4a3 Tocky reporter expression. The reporter was virtually absent in all subsets except developing T_{REG} cells where expression was very high. This digital behaviour is in keeping with NFAT dependency; the thresholded release of Ca^{2+} from intracellular stores drives switch like behaviour in the NFAT signalling pathway. Nur77 Tempo expression was much more graded, in subsets receiving low strength positive selection signals, reporter expression was low but not absent. In the $CD25^{+}$ subset reporter expression was much higher. We have previously reported that *Nr4a3* expression requires longer TCR signal duration than *Nr4a1* (Jennings and Elliot et al., 2020). It may be that whilst T_{REG} cells receive a more prolonged TCR signal, $CD25^{-}$ $CD4^{+}$ T cells receive shorter duration signals that are sufficient to drive *Nr4a1* but not *Nr4a3*.

The difference in sensitivity to TCR signal strength between the two reporters may not be due just to differential sensitivity to TCR signalling pathways. The brightness of the reporter is dependent on the number of FT Fast proteins, which is in turn dependent on the mRNA copy number. We know that when there is an increased copy number in the genomic DNA, the brightness of the reporter is higher. In fact, when we compared a single copy variant with a four copy variant in the steady state, the proportion of cells that had FT Blue expression detectable above threshold was much higher in the four copy variant, despite both individuals being at steady state. Therefore, in the single copy variant, there was likely a proportion of cells that had received a recent TCR signal sufficiently strong enough to elicit transcription of the *FT Fast* gene, but not enough copies were present for FT Blue expression to be detectable above background noise by our flow cytometry system. It may then also be the case that in single positive thymocytes of Nr4a3 Tocky mice, *FT Fast* is being transcribed at very low levels but not enough to detect FT Blue by flow cytometry. We estimate that the Nr4a3 Tocky mouse carries 4-6 copies of the *FT Fast* transgene, higher than the single copy Nur77 Tempo variant we used in these experiments. However, we also know that

endogenous *Nr4a1* expression is much higher than endogenous *Nr4a3* expression. Therefore, in addition to differential regulation by signalling pathways downstream of the TCR, the regulatory elements upstream of the *Nr4a1* gene that regulate *FT Fast* expression in the Nur77 Tempo mouse create more transcripts, impacting reporter brightness.

We utilised the Nur77 Tempo mice to investigate TCR signalling dynamics in T cells that reside in the lung and the liver. In lymphoid organs, CD69 is a marker of recent antigen recognition. CD69 antagonises that activity of S1PR1, which allows T cells to migrate along gradients of sphingosine-1-phosphate, which is concentrated in the blood. CD69 prevents egress into the circulation, retaining T cells in the lymphoid environment to promote their full activation after initial TCR signal. In peripheral organs such as the liver, T cells can express CD69 long-term to promote their tissue residency. The liver has a large population of resident T cells that are vital in the response against local infection.

In the spleen we found that CD69 expression was associated with FT Blue, confirming the utility of the Nur77 Tempo model to identify T cells that have received a recent TCR signal in the lymphoid environment. In the liver, CD69 expression was not associated with FT Blue but instead a reduction in FT Red. These results contradict suggestions in the literature (Lee et al., 2011; Schenkel & Masopust, 2014) that peripheral antigen recognition is important to sustain resident T cell populations and instead supports a model where resident T cells are sustained by soluble factors in the tissue microenvironment. Loss of FT Red is likely a result of prolonged withdrawal from the lymphoid environment and loss of tonic TCR signalling that occurs there. $CD69^-$ populations sustained their expression of FT Red as they are likely able to recirculate through lymphoid organs and receive tonic self-antigen signals.

Intra-epithelial lymphocytes in the small intestine can be $CD8\alpha\beta^+$ 'induced' IELs or $CD8\alpha\alpha^+$ 'natural' IELs. It has been proposed that these populations have different origins, with natural

IELs being selected for in the thymus during early age and residing there for life (McDonald et al., 2018). Induced IELs are proposed to arrive at the intestine from the circulation and migrate into the epithelial layer in response to local signals (McDonald et al., 2018). The FT expression patterns were markedly different between natural and induced IELs. Induced IELs had an expression pattern that resembled $CD69^+$ T cells in the liver, supporting the hypothesis that these cells arrive form the circulation. Induced IELs had very high expression of FT Red but low FT Blue, more similar to steady state splenic T cells. These findings suggest that natural IELs receive TCR signals in the epithelial layer to support their survival whilst induced IELs do not. In particular, $TCR\gamma\delta^+$ IELs had the highest expression of FT; γδ TCRs can be ligated by butyrophillin and butyrophillin-like proteins. For example, in mice and humans Vγ4 TCR chains can bind to butyrophillin-3 that is expressed by intestinal epithelial cells (Willcox et al., 2019). The ligands for $CD8\alpha\alpha^+$ $TCR\alpha\beta^+$ T cells are not well defined, but our data suggests that they are likely present on host IECs and important for survival.

Finally, we demonstrated that Nur77 Tempo reporter expression could be induced by *in vivo* administration of αCD3. This validates the utility of Nur77 Tempo for studying TCR signalling in *in vivo* disease models.

Although both distal reporters of TCR signalling, Nr4a3 Tocky and Nur77 Tempo report on different aspects of the TCR signalling cascade with different sensitivities. This imparts a slightly different utility to the two reporter systems. Studies that investigate low strength signals such as positive selection are likely to benefit from the increased sensitivity of Nur77 Tempo. Nur77 Tempo is also likely to be beneficial in studying alterations to TCR signalling strength, due to its more graded expression patterns compared to Nr4a3 Tocky. A drawback to Nur77 Tempo is the high levels of FT Red background expression that occurs as a result of its high sensitivity. Experimental models in which it is important to detect historic TCR signalling events with a low level of background

noise would benefit from using Nr4a3 Tocky over Nur77 Tempo. Furthermore, Nr4a3 Tocky may be particularly useful for studying the TCR signals that drive thymic T_{REG} development, as they are the main drivers *of Nr4a3* expression during development.

It is of note that our findings here are limited to T cell development and experimental modelling of acute stimulation. TCR signalling is a dynamic process; much of the research interest surrounding the regulation of TCR signalling is related to chronic TCR stimulation. ICB therapies that aim to modulate TCR signalling are used to treat cancer, in which T cells are exposed to chronic antigen stimulation. NFAT and ERK signalling pathway dynamics change over time (Wither et al., 2023); our observations that Nur77 Tempo is more sensitive to lower strength or duration TCR signals may be limited to the context of acute stimulation. Further work is required to determine whether these models are applicable to chronic TCR stimulation.

4 TRACKING TCR SIGNALLING DURING CHRONIC STIMULATION

4.1 INTRODUCTION

TCR regulated functions are shut down during T cell exhaustion through the combined activity of epigenetic re-wiring and negative signalling at the immune synapse by co-inhibitory receptors. During chronic TCR stimulation, multiple co-inhibitory receptors are expressed that have distinct mechanisms of action and may have non-redundant functions. The complex make-up of co-inhibitory and co-stimulatory receptors, and whether they are engaged with their ligands, has an important role in regulating TCR signalling. However, the precise mechanism of action of many such receptors is not clear, meaning we have an incomplete understanding of how different co-inhibitory receptors impacts different signalling pathways downstream of the TCR. As such, we do not know which specific pathways downstream of the TCR are impacted by ICB therapy in certain contexts.

4.1.1 Divergence of NFAT and ERK Pathways

Many studies investigating TCR signalling pathways have focussed on the immediate response to pMHC stimulation, this has led to the dogma that all signalling pathways trigger simultaneously, almost instantly after TCR ligation. Failure to make longer term observations to the dynamics of TCR signalling pathway activity may have limited the scope of many previous studies. An *in vitro* NFAT/ERK dual reporter system has been used to study the dynamics of Calcineurin-NFAT and Ras-ERK signalling pathways over time in response to different strengths of TCR signal (Wither et al., 2023). TCR transgenic $CD8^+$ T cells were stimulated with different doses of either a cognate peptide or partial agonist. In agreement with previous studies that have proposed binary signalling models for both pathways, stimulation with any dose of either peptide triggers rapid

and synchronised activity of both pathways that did not differ based on the strength of TCR signal. This experimental data fits with a model in which a threshold must be crossed in order to induce a stereotyped response and all peptide doses tested here were sufficient. However, longer term observation over thirty hours showed that higher affinity peptide was associated with a higher magnitude of signalling pathway activity. Although peptide dose did not change the magnitude of ERK signalling, a low dose of cognate peptide reduced NFAT pathway activity such that it was equivalent to a high dose of low affinity peptide. Therefore, these two pathways can show divergent behaviour in response to antigen signals over longer periods of time.

The study went on to investigate the transcriptional response to signalling via either Ras-ERK or Calcineruin-NFAT in isolation using small molecule inhibitors of Calcineurin (Cyclosporine A) or MEK (Trametinib). A high number of genes were activated or repressed in response to TCR signalling; multiple linear regression analysis grouped genes into modules based on whether they were activated or repressed, and whether this was more highly dependent on Ras-ERK or Calcineurin-NFAT pathway activity. In keeping with our work in chapter one using small molecule inhibitors, *Nr4a3* was activated in a highly NFAT dependent manner. In contrast, *Fos,* which is activated directly downstream of ERK, was largely unaffected by Cyclosporine A but acutely sensitive to Trametinib, as expected. The distinct gene modules showed that many TCR regulated genes important for T cell functionality have different pathway dependencies. For example, *Cxcr6* was acutely ERK dependent, but *Ifng* was acutely NFAT dependent. Downregulation of *Il7r* was very ERK dependent, but downregulation of *Gata3* was very NFAT dependent.

By controlling expression of TCR regulated gene modules via different pathways and diverging pathways in response to different strengths of long-term stimulation, T cells may be able to encode qualitatively different input signals into qualitatively different functional outputs.

4.1.2 Role of NFAT Signalling in CD8$^+$ T Cell Exhaustion

Divergence of Calcineurin-NFAT and RAS-ERK signalling pathways is a critical feature of T cell dysfunction during chronic stimulation. During early stimulation, when both pathways are active, NFAT:AP-1 dimers play a critical role in regulating the expression of key cytokines (Mognol et al., 2017). Divergent activity of Ras-ERK and Calcineurin-NFAT signalling pathways may have an important functional role in driving T cell dysfunction during chronic TCR stimulation, particularly in the absence of co-stimulation. An early study in murine CD4$^+$ T cells found that overnight stimulation with plate-bound αCD3 rendered T cells incapable of producing IL-2 in response to a subsequent αCD3/αCD28 stimulation (Li et al., 1996). ERK and NFAT activity were measured by western blotting for NFAT from the cytosolic compartment or pERK from total cell lysate. The investigators found that αCD3 stimulation induced rapid activation of both Calcineurin-NFAT and Ras-ERK pathways upon primary stimulation. However, overnight treatment with αCD3 followed by re-stimulation was unable to induce ERK phosphorylation but a very minor effect on the presence of cytosolic NFAT. This is early evidence that during T cell dysfunction, NFAT signalling might remain intact whilst ERK signalling. Interestingly, the investigators found that ERK phosphorylation could be induced by PMA stimulation, suggesting that the pathway machinery was intact, but a signalling event proximal to the TCR was responsible for shutting down the RAS-Erk pathway.

A study in 2002 demonstrated that CD4$^+$ T cell anergy could be induced by activation of that NFAT pathway alone (Macián et al., 2002). Anergy could be effectively induced by sixteen hour treatment with ionomycin, a Ca^{2+} ionophore. Ionomycin treatment did not induce AP:1 activation and anergy induction was blocked by knockout of *Nfat1*, confirming the role of NFAT signalling in T cell negative feedback. These findings of differential pathway activity during CD4$^+$ anergy have been re-capitulated in chronically stimulated CD8$^+$ T cells during LCMV infection. Transcriptional

comparison of exhausted $CD8^+$ T cells arising during chronic infection and effector $CD8^+$ T cells arising during acute infection has revealed an upregulated of *Nfatc1* and a downregulation of *Fos* and *Jun* in the exhausted population (Shin et al., 2007).

Further evidence for the role of NFAT in negative feedback control of $CD8^+$ T cells comes form a study that utilised a constitutively active form of NFAT1 that carries a mutation in the region that binds to AP1 during dimer formation (CA-RIT-NFAT1) (Martinez et al., 2015). This allows investigation into the functional outcomes of NFAT signalling in the absence of ERK signalling. CA-RIT-NFAT1 mice showed high expression of multiple co-inhibitory receptors at steady state; CA-RIT-NFAT1 was able to bind to regulatory regions of genes of *Pdcd1* and *Havcr2* without any TCR stimulation. As a result, in disease models the CA-RIT-NFAT1 mice had a higher tumour burden and viral load, highlighting how NFAT signalling alone can cause severe T cell dysfunction.

Although there are many similarities between effector T cells that arise during acute stimulation and exhausted T cells that arise during chronic stimulation, there are transcriptional signatures unique to each subset (Shin & Wherry, 2007). A study in 2016 aimed to compare the transcriptional profiles of exhausted vs non-exhausted effector $CD8^+$ TILs (Singer et al., 2016). PD-1^+ TIM-3^- and PD-1^+ TIM-3^+ cells were sorted and analysed by RNA-seq. Whilst there were many transcriptional similarities, the double-positive population had some uniquely upregulated genes. One of these was Mt1 which encodes Metallothionein 1, a protein involved in zinc metabolism and cytolytic granule release. Knockout of both Metallothionein genes results in better control of tumour growth and restored cytokine production to TIM-3^+ exhausted $CD8^+$ T cells. RNA-seq analysis of TIM-3^+ $CD8^+$ T cells from Metallothionein deficient and wild-type mice allowed an uncoupling of genes associated with T cell activation and those specifically associated with T cell dysfunction. It may be the case that the altered dynamics of NFAT and ERK

signalling during chronic TCR stimulation allows T cells to encode different antigenic stimuli into these transcriptional programmes that specifically modulate effector function vs. T cell exhaustion.

4.1.3 Pathway Targeting by Co-inhibitory Receptor Blockade

It remains unclear as to what extent different ICB therapies are able to reinvigorate different TCR signalling pathways. This has important functional consequences. For example, if an exhausted T cell has shut down ERK signalling pathways, restoration of ERK signalling may then drive the formation of NFAT:AP1 dimers that are critical for cytokine production. If ICB therapy instead only invigorates NFAT signalling pathways, this may reinforce T cell exhaustion without restoring T cell functionality. Others have described T cell exhaustion as being dependent on TCR signalling in the absence of co-stimulation. Previous studies have shown that whilst the phosphorylation status of CD3ζ and CD28 are both sensitive to inhibitory signalling by PD-1, CD28 is more sensitive and spatially more related to PD-1 (Hui et al., 2017). Other studies have shown that PD-1 still has a potent effect on IL-2 production when antigen presenting cells are deficient for CD80 and CD86, the ligands for CD28 (Mizuno et al., 2019). Both studies were performed in slightly different *in vitro* systems.

In all likelihood, PD-1 can target CD28 and the TCR depending on context. In co-stimulation rich environment, blockade of PD-1 may therefore restore co-stimulatory signalling and perhaps revert T cell exhaustion. In an environment where co-stimulation is not possible, such as within a tumour where the ligands may not be present, PD-1 blockade might reinforce NFAT signalling and the exhaustion programme. This may explain why PD-1 blockade seems to have a potent effect on T cells in the co-stimulation rich environment of the lymph node (Dammeijer et al., 2020) but

lead to upregulation of alternative co-inhibitory receptors on intratumoural T cells (Koyama et al., 2016).

Successful ICB therapy must aim to, if possible, restore TCR signalling pathways that are essential for a productive and long-lasting anti-cancer functionality such as proliferation and cytokine production. This will involve a better understanding of how pathway dynamics change during chronic stimulation and how these pathways respond to ICB therapy. Here we utilised Nur77 Tempo and Nr4a3 Tocky mice, that are reporters of NFAT independent and NFAT dependent signalling respectively, to track pathway dynamics during chronic stimulation. We used both a sub-cutaneous tumour model and a chronic *in vitro* stimulation model, TCR signalling pathway are rapidly re-wired to bias NFAT-dependent over NFAT-independent pathways. Furthermore, we tested the sensitivity of NFAT-independent TCR signalling to therapeutic re-activation with ICB therapy and αCD3 stimulation, finding it to be refractory to both. Finally, we tested the impacts of transient NFAT pathway inhibition on development of $CD8^+$ T cell functional exhaustion and TCR pathway dynamics.

4.2 RESULTS

4.2.1 Tracking TCR Signalling in MC38 Tumours

In order to track TCR signalling dynamics under chronic stimulation in the tumour environment, we injected MC38 colon carcinoma cell line sub-cutaneously into Nur77 Tempo mice. We chose the MC38 tumour model because it is immunogenic and responsive to checkpoint blockade in other labs and also in our hands (Dr. Lozan Sherif, unpublished data). The MC38 cell line drives an aggressive $CD8^+$ T cell mediated response against an envelope protein of retrovirus MulV (Ye et al., 2020) that is found in the germline of C57BL/6 mice. The p15E peptide (KSPWFTTL) is presented by H2-Kb to $CD8^+$ T cells; a commercially available H2-Kb KSPWFTTL pentamer (ProImmune) can be used to track $CD8^+$ T cells reactive for this peptide, identifying antigen reactive $CD8^+$ T cells in the tumour microenvironment.

As a pilot experiment, we injected MC38 cells subcutaneously into Nur77 Tempo mice before culling at day 7 (tumour diameter ~2mm) and day 13 (tumour diameter ~8mm). Tumours were resected and digested to single cell suspension for analysis by flow cytometry. We gated on live $CD8^+$ T cells and stained p15E reactive cells with KSPWFTTL pentamer (Figure 4.1). We found that at both day 7 and day 13 there was a sizeable portion of p15E specific $CD8^+$ T cells.

When we compared FT profiles of both the bulk and Pentamer+ populations between day 7 and 13 we made a qualitative observation that a higher proportion of $CD8^+$ T cells were FT $Blue^+$ at day 7, particularly in the $Pentamer^+$ population (Figure 4.2). The day 13 stage of tumour development was associated with much higher expression levels of negative regulators of TCR signalling PD-1 and CD39 (Figure 4.3). PD-1 expression displayed as a heatmap on the FT plots shows that at day 7, PD-1 expression is associated with FT Blue expression (Figure 4.4). However, at day 13, particularly in the $Pentamer^+$ population, PD-1 expression is more ubiquitous. There is a population of antigen reactive $CD8^+$ T cells that have infiltrated the tumour environment but are

not receiving a TCR signal that we can detect through the Nur77 Tempo reporter. We hypothesised that at an early stage of tumour development at ~day 7, TCR signals drive expression of negative regulators of TCR signalling such as PD-1, which then shut down antigen induced *Nr4a1* expression via negative signalling at the immune synapse.

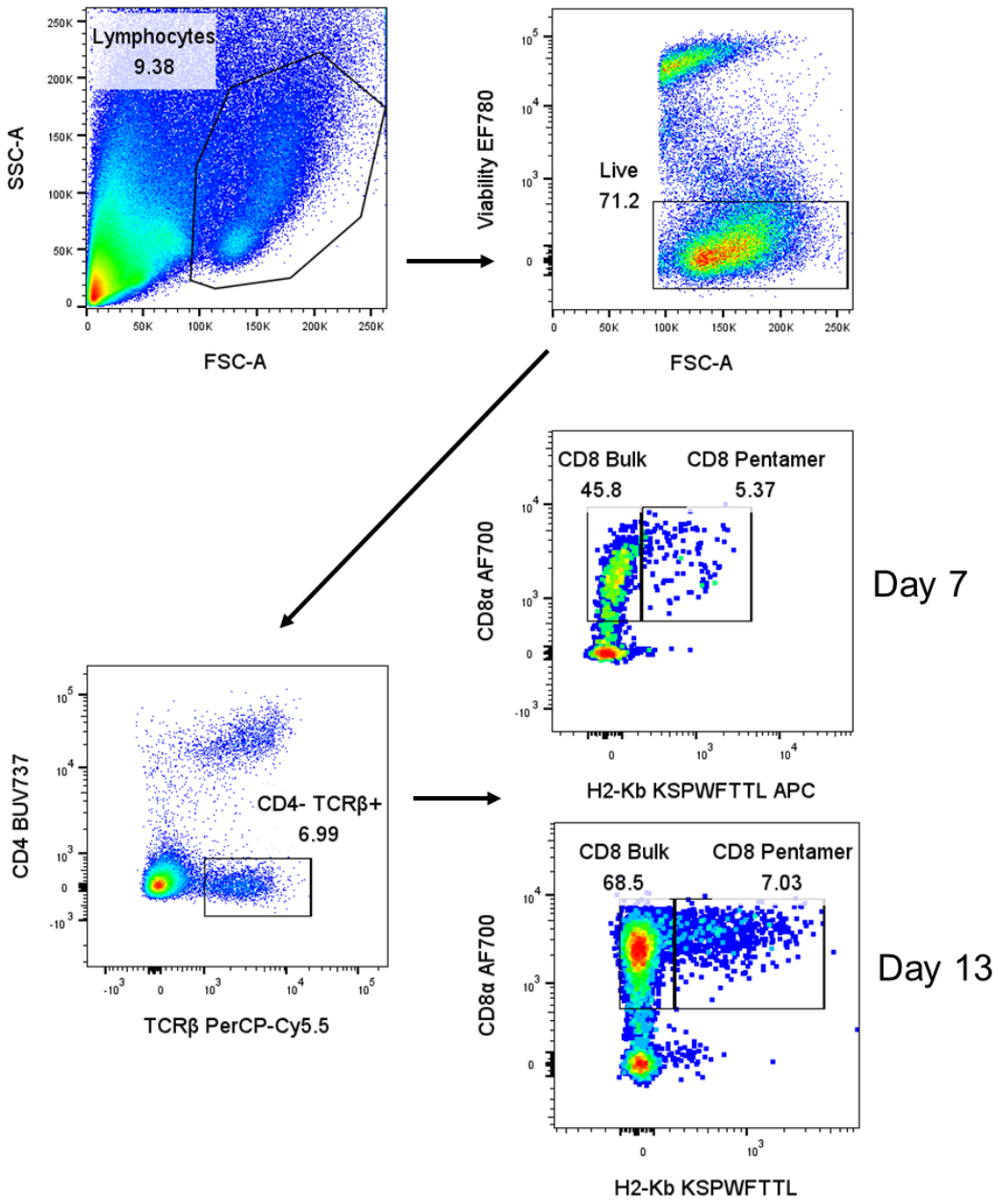

Figure 4.1. ***Gating strategy for CD8⁺ T cells in MC38 tumours****. Staining with H2-Kb KSPWFTTL pentamer is shown for day 7 and day 13.*

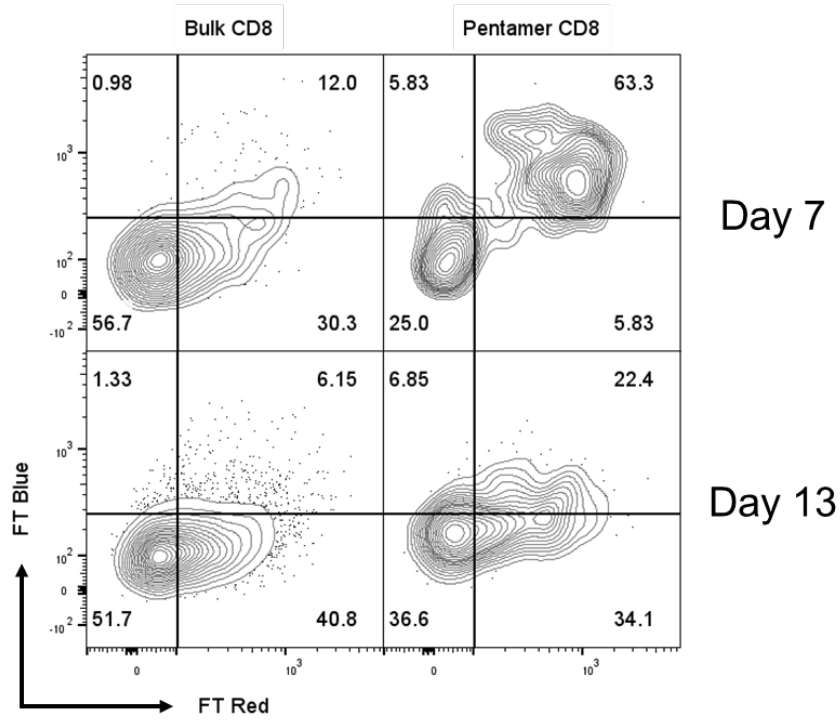

Figure 4.2. ***FT Analysis in MC38 tumour infilrating CD8 T cells at day 7 and 13.*** *FT blue and FT Red expression in bulk CD8⁺ T cell and pentamer⁺ CD8⁺ T cell populations at day 7 and day 13 post implantation. N=1/time point.*

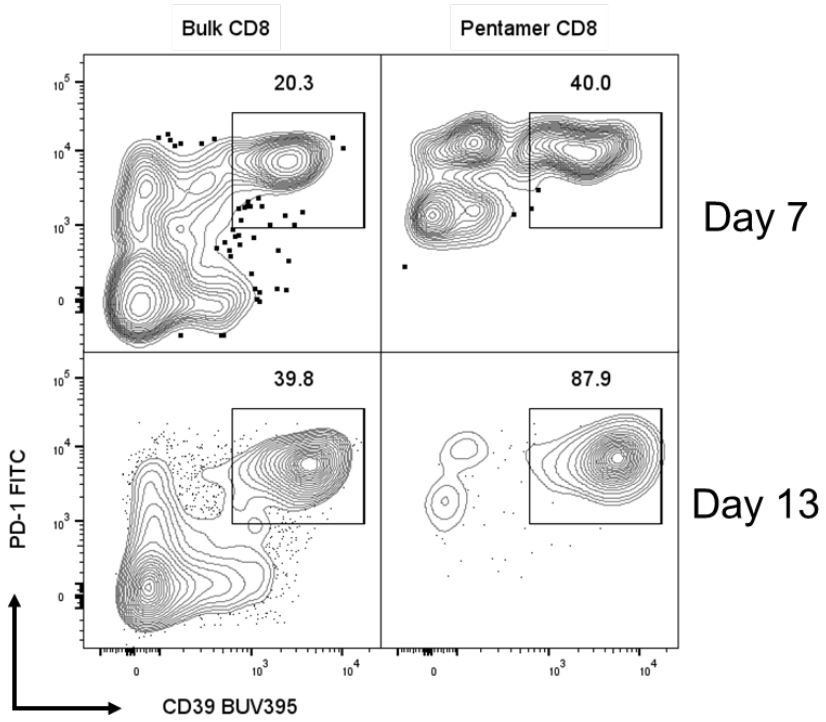

Figure 4.3. ***Inhibitory receptor analysis in MC38 tumour infiltrating CD8 T cells at day 7 and day 13.*** *PD-1 and CD39 expression in bulk CD8⁺ T cell and pentamer⁺ CD8⁺ T cell populations at day 7 and day 13 post implantation. N=1/time point.*

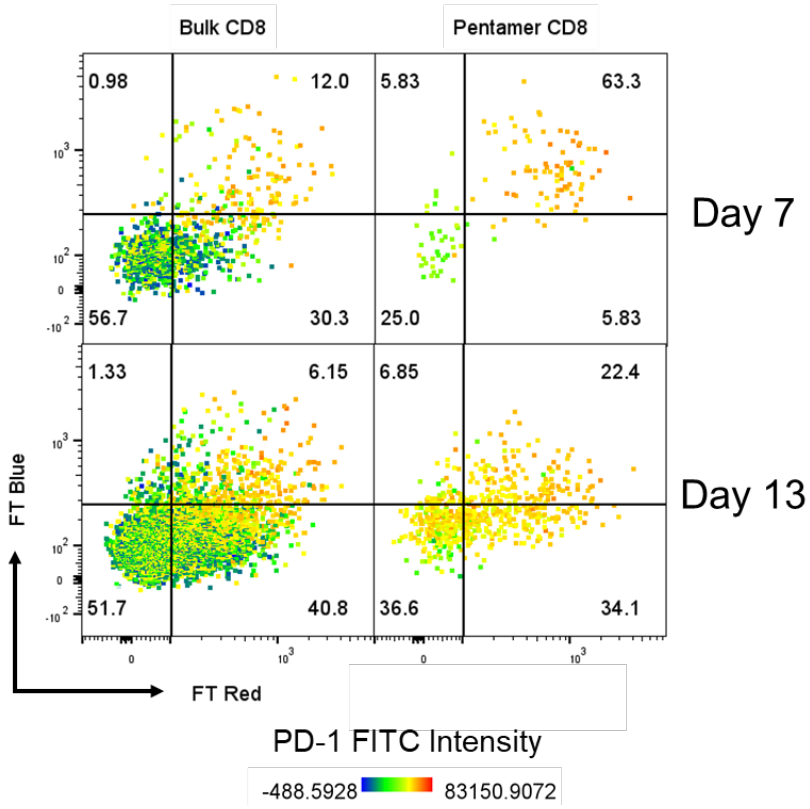

Figure 4.4. ***. FT Analysis in MC38 tumour infilrating CD8 T cells at day 7 and 13.*** *FT blue and FT Red expression in bulk CD8⁺ T cell and pentamer⁺ CD8⁺ T cell populations at day 7 and day 13 post implantation. Heatmap represents fluorescent intensity of PD-1 staining. N=1/time point.*

We repeated this experiment in a greater number of mice, comparing Nur77 Tempo to Nr4a3 Tocky. We found that in Nur77 Tempo mice, there was an increase in the proportion of Blue⁻Red⁺ CD8⁺ T cells, indicative of a history of TCR signalling, but no increase in the proportion of Blue⁺ Red⁺ CD8⁺ T cells, suggesting that the pathway detected by the Nur77 Tempo reporter is active only for a short period of time (Figure 4.5.A). In contrast, Nr4a3 Tocky mice showed an increase in the proportion of Blue⁺ Red⁺ and Blue⁻ Red⁺ CD8⁺ T cells (Figure 4.5.B), suggesting the pathway detected in this model is sustained during tumour development.

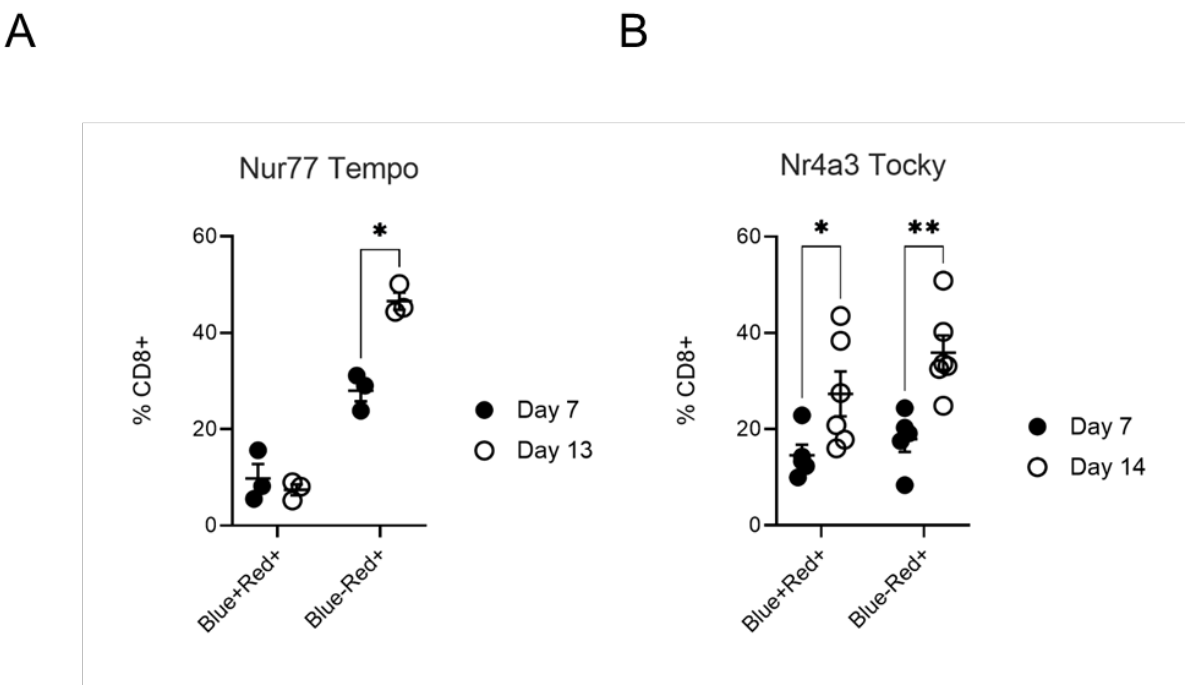

Figure 4.5. ***Quantification of FT Blue and FT Red expression in MC38 tumour infiltrating CD8 T cells at day 7 and day 13.*** *MC38 cells were implanted sub-cutaneously into Nur77 Tempo (A) or Nr4a3 Tocky mice (B). After 7 or 13/14 days, mice were euthanised and tumours were digested into single cell suspension for analysis by flow cytometry. Cells were pre-gated on Live CD8⁺ TCRβ⁺ singlets. Shown is proportion of cells FT Blue⁺ FT Red⁺ or FT Blue⁻ FT Red⁺. Error bars indicate mean and SEM. Stats test shown are two-way ANOVA. *P ≤ 0.05, **P ≤ 0.01, ***P ≤ 0.001, ****P ≤ 0.0001. N=3-6/group.*

4.2.2 Nur77 Tempo Response to Immunotherapy

In order to test whether this process is reversible, we again inoculated Nur77 Tempo mice with MC38 cells and injected 10mg/kg αPD-L1 blocking antibody (Clone 80, AstraZeneca) intra-peritoneally on days 8 and 11 before tumour resection and analysis on day 13 (Figure 4.6.A). In both the isotype and αPD-L1 treated groups, FT Blue expression remained low (Figure 4.6.B). There was no difference in median intensity or frequency of FT Blue in response to αPD-L1, this was true for both the bulk CD8⁺ T cell population and the Pentamer⁺ population (Figure 4.6.C&D). There was a trending decrease in the expression of FT Red, this may be a result of αPD-L1 induced proliferation, causing a dilution of the FT Red protein as cells divide. We did observe a modest increase in the expression of co-inhibitory receptors PD-1 and NKG2A (Figure 4.7).

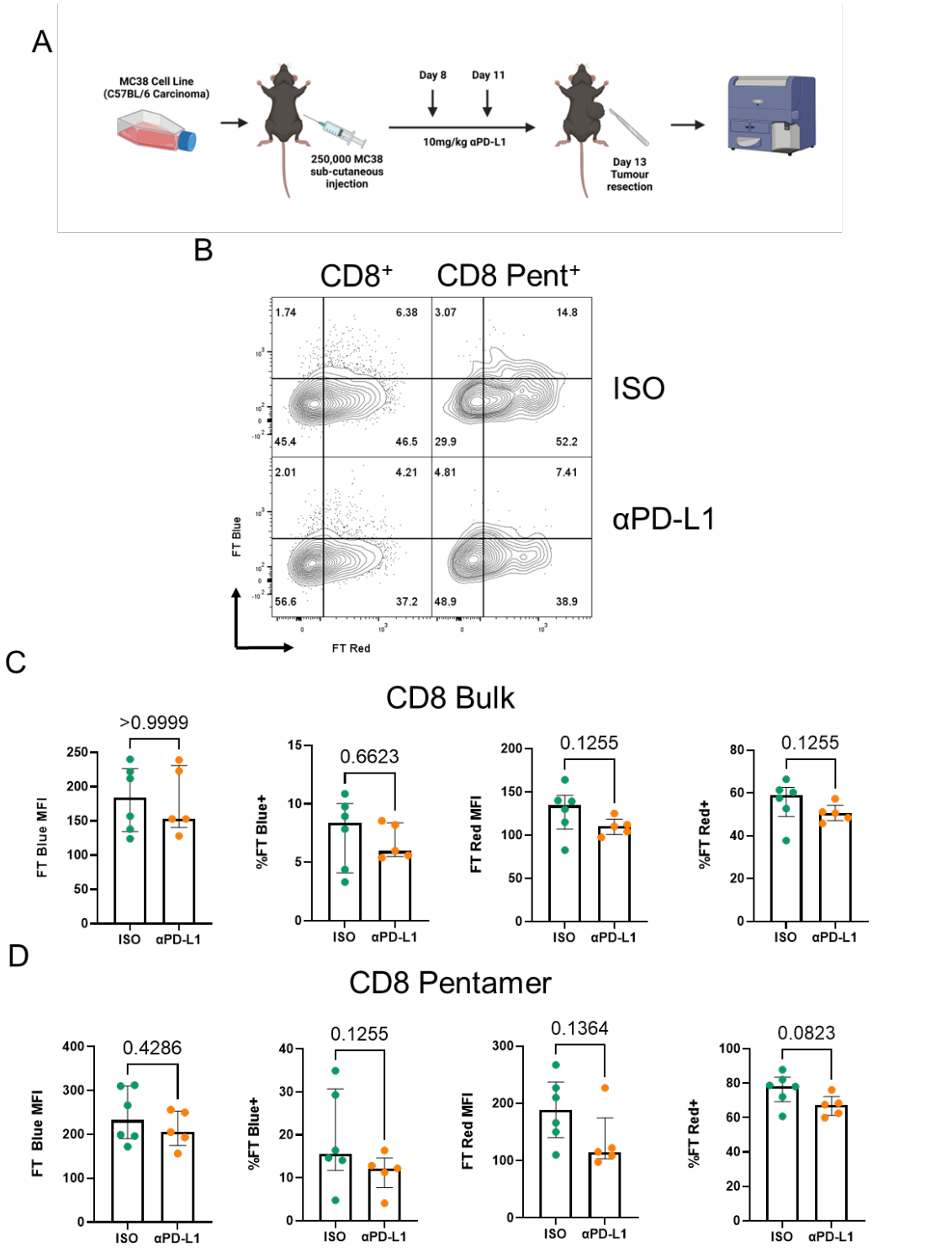

Figure 4.6. ***Analysis of FT expression in MC38 tumour infiltrating CD8 T cells following day 8&11 PD-L1 blockade in Nur77 Tempo mice.*** *A) Representative flow plots of FT expression in bulk and pentamer⁺ CD8⁺ tumour infiltrating T cells after treatment with αPD-L1 or isotype control. B&C) Quantification of (A). Statistical test shown are Mann-Whitney. Error bars indicate median and inter-quartile range. N=5-6/group.*

We reasoned that αPD-L1 may restore TCR signalling and FT Blue expression, but that this may be very short lived. If there was a sustained increase in FT Blue expression, this would likely be

detectable by an increase in the intensity of FT Red, but we did not make this observation.

As we and others have described, ICB induced increase to TCR signal strength can drive compensatory upregulation of co-inhibitory receptors. We hypothesised that a rapid upregulation of FT Blue might be associated with a rapid increase in negative regulation of TCR signalling, quickly attenuating *Nr4a1* expression. A small increase in the fluorescent intensity of Nur77 GFP reporter has been observed following αPD-L1 treatment of mice infected with chronic LCMV

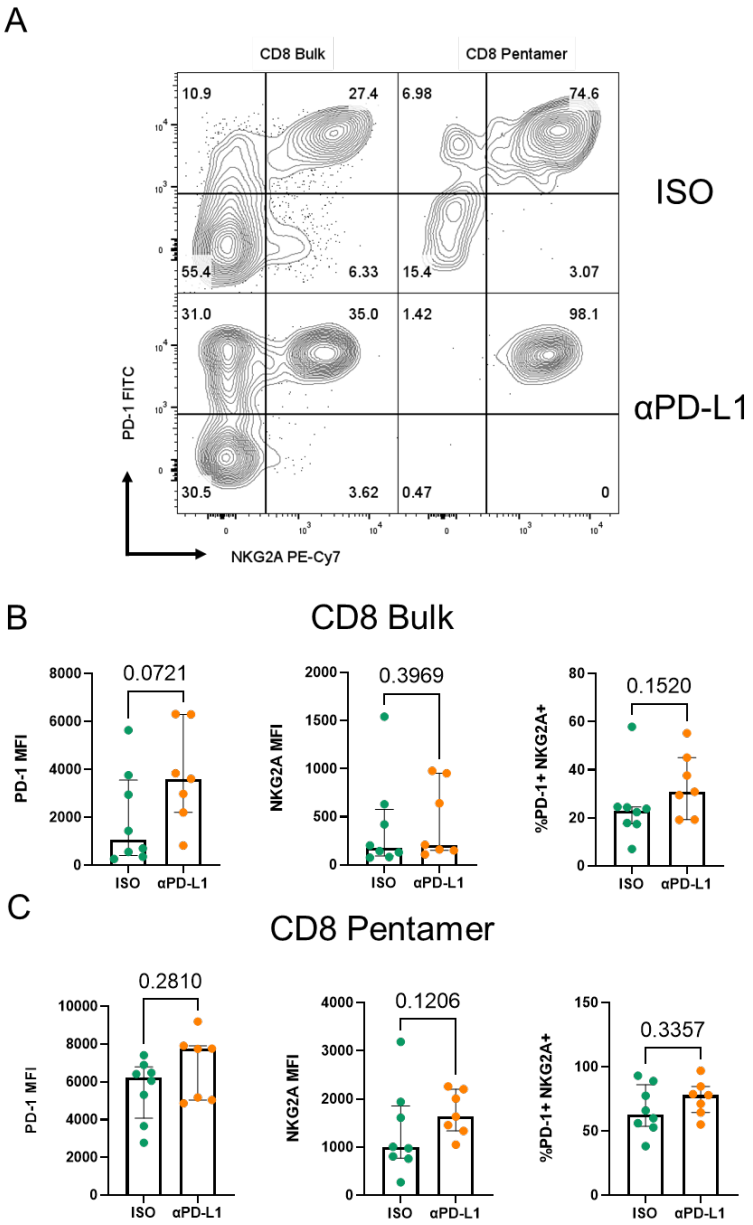

Figure 4.7 ***Analysis of inhibitory receptor expression in MC38 tumour infiltrating CD8 T cells following day 8&11 PD-L1 blockade in Nur77 Tempo mice.*** *A) Representative flow plots of PD-1 and NKG2A expression in bulk and pentamer⁺ CD8⁺ tumour infiltrating T cells after treatment with αPD-L1 or isotype control. B&C) Quantification of (A). Statistical test shown are Mann-Whitney. Error bars indicate median and inter-quartile range. N=7-8/group.*

(Sandu etal., 2020), but only six hours after treatment. Furthermore, others have described a TCF1/SLAMF6^{+} TIM-3^{-} T_{PEX} population that are the selective responders to ICB therapy. It may be that in our experiment, there was an increase in FT Blue expression, but this only occurred in a small subset of CD8^{+} T cells that we were not able to gate on with our staining panel and occurred for only a short time.

In order to observe this hypothesised increase to FT Blue expression, we repeated our experiment but culled the mice for analysis six hours after one dose of αPD-L1 therapy at day 12 (Figure 4.8.A). Within the PD-1^{+} population of TILs, we gated on SLAMF6^{+} TIM-3^{-} T_{PEX} and SLAMF6^{-} TIM-3^{+} T_{EX} populations, the majority of cells falling into the latter category (Figure 4.8.B). In the draining lymph node, the majority of PD-1^{+} cells were T_{PEX} (Figure 4.8.C). Treatment with αPD-L1 did not impact the T_{PEX}/T_{EX} ratio at this short time point (Figure 4.8.D). We could not observe any difference in FT Blue expression between isotype and αPD-L1 treated groups among either T_{PEX} or T_{EX} populations (Figure 4.9) (Figure 4.10.A&B). Nor could we detect any difference when we gated on all PD-1^{+} CD8^{+} T cells (Figure 4.10.C) or Pentamer^{+} CD8^{+} T cells (Figure 4.10.D). There was no difference in FT Blue frequency between T_{PEX} and T_{EX} populations irrespective of αPD-L1 treatment (Figure 4.10.E).

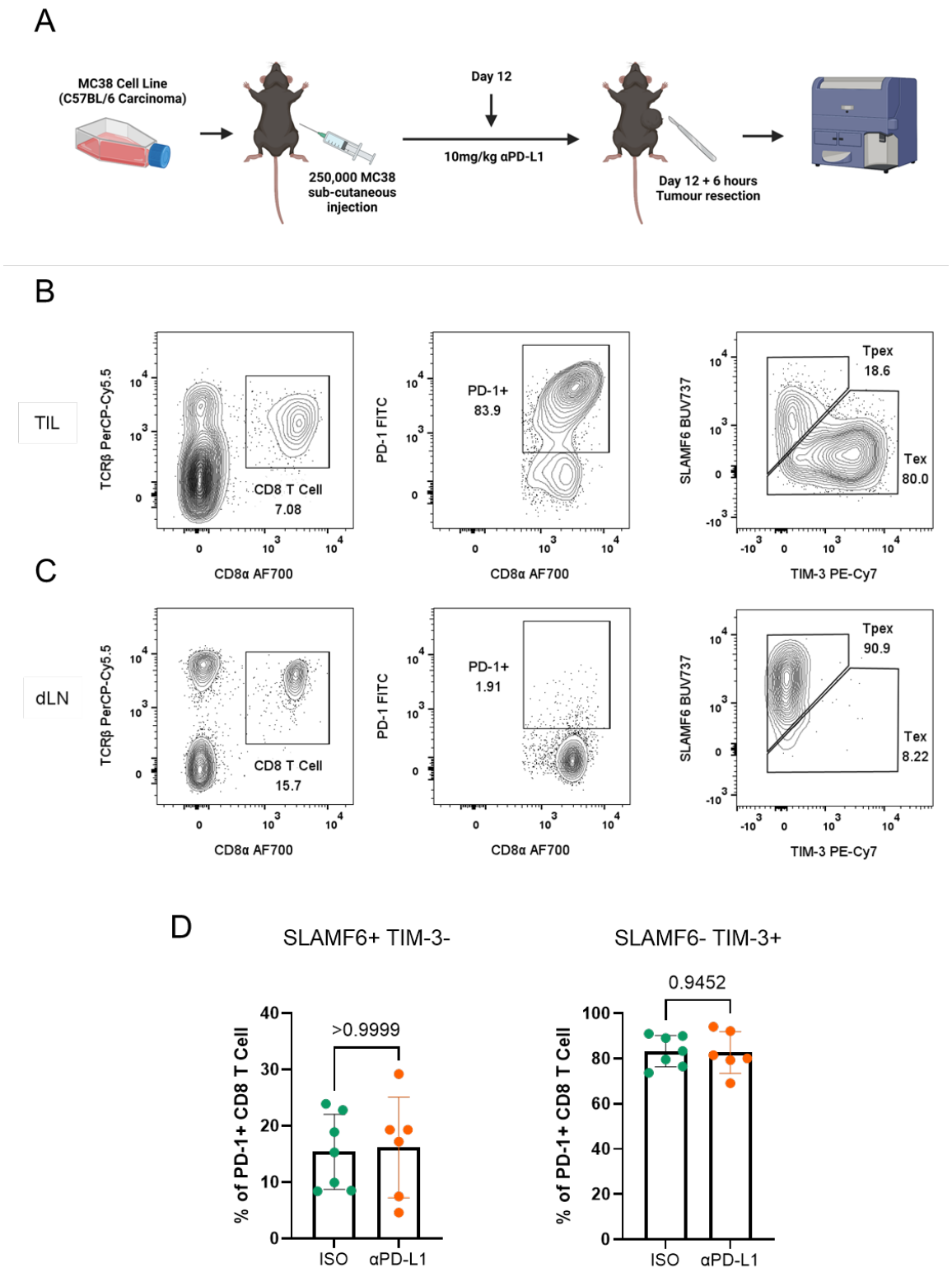

Figure 4.8. ***Example gating of T_{PEX} and T_{EX} CD8 T cells in MC38 tumours, quantification of population frequencies.*** *Gating strategy for T_{PEX} and T_{EX} cells in the tumour (A) and draining lymph node (B) of MC38 tumour bearing Nur77 Tempo mice. C) Quantification T_{PEX} and T_{EX} cells in MC38 tumours after treatment with αPD-L1 or isotype control. Statistical test shown are Mann-Whitney. Error bars indicate median and inter-quartile range. N=7-8/group.*

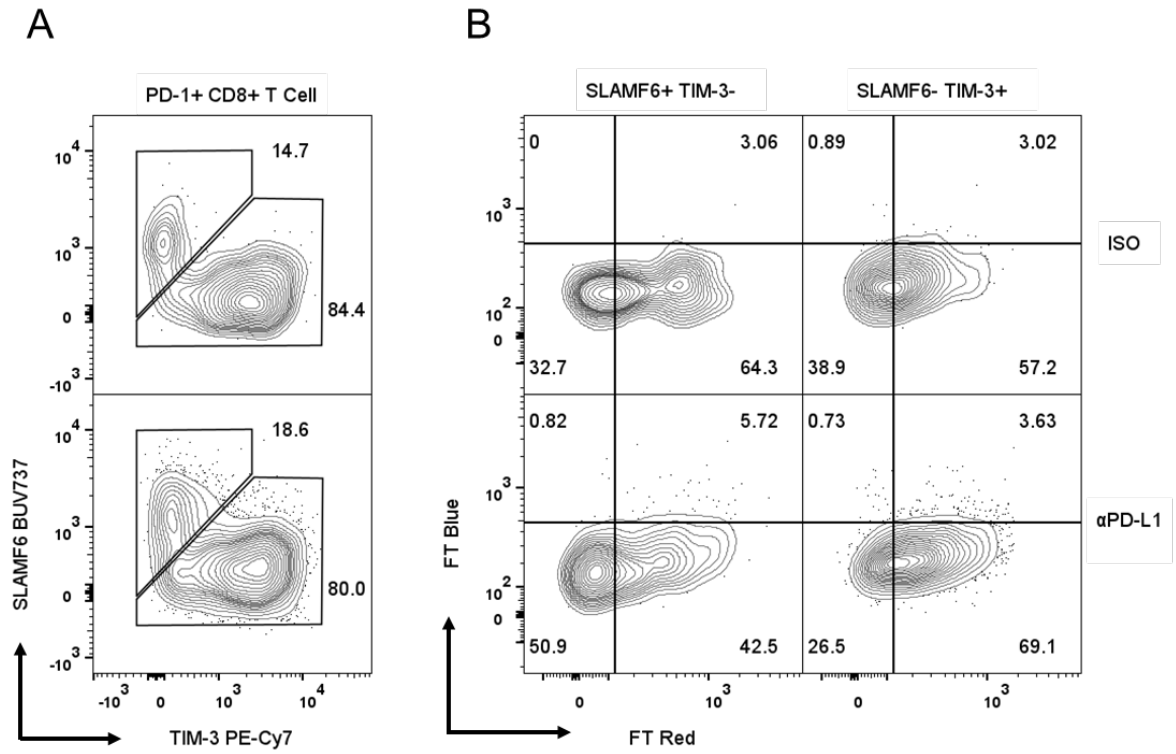

Figure 4.9. ***Analysis of FT expression in MC38 tumour infiltrating CD8 T_{PEX} and T_{EX} cells following day 12 PD-L1 blockade in Nur77 Tempo mice.*** *A) Gating of T_{PEX} and T_{EX} cells. B) Representative plots of FT Expression in T_{PEX} and T_{EX} cells after treatment with αPD-L1 or isotype control.*

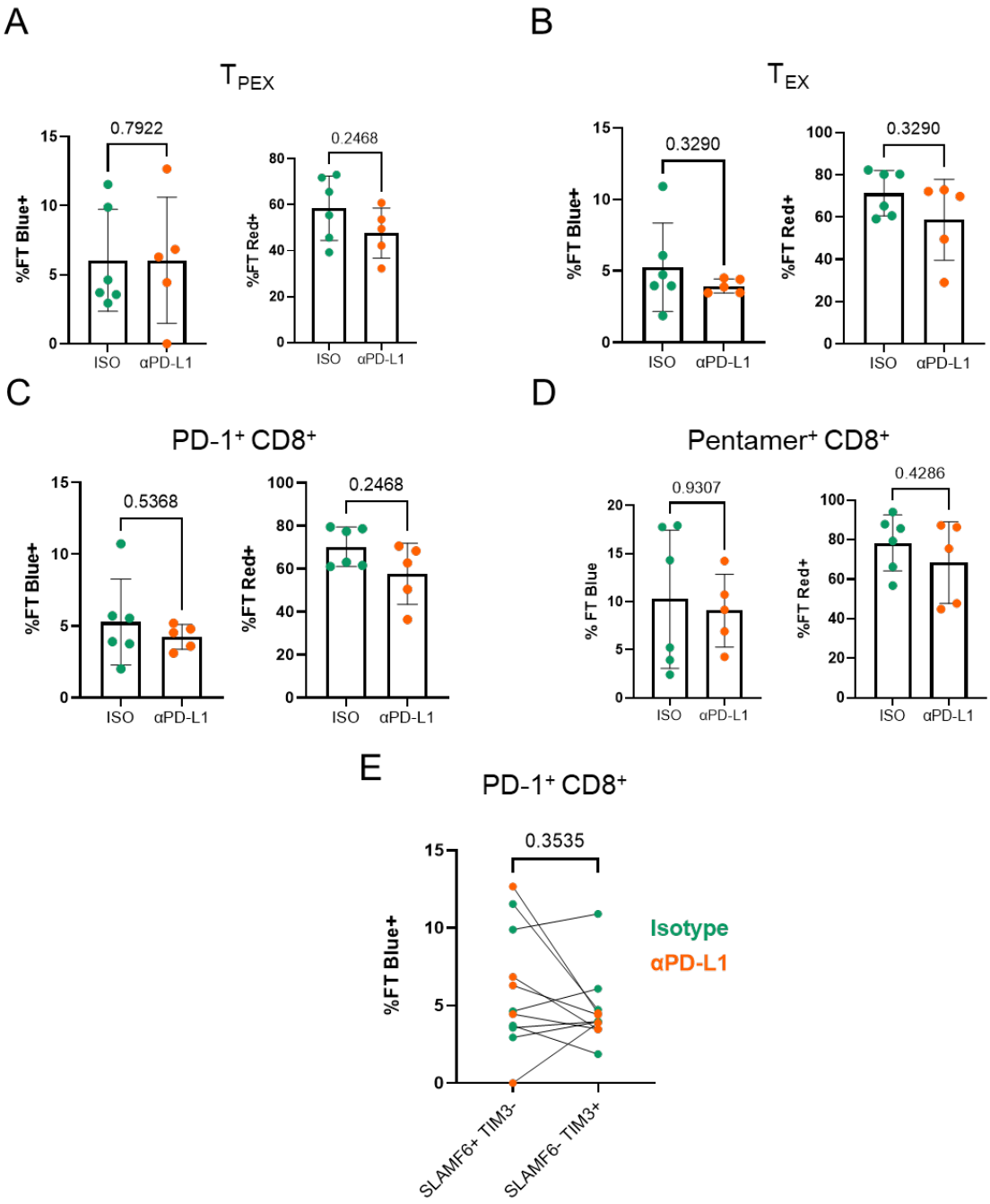

Figure 4.10 ***Analysis of FT expression in MC38 tumour infiltrating CD8 T cells following day 12 PD-L1 blockade in Nur77 Tempo mice.*** *Quantification of FT Blue and FT Red frequency in T_{PEX} cells (A), T_{EX} cells (B), PD-1⁺ CD8⁺ T cells (C), Pentamer⁺ CD8⁺ T cells (E). Comparison of FT Blue frequency in T_{PEX} and T_{EX} cells from paired samples (F). Statistical test shown are Mann-Whitney (A-D) and Wilcoxon matched-pairs (F). Error bars indicate median and inter-quartile range*

Our in vitro work on splenic CD8$^+$ T cells has shown that Nur77 Tempo is more sensitive to lower strength TCR signals than Nr4a3 Tocky. Additionally, our previous work has shown that *Nr4a1* is more sensitive to shorter duration TCR signals than *Nr4a3* (Jennings and Elliot et al., 2020). Importantly, all this work was performed during an acute stimulation and on the populations of largely naïve and memory cells that reside in lymphoid tissue. Our previous work has shown that Nr4a3 Tocky reporter can be expressed in ~40% of CD8$^+$ TILs as late as day 14 with >90% of cells expressing both PD-1 and LAG-3 (Elliot et al., 2021). Work from others in the lab has shown that the intensity of Nr4a3 Tocky FT Blue increases following ICB (Dr. Lozan Sherif, unpublished data). Despite this, CD8$^+$ TILs did not express Nur77 Tempo FT Blue after >1 week of tumour development and were not sensitive to ICB. We hypothesised that there may be a reversal in the relative sensitivities of the two reporters during tumour development and something about the process of chronic stimulation elevated the TCR signalling threshold required for expression of *Nr4a1*. We also considered it possible that Nur77 Tempo may not be expressed due to a technical issue with the reporter. T cells undergo significant epigenetic re-wiring during chronic stimulation; during development of the mouse line, the BAC is inserted into random sites of chromosomal DNA. If the BAC were inserted into a region epigenetically accessible in naïve T cells but not chronic stimulated ones, for example proximal to the *Il2* locus, this may explain our findings in the MC38 tumour model.

In order to test these hypotheses, we grew tumours out to day 11 in two strains of the Nur77 Tempo line. We reasoned that if the BAC were inserted into an epigenetically inaccessible region, it would be unlikely to have happened in two different founder lines, were the chances of insertion into a similar genomic locus is highly unlikely. We also grew MC38 tumours in Nr4a3 Tocky mice to use as a comparator. We then injected the mice intra-peritoneally with an isotype control or 10mg/kg αCD3 stimulating antibody to give a very strong systemic TCR signal (Figure 4.11.A). After four hours we culled the mice and dissected tumours and draining lymph nodes for analysis. We

chose four hours post-stimulation as our previous work in chapter 3 had shown almost ubiquitous FT Blue expression in splenic $CD8^+$ T cells four hours after *in vivo* αCD3 injection (Figure 3.14). In the tumour draining lymph node, we saw a large upregulation of CD69 confirming that the antibody had circulated by four hours (Figure 4.11.B). When we stained $CD8^+$ TILs for CD3ε and TCRβ, we observed a reduction in staining after αCD3 injection compared to isotype control, as the stimulating antibody blocked binding between fluorophore conjugated antibodies and their epitopes (Figure 4.11.C). This confirmed that the stimulating antibody was able to access $CD8^+$ TILs.

In the Nr4a3 Tocky mice, there was a considerable amount of FT Blue expression in $CD8^+$ T cells of the isotype treated mouse, which was significantly increased when in the mouse treated with αCD3. In contrast, both strains of Nur77 Tempo mice had very low expression of FT Blue as previously observed and only showed very modest FT Blue upregulation after αCD3 treatment (Figure 4.12). We made the qualitative observation that those $CD8^+$ T cells that did turn FT $Blue^+$ had very low levels of FT Red expression and that a history of TCR signalling seemed to render $CD8^+$ T cells more refractory to Nur77 Tempo reporter expression. This phenomenon was limited to $CD8^+$ T cells, as expression of FT Blue was high in $CD4^+$ T cells of both isotype and αCD3 treated mice and was equivalent between Nur77 Tempo and Nr4a3 Tocky mice.

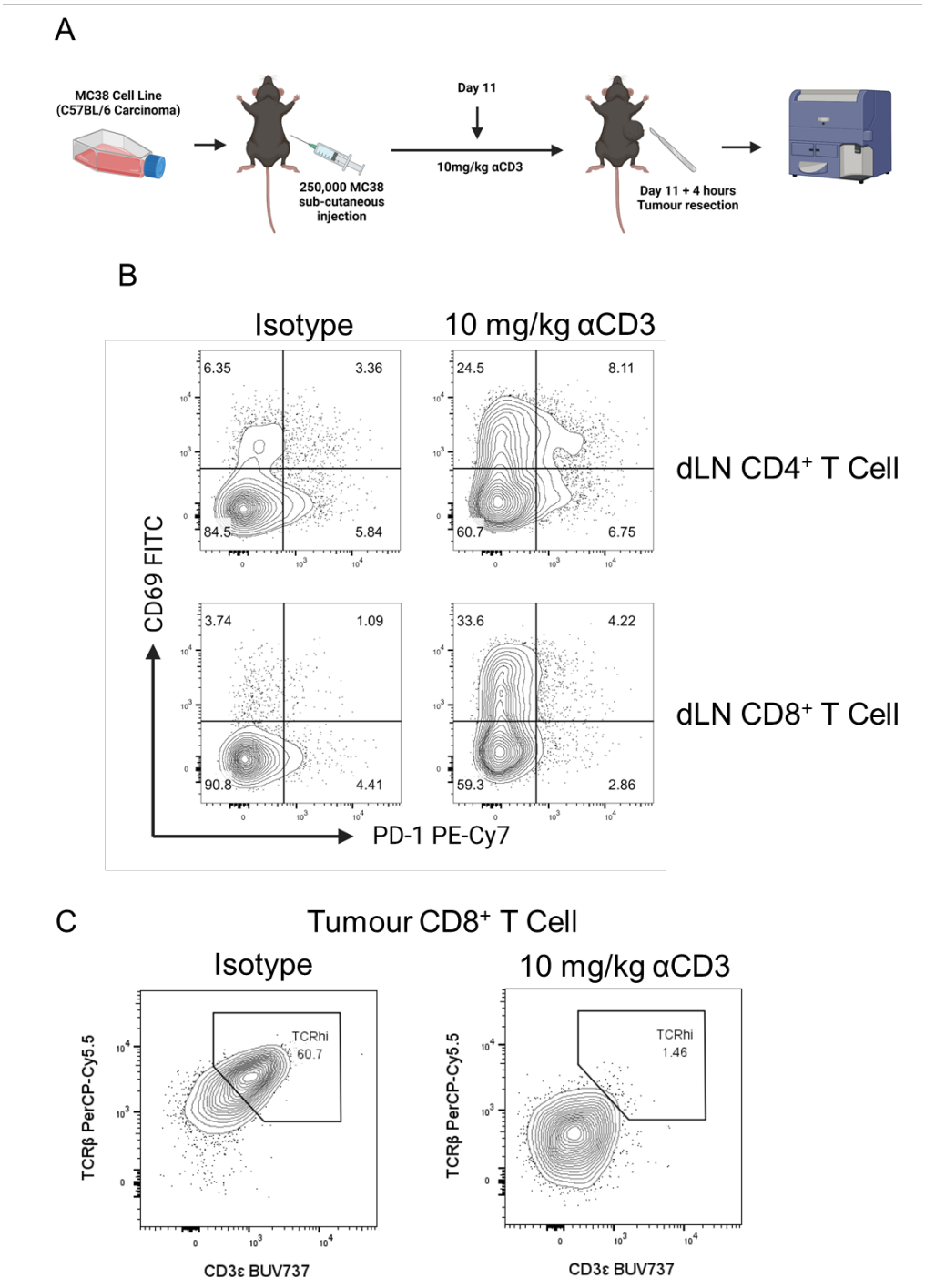

Figure 4.11. ***Analysis of CD69 and CD3 surface staining in MC38 tumour infiltrating and tumour draining lymph node CD8 T cells following day 11 αCD3 treatment in Nur77 Tempo mice.*** *Schematic detailing experimental design of αCD3 treatment at day 11 of MC38 tumour bearing Nur77 Tempo mice. B) CD69 and PD-1 expression in CD4⁺ and CD8⁺ T cells in the draining lymph node of MC38 tumour bearing mice after treatment with αCD3 or isotype control. C) CD3ε and TCRβ expression on tumour infiltrating CD8⁺ T cells after treatment with αCD3 or isotype control.*

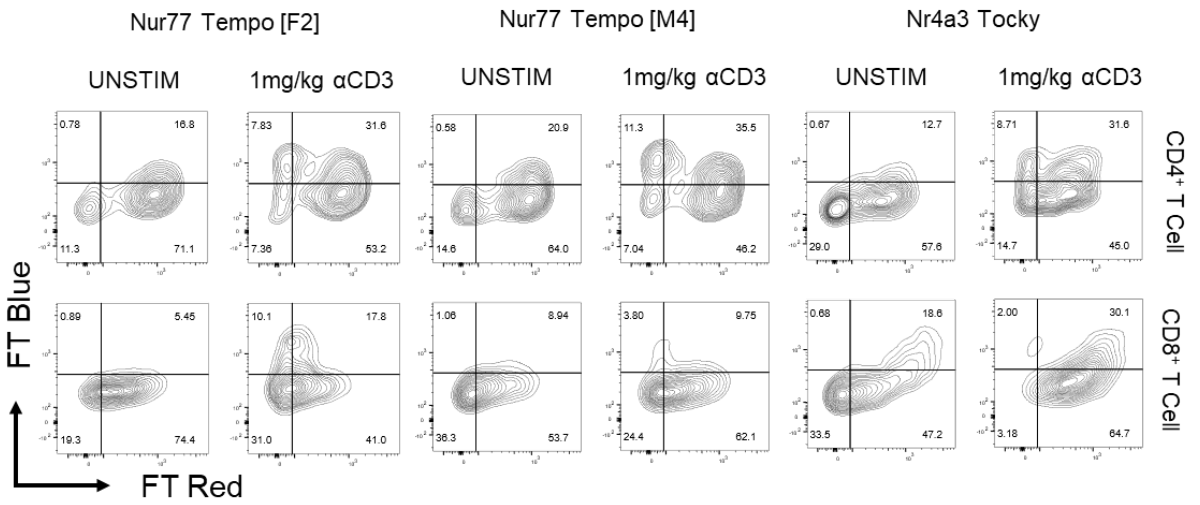

Figure 4.12. ***Analysis of FT expression in MC38 tumour infiltrating CD8 T cells following day 11 αCD3 treatment in Nur77 Tempo mice.*** *Expression of FT in CD4⁺ and CD8⁺ T cell infiltrating MC38 tumours of Nur77 Tempo and Nr4a3 Tocky mice following treatment with 1mg/kg αCD3 or isotype control.*

4.2.3 TCR Signalling Dynamics during *In Vitro* Exhaustion

We next sought to determine whether the shutting down of Nur77 Tempo reporter expression was due to the tumour microenvironment or was an inherent feature of chronic TCR stimulation. In order to study the effects of chronic TCR stimulation under controlled conditions, we sorted CD8⁺ T cells from pooled spleens and inguinal lymph nodes of Nur77 Tempo mice for an *in vitro* stimulation assay. We designed 3 conditions: naïve in which cells were not stimulated, acute in which cells were stimulated for two days and then rested for four days, or chronic in which cells were stimulated for all six days (Figure 4.13). CD8⁺ T cells were sorted with >90% purity (Figure 4.13), and the culture medium was supplemented with 1 ng/ml of IL-7 and 1 ng/ml of IL-15, important homeostatic cytokines for CD8⁺ T cells. Cells were stimulated with αCD3/αCD28 coated nanobeads that act as artificial APCs. The nanobeads are magnetic, this allows for their effective removal with a magnetic 96 well plate stand. Light microscope observation of the three

stimulation conditions after day 2 show cells in the acute condition have blasted and are clearly larger than the naïve condition but have had the magnetic beads effectively removed. The chronic condition contains nanobeads in an approximate 1:1 cell:bead ratio (Figure 4.14).

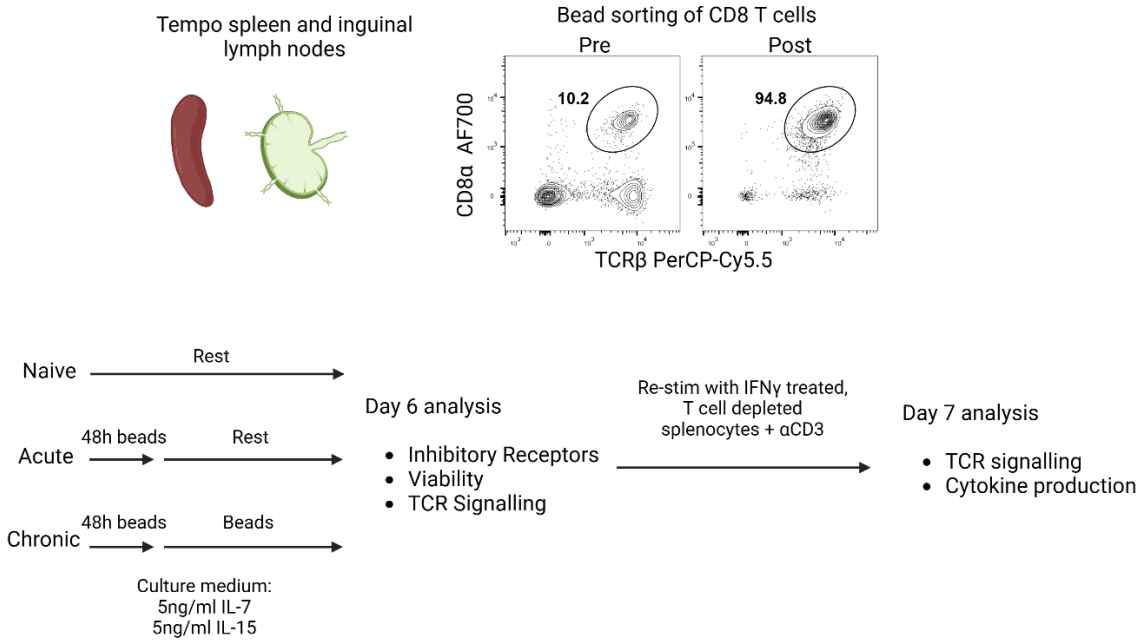

Figure 4.13. ***Schematic detailing experimental procedure of Naïve Acute and Chronic stimulation conditions of sorted CD8⁺ T cells form spleens and inguinal lymph nodes of Nur77 Tempo mice.*** *Naïve Acute and Chronic cells were re-stimulated with T cell depleted splenocytes and αCD3.*

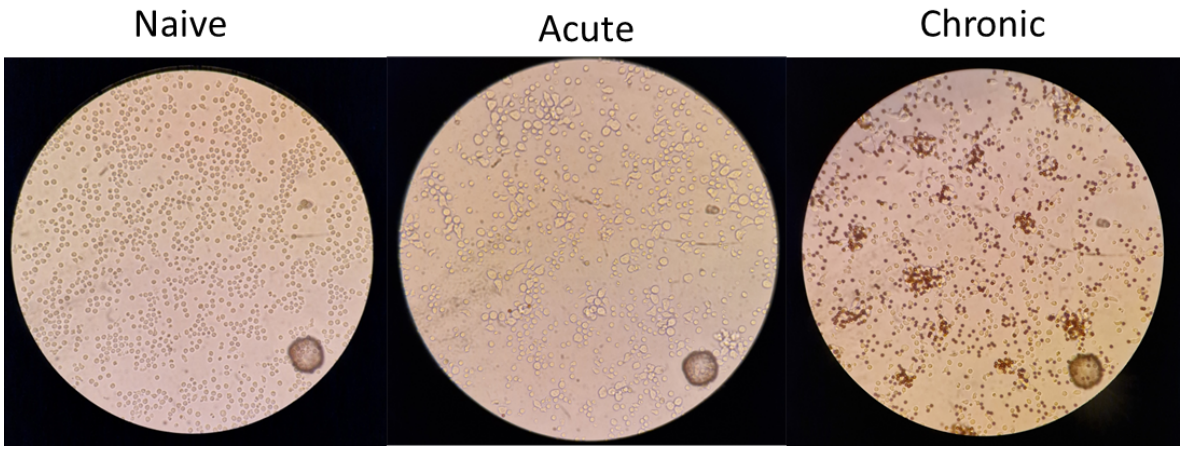

Figure 4.14. ***Representative brightfield images of Naïve Acute and Chronic stimulation conditions after 48 hours, following removal of magnetic beads from Acute and Chronic conditions and replacement of beads in Chronic condition.*** *Images taken at 4X zoom.*

Analysis at day 6 of the protocol found that whilst unstimulated cells were able to survive in the presence of IL-7 and IL-15, acute stimulation, and to a greater extent chronic stimulation, caused a decrease in cell viability (Figure 4.15.A). Visual observation of the culture showed overgrowth in the chronic stimulation condition and colour change of phenol red pH indicator suggesting acidification of the culture medium. Within the remaining live cells, expression levels of FT Blue were very low indicating a lack of ongoing TCR signalling (Figure 4.15.B). Chronic stimulation did drive a modest increase in the expression levels of some negative regulators of TCR signalling such as PD-1, LAG-3, and CD39 (Figure 4.15.C). However, the upregulation of TIM-3 and downregulation of SLAMF6 that is characteristic of $CD8^+$ T cell exhaustion was not observed.

We rested the cells overnight in IL-7 and IL-15 supplemented media to test their re-stimulation capacity. In order to model the effects of increased co-inhibitory receptor expression, we could not re-stimulate using nanobeads as they do not express the required ligands. Instead, we used a CD90.2 negative selection kit to remove all T cells from the splenocytes of another mouse, leaving a population of largely B cells (not shown). We stimulated the T cell depleted splenocytes overnight with 10 ng/ml of IFNγ, which caused an upregulation of PD-L1 and IA/IE, the primary ligands for PD-1 and LAG-3 respectively (Figure 4.16). We then co-cultured the rested $CD8^+$ T cells and the IFNγ primed APCs in a 1:1 ratio for four hours in the presence of 1 µg/ml αCD3, PdBU/Ionomycin, or an unstimulated control. PdBU is a phorbol ester and potent activator of PKC and ionomycin is a Ca^{2+} ionophore that drives calcium flux and activation of the NFAT pathway, this bypasses the TCR by directly activating downstream signalling pathways. These were used in combination with αCD3 stimulation as means to determine whether any chronic stimulation induced T cell dysfunction was due to inhibitory signalling at the immune synapse (impacting only αCD3 stimulation) or blockade of downstream signalling (impacting both).

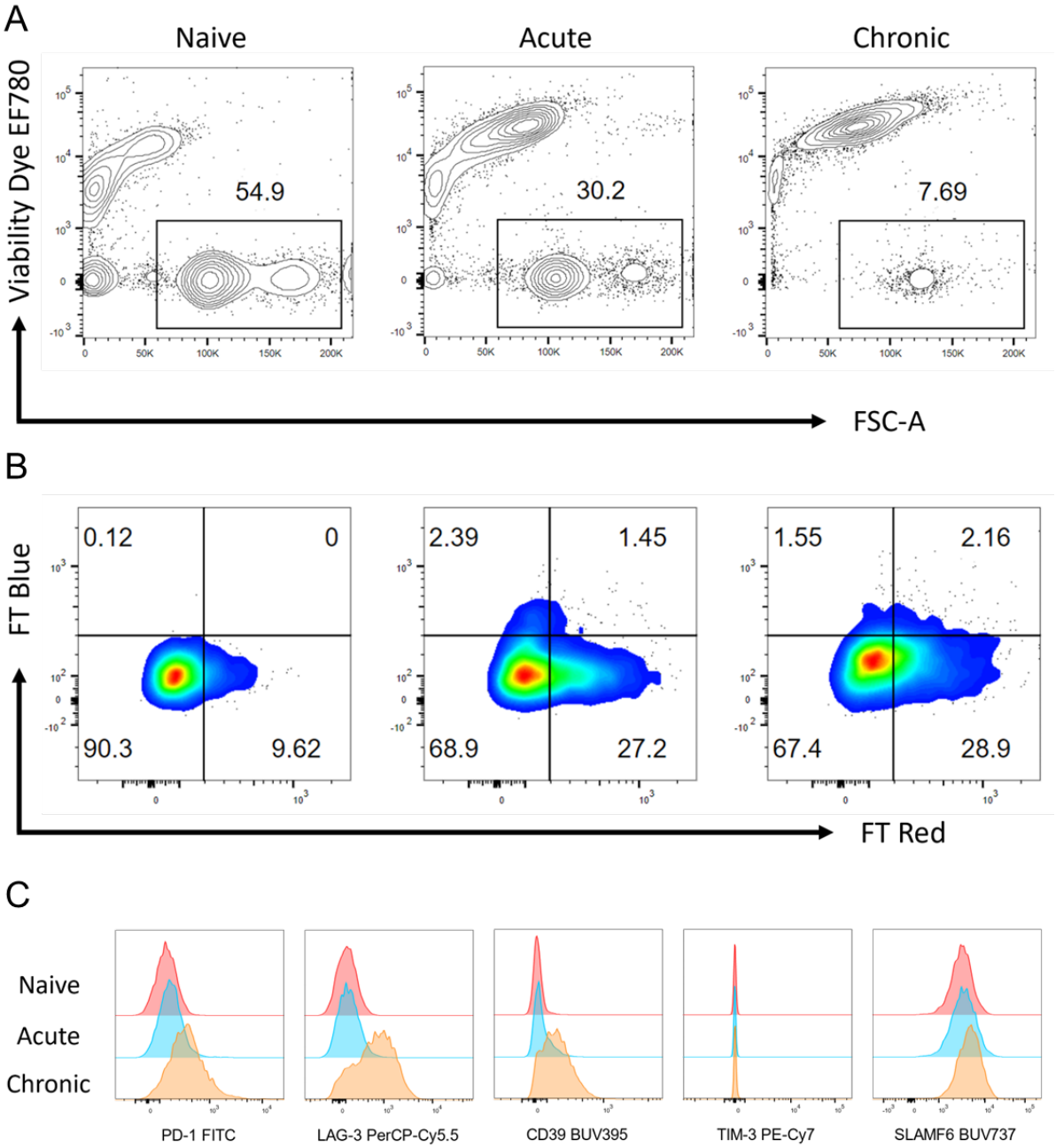

Figure 4.15 ***Analysis of viability, FT expression, and co-inhibitory receptor expression following naïve acute and chronic stimulation protocols.*** *Representative plots of A) Viability dye staining B) FT Expression C) Coinhibitory receptor expression in Naïve Acute and Chronic stimulation conditions detailed in Figure 4.14.*

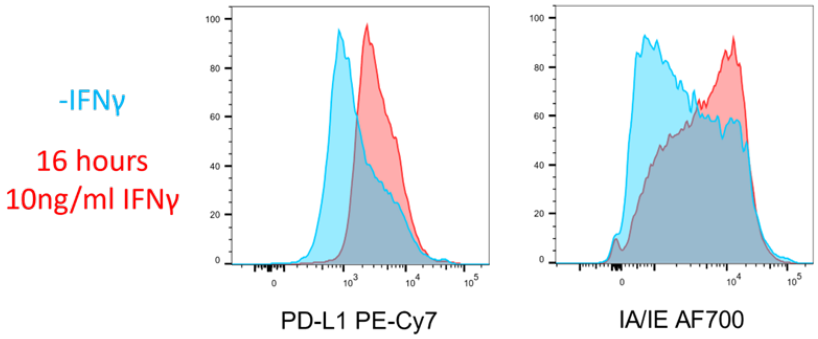

Figure 4.16 ***Pre-treatment of APCs with IFNγ increased co-inhibitory receptor ligand expression.*** *Expression of PD-L1 and IA/IE on T cell depleted splenocytes with and without 16-hour stimulation with 10 ng/ml recombinant IFNγ. Pre-gated on live singlets.*

To assay for functional T cell exhaustion, cells were re-stimulated in the presence of Brefeldin A and intracellular staining for IFNγ and TNFα was performed. Cytokine production was in fact higher in the cells that had been chronically stimulated suggesting that our protocol had not produced exhausted $CD8^+$ T cells (Figure 4.17). Cells from all conditions also expressed high levels of FT Blue upon re-stimulation (Figure 4.18), failing to re-capitulate our results from MC38 tumour experiments. The low viability and absence of $TIM\text{-}3^+$ $SLAMF6^-$ cells suggested that any exhausted cells that were generated during the chronic stimulation died.

In order to combat low levels of viability, we modified the assay to include 20 ng/ml of IL-2 to the media, and regular cell passaging to prevent overgrowth due to proliferation (Figure 4.19). This would act to prevent acidification of the culture medium but also to ensure an approximate 1:1 bead:cell ratio as the sorted $CD8^+$ T cells proliferate.

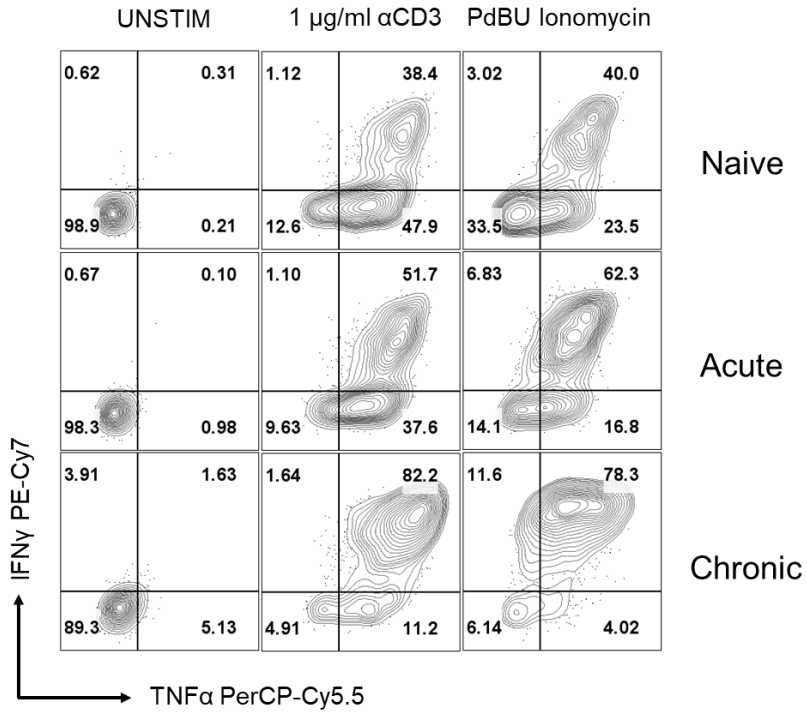

Figure 4.17. ***Analysis of cytokine production following naïve acute and chronic stimulation protocols and re-stimulation with T-cell depleted splenocytes.*** *Cells from Naïve Acute and Chronic conditions were re-stimulated with T cell depleted splenocytes and αCD3 or PdBU/Ionomycin for six hours with Brefeldin A. Representative plots show expression of TNFα and IFNγ.*

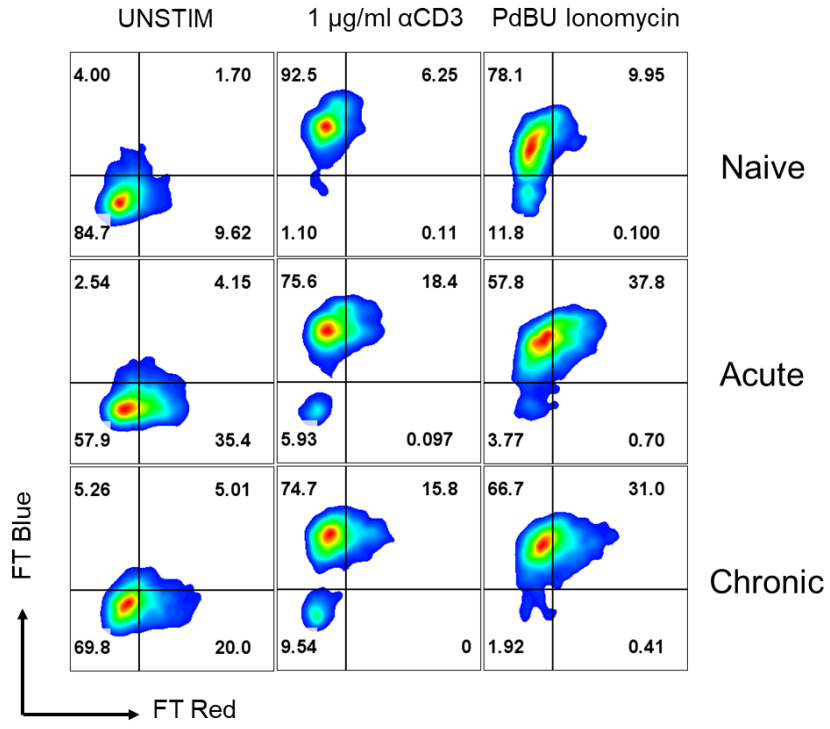

Figure 4.18. ***Analysis of FT expression following naïve acute and chronic stimulation protocols and re-stimulation with T-cell depleted splenocytes*** *Cells from Naïve Acute and Chronic conditions were re-stimulated with T cell depleted splenocytes and αCD3 or PdBU/Ionomycin for six hours. Representative plots show expression of FT.*

At day six, we observed higher levels of viability compared to our previous experimental design (Figure 4.20.A) and a small proportion of $CD8^+$ T cells expressing FT Blue (Figure 4.20.B). We observed a population of live TIM-3^+ LAG-3^+ cells (Figure 4.21.A) and downregulation of SLAMF6 (Figure 4.21.B), suggesting our protocol had effectively produced $CD8^+$ T cells with an exhausted phenotype. When we rested overnight and re-stimulated with IFNγ primed T cell depleted splenocytes and 1 μg/ml αCD3, chronically stimulated $CD8^+$ T cells showed a marked reduction in expression of TNFα and IFNγ (Figure 4.22.A). Acute, and to a greater extent chronic, stimulation caused a reduction in the intensity of FT Blue expression following re-stimulation (Figure 4.23). Although this iteration did produce live cells that express cell surface markers of $CD8^+$ T cell exhaustion, we were again not able to re-capitulate the almost absence of FT Blue expression that we observed in MC38 tumours.

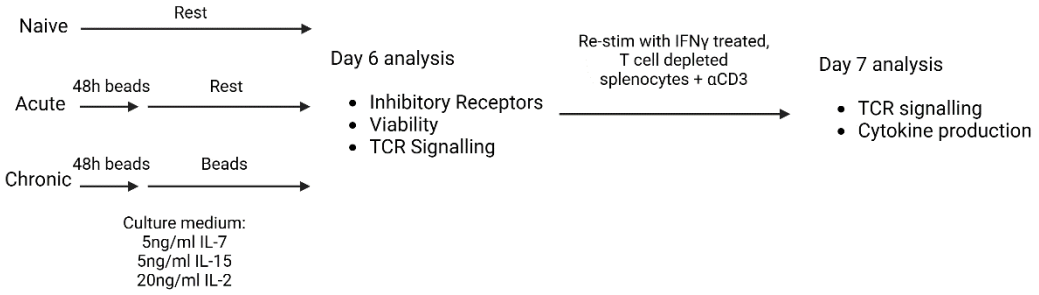

Figure 4.19. ***Schematic detailing experimental procedure of Naïve Acute and Chronic stimulation conditions of sorted CD8⁺ T cells form spleens and inguinal lymph nodes of Nur77 Tempo mice.*** *Naïve Acute and Chronic cells were re-stimulated with T cell depleted splenocytes and αCD3.*

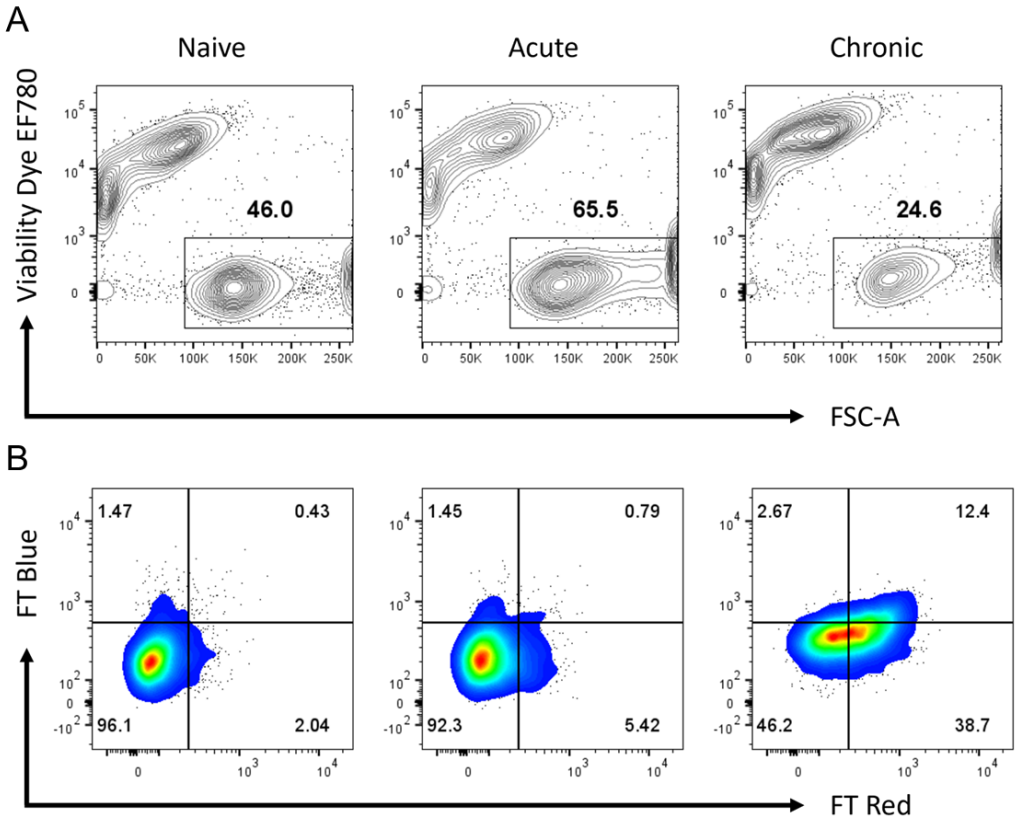

Figure 4.20. ***Analysis of viability and FT expression following naïve acute and chronic stimulation protocols.*** *Representative plots of viability dye staining (A) and FT expression (B) in Naïve Acute and Chronic stimulation conditions detailed in Figure 4.19.*

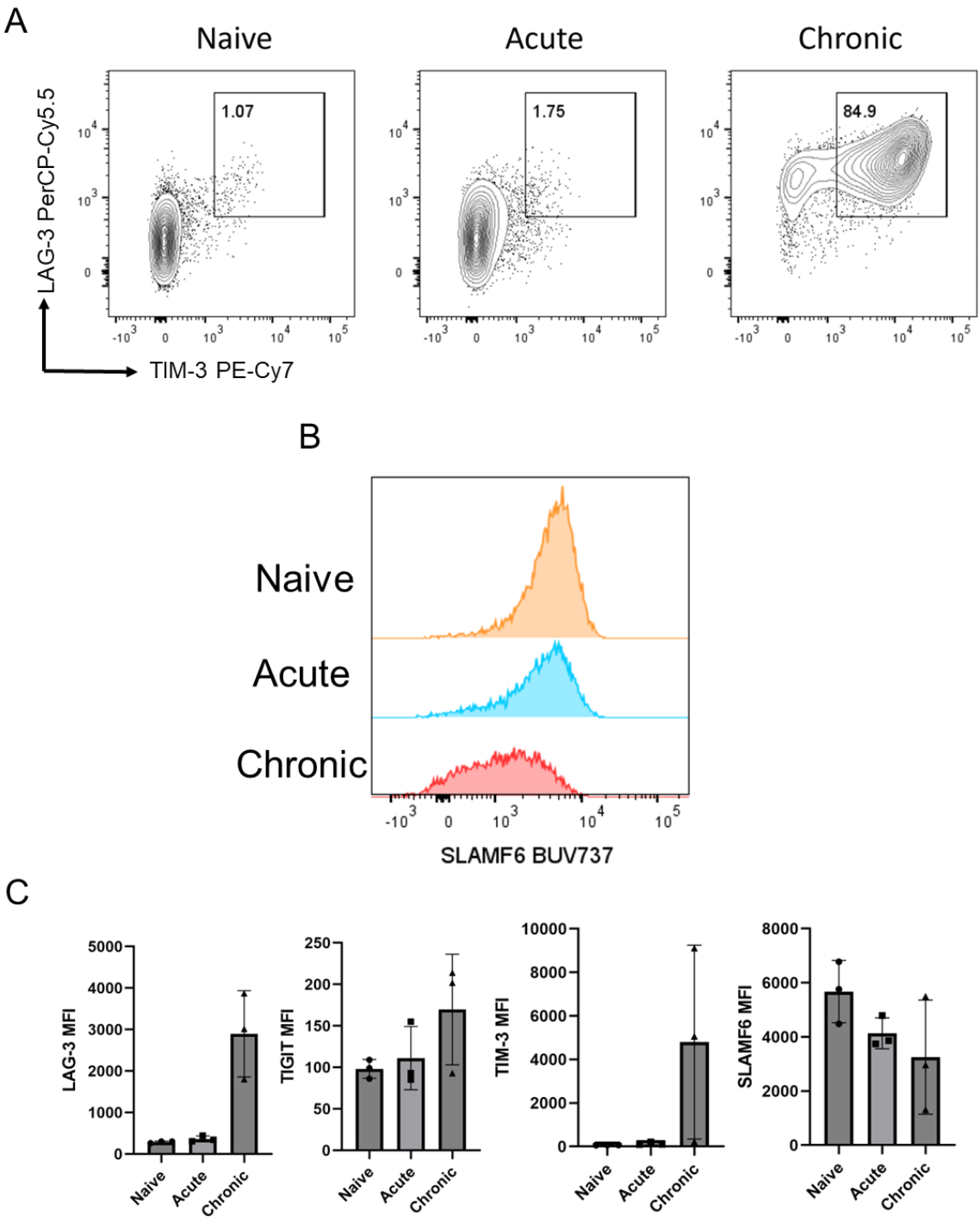

Figure 4.21. ***Chronic stimulation drives changes to cell surface inhibitory receptors.*** *Representative plots of LAG-3 and TIM-3 expression following naïve, acute or chronic stimulation protocols (A) histogram of SLAMF6 expression following naïve, acute or chronic stimulation protocols. C) MFI of LAG-3, TIGIT, TIM-3, SLMAF6 is plotted N=3. Bar graphs plot mean values and error bars indicate SEM.*

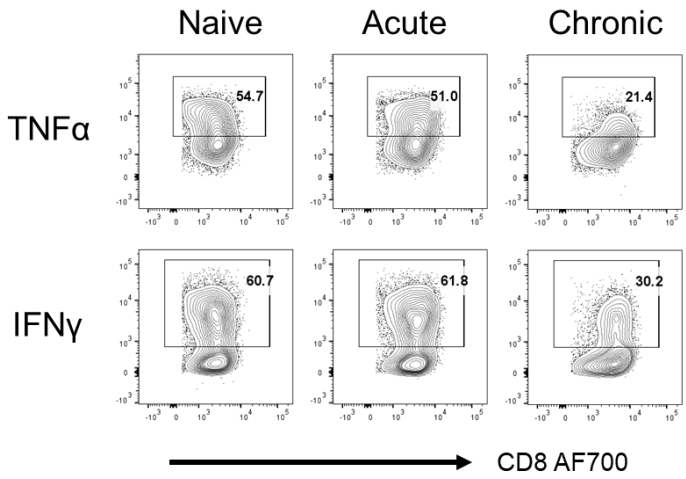

Figure 4.22. ***Chronic stimulation drives changes to cytokine production capacity upon re-stimulation.*** *Sorted CD8⁺ T cells from Naïve Acute and Chronic stimulation conditions were re-stimulated with T cell depleted splenocytes and 1 µg/ml αCD3 for six hours in the presence of Brefeldin A before intracellular cytokine staining and analysis by flow cytometry. Representative plots for TNFα, IFNγ.*

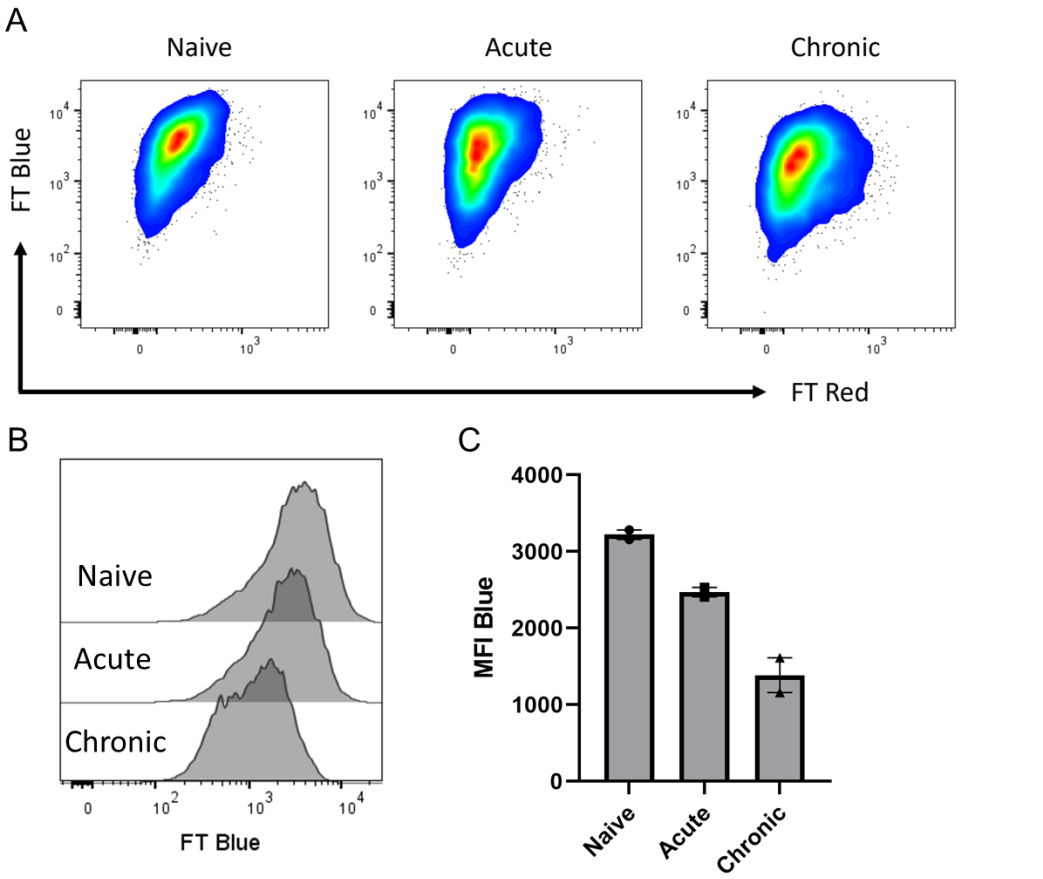

Figure 4.23 ***Chronic stimulation drives changes to FT Blue expression upon re-stimulation.*** *A&B) Representative plots of FT expression following re-stimulation of Naïve, Acute and Chronic conditions with t cell depleted splenocytes and 1 µg/ml αCD3 for six hours. C) MFI of FT Blue following re-stimulation. N=2.*

We reasoned that we may again be seeing death of those cells that become refractory to TCR induced *Nr4a1* expression. We modified the protocol to increase concentrations of cytokines in the culture medium to 10 ng/ml IL-7, 10 ng/ml IL-15, 100 ng/ml IL-2. Furthermore, others have described T cell dysfunction caused by TCR stimulation in the absence of co-stimulation. During an anti-cancer T cell response, T cells are primed within the lymph node which is a co-stimulation rich environment and then receive a second TCR signal after migration to the tumour, often in the absence of co-stimulation. In order to model this process more faithfully, we compared conditions where cells were stimulated with αCD3/αCD28 nanobeads for two days and then either rested (acute stimulation) or stimulated with plate bound αCD3 (chronic stimulation) for six days. To track the progression of the exhausted phenotype and TCR signalling status over time, we analysed the cells when they were passaged every two days (Figure 4.24). We also included Nr4a3 Tocky mice in this iteration to compare how TCR signalling was detected by the two reporters over time.

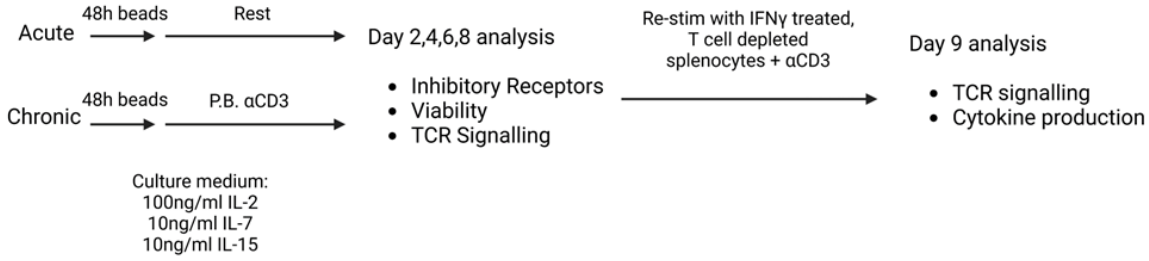

Figure 4.24 ***Schematic detailing experimental procedure of Acute and Chronic stimulation conditions of sorted CD8⁺ T cells form spleens and inguinal lymph nodes of Nur77 Tempo and Nr4a3 Tocky mice.*** *Acute and Chronic cells were re-stimulated with T cell depleted splenocytes and αCD3.*

Acute stimulation caused an uptick in expression of co-inhibitory receptors that was reduced when cells were rested without significantly impacting SLAMF6 expression (Figure 4.25.A). Chronic stimulation led to a progressive increase in the expression of co-inhibitory receptors and eventual downregulation of SLAMF6 (Figure 4.25.B). By day eight there was a significant increase in expression of PD-1, LAG-3, TIGIT, CD39, and TIM-3 (Figure 4.26) and the emergence of a proportion of TIM-3^{+} SLAMF6^{-} cells, indicative of terminal exhaustion (Figure 4.27).

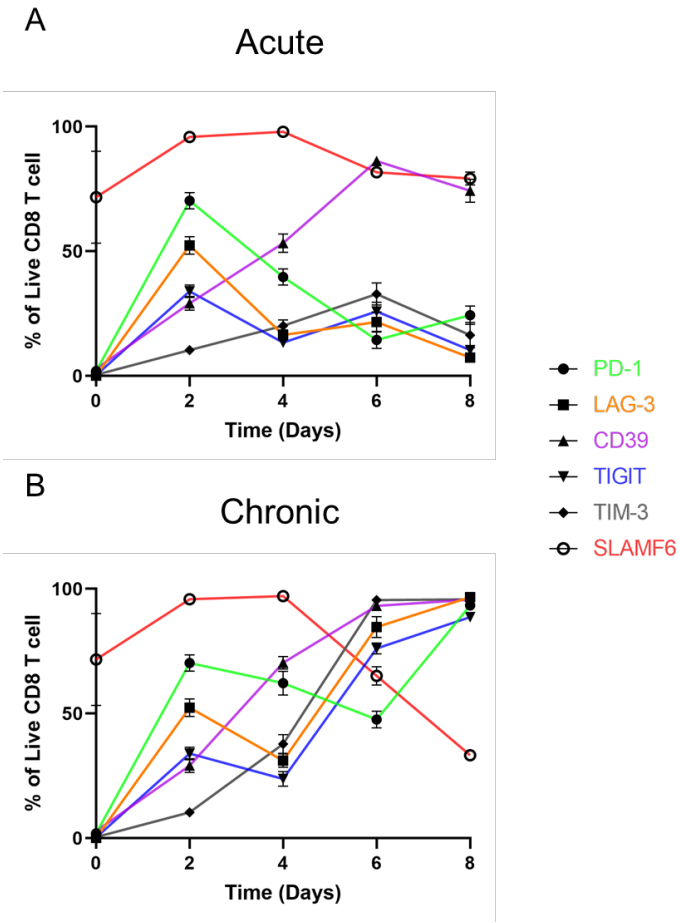

Figure 4.25. ***Chronic stimulation drives changes to cell surface inhibitory receptors.*** *A) Expression of indicated markers over time in Acute and Chronic stimulation conditions detailed in Figure 4.24. Error bars indicate mean and 95% CI. N=9.*

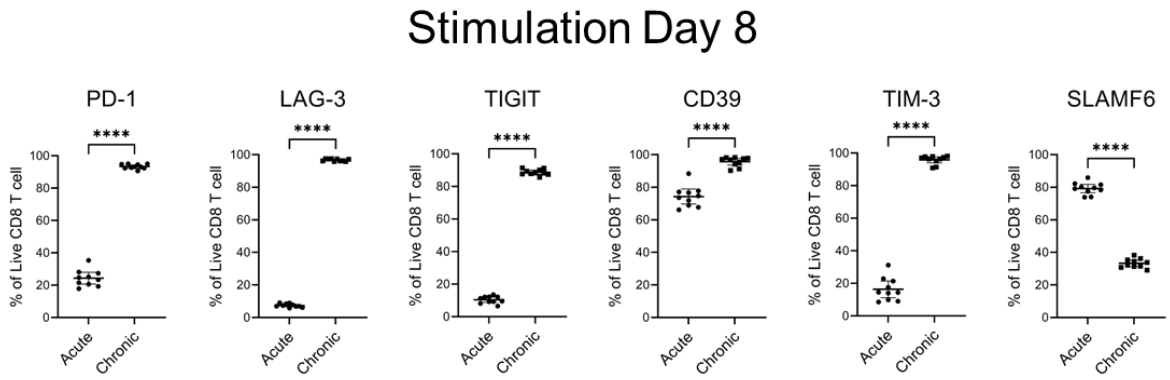

Figure 4.26. ***Chronic stimulation drives changes to cell surface inhibitory receptors.*** *Expression of indicated markers at day 8 of Acute or Chronic stimulation. Statistical test shown is paired t-test. *P ≤ 0.05, **P ≤ 0.01, ***P ≤ 0.001, ****P ≤ 0.0001. N=9.*

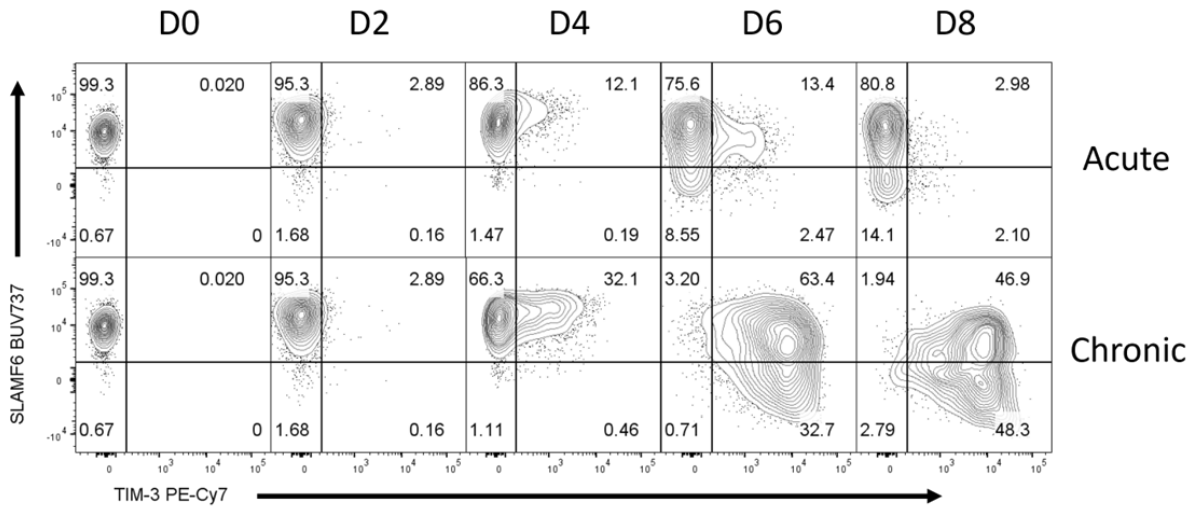

Figure 4.27. ***Chronic stimulation drives characteristic T_{EX} phenotype.*** *Representative plots of SLAMF6 and TIM-3 expression in Acute and Chronic stimulation conditions over time.*

Re-stimulation with IFNγ primed T cell depleted splenocytes showed a defect in IL-2 production in the chronic stimulation condition (Figure 4.28) but IFNγ and TNFα production remained intact (Figure 4.29).

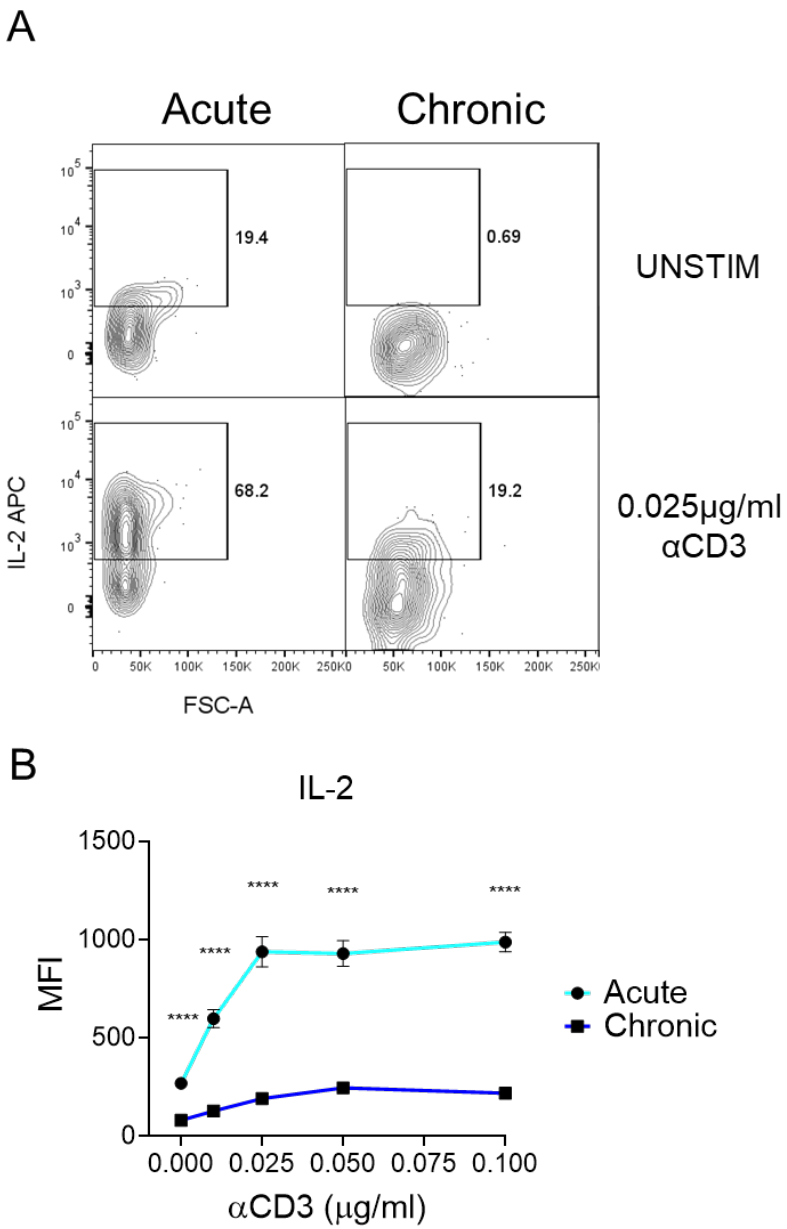

Figure 4.28. ***Chronic stimulation decreases IL-2 production capacity upon re-stimulation.*** *Cells form Acute and Chronic stimulation conditions were re-stimulated with T cell depleted splenocytes and a dose titration of αCD3 for six hours in the presence of Brefeldin A before intracellular cytokine staining and analysis by flow cytometry. A) Representative plots of IL-2 for 0.025 µg/ml αCD3 stimulation. B) MFI of IL-2 is plotted against αCD3 concentration for Acute and Chronic stimulation conditions. Error bars indicate mean and SEM. Multiple paired t-tests compare Acute vs Chronic at each αCD3 concentration. *P ≤ 0.05, **P ≤ 0.01, ***P ≤ 0.001, ****P ≤ 0.0001. N=9.*

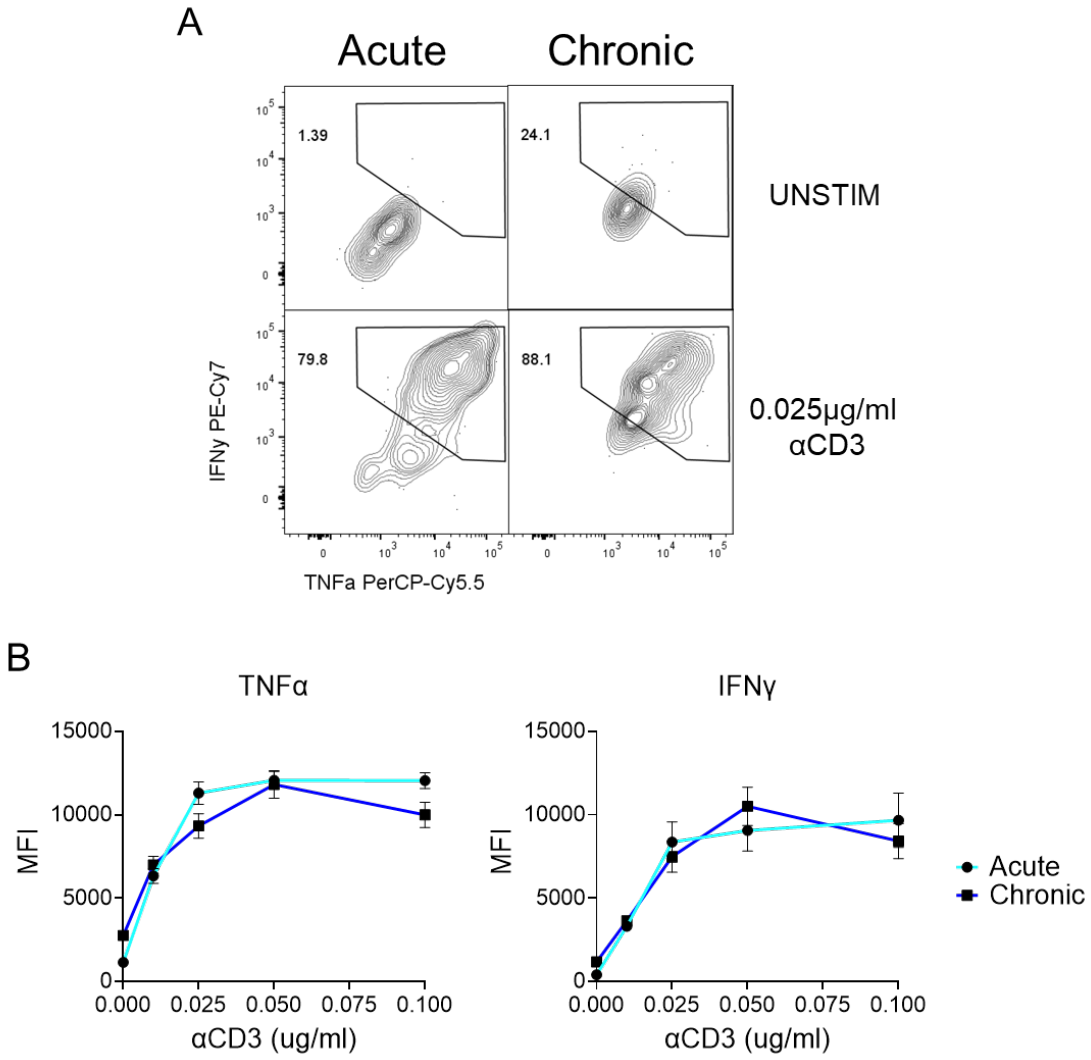

Figure 4.29. ***Chronic stimulation does not change capacity for production of IFNγ or TNFα upon re-stimulation.*** *Cells form Acute and Chronic stimulation conditions were re-stimulated with T cell depleted splenocytes and a dose titration of αCD3 for six hours in the presence of Brefeldin A before intracellular cytokine staining and analysis by flow cytometry. A) Representative plots of IFNγ and TNFα for 0.025 µg/ml αCD3 stimulation. B) MFI of indicated cytokine is plotted against αCD3 concentration for Acute and Chronic stimulation conditions. Error bars indicate mean and SEM. Multiple paired t-tests compare Acute vs Chronic at each αCD3 concentration. *P ≤ 0.05, **P ≤ 0.01, ***P ≤ 0.001, ****P ≤ 0.0001. N=9.*

Chronically stimulated $CD8^+$ T cells are much larger than those that received acute stimulation, this dramatically alters the auto fluorescent profile detected by some filters. For example, chronically stimulated cells autofluoresce in the 450/50 filter used to detect FT Blue, necessitating a wild-type mouse to act as a fluorescence minus one (FMO) control. It may be possible that autofluorescence in the 670/30 and 780/60 filters used to detect TNFα PerCP-Cy5.5 and IFNγ PE-Cy7 prevent a direct comparison between the acute and chronic stimulation conditions. Using the 0 μg/ml αCD3 re-stimulation control to set the negative gate on acute and chronic stimulation conditions (Figure 4.30) indicates a reduced frequency of IFNγ and TNFα expression in the chronically stimulated condition (Figure 4.31). Nevertheless, it is not possible to distinguish between autofluorescence and genuine cytokine expression in those cells that were not re-stimulated.

At day eight of chronic stimulation there was a marked difference in FT profiles between Nur77 Tempo and Nr4a3 Tocky mice (Figure 4.32.A). Nr4a3 Tocky mice expressed high levels of FT Blue whilst Nur77 Tempo FT Blue levels were hardly detectable over the wild-type control. The median intensity of FT Red can be used as a read-out of the history of reporter expression. Whilst expression is low at day 4, likely due to very high levels of proliferation diluting the fluorescent protein, by day six there is a much more significant accumulation of FT Red in Nr4a3 Tocky mice over Nur77 Tempo (Figure 4.32.B).

Upon re-stimulation, $CD8^+$ T cells that had received a prior acute stimulation were able to express FT Blue in both Nur77 Tempo and Nr4a3 Tocky mice (Figure 4.33.A). Cells that had received a prior chronic stimulation were only able to express FT Blue in Nr4a3 Tocky mice (Figure 4.33.A); intensity of the reporter was dependent on dose of αCD3 (Figure 4.33.B). These results re-capitulate the sustained expression of Nr4a3 Tocky, but not Nur77 Tempo, in $CD8^+$ T cells infiltrating MC38 tumours, confirming that the effect we saw was not dependent on the tumour

microenvironment. The association of Nr4a3 Tocky, but not Nur77 Tempo, expression with an exhausted phenotype indicates that prolonged NFAT signalling in the absence of AP:1 signalling may be responsible for terminal exhaustion differentiation.

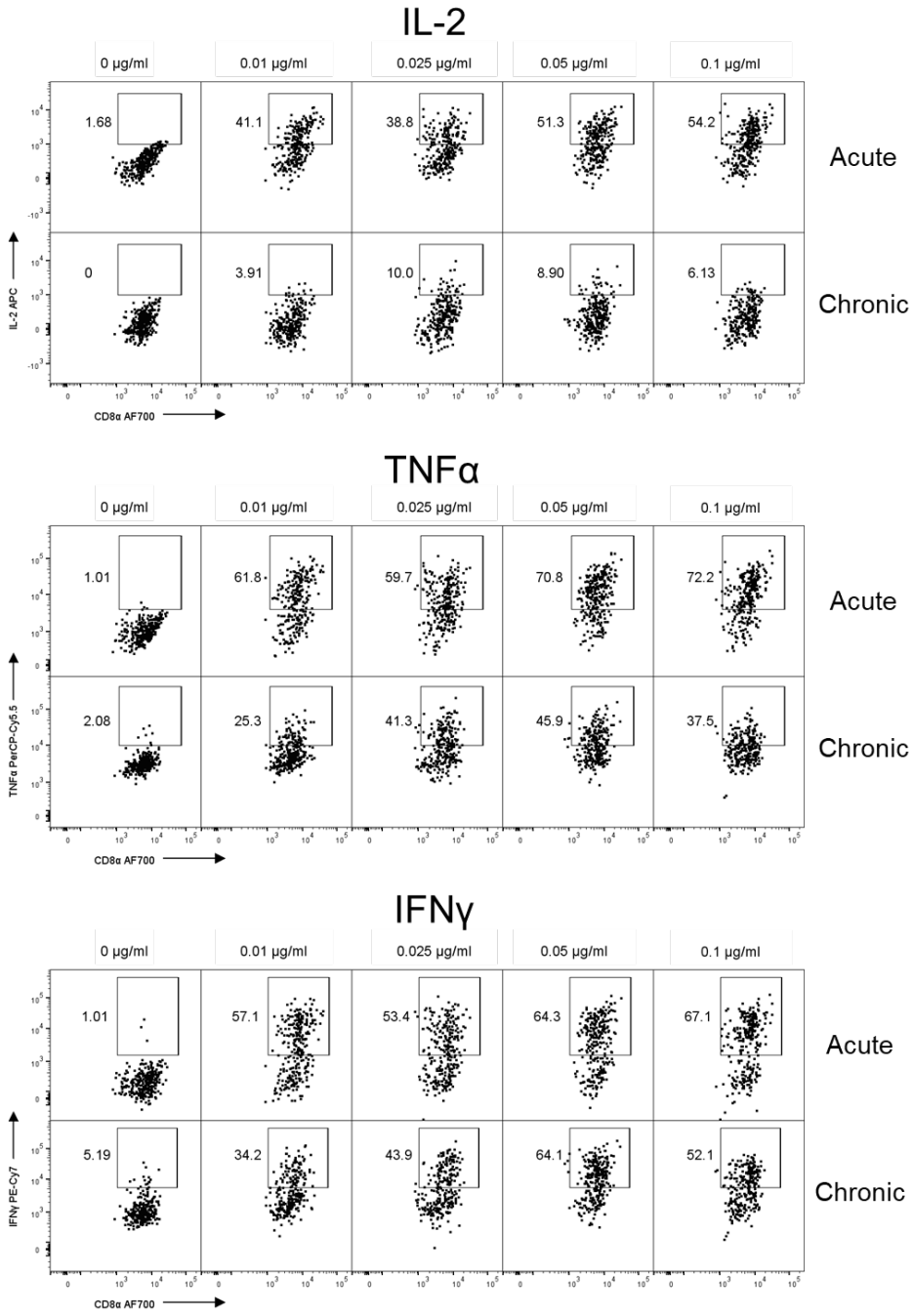

Figure 4.30. ***Re-gating of intracellular cytokine staining following re-stimulation.*** *Intracellular cytokine staining of cells from Acute and Chronic conditions (Figure 42) following re-stimulation. Gating strategy based on fluorescent intensity of cells from Acute and Chronic conditions co-cultured with T cell depleted splenocytes in the absence of αCD3 stimulation.*

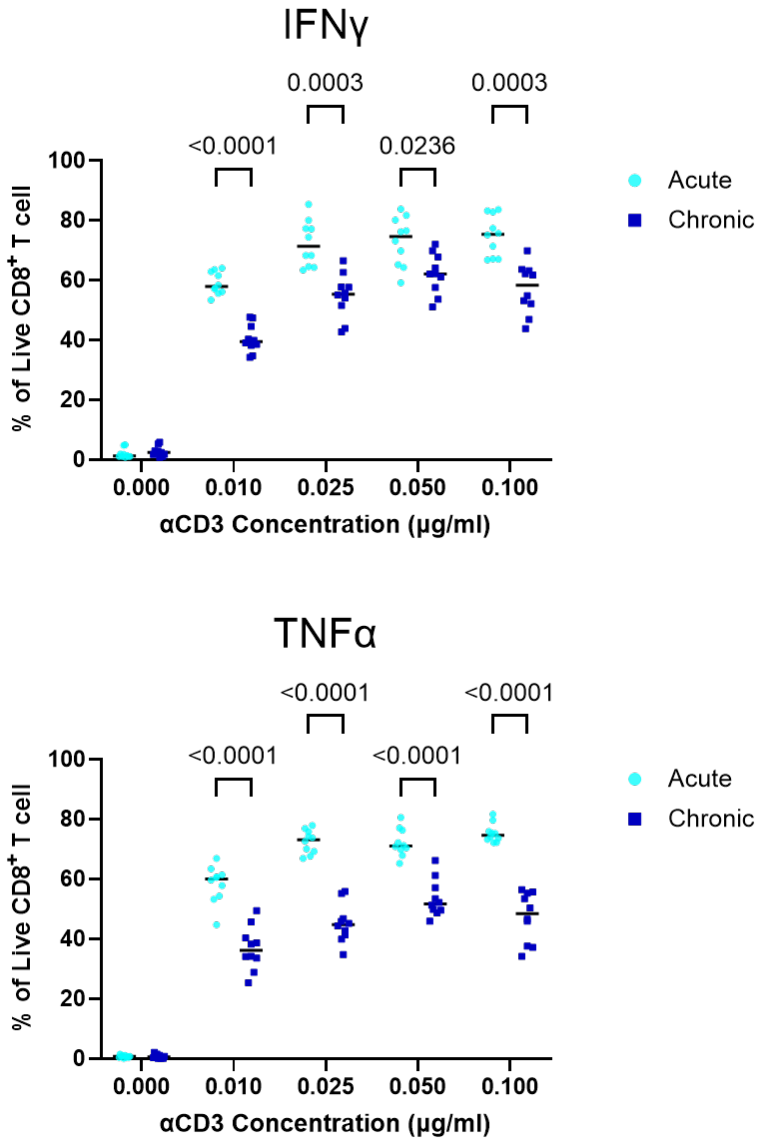

Figure 4.31. ***Quantification of intracellular cytokine staining following re-gating.*** *Quantification of IFNγ and TNFα expression, gating strategy as shown in Figure 4.30. Statistical test shown in paired two-way ANOVA with Geisser-Greenhouse correction and Šìdáks multiple comparisons between means of Acute and Chronic conditions. N=9.*

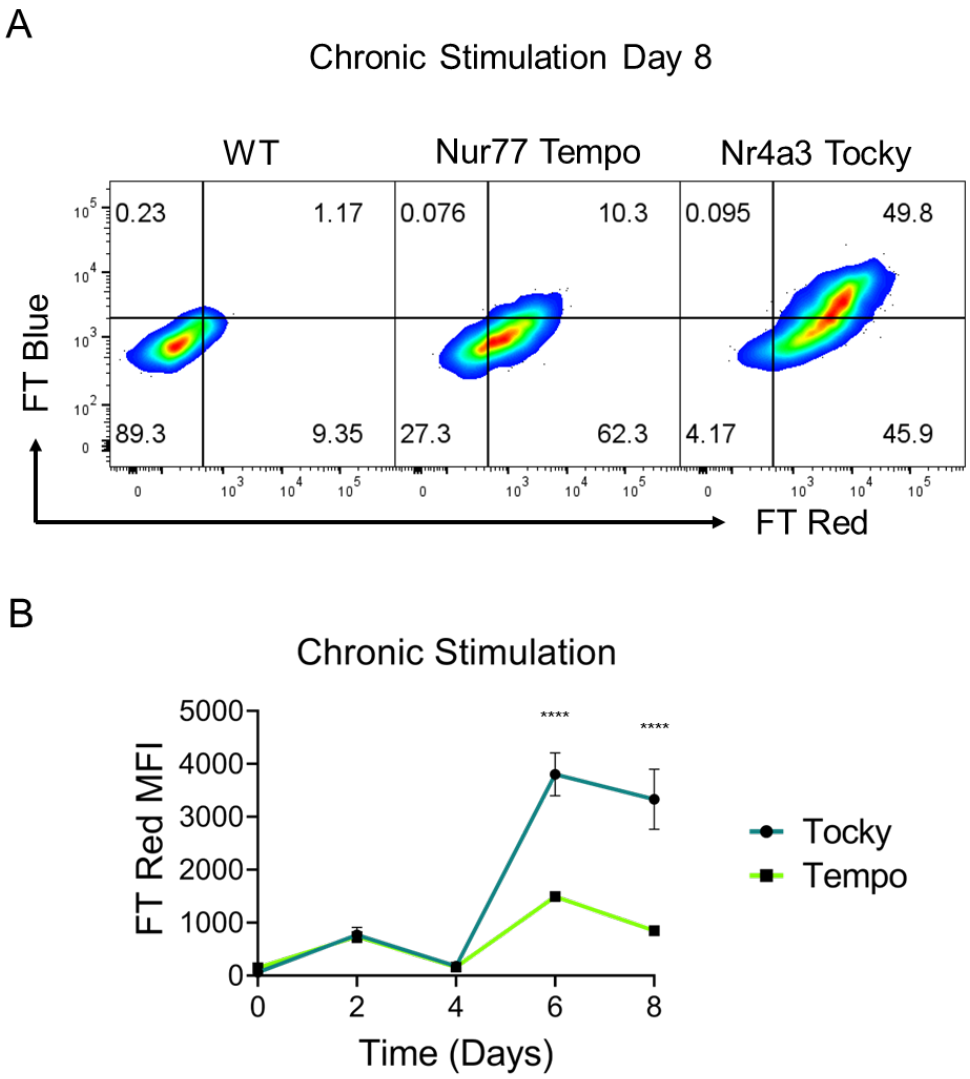

Figure 4.32. ***Chronic stimulation of sorted CD8 T cells drives persistent FT expression in Nr4a3 Tocky but not Nur77 Tempo mice.*** *A) Representative plots of FT expression after eight days of chronic stimulation in wild-type, Nur77 Tempo, or Nr4a3 Tocky mice. B) MFI of FT Red in Nur77 Tempo and Nr4a3 Tocky mice at different time points during chronic stimulation. Error bars indicate mean and SEM. Multiple paired t-tests compare Nur77 Tempo vs Nr4a3 Tocky at each indicated time point. *P ≤ 0.05, **P ≤ 0.01, ***P ≤ 0.001, ****P ≤ 0.0001. N=4-5/group.*

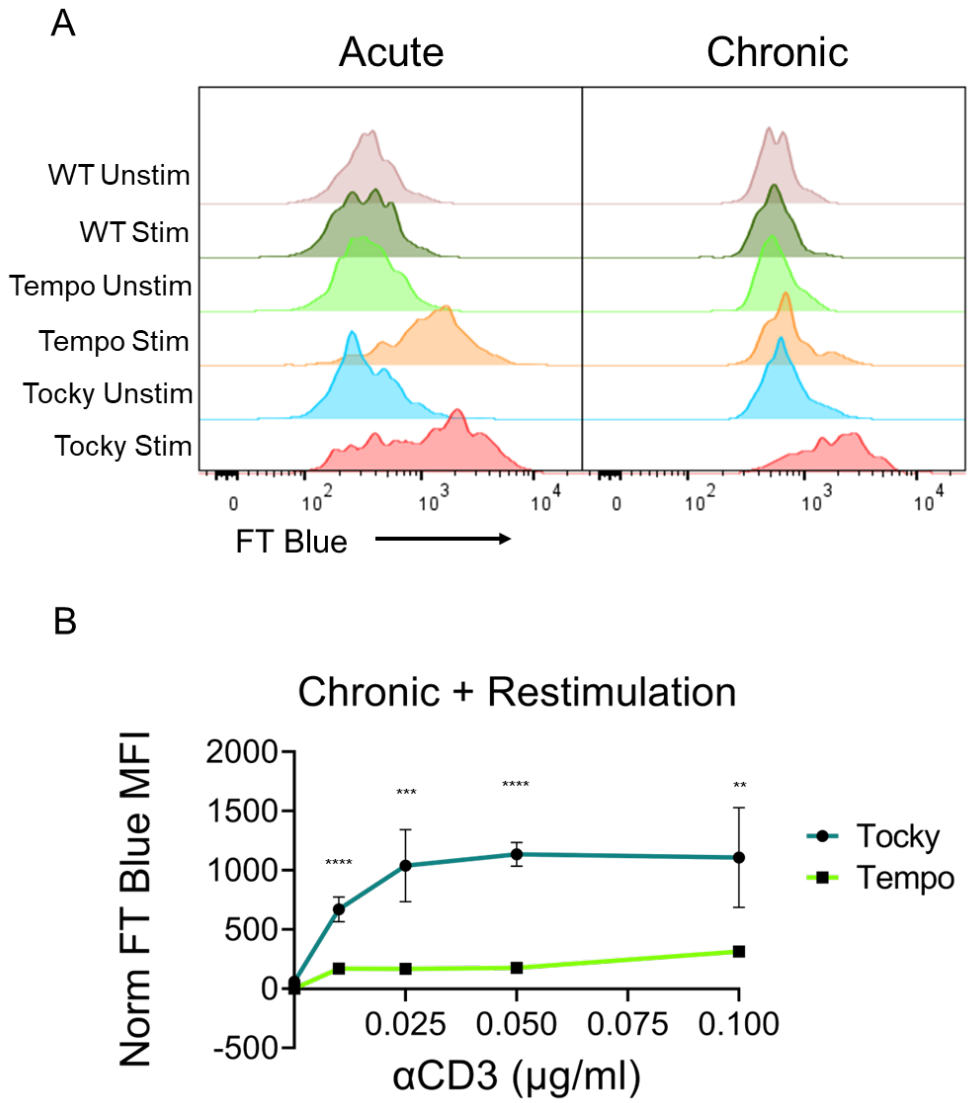

Figure 4.33. ***Chronic stimulation of sorted CD8 T cells drives persistent FT expression in Nr4a3 Tocky but not Nur77 Tempo mice.*** *Cells from Acute and Chronic conditions were re-stimulated with T cell depleted splenocytes and a dose titration of αCD3. A) Representative histograms of FT blue expression with or without re-stimulation with 0.05 μg/ml αCD3 in indicated mouse genotypes. B) Normalised FT Blue MFI plotted against αCD3 concentration. Data is normalised by (FT Blue MFI(X) – FT Blue MFI(Wild-Type)). Error bars indicate mean and SEM. Multiple paired t-tests compare Nur77 Tempo vs Nr4a3 Tocky at each indicated αCD3 concentration. *P ≤ 0.05, **P ≤ 0.01, ***P ≤ 0.001, ****P ≤ 0.0001. N=4-5/group.*

Recent work from the Wherry group has found that STAT5 signalling can antagonize the activity of TOX, preventing terminal exhaustion and prolonging an 'intermediate-exhausted' state, where cells that express cell surface markers of exhaustion retain effector functions such as cytokine production. We reasoned that the very high concentration of IL-2 used in our experimental design may be responsible for sustained cytokine expression despite chronic stimulation.

To test the role of NFAT signalling in exhaustion differentiation, we repeated the acute and chronic stimulation procedure, this time including a chronic + CsA condition, where 1 μM of cyclosporine A was added to the culture when cells were transferred to plate-bound αCD3. We also significantly decreased the concentration of IL-2 to 10 ng/ml and removed IL-7 and IL-15, to prevent the 'intermediate exhaustion' state described by Wherry and colleagues (Figure 4.34). We also planned to include FMO controls for intracellular cytokine staining to account for the different autofluorescent profiles of acute and chronically stimulated $CD8^+$ T cells.

Culture with 1 ng/ml IL-2 prevented proliferation of $CD8^+$ T cells (data not shown) to the point that they did not need to be passaged. Additionally, the viability was very low among all conditions (Figure 4.35). Whilst FT expression was almost absent in the acute stimulation condition, chronically stimulated cells expressed high levels of FT red (Figure 4.36) (Figure 4.37.B). FT Blue expression was higher in Nr4a3 Tocky compared to Nur77 Tempo in chronically stimulated cells (Figure 4.36) (Figure 4.37.A). Treatment with CsA reduced expression of Nr4a3 Tocky to acute stimulation levels whilst not significantly reducing Nur77 Tempo expression (Figure 4.36) (Figure 4.37.B), in agreement with our previous work (Figure 3.8). As before, chronic stimulation caused an increase in multiple co-inhibitory receptors (Figure 4.38.A) (Figure 4.39), although downregulation of SLAMF6 was not observed (Figure 4.38.B). CsA treatment significantly reduced the expression of PD-1, LAG-3, and TIGIT but CD39 and TIM-3 were unaffected (Figure 4.39).

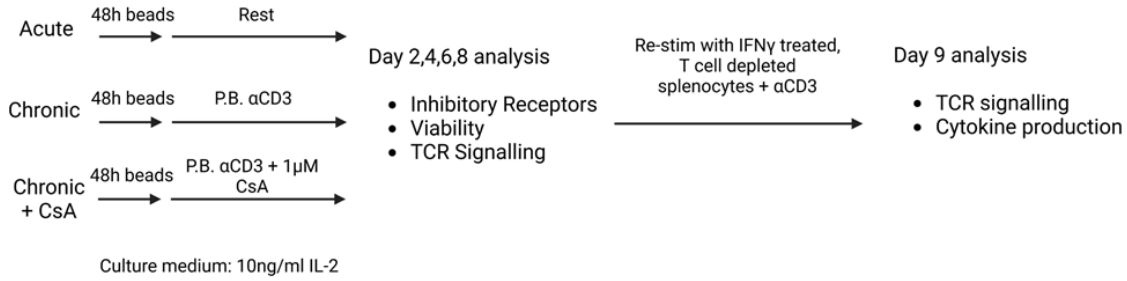

Figure 4.34. ***Schematic detailing experimental procedure of Acute, Chronic and Chronic + CsA stimulation conditions of sorted CD8⁺ T cells form spleens and inguinal lymph nodes of Nur77 Tempo and Nr4a3 Tocky mice.*** *Acute and Chronic cells were re-stimulated with T cell depleted splenocytes and αCD3.*

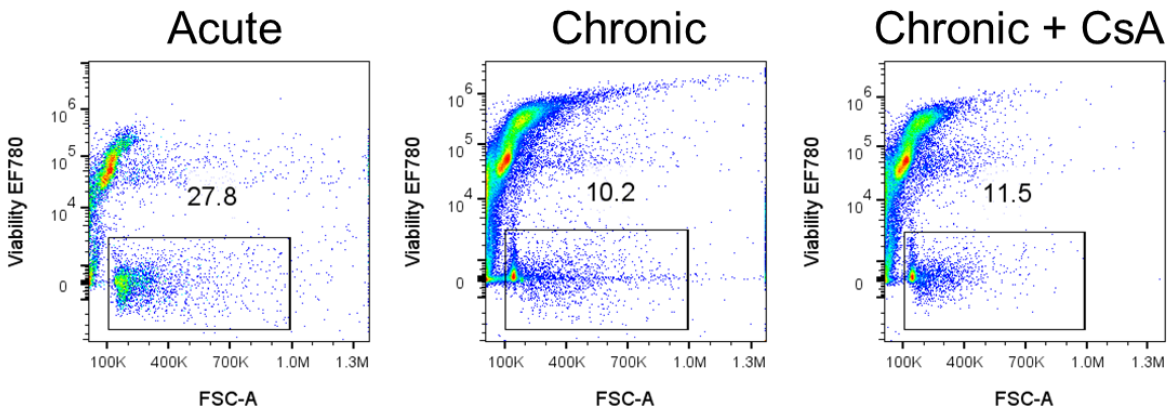

Figure 4.35. ***Chronic stimulation drives loss of viability in low IL-2 culture conditions.*** *Representative plots of viability dye staining for Acute, Chronic and Chronic + CsA conditions.*

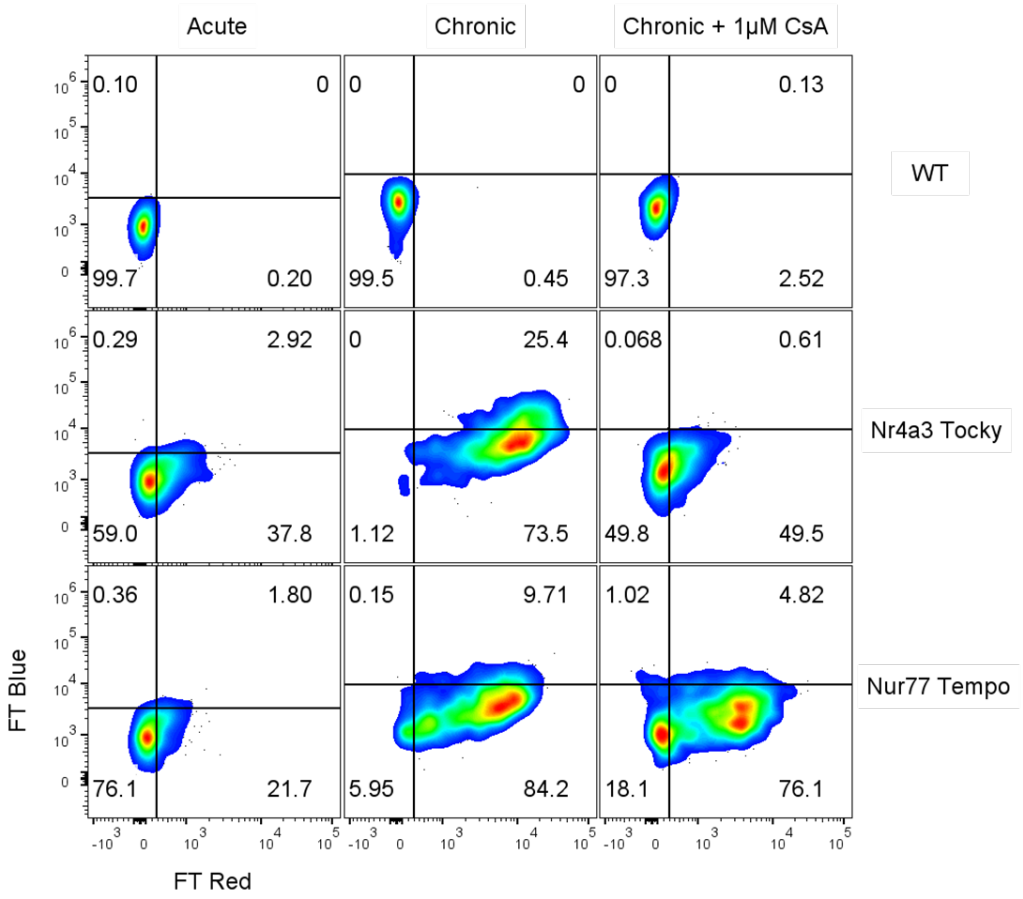

Figure 4.36. ***Cyclosporine reduces expression of FT Blue in Nr4a3 Tocky mice.*** *Representative plots of FT expression in Acute, Chronic, and Chronic + CsA conditions at day 8 in wild-type, Nur77 Tempo, and Nr4a3 Tocky mice.*

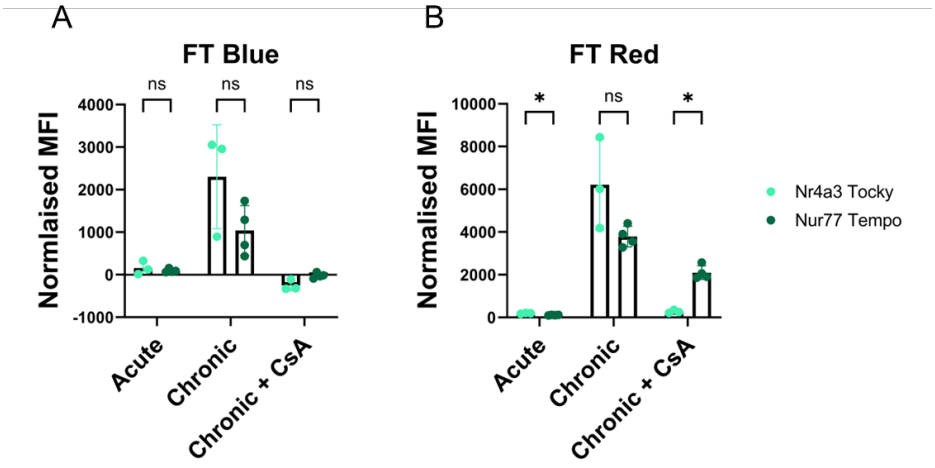

Figure 4.37. ***Cyclosporine reduces expression of FT in Nr4a3 Tocky mice.*** *Normalised MFI of FT Blue (A) and FT Red (B) in Acute, Chronic, and Chronic + CsA conditions in wild-type, Nr4a3 Tocky, and Nur77 Tempo mice. Data normalised by (MFI(X) – MFI(Wild-Type)). Statistical test is unpaired t-test. *P ≤ 0.05, **P ≤ 0.01, ***P ≤ 0.001, ****P ≤ 0.0001. N=3-4/group.*

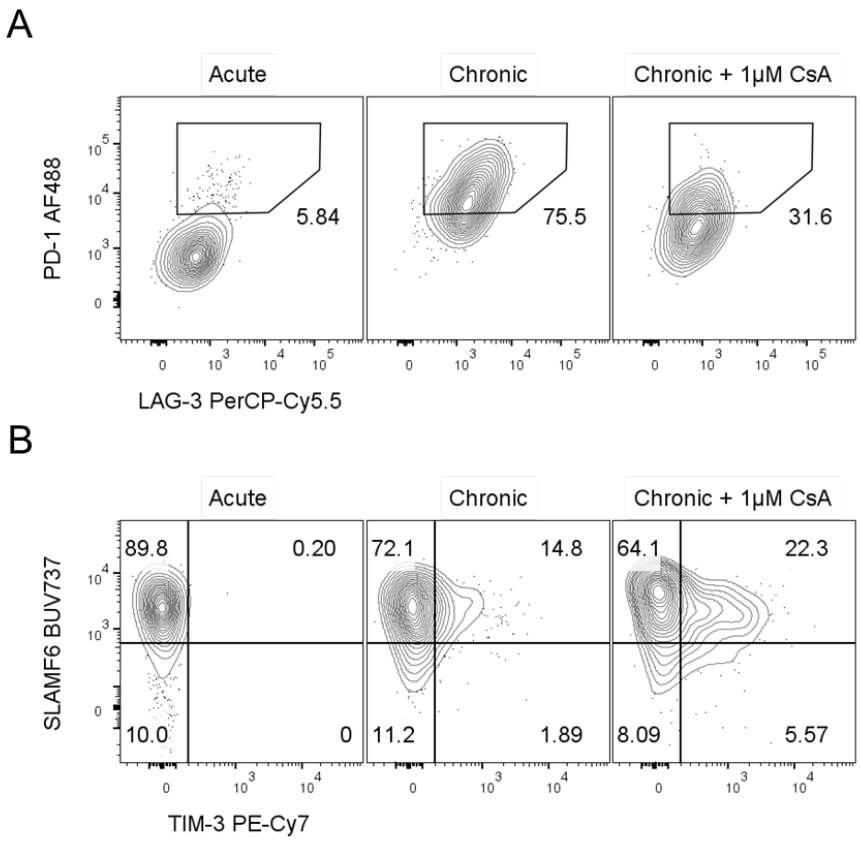

Figure 4.38. ***Cyclosporine reduces expression cell surface co-inhibitory receptors following chronic stimulation.*** *Representative plots of PD-1 and LAG 3 expression (A) and SLAMF6 and TIM-3 expression (B) in Acute, Chronic, and Chronic + CsA conditions at day 8.*

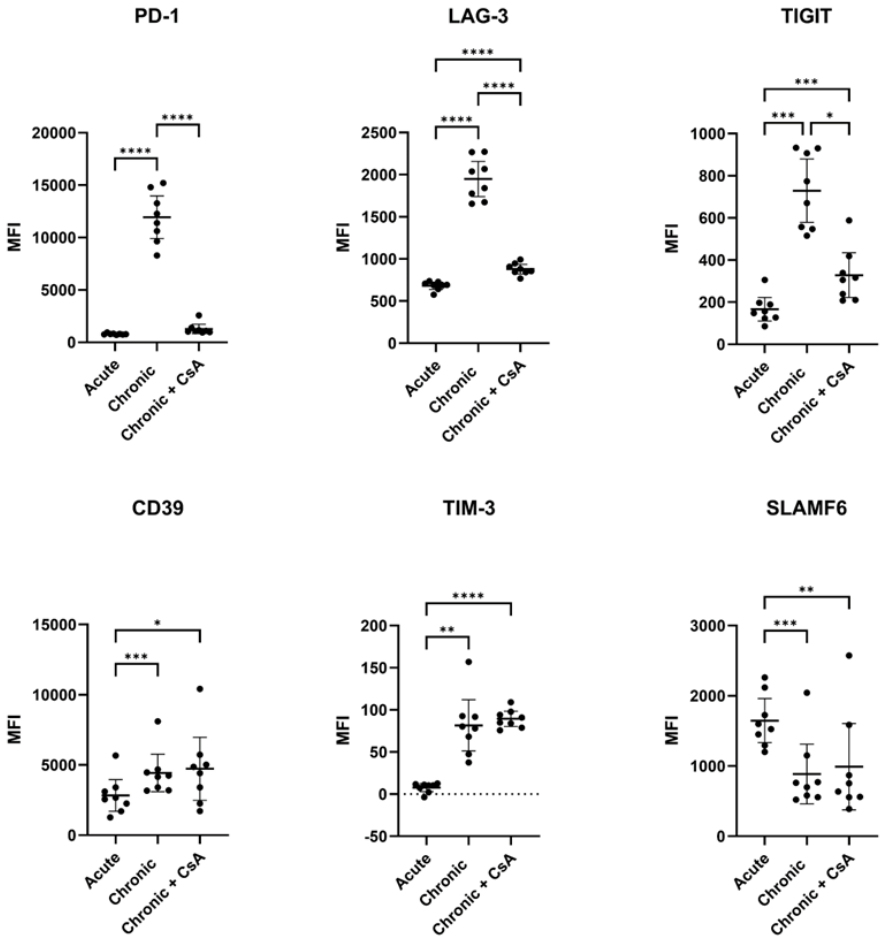

Figure 4.39. ***Cyclosporine reduces expression cell surface co-inhibitory receptors following chronic stimulation.*** *MFI Values of indicated markers in Acute, Chronic, and Chronic + CsA conditions at day 8. Statistical test shown is paired one way ANOVA with Geisser-Greenhouse correction, Dunnett's multiple comparisons between means of each group. *P ≤ 0.05, **P ≤ 0.01, ***P ≤ 0.001, ****P ≤ 0.0001. N=8.*

We accessed RNAseq data from sorted TCR transgenic CD8⁺ T cells that were stimulated *in vitro* with cognate peptide (Wither et al., 2023) (GSE242418). DMSO vehicle control, Cyclosporine A, MEK inhibitor Trametinib, or a combination of both inhibitors were added after 9 hours before RNA extraction at 30 hours. We plotted mean transcript per million values normalised against the DMSO control for (*Nr4a1, Nr4a3, Pdcd1, Lag3, Tigit*) (Figure 4.40). In agreement with our short-term small molecule inhibitor studies, normalised expression of *Nr4a1* was reduced by inhibition of the ERK pathway but increased by inhibition of the NFAT pathway, whilst the inverse was true for *Nr4a3*. *Pdcd1, Lag3,* and *Tigit* that showed a dependency on NFAT signalling over ERK signalling, confirming our findings that these inhibitory receptors can be sustained by NFAT signalling alone.

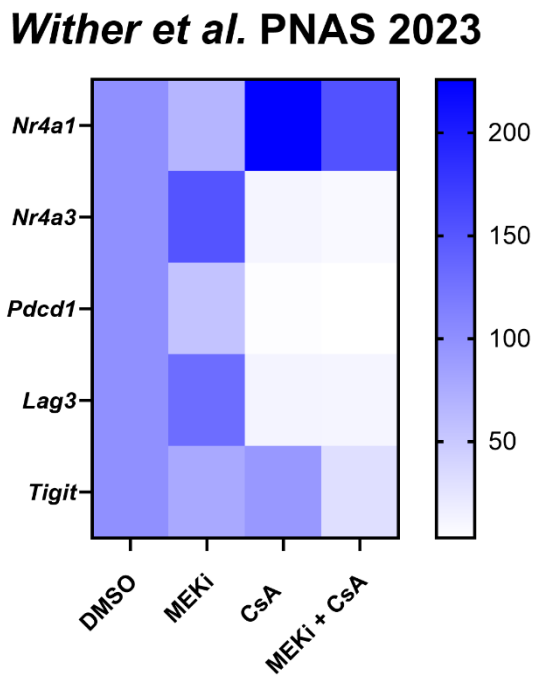

Figure 4.40. ***Nr4a1 shows differential pathway sensitivity to Nr4a3 and inhibitory receptors.*** *Sorted CD8⁺ T cells were stimulated for 30 hours, with indicated small molecule inhibitors added to the culture after 9 hours before analysis by RNAseq. Mean transcript per million read counts (2 biological repeats) for annotated genes were normalised against the DMSO control by (TPM(x)/TPM(DMSO)*100). Dataset accessed from Wither at al., 2023 GSE242418.*

FMO controls were used to gate on cytokine expressing cells following re-stimulation with T cell depleted splenocytes and αCD3 (Figures 4.41-4.43). Again, expression of cytokines was not significantly different between acute and chronic stimulation conditions (Figure 4.44). Frequency of cytokine expressing cells was notably lower than the previous iteration of this assay.

Our results indicate that the optimal methodology to generate exhausted $CD8^+$ T cells *in vitro* is to culture in the presence of IL-2, IL-7, and IL-17 to support optimal viability. With this methodology we were able to generate functionally exhausted cells that displayed a clear bias towards NFAT-dependent signalling during chronic stimulation (Table 4.1). Furthermore, we highlight that transient inhibition of NFAT pathway activity is able to partially restore phenotypic features of exhaustion.

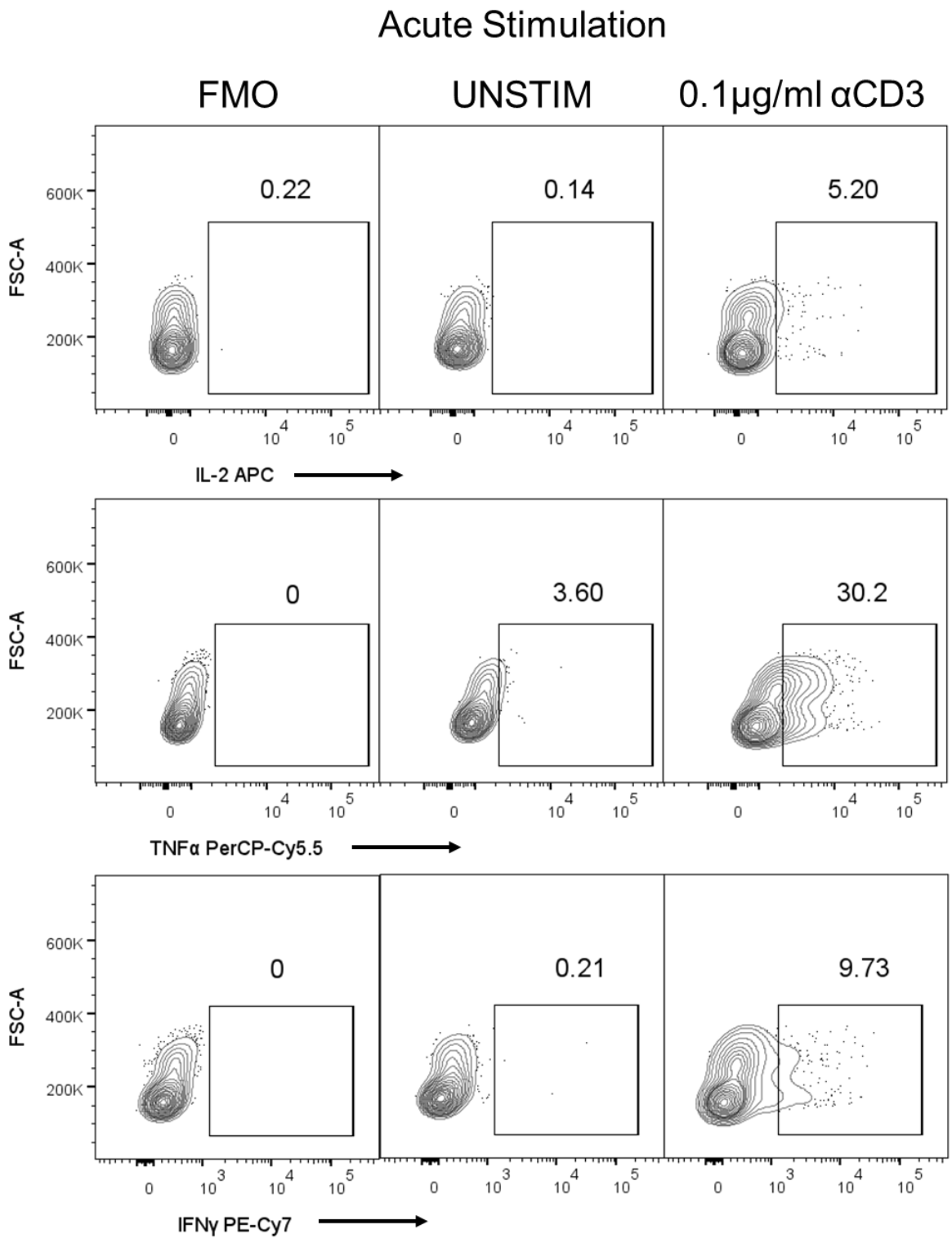

Figure 4.41. ***FMO staining control and gating strategy for cytokine intracellular staining in cells from Acute condition (Figure 4.34) following re-stimulation.***

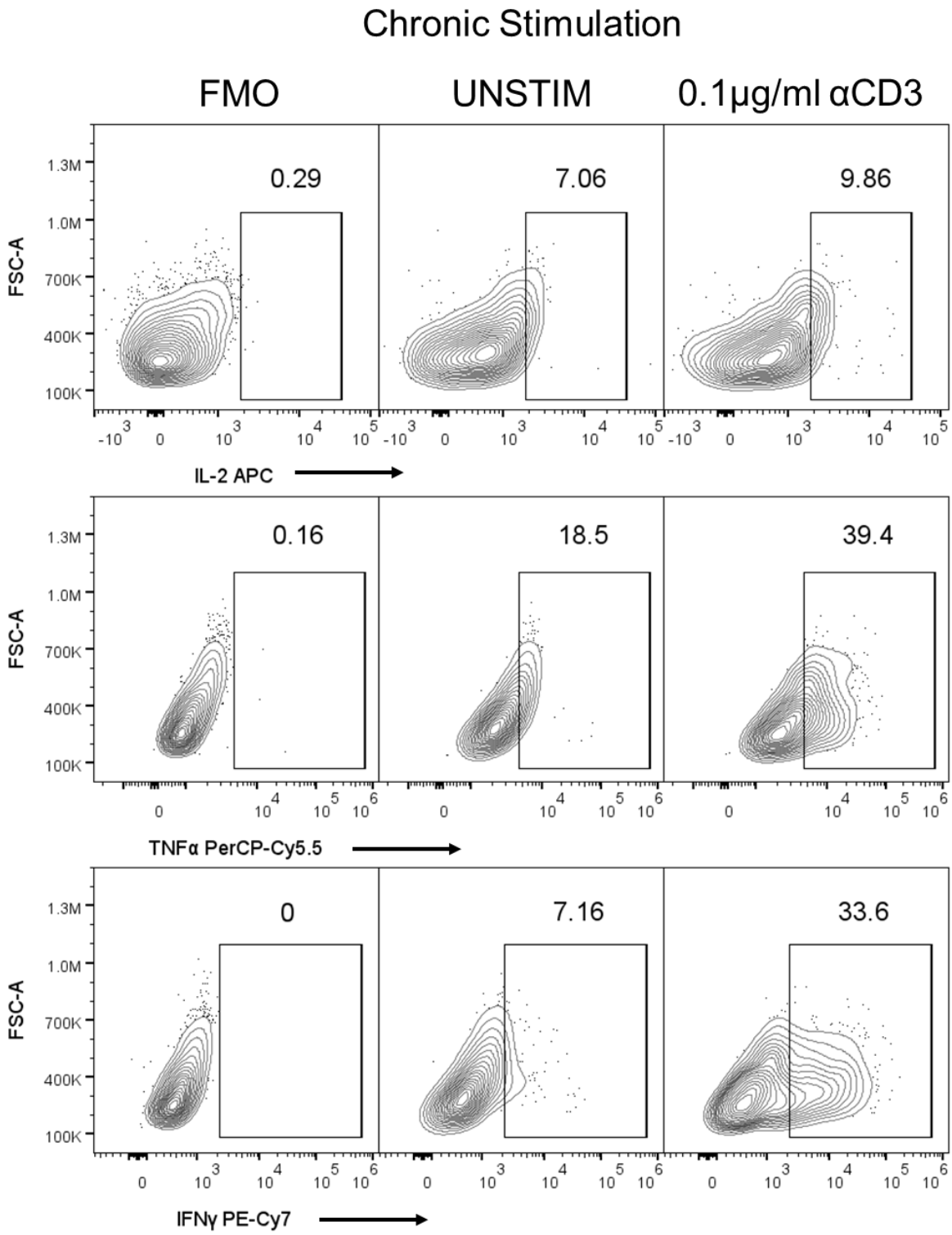

Figure 4.42. ***FMO staining control and gating strategy for cytokine intracellular staining in cells from Chronic condition following re-stimulation.***

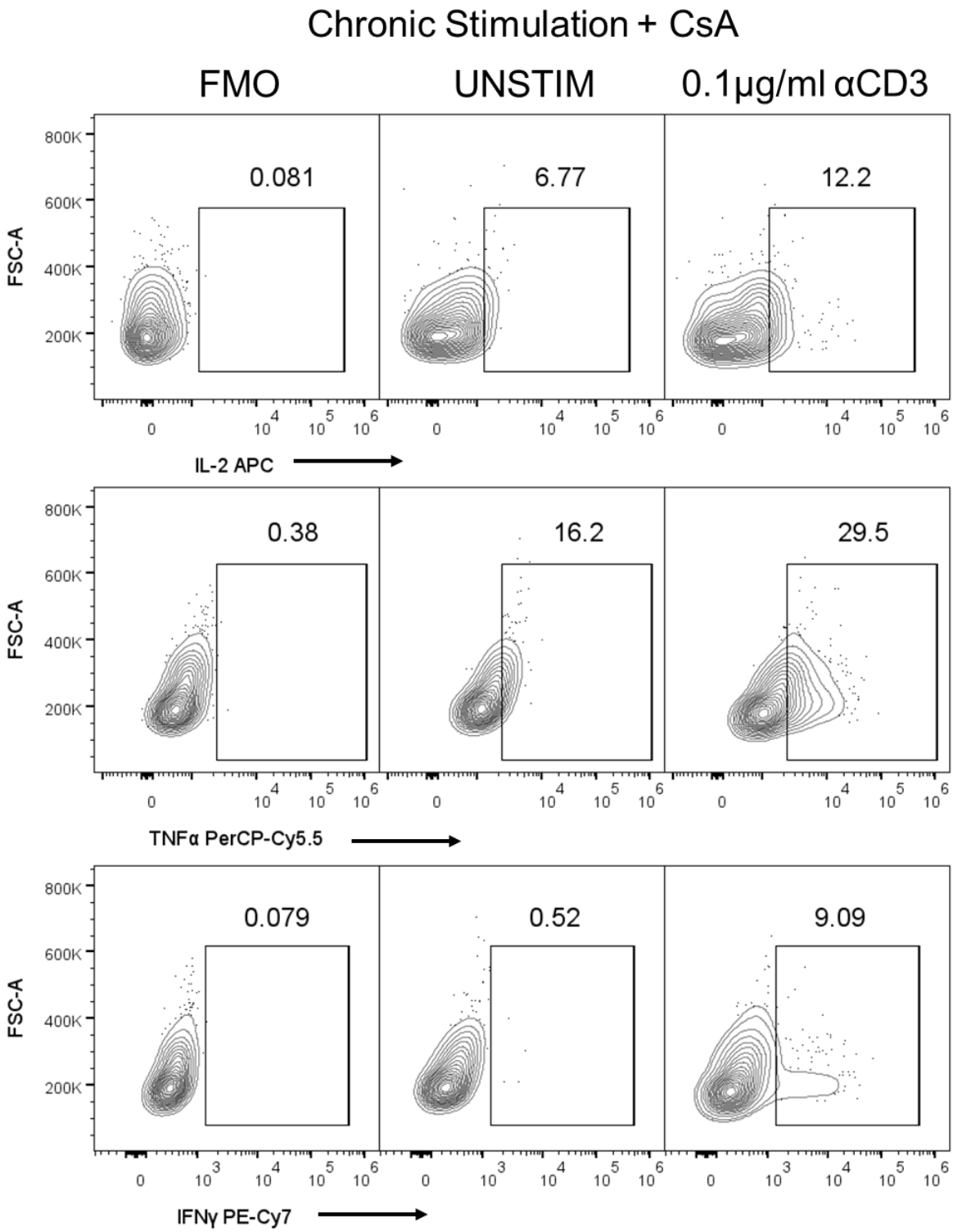

Figure 4.43. ***FMO staining control and gating strategy for cytokine intracellular staining in cells from Chronic + CsA condition following re-stimulation.***

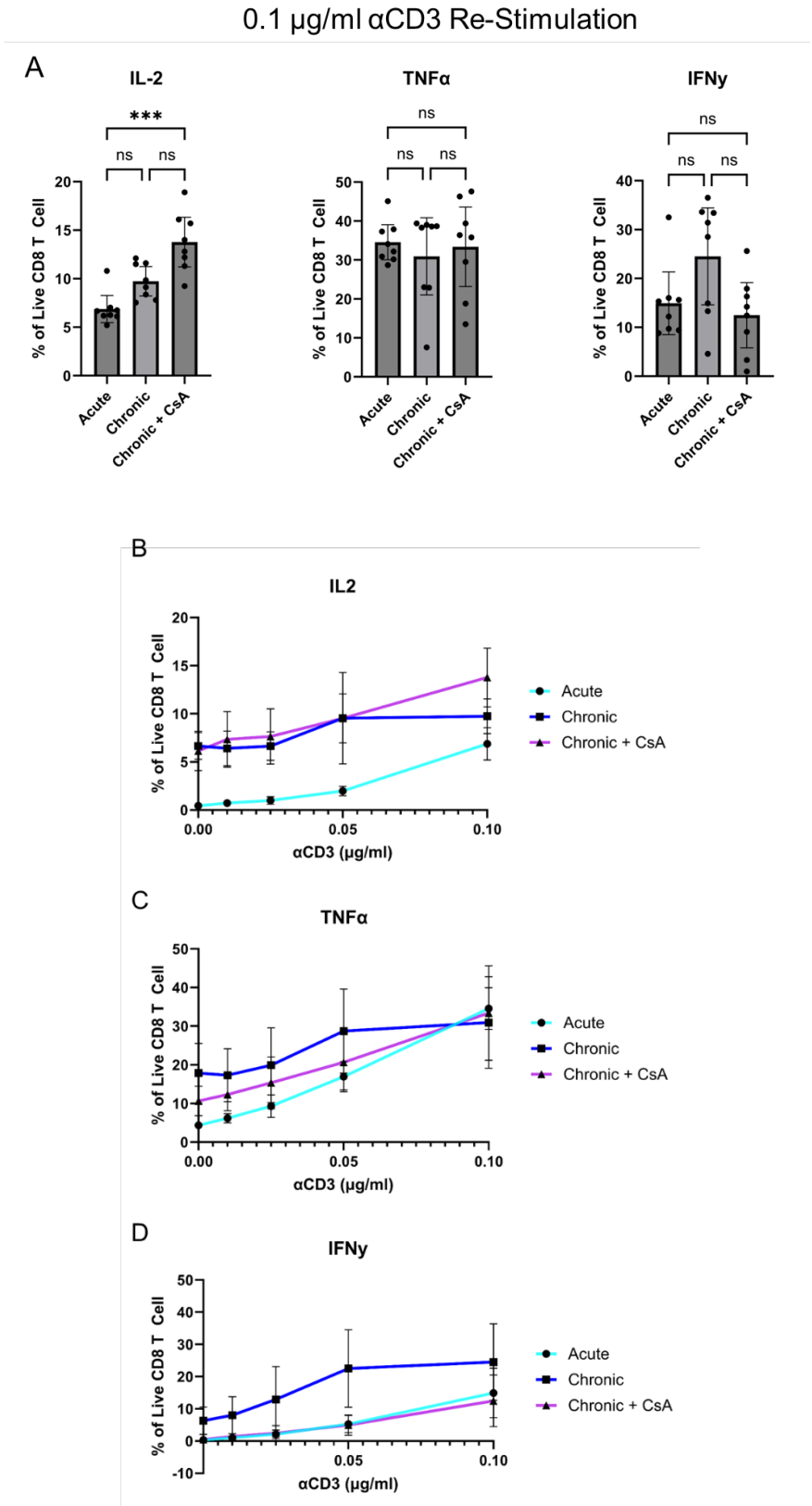

Figure 4.44. ***Cyclosporine shows no effect on production of cytokines upon re-stimulation of chronically stimulated cells.*** *Cells from Acute, Chronic, and Chronic + CsA conditions were re-stimulated with T cell depleted splenocytes and a dose titration of αCD3 for six hours with Brefeldin A before intracellular cytokine staining and analysis by flow cytometry. Expression of indicated markers is shown. Statistical test shown is paired one way ANOVA with Geisser-Greenhouse correction, Dunnett's multiple comparisons between means of each group. *P ≤ 0.05, **P ≤ 0.01, ***P ≤ 0.001, ****P ≤ 0.0001. N=8.*

Summary Figure	4.19	4.24	4.34
Chronic Stimulation Method	CD3/CD28 beads	Plate bound αCD3	Plate bound αCD3
Media IL-2 conc.	/	100 ng/ml	10 ng/ml
Media IL-7 conc.	5 ng/ml	10 ng/ml	/
Media IL-15 conc.	5 ng/ml	10 ng/ml	/
Viability	good	good	poor
Inhibitory Receptor Expression	High	High	High
Downregulated SLAMF6	Yes	Yes	NO
IL-2 Production	N/A	Reduced	Unchanged
TNFα Production	Reduced	Unchanged	Unchanged
IFNγ Production	Reduced	Unchanged	Unchanged
Loss of Nur77 Tempo Expression	No	Yes	Yes

*Table 4.1.**A Summary table of different in vitro chronic stimulation protocols.***

4.3 DISCUSSION

Here we have utilised Nur77 Tempo mice to demonstrate that NFAT independent signalling is shut down during chronic stimulation of $CD8^+$ T cells in the tumour environment. Previous work has shown that NFAT dependent signalling detected by Nr4a3 Tocky reporter is equivalent between $CD4^+$ and $CD8^+$ T cells infiltrating MC38 tumours, furthermore the frequency of FT Blue expression does not significantly decrease over time, remaining at a median of >20% by day 14. In contrast, FT Blue expression decreased over time in Nur77 Tempo mice with a median of 5-10% by day 13. We found that FT Blue expression was not sensitive to PD-L1 blockade or even treatment with αCD3 stimulating antibody. Insensitivity to PD-L1 blockade was observed even in the PD-1^+ SLAMF6^+ TIM-3^- T_{PEX} population. Although T_{PEX} cells have been reported as selective responders to ICB, transfer experiments in LCMV infected mice have confirmed that they are epigenetically committed to the exhaustion programme. It may be that the pathways that controls *Nr4a1* expression are switched off early in the trajectory of exhaustion differentiation.

In vitro experiments confirmed that maintenance of NFAT dependent pathways and cessation of NFAT independent pathway was not due to environmental factors within the tumour, but is rather an intrinsic feature of chronic TCR stimulation. Our *in vitro* exhaustion protocol was able to re-capitulate many phenotypic characteristics of $CD8^+$ T cell exhaustion such as TIM-3 upregulation and SLAMF6 downregulation. However, we were unable to convincingly cause the reduction in production of effector cytokines that is characteristic to $CD8^+$ T cell exhaustion. There are a number of possible reasons for this discrepancy. Firstly, it may be that addition of T cell homeostatic cytokines may have retained chronically stimulated $CD8^+$ T cells in an 'intermediate exhausted' state. This has been described by Ansuman Satpathy's lab in chronic LCMV infection, where 'T_{EX}^{KLR}' cells that are PD-1^+ SLAMF6^- express CXCR1 and effector marker KLRG1, and retain their ability to produce IFNγ (Daniels et al., 2019). Satpathy and colleagues suggest that during

LCMV infection this state is restricted to lower affinity clones and represent a divergence from terminal exhaustion. Wherry and colleagues have recently proposed that STAT5 signalling downstream of IL-2 is a critical determinant in this fate decision, such that constitutively active STAT5 prevents terminal exhaustion altogether (Beltra et al., 2023). Our experimental design as shown in Figure 4.24 included high concentrations of IL-2 in the culture media, as well as IL-7 and IL-15 that also signal via STAT5, possibly retaining cytokine production despite chronic TCR stimulation. When we reduced levels of IL-2 and removed IL-7 and IL-15, we saw a very significant loss in viability. It was not possibly to distinguish a difference between cytokine expression between acute and chronic stimulation conditions following such a large amount of cell death.

The *in vitro* protocol likely needs further refining, to generate functionally exhausted $CD8^+$ T cells that survive long enough to thoroughly assay their TCR signalling capacity. Many studies have studied $CD8^+$ T cell exhaustion *in vitro* by utilising TCR transgenic models. Repeated stimulation of sorted OTI $CD8^+$ T cells with cognate OVA peptide leads to multiple co-inhibitory receptor expression, blunted cytokine production, and promoter hypermethylation of genes involved in T cell functionality (Zhao et al., 2020). Here, the culture was supported with IL-7 and IL-15 but no IL-2. Another study also using OTI $CD8^+$ T cells was able to re-capitulate phenotypic and epigenetic features of exhaustion, this time pulsing with OVA peptide in the presence of low concentration of IL-2 and bone-marrow derived dendritic cells (J. E. Wu et al., 2023). Although this protocol does mirror the function and phenotype of exhausted $CD8^+$ T cells *in vivo* it may not be a faithful model due to high levels of co-stimulatory ligands expressed by bone marrow-derived dendritic cells. $CD8^+$ T cell exhaustion, particularly in the tumour microenvironment, is likely driven by TCR stimulation in the absence of co-stimulation (Wherry & Kurachi, 2015). Phenotypic and epigenetic features of exhaustion have been replicated by a two-phase *in vitro* stimulation protocol, with two days of CD3/CD28 stimulation followed by eight days of CD3 stimulation (Belk et al., 2022). This likely mimics the two-stage stimulation of cancer antigen specific $CD8^+$ T cells

that are primed in the co-stimulation rich environment of the lymph node before a longer duration TCR only stimulation in the tumour microenvironment (Prokhnevska et al., Immunity 2023). Belk and colleagues cultured sorted $CD8^+$ T cells with 10 ng/ml IL-2, we attempted to replicate their protocol (Figure 4.34) but saw much higher levels of cell death and did not observe the same changes to cytokine production. This discrepancy may be due to our use of CD3/CD28 coated beads opposed to coated plates, and our use of 1 µg/ml αCD3 compared to their 5 µg/ml αCD3. Use of coated nanobeads to stimulate cells that are actively proliferating represents a technical challenge. The culture is started with a 1:1 bead:cell ratio but proliferation of T cells disrupts this ratio such that many cells are likely not in contact with the nanobeads by the time they are passaged. If this assay were to be repeated, it would likely require an optimisation stage, where a number of stimulation conditions (seeding density, supporting cytokine concentration, beads vs. plate bound stimulation) would be tested to identify the conditions required for survival of functionally exhausted $CD8^+$ T cells. This particular stimulation condition could then be used to thoroughly investigate TCR signalling dynamics associated with functional exhaustion.

It is of interest that NFAT-independent pathways were shut down during chronic stimulation without causing functional exhaustion. Early commitment to the exhaustion lineage, prior to functional exhaustion, via epigenetic modifications has been described in LCMV models (Utzschneider et al., 2016). It may well be that loss of NFAT-independent signalling occurs prior to many functional features of exhaustion. In the experimental design detailed in Figure 4.24, chronic stimulation was associated with a loss of IL-2, but not IFNγ or TNFα despite loss of NFAT-independent signalling. This may be a result of different signalling pathway dependencies of the different cytokines. IL-2 is highly dependent on NFAT:AP-1 dimers (Macián et al., 2001) but TNFα expression can be sustained when NFAT is prevented from binding to AP-1 (Macian et al., 2000). Furthermore, IFNγ can be expressed at high levels when MEK activity is blocked by a small molecule inhibitor, but not in the presence of Cyclosporine A (Wither et al., 2023).

Due to our observation of sustained NFAT-dependent signalling during chronic stimulation and work by other linking NFAT to exhaustion, we hypothesised that transient blockade of the NFAT pathway may be able to limit exhaustion. Treatment with 1 μM Cyclosporine A during the chronic αCD3 stimulation stage of the *in vitro* protocol significantly reduced the expression of PD-1, LAG-3, and TIGIT but did not impact expression levels of TIM-3 or CD39 (Figure 4.39). Cyclosporine A was washed off the cells before re-stimulation and assessment of cytokine production capacity. NFAT signalling essential for many T cell effector functions, however cytokine production seemed to be largely unaffected by Cyclosporine treatment, suggesting that an overnight rest in its absence is sufficient to allow NFAT signalling upon re-stimulation.

In order to fully test the role of chronic NFAT signalling in $CD8^+$ T cell exhaustion, we must have a reliable protocol to replicate functional exhaustion. We hypothesise that under chronic stimulation conditions that reduce cytokine production capacity, transient Cyclosporine treatment may be able to restore it. Our testing of this hypothesis would be dependent on further optimisation of chronic *in vitro* stimulation protocol. Use of Cyclosporine to prevent T cell exhaustion may be an attractive therapy strategy. Cyclosporine is well tolerated and is used often for treatment of graft versus host disease. Additionally, Calcineurin inhibitors have been trialled in the treatment of ICB induced colitis (Zhang et al., 2021), they were found to reduce colitis symptoms with minimal side effects. It may well be the case that Calcineurin inhibitors reduce T cell effector function and dampen the anti-cancer impact of ICB therapy, further trials would be required to investigate whether this is the case.

The life cycle of a cancer-specific $CD8^+$ T cell is proposed to begin with priming in the lymph node and trafficking to the tumour, at this stage both NFAT and NFAT-independent signalling are active, and the cell maintains expression of TCF1, ability to proliferate, and produce multiple cytokines. Following arrival at the tumour site, the $CD8^+$ T cell receives another TCR signal following immune

synapse formation with a tumour cell. This TCR signal is of a longer duration and usually lacks co-stimulation. Our evidence suggests this prolonged TCR ligation signals only via the NFAT pathway and leads to downregulation of TCF1/SLAMF6, loss of proliferative capacity, and loss of cytokine production. When patients are treated with ICB, there is a clonal replacement of $CD8^+$ T cells within the tumour. This suggests that ICB does not re-activate ERK signalling in those cells that have transitioned to NFAT only signalling pathways but prolongs the phase in which newly entering $CD8^+$ T cells can signal via both ERK and NFAT. This model is in keeping with experimental data in mice, where TCF1 expressing cells selectively respond to ICB therapy (Utzschneider et al., 2016) (Im et al., 2016). We observed an almost complete loss of NFAT-independent signalling by day 13 of MC38 tumour development and treatment with αPD-L1 had no effect on Nur77 Tempo FT Blue expression. This further supports a model in which NFAT-dependent signalling negatively regulates NFAT-independent signalling, and this process cannot be reversed by ICB. We proposed that blockade of NFAT-dependent signalling via treatment with Cyclosporine or Tacrolimus may be able to prevent this re-wiring of TCR signalling pathways. Cyclosporine/Tacrolimus treatment could be administered as a condition regiment for several weeks prior to ICB therapy. Blockade of NFAT signalling in this way may be able to increase the number and repertoire of cancer-specific $CD8^+$ T cells that have yet to shut down NFAT-independent signalling and are therefore amenable to ICB therapy. The next steps would involve confirming the *in vitro* experimental data by optimising the *in vitro* exhaustion process and restoration of cytokine production by transient Cyclosporine treatment. Following this, transient treatment of MC38 tumour bearing Nur77 Tempo mice with cyclosporine prior to ICB could be used to investigate the impacts on NFAT-independent signalling and tumour growth.

5 INVESTIGATING DRIVERS OF IMMUNITY IN LOW MUTATIONAL BURDEN COLORECTAL CANCER

5.1 INTRODUCTION

In contrast to experimental mouse models of cancer, immune responses to human cancer are highly heterogeneous. Our work using MC38 sub-cutaneous implantation and in vitro stimulations allows us to control the level of antigen recognition in our models. This may, however, have limited applicability to human cancer. The mutational landscapes of human cancers vary greatly (Alexandrov et al., 2020) with important ramifications for antigen recognition the anti-cancer immune response (Schumacher and Schreiber 2015). Colorectal cancer (CRC) patients have a wide range of mutational burdens and patient sub-groups differ greatly in the magnitude of their anti-cancer immune response (Guinney et al., 2015). In a body of work related to, but distinct from, our work on TCR signalling in mouse models, we aimed to use CRC as a platform to investigate drivers of anti-cancer immunity in humans.

CRC is a malignancy of the colonic or rectal epithelium and is the third leading cause of cancer death worldwide (Rawla et al., 2019). Colorectal cancer can occur sporadically or as a result of germline mutations that cause hereditary cancer syndromes such as hereditary non-polyposis colorectal cancer (HNPCC/Lynch syndrome) or familial adenomatous polyposis (FAP); the latter with almost 100% incidence (Medema & Vermeulen, 2011). Several risk factors are associated with CRC including smoking, high body-mass index, low physical activity, diets low in fibre and high in red meat. In addition, prevalence is higher in men and varies greatly by country (Safiri et al., 2019).

The most common and most effective curative treatment for colorectal cancer remains surgical resection. Chemotherapy and radiotherapy can be given either as a neoadjuvant therapy before

surgery or post operatively to prevent recurrent disease (Morton et al., 2023). In metastatic disease, monoclonal antibodies directed at epidermal growth factor receptor (EGFR) (Cetuximab) (Jeong et al., 2016) or vascular endothelial growth factor A (VEGF-A) (Bevacizumab) (Rosen et al., 2017) may be used to target growth signalling (in RAS and RAF wild type cancers only) and angiogenesis, respectively. However, increase in median survival rates are modest for both drugs. Additionally, monoclonal antibodies targeting immune regulatory pathways including PD-1 (Pembrolizumab, Nivolumab) and CTLA-4 (Ipilumimab) are now approved by NICE for the treatment of CRC in a small subset of UK patients. The majority of patients that do not respond to immunotherapy represent a patient group of significant unmet clinical need.

5.1.1 The Origin of CRC

The colonic epithelium has capacity for maintenance and self-renewal via intestinal stem cells (ISCs) that reside in colonic crypts. ISCs give rise to highly proliferative transit amplifying cells, that migrate up the crypt, differentiating into enterocytes and enteroendocrine cells before death and ejection into the gut lumen. The lifespan of a colonic epithelial cell is less than a week, whilst ISCs are long lived; a single crypt can generate around 200 cells a day from its pool of ISCs (Reya & Clevers, 2005). Proliferation and differentiation in the crypt are tightly controlled by a number of signalling pathways including Wnt, Notch, BMP, and Hedgehog. Colorectal polyp formation is initiated almost exclusively by dysregulation of the Wnt signalling pathway (Schatoff et al., 2017), often by mutation of the gene encoding Adenomatous Polyposis Coli (*APC*). Subsequent mutations in genes such as *TP53*, *KRAS*, *BRAF*, *SMAD4*, *PIK3CA* mediate progression to carcinoma and metastasis (D. Huang et al., 2018).

Several proteins, such as LGR5 (Barker et al., 2007), have been identified as markers for ISCs via fate mapping experiments in mice, demonstrating that most intestinal epithelial cells arise from $LGR5^+$ progenitors. There is heterogeneity among ISCs; a distinct pool of $BMI1^+$ ISCs render $LGR5^+$

ISCs redundant for intestinal homeostasis, as shown by their ablation in mice (H. Tian et al., 2011). Such markers have been valuable in determining the cell type of origin in murine models of intestinal cancer. Conditional knockout of *Apc* in ISCs by tamoxifen inducible expression of Cre recombinase, under the influence of *Lgr5* regulatory regions, leads to rapid formation of adenomas. In contrast, oral administration of Cre recombinase, to target transit amplifying cells and spare crypt stem cells, leads to micro-adenomas that fail to progress to macro adenomas (Barker et al., 2009). However, microadenomas did persist (>200 days) for longer than wild-type counter parts under normal homeostasis (<7 days). Non-crypt cell derived microadenomas can form macroadenomas if the NFκB pathway is subsequently activated by inflammation or *Kras* mutations (Huels & Sansom, 2015).

In human cancers, lesions have been observed in which epithelial cells at the luminal end of the crypt carry *APC* mutations whilst crypt stem cells are *APC* wild-type, suggesting human cancer does not always arise from stem cell populations (Shih et al., 2001).

5.1.2 Genetic Instability in CRC

Microsatellites are regions of repeated nucleotide sequences often located near coding regions, and due to their repetitive structure, they are particularly vulnerable to mismatch mutations. Mismatch repair (MMR) machinery excises single strand regions containing mismatch mutations allowing DNA polymerase to re-synthesise the single strand, correcting errors. Defective MMR leads to microsatellite instability - expansions/contractions of microsatellite regions resulting in accumulation of frameshift and missense mutations, which can drive tumorigenesis (Pećina-Šlaus et al., 2020). Hereditary non-polyposis colorectal cancer (HNPCC), or Lynch syndrome, is an inherited cancer syndrome that pre-disposes patients to development of CRC and cancers at other sites. HNPCC is caused by germline mutations in genes that encode proteins responsible for MMR (*MLH1, MSH2, MSH6, PMS2*), leading to microsatellite instability in a small proportion of

patients. Microsatellite instability can also be caused by somatic mutations to MMR genes. Whilst microsatellite instable (MSI) disease accounts for around 15% of CRC patients, the majority of CRC cases are microsatellite stable (MSS) with functioning MMR machinery. Around 65% of patients show chromosomal instability (CIN), leading to aneuploidy and chromosomal rearrangement. The remaining ~20% of patients display a CpG island methylator phenotype (CIMP) characterised by epigenetic suppression of tumour suppressor genes (Orsetti et al., 2014). Microsatellite instability may arise as a consequence of CIMP, if promoter regions of genes involved in MMR become hyper-methylated (Boland & Goel, 2010).

5.1.3 Immune Responses to CRC

Early evidence for adaptive immune responses to colorectal cancer came in 1998. A predominance of Vβ9 TCR chains in colorectal cancers indicated clonal expansion of T cells, suggesting tumour reactivity (Baier et al., 1998). Subsequent studies demonstrated that infiltration of $CD8^+$ T cells into the tumour nest (Naito et al., 1998) and a high ratio of CD8:CD4 T cells (Diederichsen et al., 2003) are positive prognostic indicators of survival. A more comprehensive analysis in 2006 went on to consider the function of T cells within tumours, highlighting that relapse free survival correlated with elevated transcripts of a Th1 associated gene module (*IRF1, CD3z, CD8a, GNLY, GZMB, IFNG, TBX21*) that showed co-ordinated expression patterns (Galon et al., 2006). Furthermore, Galon and colleagues expanded on previous immuno-histochemistry (IHC) analysis, finding prognostic value to high staining density of CD3, CD8, GZMB, CD45RO. The latter two markers indicated that T cells with a cytotoxic (GZMB) and memory (CD45RO) phenotype correlate with survival.

Subsequently, Galon and colleagues have developed the Immunoscore (Galon et al., 2014), an IHC approach that scores staining of intra-tumoural CD3 and CD8 expression. It has been internationally validated as a more effective prognostic tool than traditional TNM staging (Pagès

et al., 2018). However, the Immunoscore may be a somewhat reductionist approach to quantifying adaptive responses; CRCs often contain large numbers of 'bystander' CD8 T cells that recognise antigens unrelated to cancer (Simoni et al., 2018) and therefore the presence of CD8 T cells may not necessarily be indicative of an antigen-specific anti-cancer response. In addition, the Immunoscore may be of limited usefulness to clinical practice if it is purely prognostic and cannot inform therapy decisions.

Lal and colleagues have made efforts to quantify the immune response in CRC, identifying a transcriptional signature of co-regulated genes (the coordinated immune response cluster (CIRC)) (Lal et al., 2015). The CIRC signature contains genes associated with a type 1 immune response including Th1 cytokine *IFNG*, Th1 master transcription factor *TBX21*, a number of MHC II genes, co-stimulatory and co-inhibitory receptors, and chemokines. Notably the CIRC signature does not include transcripts for *CD3E* or *CD8A*/*CD8B* and therefore, whilst likely to correlate, can be seen as distinct from the Immunoscore. The CIRC signature is arguably a more detailed quantification of the immune response to CRC that the immunoscore due to its consideration of the function of infiltrating T cells as opposed to just their presence. Despite this, no studies have correlated CIRC signature scores with survival data, so the CIRC does not yet have the same validated prognostic value as the Immunoscore. Furthermore, the immunoscore not only quantifies the staining of $CD8^+$ T cells but scores their proximity to tumour nests, providing more spatial data than the CIRC score. In clinical settings, RNA sequencing of CRC samples to determine CIRC scores is impractical, however, IHC staining density using a pan-MHC II antibody is an accurate predictor of CIRC score and can act as a more practical read-out (McMurray, 2021).

It is of critical importance to understand how cancers are immunogenic. Cancers are derived from healthy tissue; this presents a challenge to the adaptive immune system as autoreactive T

cells are deleted in the thymus, creating tolerance to self-peptides within the immune system. Somatic mutations in cancer cells can give rise to novel immunogenic amino acid sequences called neoantigens. Therefore, the type and degree of genetic instability is a key factor in determining the immunogenicity of a cancer. MSI cancers are characterised by improved prognosis at stage I-III (Guidoboni et al., 2001; Kang et al., 2018), increased infiltration of cytotoxic lymphocytes (De Smedt et al., 2015; Galon et al., 2006; Guidoboni et al., 2001; Mlecnik et al., 2016), elevated expression of Th1 transcriptional signatures (Galon et al., 2006; Lal et al., 2015; Mlecnik et al., 2016), increased expression of co-inhibitory receptors (Llosa et al., 2015) and improved responses to checkpoint blockade immunotherapy (Le et al., 2015). As a result, only patients with defective MMR machinery are approved for immunotherapy treatment in the UK (CRUK).

In comparison to MSS CRCs, MSI CRCs have an expected increase in the number of both missense and frameshift mutations (Mlecnik et al., 2016). Whole exome sequencing allows for enumeration of transcribed neo-antigens and HLA binding algorithms can predict whether neo-antigens can be presented by MHC I or MHC II alleles. MSI CRCs have an abundance of neo-antigens that are predicted to bind a variety of both MHC I and MHC II alleles whereas MHC binding neoantigens are much rarer in MSS CRC patients, consistent with the considerably lower overall level of mutations. Indeed, specific responses to tumour neoantigens have been directly demonstrated in MSI patients (Mlecnik et al., 2016).

It is likely that the mutational load associated with microsatellite instability can initiate an adaptive immune response against tumour derived neoantigens, rendering MSI CRCs amenable to checkpoint blockade immunotherapy. However, quantification of the immune response by either Immunoscore (Mlecnik et al., 2016) or CIRC score (Lal et al., 2015) reveals that whilst the high-immunity subset of CRC patients is enriched for MSI patients, it does contain some MSS

patients. Conversely, some MSI patients fall into the low immunity subsets. A study in 2019 that performed whole exome sequencing on a small number of CRC patients (7 MMR proficient 2 MMR deficient) found that although the number of non-synonymous mutations was much higher in MMR deficient patients, numbers ranged from 15-49 in MMR proficient patients but reached around 600 in MMR deficient patients (Bulk et al., 2019). Phenotyping of TILs revealed a $CD103^+$ $CD39^+$ population of $CD8^+$ T cells in dMMR tumours, a phenotype that has been previously associated with tumour reactivity (Duhen et al., 2018). This population of CD8 T cells produced IFNγ in response to synthetic peptides derived from non-synonymous mutations identified by whole exome sequencing, indicating that a proportion of MSS patients do mount antigen specific responses against MSS CRCs and the immune stratification of CRC patients is not as simple as MSI vs MSS. It is of note that many synthetic peptides generated from non-synonymous mutations did not induce IFNγ production, highlighting the importance of experimental validation of putative neoantigens. What drives the extreme differences in immune responses to CRCs with seemingly similar mutational burdens remains a significant unanswered question.

5.1.4 MHC II and the Microbiome

A critical feature of the CIRC signature is the inclusion of several MHC II genes. Although MHC II expression has typically been considered restricted to specialised antigen presenting cells (APCs), colonic epithelial cells can express MHC II under inflammatory conditions (Heuberger et al., 2020). MHC II expression is controlled by the master regulator, class II transcriptional activator (CIITA); in non-haematopoietic cells such as intestinal epithelial cells (IECs), CIITA expression is dependent on its pIV promoter (Waldburger et al., 2001) which is regulated by STAT-1, downstream of IFNγ signalling (Muhlethaler-Mottet et al., 1997). IFNγ can come from multiple sources in the intestinal epithelium, including $CD8^+$ T cells, $CD4^+$ T cells, NK T cells, NK cells, MAIT cells, ILC1 cells, or γδ T cells. IFNγ expression in lymphocytes can be driven by activation of

antigen or innate immune receptors or by exposure to inflammatory cytokines such as IL-18 (Okamura et al., 1995) and IL-12 (Chan et al., 1991; Kubin et al., 1994).

Koyama and colleagues demonstrated that MHC II expression by IECs in mice is elevated by disruption to gut microbiome population distributions or total body irradiation (TBI) but abolished by germ free housing conditions (M. Koyama et al., 2019). Following TBI, mucosal barrier breakdown and translocation of bacteria into the epithelium was observed and the intestines of mice were enriched for IFNγ$^+$ CD4$^+$ T cells and ILC1 cells; the TBI mediated upregulation of MHC II was dependent on expression of *Infgr*, *Myd88*, *Trif*, *Il12p35*. The authors suggest a mechanism whereby microbiota that translocate to the epithelium drive IL-12 expression in macrophages, which stimulates TCR-independent IFNγ expression in lamina propria CD4$^+$ T cells, leading to MHC II upregulation on IECs. Critically, MHC II$^+$ IECs were able to express co-stimulatory molecule CD80 and activate naïve CD4$^+$ T cells through cognate antigen presentation, and naive CD4 T cell activation was prevented by CD80 blockade, highlighting the importance of co-stimulation in this process. Cognate antigen recognition by CD4$^+$ T cells would lead to IFNγ production, causing a resultant increase MHC II expression; it is easy to envisage how a positive feedback loop could be established. Although this report examines IEC MHC II expression in the context of graft versus host disease, it is tempting to speculate that such a feedback loop drives the expression of MHC II genes in CRCs with an elevated CIRC signature. Indeed, if IFNγ and subsequent MHC II expression was driven by a TCR independent microbiota/IL-12 axis, it would explain why some MSS CRCs can have a high CIRC score despite most likely having a similar neo-antigen burden to low CIRC MSS CRCs.

A separate study noted that the expression level of MHC II on IECs differed greatly between mice of the same strain housed in different facilities (Van Der Kraak et al., 2021). IEC MHC II expression was ablated by antibiotic treatment and was transferrable between mice by co-housing,

confirming a bacterial mechanism. Elevated MHC II expression was associated with increased serum IL-18 and reduced by antibody blockade of IL-12 or IL-18R. IL-18 is initially translated in its inactive pro-IL-18 form. Inflammasomes are large multimolecular complexes that can detect intracellular PAMPs, cleaving Caspase-1 into its active form, which can then cleave pro-IL-18 and pro-IL-1β into their active forms. Induction of IL-18 release by IECs by experimental inflammasome activation, either by mutations to *NLRC4* or *Tritrichomonas* colonisation was sufficient to induce IEC MHC II expression, dependent on IFNγ signalling. These two studies demonstrate that the intestinal microbiome is able to induce expression of MHC II in an antigen independent manner, either through a TLR-MYD88-IL-12 axis or an inflammasome-IL-18 axis.

In support of microbiota-driven heterogeneity in immune responses, CRC patients exhibit differences in their microbiome composition compared to healthy controls (Flemer et al., 2018). Changes to the microbiome can be observed in adjacent healthy tissue and in early-stage polyps, suggesting that bacterial population changes can precede CRC development as opposed to occurring as a result of CRC related inflammation, although the mechanism is unclear. Many studies have examined the diversity of the gut microbiome in CRC using 16s rRNA sequencing. One such study correlated the abundance of bacterial taxonomic units with immune signatures identified by RNA sequencing of paired samples, noting a positive association between one unit and several cytokines (Flemer et al., 2017).

Another possible reason for immune response heterogeneity is that there is simply a higher degree of antigen recognition occurring in high CIRC MSS cancers. As previously discussed, neoantigen specific responses have been detected in MSS cancers albeit at low levels (Bulk et al., 2019). One may hypothesise that the high CIRC MSS patients simply have an effective neoantigen response whereas the low CIRC patients do not. This hypothesis is hard to validate or indeed exclude. Although neoantigen prediction algorithms exist, the majority of putative

neoantigens cannot be validated experimentally. For example, Bulk and colleagues detected 15-49 non-synonymous, transcribed mutations in MSS CRCs however the number of mutation-derived synthetic peptides that elicited a response from TILs ranged from 0-3, and this low level was consistent with other studies (McGranahan et al., 2016; Simoni et al., 2018). If high CIRC scores in MSS patients were being driven by a higher neo-antigen burden, a correlation between mutational burden and CIRC score might be expected. There appears to be no trend (unpublished data, Lal), however small differences may be hard to observe among patients with such uniformly low mutation counts.

The microbiome has been shown to promote tumourigenesis by remodelling the immune microenvironment in murine models of CRC. Commensal *F.Nucleatum* is over-represented in the colonic microbiome of CRC patients (Castellarin et al., 2012) and gavage into APCmin/- mice accelerates tumour growth, associated with an influx of myeloid derived suppressor cells (MDSCs) (Kostic et al., 2013). The commensal B. fragilis can also accelerate tumourigenesis in APCmin/- mice by inducing IL-17-dependent colitis (S. Wu et al., 2015). The authors suggest that this evidence is indicative of a causative role for dysbiosis in the development of human CRC, but these results should be interpreted cautiously, as they were generated in mice with germline APC mutations which are only present in a small proportion of human CRCs and may be of limited relevance to patients without germline APC mutations. The microbiome of humans is more diverse than mice and niche competition is likely to be different.

In contrast, some commensals may support an anti-cancer response. Murine Bifidobacterium commensals have been shown to augment anti-cancer adaptive immune responses and are necessary for the response to anti PD-L1 immunotherapy in sub-cutaneous transplant cancer models (Sivan et al., 2015). The mechanism by which this occurs remains unclear. A later study showed that mice inoculated with sub-cutaneous sarcoma cells were incapable of clinically

responding to anti CTLA-4 immunotherapy when housed in germ-free conditions, and that anti CTLA-4 therapy remodelled the faecal microbiome (Vétizou et al., 2015). The authors suggest the primary mechanism of action as anti CTLA-4 mediated disruption of immunological tolerance in the gut allowing expansion of immunogenic commensals. Exactly how these species are immunogenic is not completely clear but may be related to barrier permeability and IL-12 expression, as observed by Koyama and colleagues. $CD4^+$ T cells isolated from spleens of CTLA-4 treated, tumour bearing mice, were co-cultured with B.fragilis-loaded DCs and transferred into germ free mice. Transfer of $CD4^+$ T cells stimulated with B.fragilis, but not control bacteria or DCs alone, slowed tumour growth. It seems unlikely that a specific response against B.fragilis antigens is responsible for slowing tumour growth as the tumours in germ free mice are likely not colonised with intestinal commensal bacteria. It is more likely that exposure to B.fragilis activates innate immune pathways in DCs which in turn may adjuvantise T cell activation and polarise $CD4^+$ T cells towards a Th1 phenotype. It would be interesting to investigate whether human commensals that colonise the gut in CRC patients are also capable of driving Th1 differentiation and impacting anti-cancer T cell responses.

A recent study provided convincing evidence that commensals can colonise tumours and initiate specific responses against bacterial antigens (Kalaora et al., 2021). The authors found that human melanomas are colonised with populations of commensal bacteria, purification of HLA-I and HLA-II molecules from fresh human melanoma samples and mass spectrometry analysis of eluted peptides (immuno-peptidomics) was cross referenced to database proteomes of colonising commensals. This revealed that peptides derived from several species of bacteria are displayed on HLA-I and HLA-II molecules of melanoma cells. Bacteria were imaged invading human melanoma cells and TILs purified from fresh melanoma samples were shown to produce IFNγ in response to peptides derived from bacterial species, including *F.nucleatum* which is known to be enriched in human colorectal cancer. To the best of our knowledge there has not

been such a comprehensive study on bacterial antigens in human CRC, however, the colon comes into contact with more bacteria than any other tissue and it seems probable that similar antigen specific responses could occur in this context.

Investigating how the bacterial populations are distributed and permeability of the mucosal barrier correlate with CIRC scores may offer mechanistic insight into the heterogeneity of CIRC scores amongst MSS patients. There are diverse mechanisms by which the colonic microbiome may modulate immune responses. Microbiome-associated inflammation may remodel the immune microenvironment, for better or for worse, and may modulate how patients respond to immunotherapy. Additionally, the microbiome may have an adjuvantising effect on T cell activation, or indeed directly activate infiltrating T cells via presentation of bacterial antigens. The microbiome may also indirectly induce MHC II expression through IL-12 or IL-18-dependent mechanisms.

The clinical significance of MHC II expression by colorectal cancer cells has been controversial; specifically, whether MHC II molecules present endogenous peptides to $CD4^+$ T cells and act as APCs. MHC II is primarily loaded with exogenous peptides in lysosomal compartments whereas MHC I is primarily loaded with proteasome-cleaved endogenous peptides in the endoplasmic reticulum (Trombetta & Mellman, 2005). Based on this dogma it seems unlikely the CRC cells would be capable of presenting neoantigens on MHC II due to the limited endocytic capacity of epithelial cells. However, endogenous cytosolic antigens can be delivered to the lysosome by macro autophagy; cytosolic proteins are captured in autophagosomes which then fuse with lysosomes and have been seen to co-localise with MHC II loading compartments in IFNγ-stimulated epithelial cell lines (Schmid et al., 2007). Indeed, in 3 different murine cancer cell lines, the majority of immunogenic peptides derived from non-synonymous mutations were MHC-II restricted and RNA-based vaccines of MHC-II binding epitopes restricted growth of

tumours in sub-cutaneous models (Kreiter et al., 2015). Therefore, MHC-II expression may be critical for presenting neoantigens.

Overexpression of CIITA in an MHC II^- murine mammary adenocarcinoma cell line prior to engraftment resulted in remodelling of the tumour immune microenvironment and ultimately tumour rejection. This process was sensitive to depletion of both $CD4^+$ and $CD8^+$ T cells and an expansion of tumour antigen-specific $CD8^+$ T cells was observed (Meazza et al., 2003). Additionally, deletion of professional APCs did not prevent rejection of CIITA-transfected tumour grafts (Bou Nasser Eddine et al., 2017), suggesting $CD4^+$ T cells were activated by tumour cells acting as APCs. As $CD8^+$ T cells were also essential for an anti-cancer response, it seems probable that activation of $CD4^+$ T cells by tumour cell MHC II leads to priming of CD8 T cells in lymphoid tissue, as opposed to direct cytotoxic activity by $CD4^+$ T cells. The authors note that CIITA-transfected cell lines do not have CD80/86 expression detectable by flow cytometry, but act as APCs nevertheless. CD80/86 costimulatory ligands deliver the critical 'second signal' in pMHC mediated T cell activation (Schwartz, 1990); other studies have also shown expression of CD80 is a critical factor for IECs to activate naïve CD4 T cells via MHC II (M. Koyama et al., 2019). However, Bou Nasser Edine and colleagues only analysed CD80/86 expression on cell lines before injection into mice and cannot rule out the possibility that CD80/86 expression occurs after engraftment or that they express different co-stimulatory molecules.

The evidence that CIITA-mediated MHC II expression on tumour cells can mediate rejection via activation of $CD4^+$ T cells is strong in murine models. This is a promising indication that it is biologically possible for MSS CRCs to present antigens to $CD4^+$ T cells via MHC II. However, whether this actually happens in human patients is unclear. Firstly, despite Bou Nasser Edine and colleague's assertions, it is highly likely that co-stimulation is essential for activation of naïve $CD4^+$ T cells by IECs, so determining CD80/86 expression on MSS CRCs will be critical. Previous

work has identified T cells reactive to tumour neoantigens infiltrating MSS CRCs (Bulk et al., 2019), and future work should aim to determine whether predicted neoantigens, or bacterial antigens, are presented by MHC II complexes on the surface of tumour cells, and whether MHC II^+ CRC cancer cells can activate autologous naïve T cells. TCR ligation in the absence of co-stimulation can be sufficient to induce cytokine production and killing but requires priming by professional APCs in lymphoid tissue prior to tumour infiltration (Proknhevska et al., 2023). However, if recognition of MHC II restricted antigens displayed by tumour cells is the key driver that distinguishes e.g. a low CIRC from a high CIRC, it will likely involve *de novo* immune responses and thus co-stimulation.

5.1.5 CRC Immunotherapy

The landmark KEYNOTE consisted of a phase 3 randomised control trial of Pembrolizumab therapy in patients with metastatic MSI colorectal cancer (T. André et al., 2020). Pembrolizumab therapy led to a significant increase in progression free survival as compared to 5FU based chemotherapy with or without Bevacizumab/Cetuximab (16.5 and 8.2 months respectively, median follow up time of 32.4 months). The CheckMate trial of Nivolumab and Ipilimumab combination therapy in patients with metastatic MSI colorectal cancer has finished recruiting for phase 3 trials (NCT04008030). Nivolumab monotherapy data published in 2017 showed a 31.1% objective response rate and a 69% disease control rate at 12.0 months median follow up time (Overman et al., 2017). Subsequent phase 2 trials presented in 2020 include low dose Ipilimumab and have shown an objective response rate of 60% (Lenz et al., 2020).

Checkpoint blockade therapy blocks delivery of inhibitory signals to T cells and augments preexisting immunity. These promising results in MSI cancers are therefore unsurprising, as they frequently have high Immunoscore and CIRC enrichment scores along with high expression of coinhibitory receptors. Regulatory approval for checkpoint blockade therapy in metastatic MSI

colorectal cancer has been achieved in the USA and UK. However, MSI disease accounts for only a small proportion of metastatic CRC patients and stage IV MSS patients have shown incredibly poor responses to checkpoint blockade therapy (0% objective response rate) (Le et al., 2015).

Such poor responses to checkpoint blockade in MSS cancers are disappointing. Although such tumours tend to exhibit lower Immunoscore and CIRC enrichment score, a subset of MSS patients have tumours with high scores that are comparable to those with MSI cancers. Therefore, one viable approach is to develop trials that aim to stratify MSS patients, to target high immunity subsets. The University of Birmingham ANICCA Phase 2 recruited patients with metastatic MSS CRC that express MHC II (a good indicator of high CIRC enrichment score) for Nivolumab therapy (NCT03981146). In contrast to results obtained from studies performed on primary resections, only 0.7% of the 455 patients screened had >50% tumour tumour-specific MHC II staining. Those that were recruited into the study had an overall response rate of 0% (Middleton et al., 2022).

A possible explanation is that the studies which concluded some MSS cancers have reasonable immune responses were performed on primary resections, whereas clinical trials are often performed on patients with stage IV metastatic, treatment resistant disease. Indeed 62.9% of patients in the ANNICA trial had liver metastases. It may well be the case that in the subgroup of patients that undergo disease progression following resection or present at stage IV, the proportion of MSS patients with high Immunoscore/CIRC enrichment score is much lower. This may be because their cancers adapt to immune pressure via immune escape mechanisms such as loss of IFNγR1 or MHC I expression. Another possibility is that the high immunity subset of stage I-III MSS patients are more likely to go into remission following surgery and are less likely to present at the clinic with stage IV disease. A similar trial, POCHI, run by the Francophone Federation of Digestive Cancer has recruited MSS CRC patients with a high density of CD3

staining and is due to report findings in 2024 (NCT04262687). Hopefully, trials such as these will provide valuable data on whether a high immunity subset of MSS CRC patients at late-stage disease respond to checkpoint blockade.

The NICHE trial (NCT03026140) has adopted an alternative approach and trialled Nivolumab and Ipilimumab in combination as a neo-adjuvant therapy prior to resection in stage I-III patients (Chalabi et al., 2020). Post-surgery resections were compared to pre-treatment biopsies to assess histopathological indicators of response to immunotherapy. A number of MSS CRCs underwent regression following immunotherapy and many showed an increase in T cell infiltration, presence of tertiary lymphoid structures, TCR clonality, and expression of genes associated with a protective immune response. It is of note that a positive immune response did not necessarily correlate with regression, however these data are promising that immunological responses to checkpoint blockade are possible in some MSS patients. The sole predictor of response to immunotherapy in MSS patients was infiltration of T cells co-expressing CD8 and PD-1. This is unsurprising as CD8 T cells are thought to be the main effector of a cytotoxic immune response and PD-1 expression indicates sensitivity to blockade. Perhaps more interestingly, intratumoural expression of CD3, CD8, CXCL13, or an IFNγ gene signature was not predictive of response, nor was tumour mutational burden. This calls into question the rationale of studies, such as POCHI, that aim to recruit MSS patients into trials based solely on the presence of intratumoural T cells and highlights the need for better patient stratification.

Some MSS patients in the NICHE study were also treated with Celecoxib, an inhibitor of COX-2, based on pre-clinical data suggesting synergy with checkpoint blockade. Although in this trial no additional benefit was seen, it follows a trend in MSS CRC immunotherapy trials of combination therapy approaches. Many trialists have aimed to augment responses to checkpoint blockade through combination therapy with a variety of other treatments. When designing trials for CRC

immunotherapy, it is important to consider the limiting factor to an anti-cancer response. Clearly, in stage 4 MSS CRC, signalling via PD-1 is not the limiting factor as blockade had no objective response (Le et al., 2015).

Due to the observed differences in MSI and MSS CRC immune microenvironments, it is possible that the limiting factor for response to PD-1 blockade in MSS is tumour immunogenicity. In the low mutational setting, aiming to generate *de novo* immune responses may be a more effective strategy than trying to re-invigorate existing ones, since spontaneous immune responses tend to be fairly poor. Although it may not currently be possible to therapeutically increase neo-antigen burden in MSS CRC, immunogenicity may be increased by other mechanisms such as cell death (Fucikova et al., 2020). Cell death results in release of damage associated molecular patterns (DAMPs) via active processes or cell lysis such as Calreticulin, HMGB1, ATP, Annexin A1, and Type I Interferons. DAMPs are recognised primarily by myeloid cells and result in recruitment and activation of immune cells and phagocytosis of cellular debris. Cell death may increase the immune response to MSS CRC by the process of 'antigen spread' whereby local uptake of antigens by APCs and trafficking to lymph nodes introduces new antigens to the adaptive immune system and activates new T cell clones. It is therefore logical that immunotherapy could be combined with cytotoxic therapies such as chemotherapy and radiotherapy to augment new responses that occur as a result of antigen spread.

PD-1 blockade is being trialled in late stage MSS CRC patients in combination with cytotoxic chemotherapy agents Temozolomide (NCT03832621), Capecitabine (NCT03396926), Irinotecan (NCT03608046) and radiotherapy (NCT03104439). In addition to cytotoxic therapy, immunogenic cell death may be augmented by manipulating DAMP signals. ATP released from dying cells acts as an 'alarm' signal and promotes recruitment and activation of immune cells. ATP and ADP are rapidly degraded into AMP by ectonucleoside CD39 which is then degraded into adenosine by

ecto-nucleotidase CD73. Adenosine is potently immunosuppressive and the sequential action of CD39 and CD73 acts to resolve the 'alarm signal' raised by ATP release in the microenvironment. Blocking antibodies directed against CD39 and CD73 have shown promising results in murine models of cancer, acting synergistically with PD-1 blockade and Oxaliplatin chemotherapy (Perrot et al., 2019); CD39 and PD-L1 blockade combinatorial blockade has completed a phase 1 trial in patients with advanced solid tumours , although the therapy was generally well tolerated, 89.5% of patients were cycled off treatment due to disease progression (Imbimbo et al., 2022) (NCT04261075).

There have been attempts to utilise cancer vaccines to generate immunity towards CRC. For example, a vaccine directed against MUC1, which is overexpressed in human CRC, was trialled to prophylactically treat patients with adenomas at risk of CRC development (Kimura et al., 2013). Significant anti MUC1 immune responses were detected in 43% of patients, but no follow-up data have been published to establish the effectiveness in preventing CRC development. Dendritic cell vaccines prepared by incubating PBMC-purified DCs with autologous tumour lysate and injected intranodally back into patients have been shown to induce expansion of tumour reactive T cells in the blood, which correlates with survival (Barth et al., 2010). This study did not have a placebo group, so efficacy is impossible to determine, but 15/25 patients showed an increase in peripheral IFNγ production in response to tumour antigens. The same group went on to demonstrate that some typical metrics of immune response to CRC such as intratumoural CD8 T cell density or mutational burden were not predictive of response to dendritic cell vaccine, but some transcriptional signatures such as PI3K, mTOR, AKT signalling pathways were highly predictive (Qian et al., 2017). This result again highlights the importance of T cell function and activity, as opposed to staining density, when stratifying patients for immunotherapy trials.

5.1.6 Future Perspectives and Project Aims

Arguably, the key challenge in CRC immunotherapy is developing treatments that are effective in MSS patients. Key to this will be understanding the mechanisms behind heterogenous levels of intra-tumoural immunity. Some MSS patients have a measurable level of intra-tumoural immunity that is equivalent to MSI-H patients. If we are able to understand the molecular mechanisms behind this process, it may inform the rational design of therapies that synergise with ICB. Here we have investigated the drivers of intra-tumoural immunity in a subset of MSS patients, aiming to understand the relative contributions of tumour antigen recognition and microenvironment adjuvantisation.

5.2 RESULTS

Previous work has shown enriched expression of CIRC score genes (Table 5.1) in a subset of MSS CRC patients (MSShiCIRC) (McMurray, 2021). The MSShiCIRC patient grouping is delineated by a CIRC score threshold that is defined by CIRC score phenographic cluster of MSI-H patients within the same cohort. The MSShiCIRC subset does not display any difference to MSS patients in age, TNM stage, frequency of mutations, position of mutations, or type of mutations (McMurray, 2021).

TCR/Co-stimulation	MHC II genes	*HLA-DQA1* *HLA-DQA2* *HLA-DRB5* *HLA-DPB1* *HLA-DPA1* *HLA-DMB* *HLA-DRA* *HLA-DMA* *HLA-DOA*
		CD247 *CD4* *CD80* *ICOS*
Co-inhibitory Signalling		*CTLA4* *LAG3* *HAVCR2* *PDCD1LG2*
Leukocyte Trafficking		*ICAM1* *CCL5* *CXCL9* *CXCL10*
Th1/IFNγ signalling		*IFNG* *IRF1* *STAT1* *TBX21*
Cytotoxicity		*GNLY*

Table 5.1. ***Co-ordinated Immune Response Cluster genes.***

5.2.1 The Role of Antigen Recognition in the MSShiCIRC Patient Subtype

The CIRC signature is an IFNγ/Th1 centric score; IFNγ expression by T cells can be induced by antigen recognition or by cytokine signalling. In order to investigate the contribution of antigen recognition to the MSShiCIRC subset, we accessed RNAseq datasets and scored patients from the TCGA-COADREAD database with transcriptional metrics generally associated with TCR signalling in $CD4^+$ T cells (T.activation) (*CD69, CD25, NR4A1, TNFRSF9*) (Figure 5.1.A) and specifically associated with $CD4^+$ T cell response to high strength TCR signalling and effective responses to ICB (Elliot et al., 2021) (TCR.strong) (*TNFRSF4, ICOS, TNIP3, STAT4, IRF8*) (Figure 5.1.B). Both metrics were elevated in the MSI-H subset as expected, but were also elevated in the MSShiCIRC subset, indicating a role for TCR signalling in high CIRC scores among MSS patients. RNAseq datasets from the TCGA-COADREAD database are performed on bulk tumour resections and therefore contain a complex mix of tumour cells, stromal cells, and immune infiltrate. Application of these transcriptional signatures is not sufficient to confirm whether conventional T cells are recognising antigen. For example, *TNFRS4* encodes OX40, which is expressed at high levels by antigen specific conventional $CD4^+$ T cells (Elliot et al., 2021), but also by T_{REG} cells (Kupiec-Weglinski, 2007).

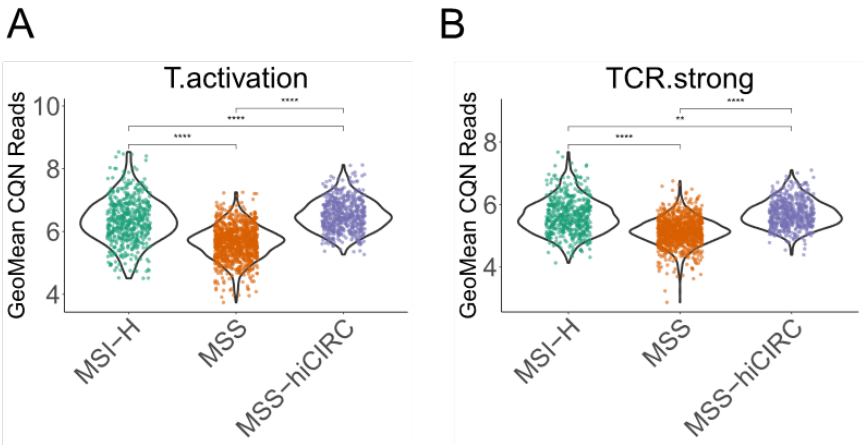

Figure 5.1. ***MSS-hiCIRC signature is associated with transcriptional signature of T cell activation and strong TCVR signalling.*** *Violin plots of transcriptional signatures calculated by geometric mean of CQN read counts A) T.activation (CD69, CD25, NR4A1, TNFRSF9) B) TCR.strong (TNFRSF4, ICOS, IRF8, TNIP3, STAT4) in MSI-H, MSS, and MSShiCIRC patients of the TCGA-COADREAD dataset. Statistical test is Mann-Whitney with multiple comparisons. *P ≤ 0.05, **P ≤ 0.01, ***P ≤ 0.001, ****P ≤ 0.0001.*

CD39 has been posited as a marker for tumour-antigen specific T cells. A 2018 study utilised whole genome sequencing of colorectal and lung cancers to design MHC pentamers loaded with patient specific neoantigens (Simoni et al., 2018). Simoni and colleagues used these to label neoantigen specific $CD8^+$ TILs, allowing their phenotypic comparison to $CD8^+$ T cells specific for non-tumour related antigens such as EBV peptides. They found that neoantigen specific cells specifically expressed CD39. $CD39^+$ $CD8^+$ T cells are the specific *in vitro* responders to synthetic peptides generated from tumour neoantigens in both $CD8^+$ T cells (Chow et al., 2023; Duhen et al., 2018)and $CD4^+$ T cells (Kortekaas et al., 2020). An MHC II^+ and an MHC II^- (data not shown) CRC patient FFPE sample were stained for CD39 (Figure 5.2). The MHC II^+ sample showed invasion of $CD39^+$ cells into the tumour epithelium which was absent in the MHC II^- sample however, both the MHC II^+ and MHC II^- samples showed strong staining on the tumour stroma.

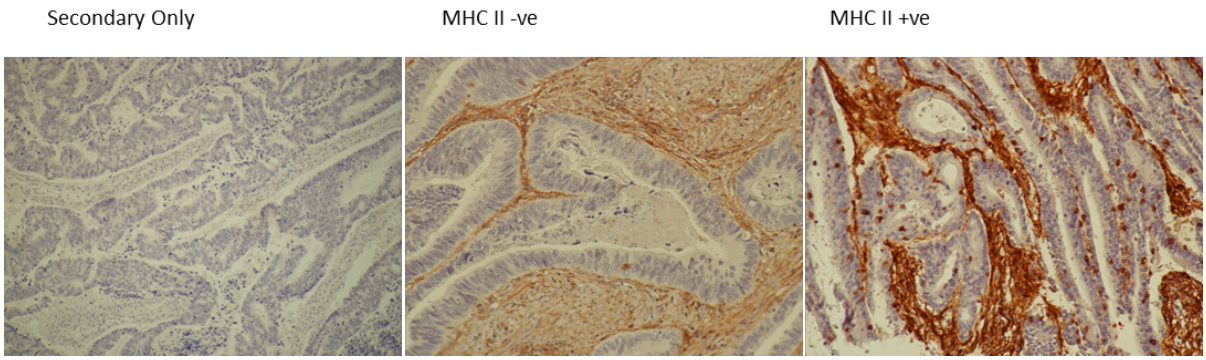

Figure 5.2. ***H-DAB staining for CD39 in colorectal cancer resections that are MHC II negative and MHC II positive.***

In order to distinguish between CD39 expression on the tumour stroma and CD39 expression by T_{REG} cells (Ahlmanner et al., 2018; Deaglio et al., 2007) from CD39 expression by tumour-antigen reactive $CD4^+$ and $CD8^+$ conventional T cells, we designed a multispectral immunofluorescent staining panel (CD4, CD8, FOXP3, CD39). Imaging of the full panel (Figure 5.3.A) or CD39 alone (Figure 5.3.B) revealed high expression levels of CD39 in the T cell rich region of an MSI-H and an

MSShiCIRC patient, but not an MSS patient. Allocated stromal and tumour epithelial regions (Figure 5.4.A) were used to train a classifier (Figure 5.4.B). The DAPI stain was used to performed automated cell detection (Figure 5.4.C) before phenotyping of individual cells as indicated in figure legend (Figure 5.4.D). MSI-H and to a lesser extent MSShiCIRC had an elevated density of $CD4^{+}$ $FOXP3^{-}$ (Figure 5.4.E) and $CD8^{+}$ (Figure 5.4.F) conventional T cells. Density of $CD39^{+}$ conventional T cells was high in all three MSI-H patients and low in all MSS patients, as expected (Figure 5.4.G&H). However, only one out of three MSShiCIRC patients showed high levels of CD39 expression. These data suggest heterogenous levels of tumour antigen recognition among MSShiCIRC patients. Whilst it is possible for a patient with intact mismatch repair machinery to have high levels of tumour antigen recognition, it is also possible to achieve high CIRC scoring without it.

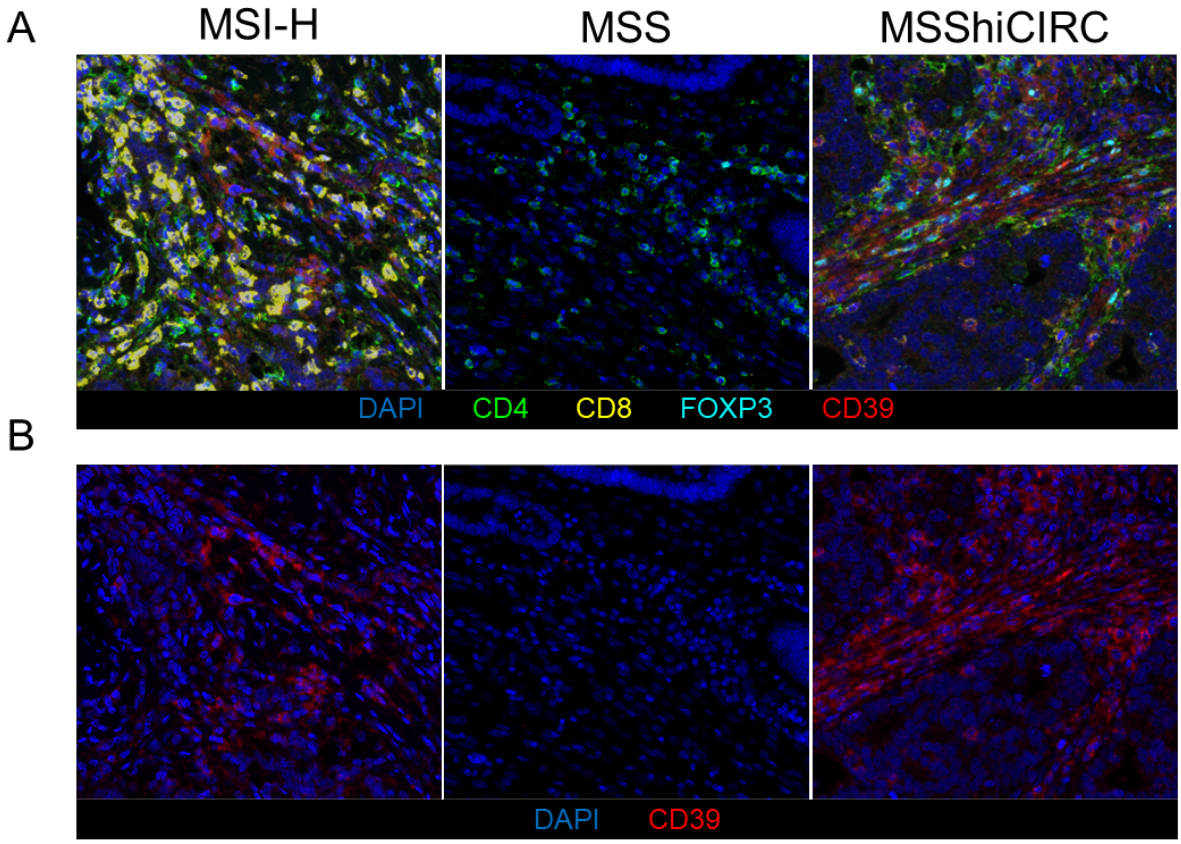

Figure 5.3. ***CD39 marks antigen reactive CD8 and CD4 T cells in MSI-H and MSS-hiCIRC tumours****. Multiplex immunofluorescence imaging of DAPI, CD4, CD8, FOXP3, and CD39 (A) or DAPI and CD39 (B) in MSI-H, MSS, and MSShiCIRC FFPE colorectal cancer sections.*

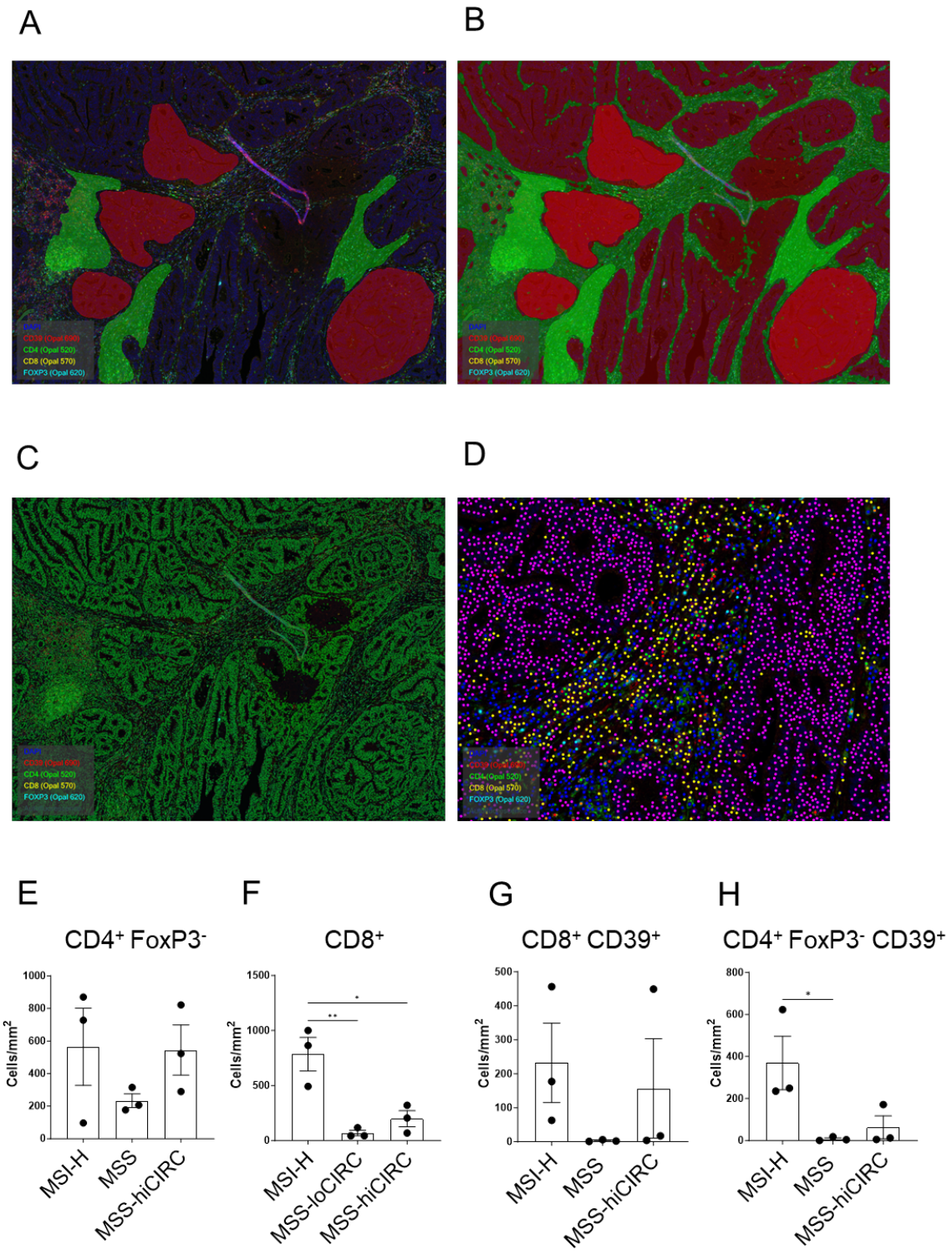

Figure 5.4. ***CD39+ TILs are abundant in MSI-H patients but rare in MSS-hiCIRC patients****. Representative images of segmentation and cell phenotyping using InForm software. A) Training regions of tumour epithelium (red) and stroma (green). B) Spatial segmentation of tumour and stroma regions. C) Cellular segmentation. D) Cell phenotyping CD8+ FoxP3- CD39- (red) CD8+ FoxP3- CD39+ (green) CD4+ FoxP3- CD39- (blue) CD4+ FoxP3- CD39+ (yellow) CD4+ FoxP3+ CD39- (brown) CD4+ FoxP3+ CD39+ (cyan) CD8- CD4- FoxP3- CD39- (purple). Quantification of indicated cell phenotypes (E-H). Statistical test is Mann-Whitney with multiple comparisons. *P ≤ 0.05, **P ≤ 0.01, ***P ≤ 0.001, ****P ≤ 0.0001. N=3/group.*

5.2.2 Metagenome sequencing of Intratumoural Bacteria

Following our observation that CIRC score can be high despite apparently low levels of tumour antigen recognition, we aimed to investigate microenvironmental drivers of high scores among MSS patients. Due to the previously discussed role of the microbiota in expression of MHC II in intestinal epithelial cells, we hypothesised that we might observe differences in the bacterial populations within the tumours. We accessed whole genome sequencing data from local cohort patients. Reads that did not align to human reference genome were aligned to microbial genomes in the NCBI database (D. Kim et al., 2016). Taxonomy data were aligned to NCBI genome IDs, differential microbe analysis and phylogenetic aggregation of reads was performed (Paulson et al., 2013).

We compared the class distribution of bacteria identified from whole genome sequencing and although the MSI-H patients showed a large enrichment of *Fusobacterium*, there were no notable differences between MSS and MSShiCIRC subtypes (Figure 5.5).

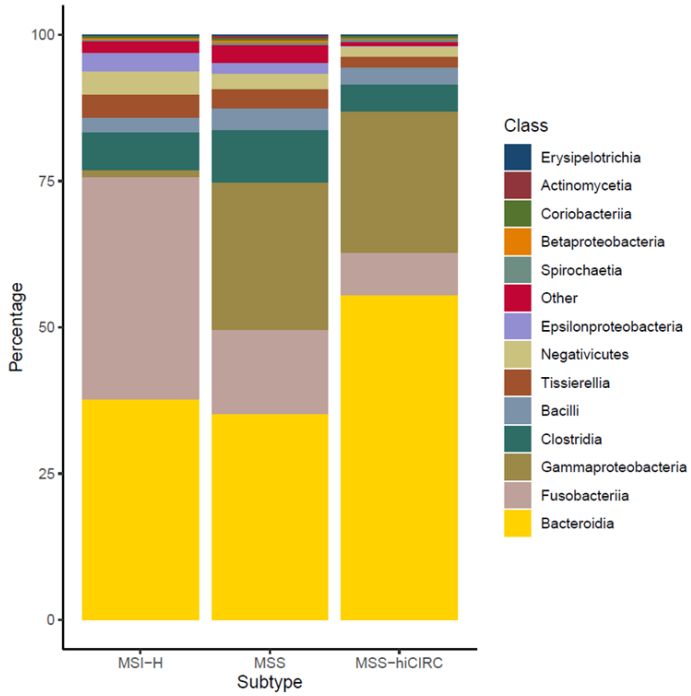

Figure 5.5. ***Distribution of bacterial classes in MSI-H, MSS, and MSS-hiCIRC local cohort patients determined by MetaGenome sequencing of tumour resections.***

Heatmap analysis of the ten most abundant bacterial classes and Z score clustering demonstrated clustering of MSI-H patients, likely due to their propensity to be right-sided (Figure 5.6). In contrast, MSShiCIRC patients appeared to be diffuse among the MSS patients. It may be that although there is no consistent difference between the bacterial makeup and the class level, there may be differences at a lower phylogenetic level. We performed heatmap and PCA analysis at every level from phylum to genus but did not observe clustering of MSShiCIRC patients at any level (data not shown). PCA analysis of the 500 most abundant operational taxonomic units (OTUs) again did not cluster MSShiCIRC patients (Figure 5.7). We observed tight clustering of MSI-H patients, PC1 appeared to be dominated by variance between MSI-H and MSS patients, likely representing differences between right-sided vs left-sided microbiota. We therefore repeated the analysis excluding MSI-H patients, but again saw no clustering of MSShiCIRC patients (Figure 5.8). We ran MSS and MSShiCIRC patients through a fixed feature model to interrogate differential abundance of individual OTUs (Paulson et al., 2013). We found that no single OTU passed statistical testing to reject the null hypothesis. Plotting relative abundance of the top five individual OTUs with highest fold change between MSS and MSShiCIRC patients (Figure 5.9.A-E) or aggregated counts of the top thirty highest fold change OTUs (Figure 5.9.F) revealed that most patients did not have detectable levels of these OTUs, and they were therefore unlikely to be a causative factor in high vs low CIRC scoring.

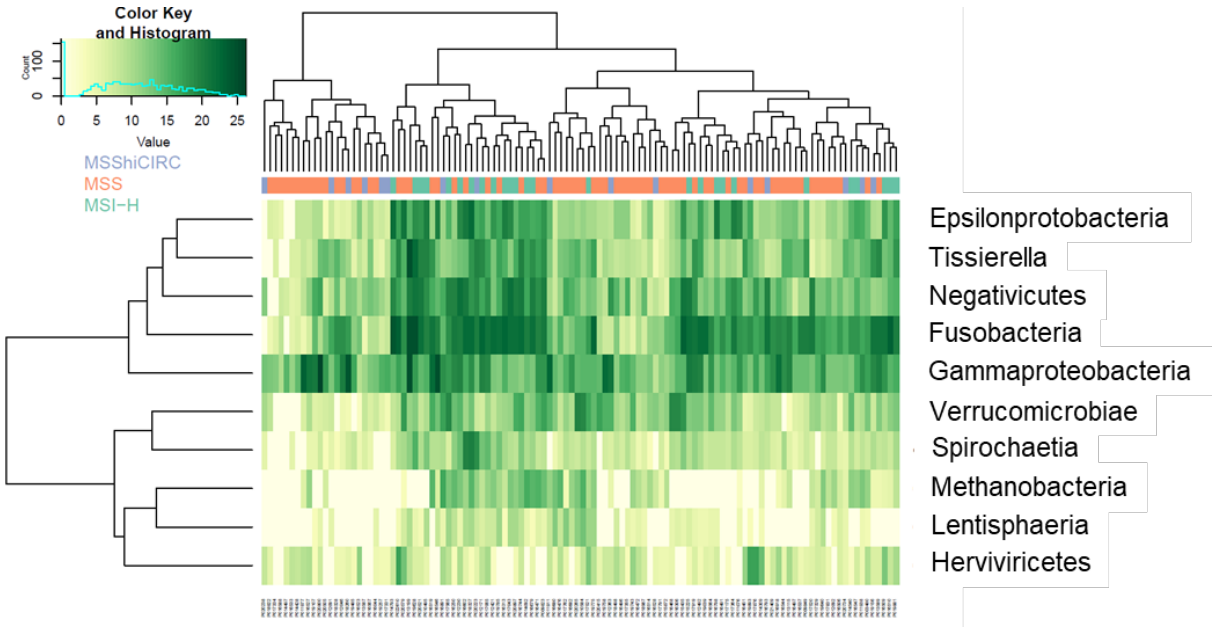

Figure 5.6. ***MetaGensome sequencing shows no difference in bacterial class distribution between MSS and MSS-hiCIRC patients****. Heatmap with Z-score clustering of the 10 most abundant bacterial classes in MSI-H, MSS, and MSS-hiCIRC local cohort patients.*

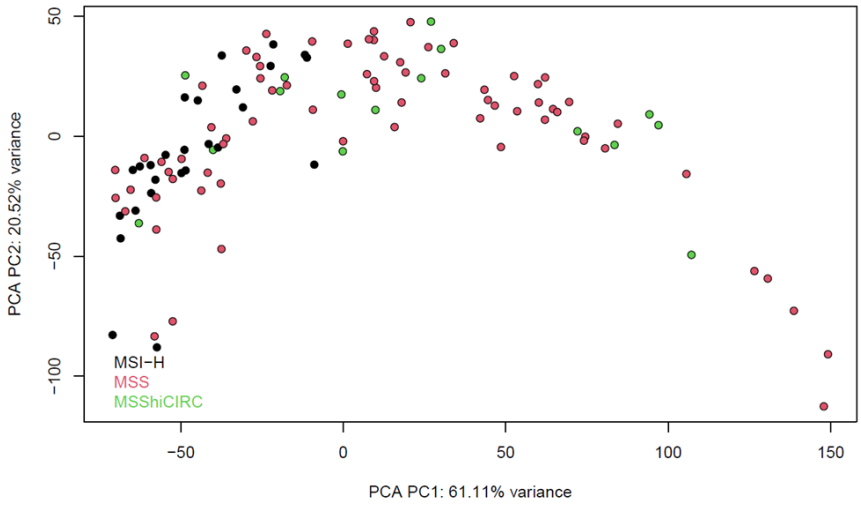

Figure 5.7. ***Only MSI-H patients show distinct OTU distributions****. PCA plot of 500 most abundant OTUs in MSI-H, MSS, and MSS-hiCIRC local cohort patients.*

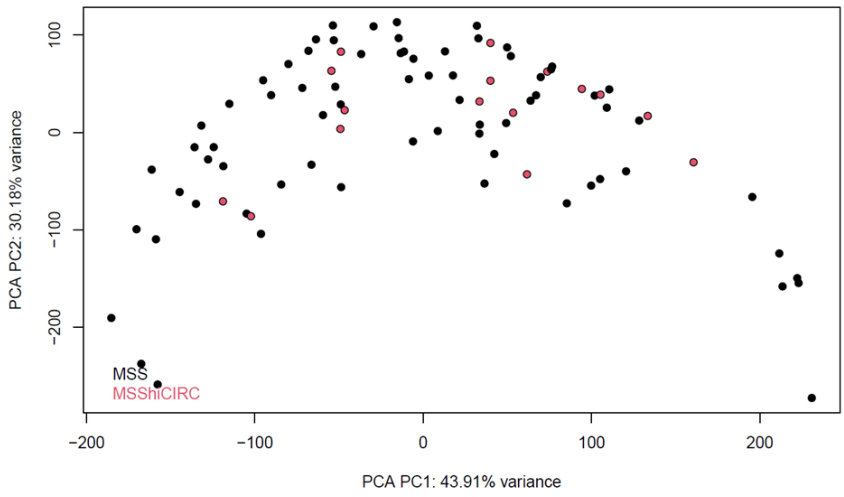

Figure 5.8. ***No variance in OUT abundance between MSS and MSS-hiCIRC patient groups. PCA*** *plot of 500 most abundant OTUs in MSS and MSS-hiCIRC local cohort patients.*

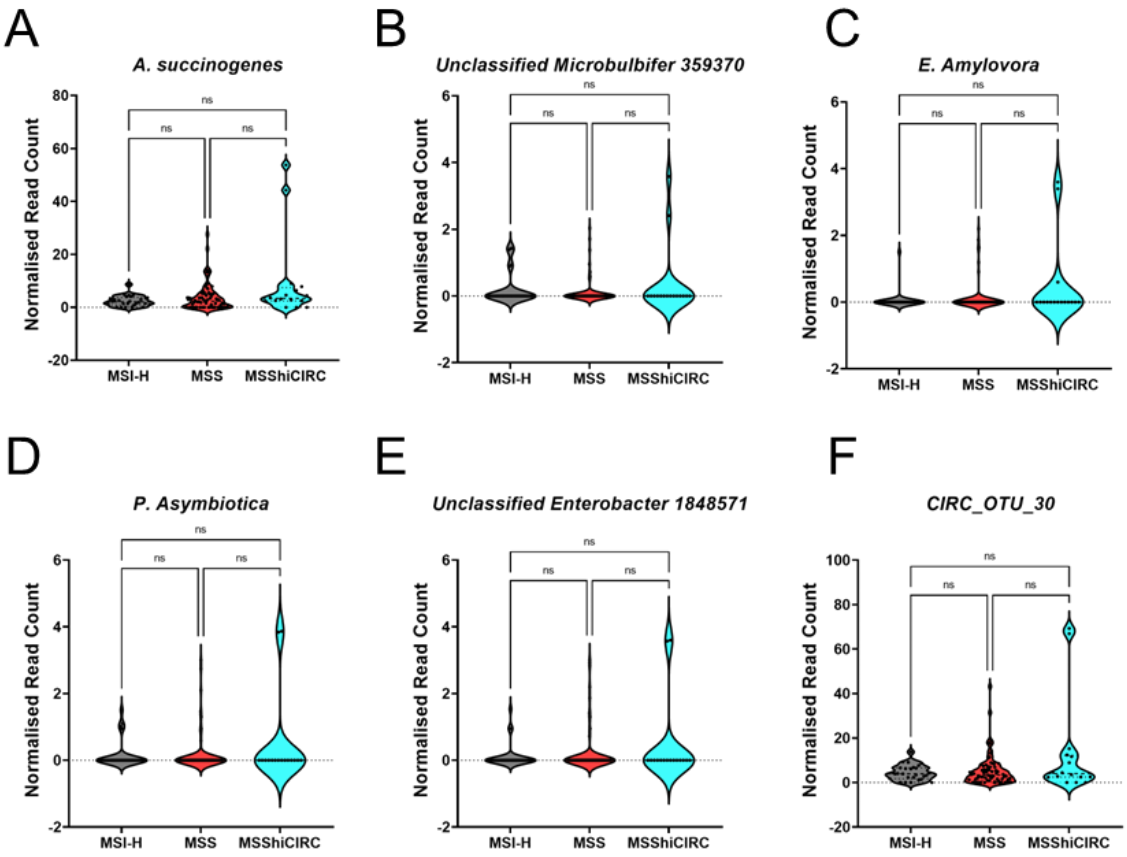

Figure 5.9. ***No individual OTUs are enriched in the MSS-hiCIRC patient group.*** *Violin plots of top 5 OTUs most differentially enriched between MSS and MSShiCIRC local cohort patients (A-E) and combined reads of the top 30 OTUs most differentially enriched (F). Stats test performed is a one way ANOVA with Tukey's multiple comparison test N=16-72/group.*

5.2.3 Altered Bacterial Detection Pathway in MSShiCIRC Patients

If the abundance of bacteria is not significantly different between MSS and MSShiCIRC patients, it may be that their ability to detect bacteria is different. Previous pathway analysis of the TCGA-COADREAD dataset revealed increased expression of pathways associated with immune responses against bacteria (McMurray, 2021). Notably, differential gene expression analysis between MSS and MSShiCIRC subtypes showed *GBP5* to be the statistically most enriched in the MSShiCIRC patients. GBP5 and other guanylate binding proteins are key mediators of innate immune responses against bacteria. For example, GBP1 is an LPS detector (Santos et al., 2020)

and GBP5 is required for NLRP3 inflammasome assembly (Shenoy et al., 2012). GBP proteins also control entry of gram-negative bacteria into the cytoplasm, which is important for innate immune responses to LPS (Man et al., 2016).

We again interrogated the TCGA-COADREAD dataset to determine differences in expression of genes associated with the innate immune that might drive IFNγ release in response to bacteria. This included all five GBP members, *TLR4* a cell surface LPS receptor, *MYD88* that mediates TLR4 downstream signalling and transcription of *IL18*, inflammasome sensor protein *NLRP3*, executor caspase of the canonical inflammasome pathway *CASP1*, inflammasome regulated cytokines *IL1B* and *IL18*, and MYD88 controlled cytokine *IL12A*. Many of these genes were enriched in MSShiCIRC and MSI-H patients compared to MSS patients, most notably GBP genes (Figure 5.10). We decided to pursue *GBP5* as a target because of its well documented role in the NLRP3 inflammasome and therefore the IL-18-IFNγ axis, and its very significant upregulation in MSShiCIRC patients.

In order to confirm increased expression, we stained samples from different patient subtypes for GBP5. We observed large differences in GBP5 expression among patients (Figure 5.11). We also observed heterogenous expression patterns (Figure 5.12), with some patients showing stromal restricted GBP5 expression but others also showing positive GBP5 staining in the epithelium. MSI-H (Figure 5.13), MSS (Figure 5.14), and MSShiCIRC (Figure 5.15) samples underwent cell detection and stroma/tumour epithelium segmentation. Individual cells from tumour epithelium regions were scored by cell DAB mean density thresholds. GBP5 expression was enriched in tumour epithelium regions of MSI-H and MSShiCIRC patients as compared to MSS (Figure 5.16.A&B). Matched adjacent healthy tissue was also stained for GBP5 (Figure 5.16.C&D) but equally low levels were observed across patient groups confirming tumour specific increased GBP5 in MSShiCIRC patients as compared to MSS.

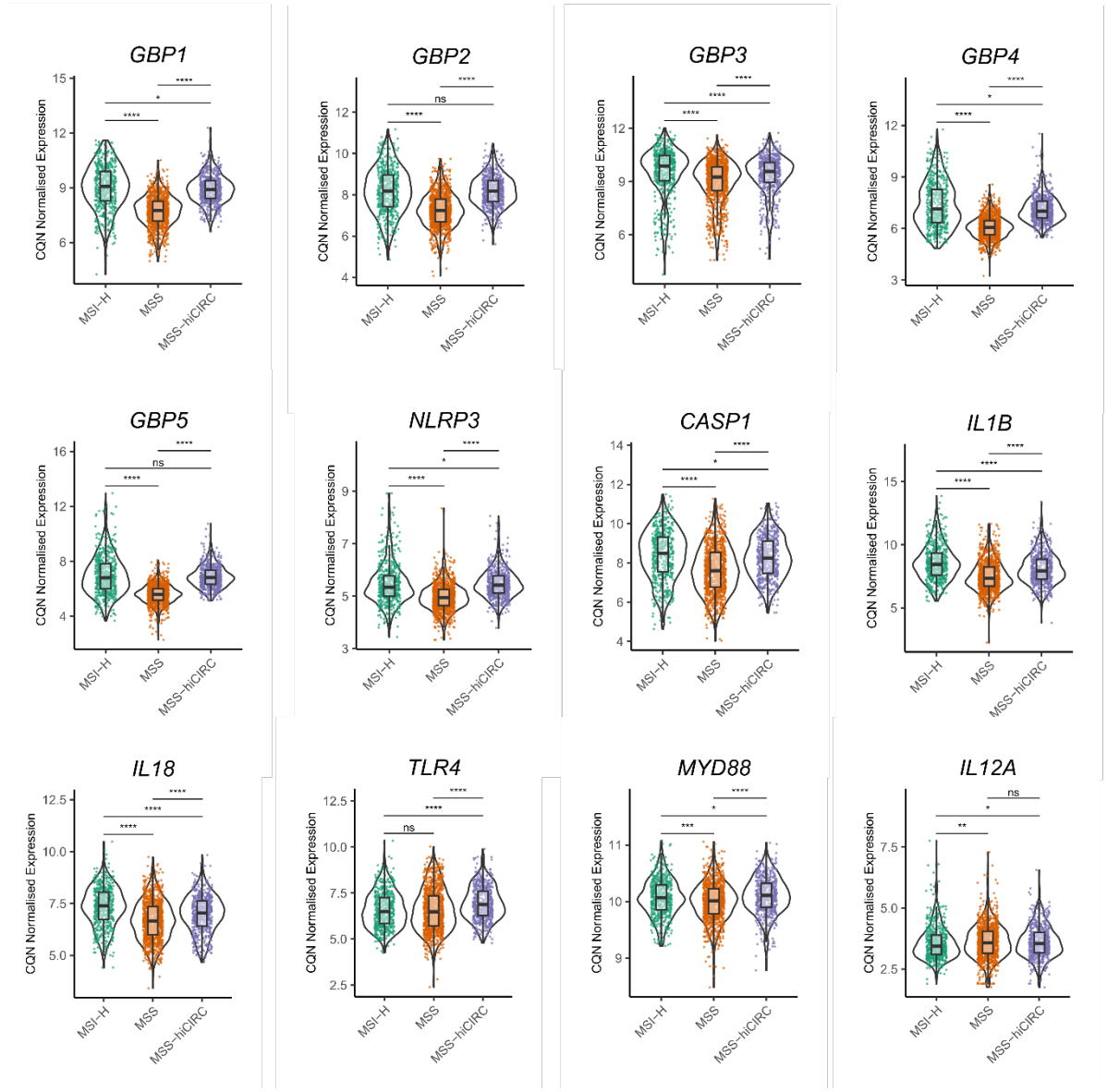

Figure 5.10. ***Genes involved in innate recognition of bacterial patterns are upregulated in MSS-hiCIRC patient tumours.*** *CQN normalised expression of indicated transcripts in MSI-H, MSS, and MSShiCIRC patients of the TCGA COADREAD dataset. Statistical test is one way ANOVA with Tukey's multiple comparisons. *P ≤ 0.05, **P ≤ 0.01, ***P ≤ 0.001, ****P ≤ 0.0001.*

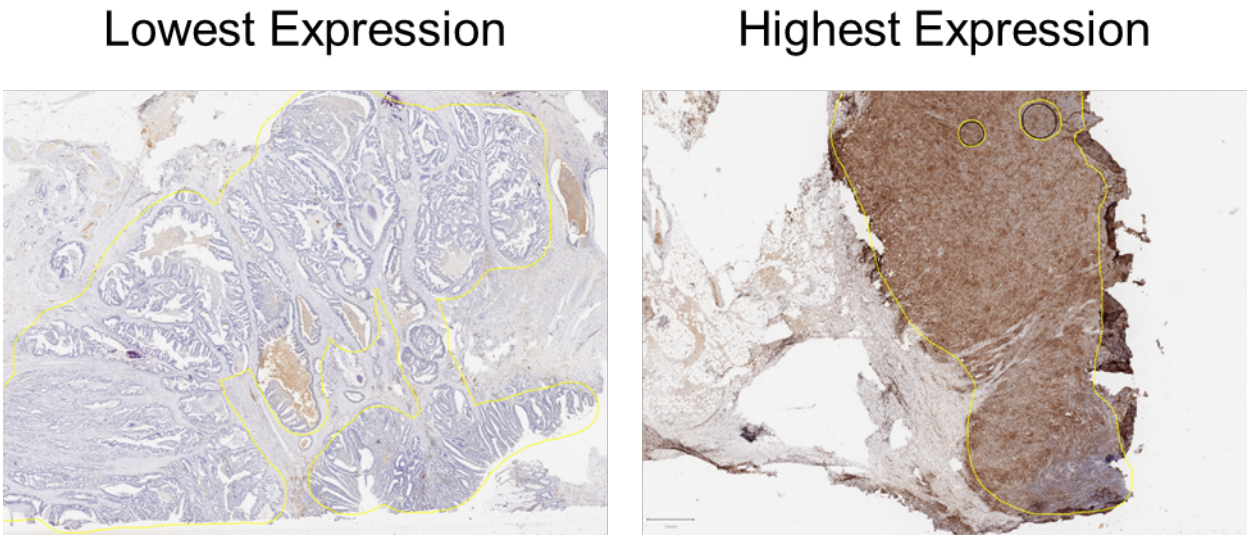

Figure 5.11. ***GBP5 shows a wide range of protein expression in resected tumours.*** *H-DAB staining of GBP5, images of highest and lowest expressors.*

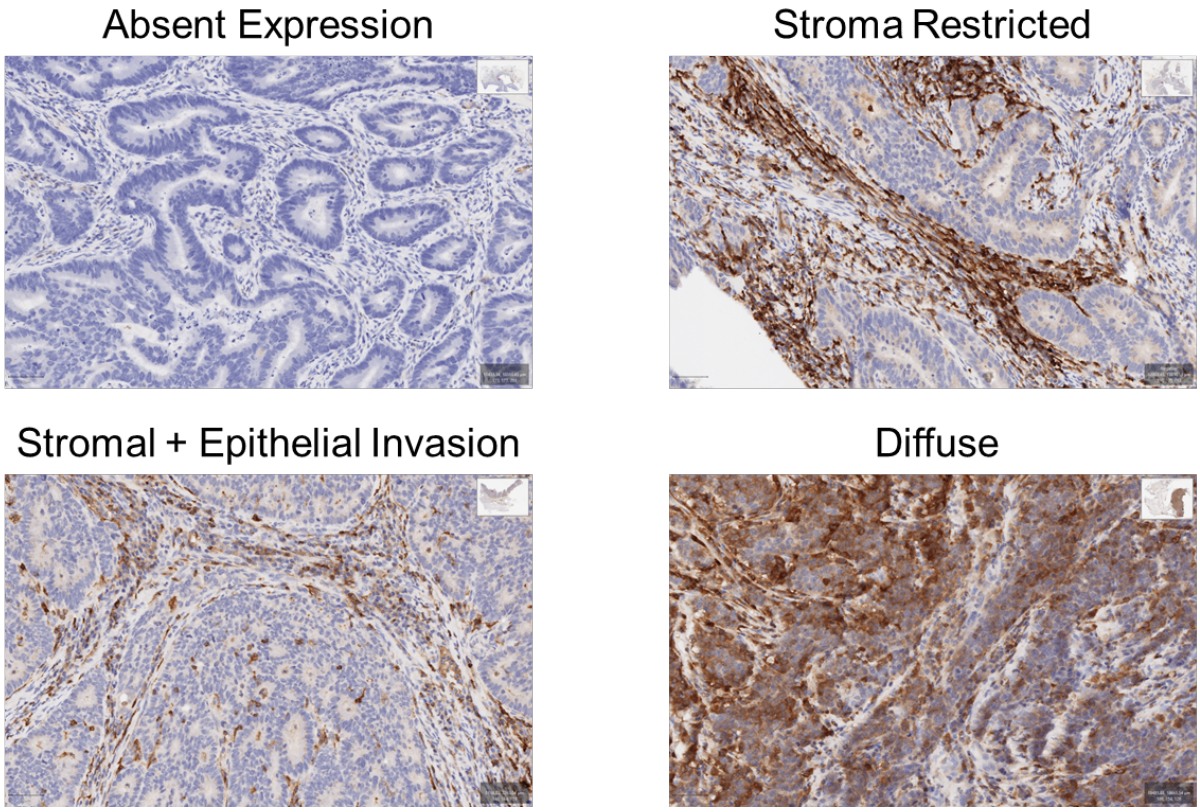

Figure 5.12. ***Representative images of the different patterns of GBP5 DAB staining observed.***

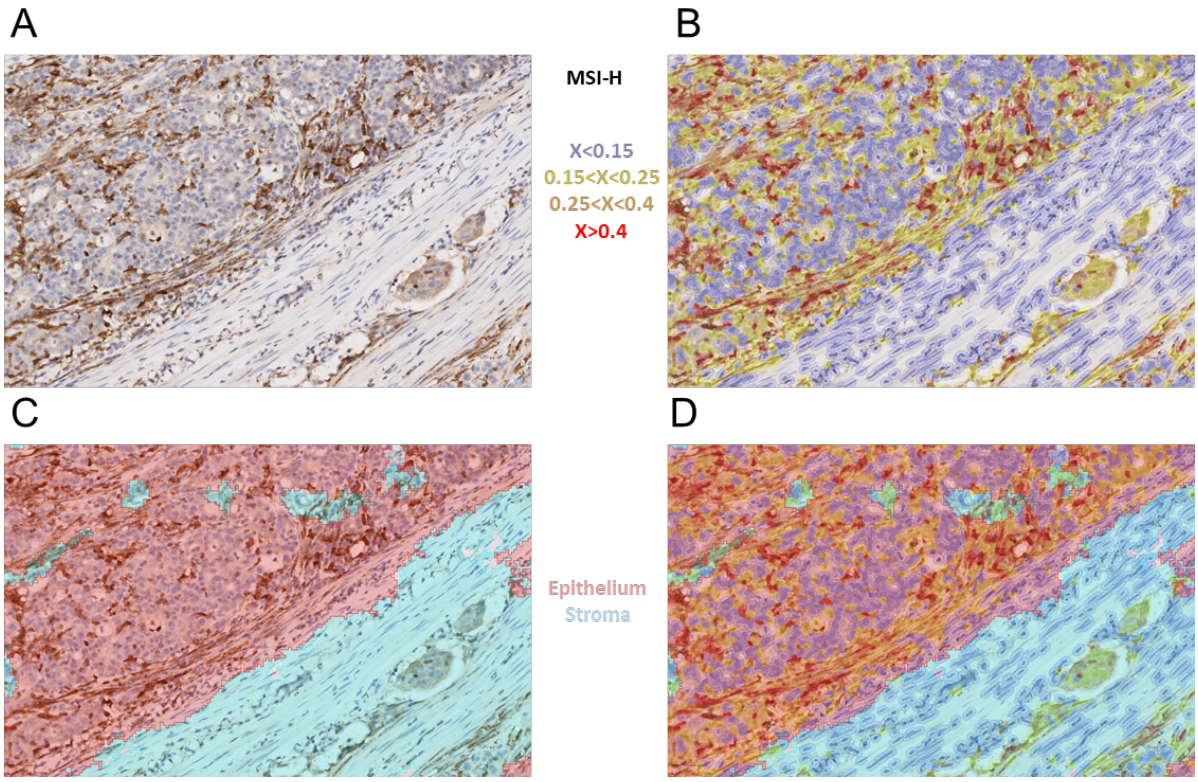

Figure 5.13. ***High expression of GBP5 in epithelial regions of MSI-H tumours.*** *A) Representative H-DAB staining of an MSI-H patient. B) Cell DAB mean intensity threshold scoring of individual cells. C) Automatic detection of tumour epithelium and stromal regions. D) Overlay of B and C.*

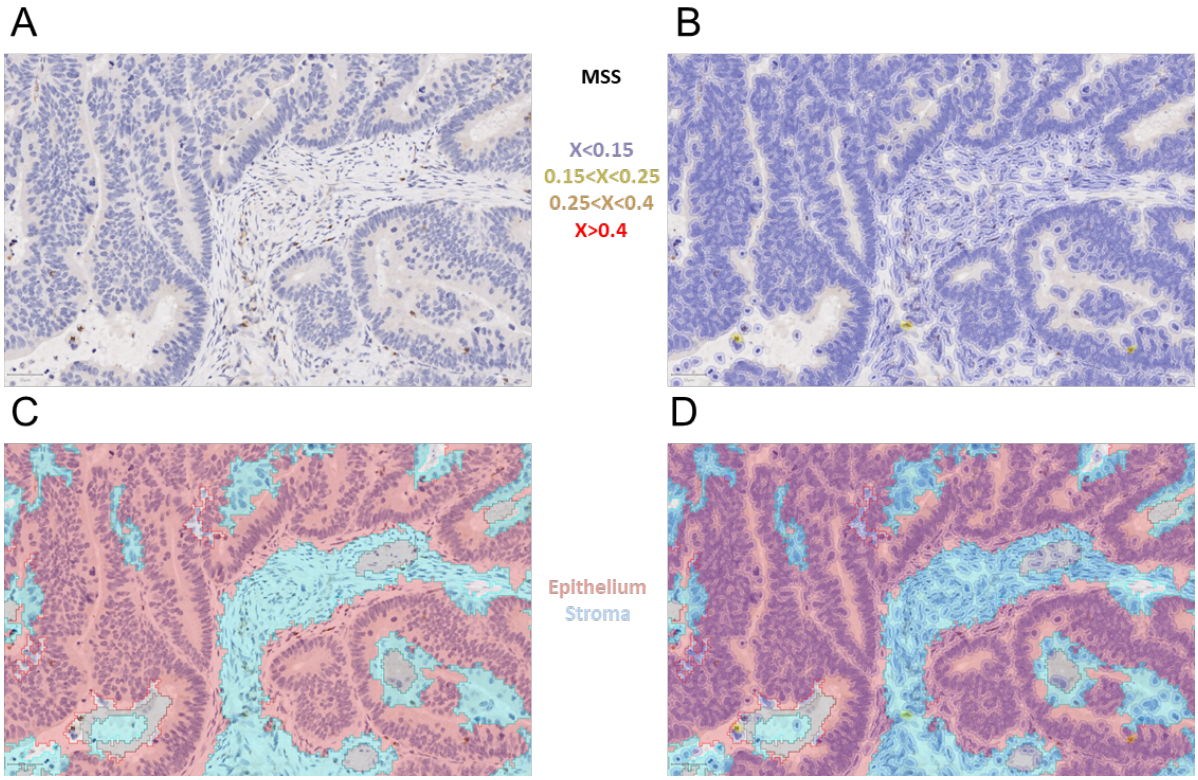

Figure 5.14. ***Low expression of GBP5 in epithelial regions of MSS tumours.*** *A) Representative H-DAB staining of an MSS patient. B) Cell DAB mean intensity threshold scoring of individual cells. C) Automatic detection of tumour epithelium and stromal regions. D) Overlay of B and C.*

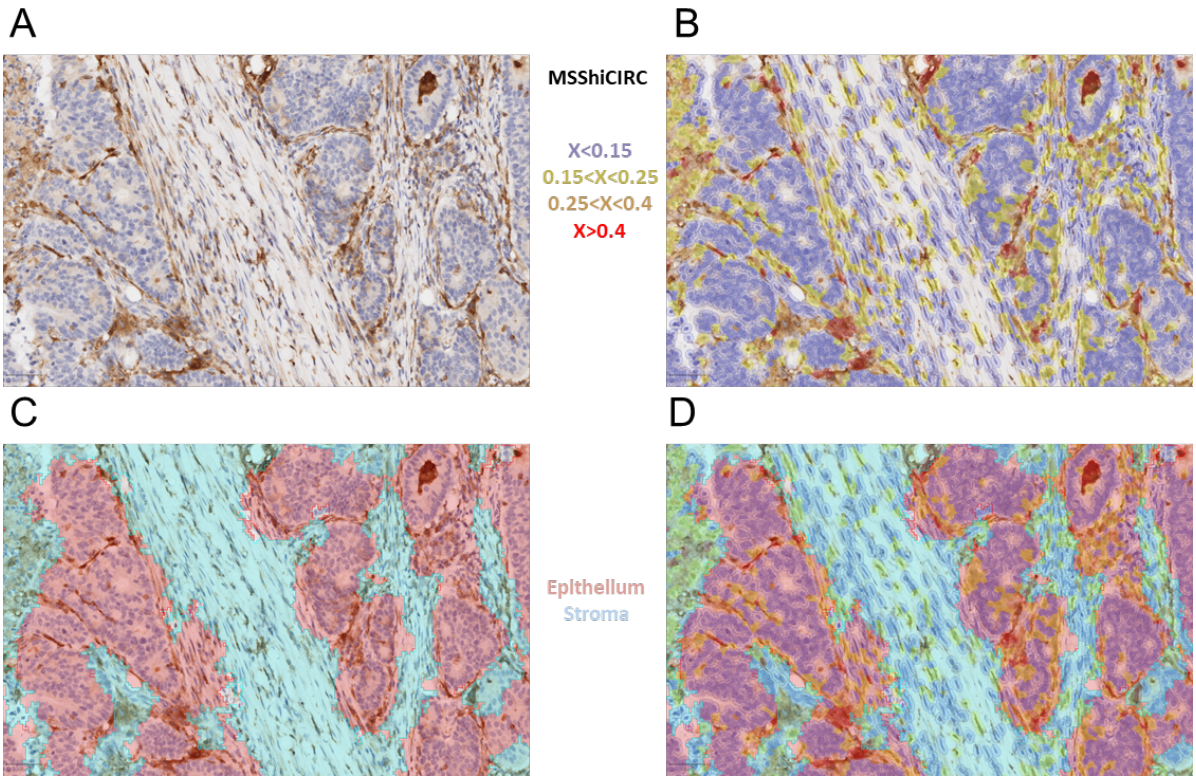

Figure 5.15. ***High expression of GBP5 in epithelial regions of MSS-hiCIRC tumours.*** *A) Representative H-DAB staining of an MSShiCIRC patient. B) Cell DAB mean intensity threshold scoring of individual cells. C) Automatic detection of tumour epithelium and stromal regions. D) Overlay of B and C.*

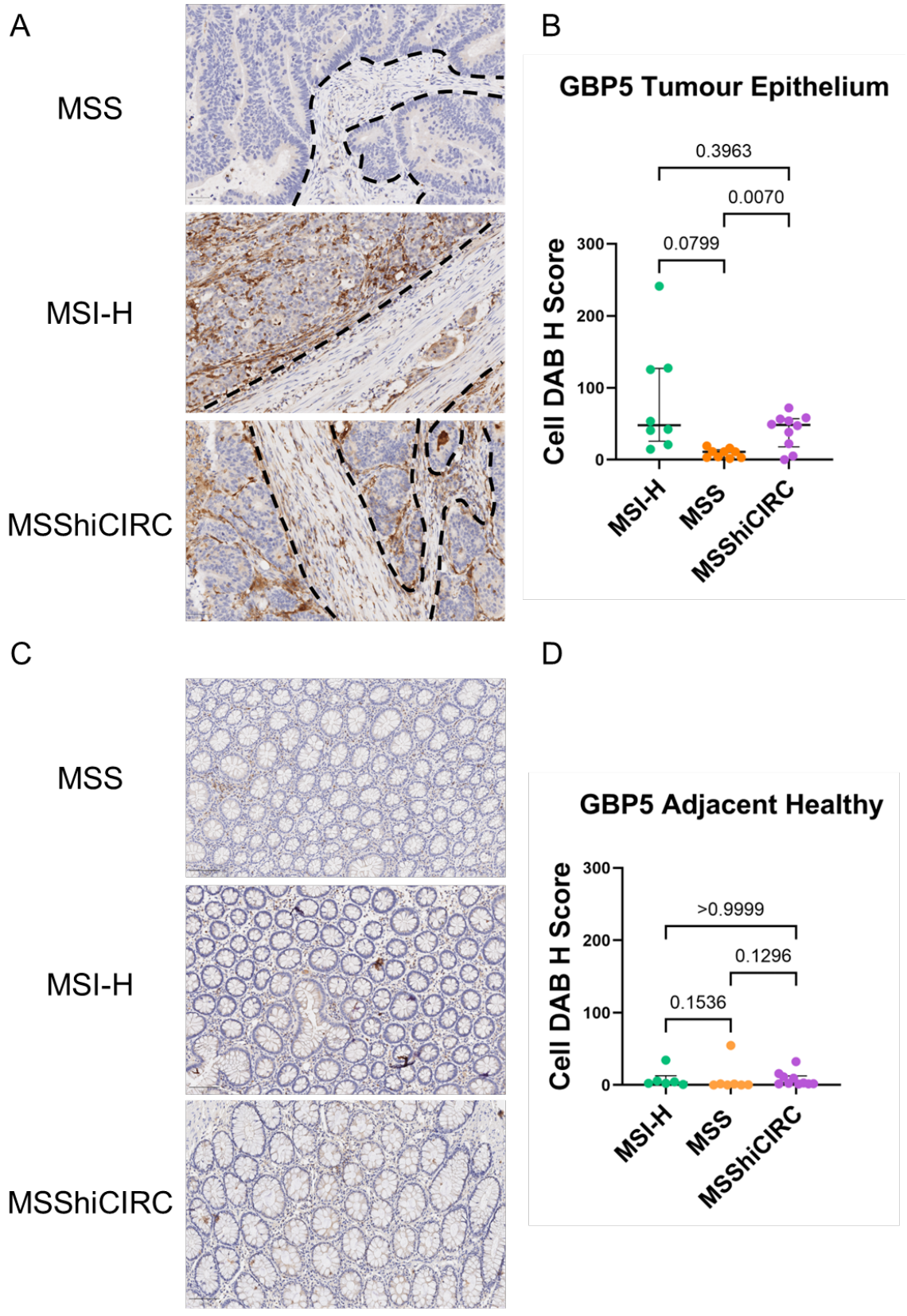

Figure 5.16. ***Elevated GBP5 expression in epithelial regions of MSI-H and MSS-hiCIRC tumours, but no change to adjacent healthy tissue.*** *A) Representative H-DAB staining of GBP5 in tumour tissue. B) Quantification of cell DAB H scoring of tumour epithelium in patient subsets. C) Representative H-DAB staining of GBP5 in matched healthy adjacent tissue. D) Quantification of cell DAB H scoring of matched healthy adjacent tissue in patient subsets. Stats test is one way ANOVA with Tukey's multiple comparisons. N=10/group.*

We hypothesised that increased levels of GBP5 may make MSShiCIRC tumour cells more amenable to activation of the NLRP3 inflammasome and subsequent caspase-1 cleavage and release of IL-18. NLRP3 inflammasome activation is well documented in human macrophages and in murine intestinal epithelium (Song-Zhao et al., 2014), but not well studied in human intestinal epithelium. In order to test whether human intestinal epithelial cells can activate the NLRP3 inflammasome we stimulated HIEC-6 cells, that are derived from healthy small intestinal epithelium, with nigericin sodium salt, a well-known agonist of NLRP3 (He et al., 2016). We lysed cell pellets and performed western blot analysis of Caspase-1 (Figure 5.17). Four hour stimulation was sufficient to induce Caspase-1 cleavage, indicating the possibility that malignant intestinal epithelial cells of MSShiCIRC patients could be driving high CIRC scores by inflammasome mediated IL-18 release.

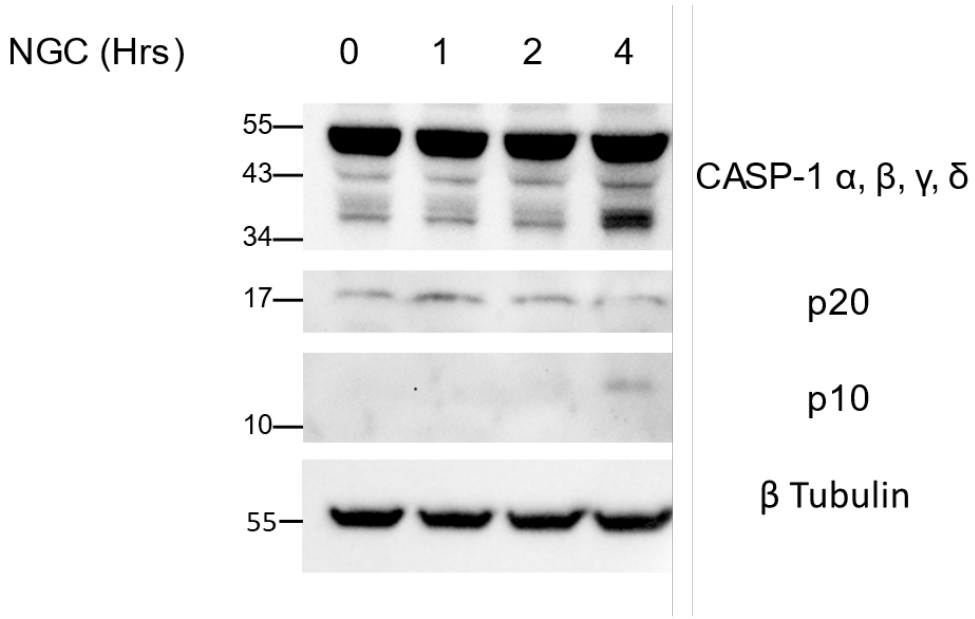

Figure 5.17. ***HIEC-6 cells cleave Caspase-1 in response to NLRP3 inflammasome stimulation.*** *Western blot analysis of HIEC-6 cell lysate following stimulation with 20μM nigericin for indicated time points*

5.3 DISCUSSION

Here we propose a model whereby recognition of bacterial patterns by detectors such as TLR4 and NLRP3 lead to production of IFNγ-inducing cytokines IL-12 and IL-18 respectively. This leads to IFNγ production by local lymphocyte populations, which are enriched for $CD161^+$ cells (Fergusson et al., 2014) such as MAIT cells and ILC1, that are proficient at responding to cytokine stimulation (Ussher et al., 2014). IFNγ signalling leads to upregulation of CIITA and subsequently cell surface MHC II, which may then lead to presentation of tumour antigens, $CD4^+$ T cell TCR ligation and further IFNγ release. IFNγ signalling also upregulates GBP5 (Krapp et al., 2016), and possibly other GBPs, leading to increase inflammasome assembly (Shenoy et al., 2012) and trafficking of gram-negative bacteria to the cytoplasm (Man et al., 2016). IFNγ may also lead to increased barrier permeability and further activation of innate immune pathways (Beaurepaire et al., 2009) completing the positive feedforward loop (Figure 5.19).

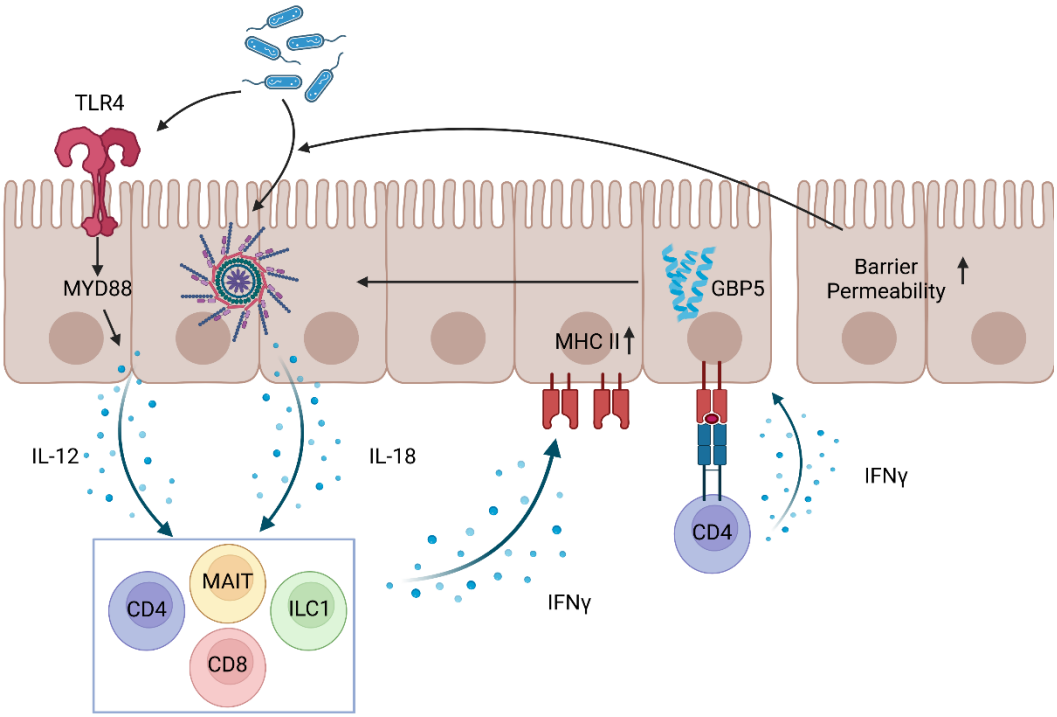

Figure 5.19. ***Proposed model of drivers of high CIRC scores in MSS patients.***

Transcriptional signatures of TCR signalling were significantly increased in MSShiCIRC patients as compared to MSS; however, these analyses were performed on bulk tumour resections where increased expression may be driven by increased T cell infiltration as opposed to specific recognition of tumour antigens. Indeed, we saw increased infiltration of T cells in all three MSShiCIRC samples analysed by multispectral immunofluorescence, but those T cells only expressed high levels of CD39 in one sample. Although limited by a small number of samples, these results suggest high levels of tumour antigen recognition is redundant for high CIRC scoring in MSS patients.

Our metagenome sequencing analysis of local cohort resections was not able to determine any difference between MSS and MSShiCIRC bacterial colonisation. MSI-H patients were included in the analysis and served as an important internal positive control. Clear clustering of the mostly right sided MSI-H patients demonstrated that our analysis was able to detect differential microbial colonisation. Additionally, some bacteria that are known to be enriched in colorectal cancer such as *Fusobacterium Nucleatum* (Mima et al., 2016) had hundreds of detectable reads in the majority of patients (data not shown). Nevertheless, these samples were not prepared with the intention of metagenome sequencing, which may have impacted the fidelity of our analysis. Best practice preparation of samples for bacterial genomics recommends immediate snap freezing (Microbiome Insights, inc.), we do not know how quickly samples were frozen before DNA extraction. Additionally, much of the colonic bacteria is embedded within the mucosal layer. If the samples were in any way washed, or rinsed in a buffer, prior to DNA extraction, this may have removed much of the potentially immunomodulatory bacteria. Our analysis was also limited to relative abundance testing of bacterial populations; without some sort of housekeeping control (such as mass of tissue) we are unable to determine total levels of bacteria. If, for example, MSShiCIRC patients had higher total numbers of bacteria than MSS but were of the same taxonomic make up – we have no way to detecting these differences. One approach could be to

image 16s rRNA using fluorescently labelled RNA probes. This would allow an estimation as to the total amount of bacteria and could provide spatial information, such as whether bacteria were spatially restricted to the mucous or invaded the epithelium. Barrier permeability could be a key contributing factor to CIRC scoring. Future work could utilise histological scoring of H&E stained sections by a blinded pathologist or serum analysis of biomarkers of barrier permeability, such as LPS.

In the absence of convincing evidence that the bacterial colonisation was a driver of high CIRC scores in MSS patients, we turned our attention to bacterial sensing pathways. Our most notable observation from analysis of TCGA-COADREAD data was the large upregulation of a number of *GBP* family genes, most notably GBP5. Other mediators of inflammasome signalling such as *CASP1, IL1B, IL18*, and *NLRP3* itself were also upregulated in MSShiCIRC patients. *TLR4* and *MYD88* were also upregulated, but *IL12A* appeared to be slightly downregulated. We confirmed increased expression of GBP5 protein in regions of tumour epithelium. When we analysed matched adjacent healthy tissue, expression of GBP5 appeared to be almost uniformly low. These findings suggest that upregulation of GBP5 is not something that precedes development of colorectal cancer, or it is extremely localised.

We propose GBP5 plays a key causative role in driving IFNγ expression in MSShiCIRC patients. However, *GBP* genes, including *GBP5,* can themselves be regulated by IFNγ signalling (Krapp et al., 2016). As we propose these networks to function in a loop (Figure 75), we are faced with a 'chicken and egg' problem. Our transcriptional analysis and imaging of FFPE resections provide information on the immune response at the point of surgical resection. However, our questions of what is responsible for the difference in intratumoural immunity between MSS and MSShiCIRC patients largely pertains to the initiation of the immune response. Many of the features we observed in MSShiCIRC patients such as elevated expression of GBP5 were also observed in MSI-

H patients. Therefore, on their own they cannot demonstrate a route to intratumoural immunity distinct from tumour antigen recognition. It may be the case that MSShiCIRC tumours drive low levels of tumour antigen recognition early on in development and this is sufficient to drive IFNγ expression, initiating the feedforward loop proposed in Figure 75. Or it may be the case that bacterial detection and IL-18 occurs prior to IFNγ production. Our analyses of resection samples have no way to distinguish these scenarios.

Stimulation of a healthy intestinal epithelial cell lines with nigericin led to cleavage of Caspase-1, suggestive of intact NLRP3 inflammasome machinery. Future work could aim to utilise an *in vitro* system to study the dynamics of our proposed feedforward loop. For example, T cells and intestinal epithelial cells or CRC cell lines could be co-cultured in a transwell system and stimulated with agonists for innate immune pathways such as nigericin. This system could be used to interrogate whether IFNγ production by T cells and subsequent MHC II upregulation by intestinal epithelial cells can occur independent of TCR ligation.

As previously described, the poor recruitment into the ANNICA trial has demonstrated that MSShiCIRC is a phenomenon largely limited to primary resections of stage I-III tumours. Poor recruitment could be due to a survivor bias if MSShiCIRC patients experience a sterilising immune response and disease-free remission following surgical resection. The TCGA-COADREAD dataset is not annotated with follow-up survival data, so we have no way to determine whether the MSShiCIRC patients that have been investigated here are still alive. If CIRC status at time of resection is associated with survival, the factors that determine MSS versus MSShiCIRC subtypes may hold valuable information that inform neo-adjuvant therapy decisions.

In comparison to trials of ICB therapy on late stage, treatment-resistant CRC patients the NICHE trial of neo-adjuvant ICB led to pathological responses in a number of MSS patients. If neoadjuvant therapy for MSS CRC becomes common practice, further investigation must aim to

understand why some patients undergo pathological responses and others do not. The NICHE study performed RNA sequencing on pre and post treatment biopsies. Although they did not find a predictive transcriptional signature, future work could aim to perform CIRC scoring should these datasets become publicly available.

We should consider whether it is therapeutically feasible to convert an MSS patient into an MSShiCIRC one. Work on pre-clinical models has shown that inflammasome activation can be experimentally induced by gavage of bacteria or pharmacological activation of TLR9 by systemic CpG (Van Der Kraak et al., 2021). Recent successes of therapeutic faecal microbiome transfer in cancer patients may be in part inflammasome mediated and may be an effective way to increase CIRC scores. Pre-clinical models have also shown that treatment with broad spectrum antibiotics is sufficient to blunt inflammasome activation in the gut and careful consideration should be given to antibiotic treatment in patients undergoing an immune response against cancer.

6 FINAL DISCUSSION

By developing the Nur77 Tempo mouse, we have developed a resource. Nur77 Tempo advances on the Nr4a3 Tocky by providing higher sensitivity, and on the Nur77 GFP model by providing higher time resolution. The high sensitivity of Nur77 Tempo comes with a drawback in that low level self-antigen recognition leads to a high level of FT Red background expression. This could be a limitation in experiments that aim to study TCR signalling events long term in the lymphoid environment. Background level is generally lost in T cells that reside with other tissues such as the liver, as they cease re-circulation into the lymphoid environment. Furthermore, when T cells are cultured long-term, FT Red protein degrades or is diluted out by proliferation in the absence of any new TCR stimulus. Therefore, studies into tissue T cells or *in vitro* studies are unlikely to have issues with background FT Red signal. The Nur77 Tempo mice are used by the Bending group and collaborators in Birmingham to investigate tolerance, immune responses to infection, and vaccination. Following the publication of our short report on Nur77 Tempo in *Discovery Immunology* we received interest from international collaborators. Notably, there was interest from labs conducting ligand identification studies for rare T cell populations. This may be a novel application of Nur77 Tempo, not only can sorted rare T cells be stimulated with putative ligands, but the *in vivo* application of the Nur77 Tempo can inform whether rare T cells are recognising ligand in situ. Furthermore, there has been interest from researchers investigating chronic infection, particularly how Nur77 Tempo can inform on chronic TCR signalling during chronic LCMV. Nur77 Tempo are deposited to the *European Mutant Mouse Archive,* and we hope that Nur77 Tempo will continue to have broad applicability to disease models and fundamental immunology research.

Our small molecule inhibitor studies allowed us to develop a system where we can track NFAT dependent and NFAT independent signals using Nr4a3 Tocky and Nur77 Tempo respectively. This

led to the findings that NFAT signalling is sustained whilst NFAT signalling is switched off during chronic TCR stimulation. Ligation of the TCR is a simple input that must be converted into a complex set of functional outcomes. This re-wiring of TCR signalling towards an NFAT bias is likely a mechanism that T cells use to activate some TCR regulated functions (such as PD-1 expression) whilst restraining others (such as proliferation). NFAT biased signalling, and the wider exhaustion programme, have probably evolved to prevent immunopathology during chronic antigen exposure. This is highlighted by the seminal 2006 study from Rafi Ahmed's lab where they found that chronic LCMV infection of a PD-L1 knockout mouse caused lethal immunopathology (Wherry 2006).

In exhausted $CD8^+$ T cells, multiple co-inhibitory receptors act to negatively regulate the TCR. The molecular pathways by which co-inhibitory receptors act are not well understood, but our evidence suggest they may be able to selectively spare NFAT signalling whilst switching other pathways off. Work from Anjana Rao's lab over the past 20 years has demonstrated how NFAT can act as a negative regulator of T cell functionality (J. Chen et al., 2019; Hogan et al., 2003; Hu et al., 2007; S.-H. Im & Rao, 2004; Macian et al., 2000; Macián et al., 2001, 2002; Martinez et al., 2015; Mognol et al., 2017; Müller & Rao, 2010; Rao et al., 1997; Sundrud & Rao, 2007). We must work to understand how co-inhibitory receptors can target some TCR downstream pathways whilst apparently sparing others, this information will be key to our understanding of which inhibitory receptors to target and in which contexts. We know that blockade of inhibitory receptors can lead to a compensatory upregulation of other receptors, likely by increasing the strength of NFAT signalling. If ICB therapy combinations can be designed to target ERK-AP-1 and PKC-NFκB pathways without reinforcing NFAT signalling, T cell functions such as cytokine production and proliferation might be restored without leading to NFAT mediated adaptive therapy resistance.

Effector T cells have many similarities to exhausted T cells, including expression of the 'master regulator' of exhaustion TOX (Sekine et al., 2020). Furthermore, T cells that show phenotypic features of exhaustion during LCMV infection contain CX3CR1^{+} KLRG1^{+} sub-groups that are polyfunctional cytokine producers (Daniels et al., 2019). Although the process of T cell exhaustion is progressive and the line between exhausted and effector populations is blurred, they are separate functional programmes that are regulated by distinct pathways.

Our evidence suggests that the switching off of NFAT independent signalling pathways happens in the early stages of CD8^{+} T cell exhaustion. Fluorescent intensity levels of FT Red diverge between Nr4a3 Tocky and Nur77 Tempo as quickly as 4 days. Furthermore, PD-1^{+} TIM-3^{-} SLAMF6^{+} T_{PEX} cells that infiltrate MC38 tumours were no more likely to express FT Blue than the TIM-3^{+} terminally exhausted cells, despite being at an early stage of exhaustion. Previous work by others has shown that T_{PEX} cells are the selective responders to ICB, proliferating and producing cytokines following therapy. How then does this then square with our observations that NFAT independent pathways are already switched off by this stage? It may be that RAS signalling pathways display 'signalling memory'. In the same way that Ca^{2+} flux can continue after the removal of a TCR stimulus, Ras signalling is characterised by 'signalling hysteresis' where positive feedback loops govern the on-off behaviour of the pathway. It may be the case that although the signals proximal to the TCR that drive NFAT independent TCR signalling are already off (as evidenced by our observations in Nur77 Tempo mice), positive feedback loops may remain active for some time to allow a proliferative response to ICB.

We posited transient inhibition of the NFAT pathway as a potential mechanism to restore T cell functionality under chronic stimulation. It is important for us to consider which populations of T cells this is likely to target in a patient with cancer and what the likely outcome could be. If we consider the life-span of a tumour reactive T cell, it begins with priming in the lymph node, which

will activate both NFAT dependent and NFAT independent signalling and lead to proliferation and migration to the tumour site. Upon arrival in the tumour microenvironment the T cell is likely in the T_{PEX} state, expressing TCF1 and able to proliferate and produce cytokines. Secondary antigen encounter in the tumour environment, likely without any co-stimulation, will lead to a shutting down of NFAT independent pathways, chronic signalling via NFAT reinforcing the expression of multiple co-inhibitory receptors, epigenetic alterations, and loss of the ability to produce cytokines or proliferate before eventual cell death. Cells that reside in tumour largely do not respond to ICB, we know this from studies that have demonstrated their clonal replacement during successful ICB therapy (Yost et al., 2019). We propose that blockade of the NFAT pathway may be able to prolong the T_{PEX} state such that a preconditioning regiment could increase the number of tumour reactive T_{PEX} able to respond to a subsequent line of ICB therapy. Of course, NFAT has important roles in T cell effector function. Many cytokines, most notably IL-2, have an absolute dependency on NFAT:AP-1 composite sites. Furthermore, NFAT is essential for cytotoxicity (Klein-Hessling et al., 2017). It remains to be seen whether Cyclosporine A could be used to prevent terminal exhaustion, without also rendering T cells functionally inert. Detailed work in pre-clinical cancer models will be important to determine the feasibility of this proposed treatment.

In our work on human CRC, our evidence suggested that high CIRC scores can be driven by mechanisms independent of tumour antigen recognition in MSS patients. Instead, we proposed that innate immune responses to bacteria may drive cytokine production that drives TCR independent IFNγ expression. Whilst conventional αβ T cells in the blood are largely insensitive to cytokine activation, the gut is enriched for innate-like T cells that are effective responders to cytokines such as Il-12 (Eftychi et al., 2019) and IL-18 (Nowarski et al., 2015). Although IL-12 production in the gut is largely mediated by myeloid cells (Eftychi et al., 2019), epithelial cells are capable of producing IL-18 (Koyama et al., 2019). Interestingly, there have been recent reports

that IL-18 production by IECs is dependent on signalling from IL-22, a cytokine produced by Th17 cells, which are also enriched in MSShiCIRC patients (McMurray, 2021). We observed elevated protein expression of GBP5, a key regulator of NLRP3 inflammasome assembly, in the tumour epithelium, but not the surrounding healthy tissue. Further mechanistic work is required to determine whether activation of the NLRP3 inflammasome is sufficient to drive MSShiCIRC features such as antigen independent IFNγ production and MHC II expression by tumour epithelium.

The best characterised driver of GBP5 expression is IFNγ itself. If upregulation of GBP5 is the true initiator of the immune response that distinguishes the MSS and MSShiCIRC patient subgroups, it would be key to understand why some patients express GBP5 whilst others do not. Our Metagenome sequencing analysis did not reveal any significant difference in the detectable bacteria between MSS and MSShiCIRC patient sub-groups. These results do not completely rule out the microbiome as a driver of the MSShiCIRC patient grouping. Human microbiome studies are notoriously difficult due to the environmental factors such as diet that make the bacterial ecosystems so diverse. It may also be the case that MSShiCIRC patients have a microbiome enriched for bacteria that have similar metabolic or immunomodulatory properties, but are not phylogenetically related.

7 COLLABORATIVE STATEMENT

Cutting of FFPE slides was performed by Michael Russel. Multiplex IF staining and imaging was performed by Ana Teodosio. Cover slipping and scanning of H-DAB stained slides was performed by Joe Flint. CIRC scoring of TCGA patients, normalisation and processing of TCGA RNAseq datasets, and processing of Genomics England MetaGenomeSeq dataset was performed by Dr. Jack McMurray. Dr. Emma Jennings performed the dose titration *in vitro* stimulation shown in Figure 3.6. Some of the MC38 tumour experiments shown in Figure 4.5.B were performed by David Lecky. The schematic shown in Figure 3.1 is based on a diagram of the bacterial artificial chromosome design provided to us by Taconic. With the exception of the examples mentioned above, the experimental data presented in this thesis was collected and analysed by myself.

8 BIBLIOGRAPHY

Abdel-Hakeem, M. S., Manne, S., Beltra, J. C., Stelekati, E., Chen, Z., Nzingha, K., Ali, M. A., Johnson, J. L., Giles, J. R., Mathew, D., Greenplate, A. R., Vahedi, G., & Wherry, E. J. (2021). Epigenetic scarring of exhausted T cells hinders memory differentiation upon eliminating chronic antigenic stimulation. *Nature Immunology*, *22*(8), 1008–1019. https://doi.org/10.1038/s41590-021-00975-5

Ahlmanner, F., Sundström, P., Akeus, P., Eklöf, J., Börjesson, L., Gustavsson, B., Lindskog, E. B., & Raghavan, S. (2018). CD39 regulatory T cells accumulate in colon adenocarcinomas and display markers of increased suppressive function. *Oncoimmunology*, *9*(97), 36993–37007.

Alexandrov, L. B., Kim, J., Haradhvala, N. J., Huang, M. N., Tian Ng, A. W., Wu, Y., Boot, A., Covington, K. R., Gordenin, D. A., Bergstrom, E. N., Islam, S. M. A., Lopez-Bigas, N., Klimczak, L. J., McPherson, J. R., Morganella, S., Sabarinathan, R., Wheeler, D. A., Mustonen, V., Alexandrov, L. B., … Stratton, M. R. (2020). The repertoire of mutational signatures in human cancer. *Nature*, *578*(7793), 94–101. https://doi.org/10.1038/s41586-020-1943-3

Altan-Bonnet, G., & Germain, R. N. (2005). Modeling T Cell Antigen Discrimination Based on Feedback Control of Digital ERK Responses. *PLoS Biology*, *3*(11), e356. https://doi.org/10.1371/journal.pbio.0030356

André, P., Denis, C., Soulas, C., Bourbon-Caillet, C., Lopez, J., Arnoux, T., Bléry, M., Bonnafous, C., Gauthier, L., Morel, A., Rossi, B., Remark, R., Breso, V., Bonnet, E., Habif, G., Guia, S., Lalanne, A. I., Hoffmann, C., Lantz, O., … Vivier, E. (2018). Anti-NKG2A mAb Is a Checkpoint Inhibitor that Promotes Anti-tumor Immunity by Unleashing Both T and NK Cells. *Cell*, *175*(7), 1731-1743.e13. https://doi.org/10.1016/j.cell.2018.10.014

André, T., Shiu, K.-K., Kim, T. W., Jensen, B. V., Jensen, L. H., Punt, C., Smith, D., Garcia-Carbonero, R., Benavides, M., Gibbs, P., de la Fouchardiere, C., Rivera, F., Elez, E., Bendell, J., Le, D. T., Yoshino, T., Van Cutsem, E., Yang, P., Farooqui, M. Z. H., … Diaz, L. A. (2020). Pembrolizumab in Microsatellite-Instability–High Advanced Colorectal Cancer. *New England Journal of Medicine*, *383*(23), 2207–2218. https://doi.org/10.1056/nejmoa2017699

Aronica, M. A., A L Mora, D B Mitchell, P W Finn, J E Johnson, J R Sheller, & M R Boothby. (1999). Preferential role for NF-kappa B/Rel signaling in the type 1 but not type 2 T cell-dependent immune response in vivo. *Journal of Immunology*, *163*(9), 5116–5124.

Arstila, T. P., Casrouge, A., Baron, V., Even, J., Kanellopoulos, J., & Kourilsky, P. (1999). A Direct Estimate of the Human αβ T Cell Receptor Diversity. *Science*, *286*(5441), 958–961. https://doi.org/10.1126/science.286.5441.958

Ashouri, J. F., & Weiss, A. (2017). Endogenous Nur77 Is a Specific Indicator of Antigen Receptor Signaling in Human T and B Cells. *The Journal of Immunology*, *198*(2), 657–668. https://doi.org/10.4049/jimmunol.1601301

Au-Yeung, B. B., Zikherman, J., Mueller, J. L., Ashouri, J. F., Matloubian, M., Cheng, D. A., Chen, Y., Shokat, K. M., & Weiss, A. (2014). A sharp T-cell antigen receptor signaling threshold for T-cell proliferation. *Proceedings of the National Academy of Sciences of the United States of America*, *111*(35). https://doi.org/10.1073/pnas.1413726111

Baier, P. K., Wimmenauer, S., Hirsch, T., von Specht, B. U., von Kleist, S., Keller, H., & Farthmann, E. H. (1998). Analysis of the T cell receptor variability of tumor-infiltrating lymphocytes in colorectal carcinomas. *Tumour Biology : The Journal of the International Society for Oncodevelopmental Biology and Medicine*, *19*(3), 205–212. https://doi.org/10.1159/000030008

Baitsch, L., Baumgaertner, P., Devêvre, E., Raghav, S. K., Legat, A., Barba, L., Wieckowski, S., Bouzourene, H., Deplancke, B., Romero, P., Rufer, N., & Speiser, D. E. (2011). Exhaustion of tumor-specific CD8+ T cells in metastases from melanoma patients. *Journal of Clinical Investigation*, *121*(6), 2350–2360. https://doi.org/10.1172/JCI46102

Balança, C. C., Salvioni, A., Scarlata, C. M., Michelas, M., Martinez-Gomez, C., Gomez-Roca, C., Sarradin, V., Tosolini, M., Valle, C., Pont, F., Ferron, G., Gladieff, L., Vergez, S., Dupret-Bories, A., Mery, E., Rochaix, P., Fournié, J. J., Delord, J. P., Devaud, C., … Ayyoub, M. (2021). PD-1 blockade restores helper activity of tumor-infiltrating, exhausted PD-1hiCD39+ CD4 T cells. *JCI Insight*, *6*(2). https://doi.org/10.1172/jci.insight.142513

Baldwin, T. A., & Hogquist, K. A. (2007). Transcriptional Analysis of Clonal Deletion In Vivo. *The Journal of Immunology*, *179*(2), 837–844. https://doi.org/10.4049/jimmunol.179.2.837

Barber, D. L., Wherry, E. J., Masopust, D., Zhu, B., Allison, J. P., Sharpe, A. H., Freeman, G. J., & Ahmed, R. (2006). Restoring function in exhausted CD8 T cells during chronic viral infection. *Nature*, *439*(7077), 682–687. https://doi.org/10.1038/nature04444

Barker, N., Ridgway, R. A., Van Es, J. H., Van De Wetering, M., Begthel, H., Van Den Born, M., Danenberg, E., Clarke, A. R., Sansom, O. J., & Clevers, H. (2009). Crypt stem cells as the cells-of-origin of intestinal cancer. *Nature*, *457*(7229), 608–611. https://doi.org/10.1038/nature07602

Barker, N., Van Es, J. H., Kuipers, J., Kujala, P., Van Den Born, M., Cozijnsen, M., Haegebarth, A., Korving, J., Begthel, H., Peters, P. J., & Clevers, H. (2007). Identification of stem cells in small intestine and colon by marker gene Lgr5. *Nature*, *449*(7165), 1003–1007. https://doi.org/10.1038/nature06196

Barth, R. J., Fisher, D. A., Wallace, P. K., Channon, J. Y., Noelle, R. J., Gui, J., & Ernstoff, M. S. (2010). A randomized trial of ex vivo CD40L activation of a dendritic cell vaccine in colorectal cancer patients: Tumor-specific immune responses are associated with improved survival. *Clinical Cancer Research*, *16*(22), 5548–5556. https://doi.org/10.1158/1078-0432.CCR-10-2138

Bauquet, A. T., Jin, H., Paterson, A. M., Mitsdoerffer, M., Ho, I.-C., Sharpe, A. H., & Kuchroo, V. K. (2009). The costimulatory molecule ICOS regulates the expression of c-Maf and IL-21 in the development of follicular T helper cells and TH-17 cells. *Nature Immunology*, *10*(2), 167–175. https://doi.org/10.1038/ni.1690

Beach, D., Gonen, R., Bogin, Y., Reischl, I. G., & Yablonski, D. (2007). Dual Role of SLP-76 in Mediating T Cell Receptor-induced Activation of Phospholipase C-γ1. *Journal of Biological Chemistry*, *282*(5), 2937–2946. https://doi.org/10.1074/jbc.M606697200

Beaurepaire, C., Smyth, D., & McKay, D. M. (2009). Interferon-γ Regulation of Intestinal Epithelial Permeability. *Journal of Interferon & Cytokine Research*, *29*(3), 133–144. https://doi.org/10.1089/jir.2008.0057

Belk, J. A., Yao, W., Ly, N., Freitas, K. A., Chen, Y.-T., Shi, Q., Valencia, A. M., Shifrut, E., Kale, N., Yost, K. E., Duffy, C. V., Daniel, B., Hwee, M. A., Miao, Z., Ashworth, A., Mackall, C. L., Marson, A., Carnevale, J., Vardhana, S. A., & Satpathy, A. T. (2022). Genome-wide CRISPR screens of T cell exhaustion identify chromatin remodeling factors that limit T cell persistence. *Cancer Cell*, *40*(7), 768-786.e7. https://doi.org/10.1016/j.ccell.2022.06.001

Beltra, J.-C., Abdel-Hakeem, M. S., Manne, S., Zhang, Z., Huang, H., Kurachi, M., Su, L., Picton, L., Ngiow, S. F., Muroyama, Y., Casella, V., Huang, Y. J., Giles, J. R., Mathew, D., Belman, J., Klapholz, M., Decaluwe, H., Huang, A. C., Berger, S. L., … Wherry, E. J. (2023). Stat5 opposes the transcription factor Tox and rewires exhausted CD8+ T cells toward durable effector-like states during chronic antigen exposure. *Immunity*, *56*(12), 2699-2718.e11. https://doi.org/10.1016/j.immuni.2023.11.005

Bending, D., Martín, P. P., Paduraru, A., Ducker, C., Marzaganov, E., Laviron, M., Kitano, S., Miyachi, H., Crompton, T., & Ono, M. (2018). A timer for analyzing temporally dynamic changes in transcription during differentiation in vivo. *Journal of Cell Biology*, *217*(8), 2931–2950. https://doi.org/10.1083/jcb.201711048

Bending, D., & Zikherman, J. (2023). Nr4a nuclear receptors: markers and modulators of antigen receptor signaling. *Current Opinion in Immunology*, *81*, 102285. https://doi.org/10.1016/j.coi.2023.102285

Bevington, S. L., Ng, S. T. H., Britton, G. J., Keane, P., Wraith, D. C., & Cockerill, P. N. (2020). Chromatin Priming Renders T Cell Tolerance-Associated Genes Sensitive to Activation below the Signaling Threshold for Immune Response Genes. *Cell Reports*, *31*(10). https://doi.org/10.1016/j.celrep.2020.107748

Bi, K., He, M. X., Bakouny, Z., Kanodia, A., Napolitano, S., Wu, J., Grimaldi, G., Braun, D. A., Cuoco, M. S., Mayorga, A., DelloStritto, L., Bouchard, G., Steinharter, J., Tewari, A. K., Vokes, N. I., Shannon, E., Sun, M., Park, J., Chang, S. L., … Van Allen, E. M. (2021). Tumor and immune reprogramming during immunotherapy in advanced renal cell carcinoma. *Cancer Cell*, *39*(5), 649-661.e5. https://doi.org/10.1016/j.ccell.2021.02.015

Boland, C. R., & Goel, A. (2010). Microsatellite Instability in Colorectal Cancer. *Gastroenterology*, *138*(6), 2073-2087.e3. https://doi.org/10.1053/j.gastro.2009.12.064

Boomer, J. S., & Green, J. M. (2010). An Enigmatic Tail of CD28 Signaling. *Cold Spring Harbor Perspectives in Biology*, *2*(8), a002436–a002436. https://doi.org/10.1101/cshperspect.a002436

Bou Nasser Eddine, F., Forlani, G., Lombardo, L., Tedeschi, A., Tosi, G., & Accolla, R. S. (2017). CIITA-driven MHC class II expressing tumor cells can efficiently prime naive CD4+ TH cells

in vivo and vaccinate the host against parental MHC-II-negative tumor cells. *Oncoimmunology*, *6*(1), e1261777. https://doi.org/10.1080/2162402X.2016.1261777

Brummelman, J., Mazza, E. M. C., Alvisi, G., Colombo, F. S., Grilli, A., Mikulak, J., Mavilio, D., Alloisio, M., Ferrari, F., Lopci, E., Novellis, P., Veronesi, G., & Lugli, E. (2018). High-dimensional single cell analysis identifies stemlike cytotoxic CD8+T cells infiltrating human tumors. *Journal of Experimental Medicine*, *215*(10), 2520–2535. https://doi.org/10.1084/JEM.20180684

Bulk, J. Van Den, Verdegaal, E. M. E., Ruano, D., Ijsselsteijn, M. E., Visser, M., Breggen, R. Van Der, Duhen, T., Ploeg, M. Van Der, Vries, N. L. De, Oosting, J., Peeters, K. C. M. J., Weinberg, A. D., Farina-sarasqueta, A., Burg, S. H. Van Der, & Miranda, N. F. C. C. De. (2019). Neoantigen-specific immunity in low mutation burden colorectal cancers of the consensus molecular subtype 4. *Genome Medicine*, *11*(87), 1–15.

Burger, M. L., Cruz, A. M., Crossland, G. E., Gaglia, G., Ritch, C. C., Blatt, S. E., Bhutkar, A., Canner, D., Kienka, T., Tavana, S. Z., Barandiaran, A. L., Garmilla, A., Schenkel, J. M., Hillman, M., de los Rios Kobara, I., Li, A., Jaeger, A. M., Hwang, W. L., Westcott, P. M. K., … Jacks, T. (2021). Antigen dominance hierarchies shape TCF1+ progenitor CD8 T cell phenotypes in tumors. *Cell*, *184*(19), 4996-5014.e26. https://doi.org/10.1016/j.cell.2021.08.020

Calvo, C. R., Amsen, D., & Kruisbeek, A. M. (1997). Cytotoxic T Lymphocyte Antigen 4 (CTLA-4) Interferes with Extracellular Signal-regulated Kinase (ERK) and Jun NH2-terminal Kinase (JNK) Activation, but Does Not Affect Phosphorylation of T Cell Receptor ζ and ZAP70. *The Journal of Experimental Medicine*, *186*(10), 1645–1653. https://doi.org/10.1084/jem.186.10.1645

Carey, K. D., Dillon, T. J., Schmitt, J. M., Baird, A. M., Holdorf, A. D., Straus, D. B., Shaw, A. S., & Stork, P. J. S. (2000). CD28 and the Tyrosine Kinase Lck Stimulate Mitogen-Activated Protein Kinase Activity in T Cells via Inhibition of the Small G Protein Rap1. *Molecular and Cellular Biology*, *20*(22), 8409–8419. https://doi.org/10.1128/MCB.20.22.8409-8419.2000

Castellarin, M., Warren, R., Freeman, D., Moore, R., & Holt, R. (2012). Fusobacterium nucleatum infection is prevalent in human colorectal carcinoma. *Genome Research*, *7*(22), 299–306. https://doi.org/10.7554/eLife.25801

Caushi, J. X., Zhang, J., Ji, Z., Vaghasia, A., Zhang, B., Hsiue, E. H. C., Mog, B. J., Hou, W., Justesen, S., Blosser, R., Tam, A., Anagnostou, V., Cottrell, T. R., Guo, H., Chan, H. Y., Singh, D., Thapa, S., Dykema, A. G., Burman, P., … Smith, K. N. (2021). Transcriptional programs of neoantigen-specific TIL in anti-PD-1-treated lung cancers. *Nature*, *596*(7870), 126–132. https://doi.org/10.1038/s41586-021-03752-4

Cavigelli, M., Dolfi, F., Claret, F. X., & Karin, M. (1995). Induction of c-fos expression through JNK-mediated TCF/Elk-1 phosphorylation. *The EMBO Journal*, *14*(23), 5957–5964. https://doi.org/10.1002/j.1460-2075.1995.tb00284.x

Cazzetta, V., Bruni, E., Terzoli, S., Carenza, C., Franzese, S., Piazza, R., Marzano, P., Donadon, M., Torzilli, G., Cimino, M., Simonelli, M., Bello, L., Villa, A., Tan, L., Ravens, S., Prinz, I., Supino, D., Colombo, F. S., Lugli, E., … Mavilio, D. (2021). NKG2A expression identifies a

subset of human Vδ2 T cells exerting the highest antitumor effector functions. *Cell Reports*, *37*(3), 109871. https://doi.org/10.1016/j.celrep.2021.109871

Chadban, TESCH, FOTI, LAN, ATKINS, & NIKOLIC-PATERSON. (1998). Interleukin-10 differentially modulates MHC class II expression by mesangial cells and macrophages in vitro and in vivo. *Immunology*, *94*(1), 72–78. https://doi.org/10.1046/j.1365-2567.1998.00487.x

Chalabi, M., Fanchi, L. F., Dijkstra, K. K., Van den Berg, J. G., Aalbers, A. G., Sikorska, K., Lopez-Yurda, M., Grootscholten, C., Beets, G. L., Snaebjornsson, P., Maas, M., Mertz, M., Veninga, V., Bounova, G., Broeks, A., Beets-Tan, R. G., de Wijkerslooth, T. R., van Lent, A. U., Marsman, H. A., … Haanen, J. B. (2020). Neoadjuvant immunotherapy leads to pathological responses in MMR-proficient and MMR-deficient early-stage colon cancers. *Nature Medicine*, *26*(4), 566–576. https://doi.org/10.1038/s41591-020-0805-8

Chan, S. H., Perussia, B., Gupta, J. W., Kobayashi, M., Pospisil, M., Young, H. A., Wolf, S. F., Young, D., Clark, S. C., & Trinchieri, G. (1991). Induction of interferon γ production by natural killer cell stimulatory factor: Characterization of the responder cells and synergy with other inducers. *Journal of Experimental Medicine*, *173*(4), 869–879. https://doi.org/10.1084/jem.173.4.869

Chen, J., López-Moyado, I. F., Seo, H., Lio, C. W. J., Hempleman, L. J., Sekiya, T., Yoshimura, A., Scott-Browne, J. P., & Rao, A. (2019). NR4A transcription factors limit CAR T cell function in solid tumours. *Nature*, *567*(7749), 530–534. https://doi.org/10.1038/s41586-019-0985-x

Chen, L., & Flies, D. B. (2013). Molecular mechanisms of T cell co-stimulation and co-inhibition. *Nature Reviews Immunology*, *13*(4), 227–242. https://doi.org/10.1038/nri3405

Chen, L., Glover, J. N. M., Hogan, P. G., Rao, A., & Harrison, S. C. (1998). Structure of the DNA-binding domains from NFAT, Fos and Jun bound specifically to DNA. *Nature*, *392*(6671), 42–48. https://doi.org/10.1038/32100

Chen, Z., Ji, Z., Ngiow, S. F., Manne, S., Cai, Z., Huang, A. C., Johnson, J., Staupe, R. P., Bengsch, B., Xu, C., Yu, S., Kurachi, M., Herati, R. S., Vella, L. A., Baxter, A. E., Wu, J. E., Khan, O., Beltra, J. C., Giles, J. R., … Wherry, E. J. (2019). TCF-1-Centered Transcriptional Network Drives an Effector versus Exhausted CD8 T Cell-Fate Decision. *Immunity*, *51*(5), 840-855.e5. https://doi.org/10.1016/j.immuni.2019.09.013

Chi, H. (2012). Regulation and function of mTOR signalling in T cell fate decisions. *Nature Reviews Immunology*, *12*(5), 325–338. https://doi.org/10.1038/nri3198

Chihara, N., Madi, A., Kondo, T., Zhang, H., Acharya, N., Singer, M., Nyman, J., Marjanovic, N. D., Kowalczyk, M. S., Wang, C., Kurtulus, S., Law, T., Etminan, Y., Nevin, J., Buckley, C. D., Burkett, P. R., Buenrostro, J. D., Rozenblatt-Rosen, O., Anderson, A. C., … Kuchroo, V. K. (2018). Induction and transcriptional regulation of the co-inhibitory gene module in T cells. *Nature*, *558*(7710), 454–459. https://doi.org/10.1038/s41586-018-0206-z

Choi, S., Warzecha, C., Zvezdova, E., Lee, J., Argenty, J., Lesourne, R., Aravind, L., & Love, P. E. (2017). THEMIS enhances TCR signaling and enables positive selection by selective

inhibition of the phosphatase SHP-1. *Nature Immunology*, *18*(4), 433–441. https://doi.org/10.1038/ni.3692

Chow, A., Uddin, F. Z., Liu, M., Dobrin, A., Nabet, B. Y., Mangarin, L., Lavin, Y., Rizvi, H., Tischfield, S. E., Quintanal-Villalonga, A., Chan, J. M., Shah, N., Allaj, V., Manoj, P., Mattar, M., Meneses, M., Landau, R., Ward, M., Kulick, A., … Rudin, C. M. (2023). The ectonucleotidase CD39 identifies tumor-reactive CD8+ T cells predictive of immune checkpoint blockade efficacy in human lung cancer. *Immunity*, *56*(1), 93-106.e6. https://doi.org/10.1016/j.immuni.2022.12.001

Colaprico, A., Silva, T. C., Olsen, C., Garofano, L., Cava, C., Garolini, D., Sabedot, T. S., Malta, T. M., Pagnotta, S. M., Castiglioni, I., Ceccarelli, M., Bontempi, G., & Noushmehr, H. (2016). TCGAbiolinks: an R/Bioconductor package for integrative analysis of TCGA data. *Nucleic Acids Research*, *44*(8), e71–e71. https://doi.org/10.1093/nar/gkv1507

Collins, A. V., Brodie, D. W., Gilbert, R. J. C., Iaboni, A., Manso-Sancho, R., Walse, B., Stuart, D. I., van der Merwe, P. A., & Davis, S. J. (2002). The Interaction Properties of Costimulatory Molecules Revisited. *Immunity*, *17*(2), 201–210. https://doi.org/10.1016/S1074-7613(02)00362-X

Conley, J. M., Gallagher, M. P., Rao, A., & Berg, L. J. (2020). Activation of the Tec Kinase ITK Controls Graded IRF4 Expression in Response to Variations in TCR Signal Strength. *The Journal of Immunology*, *205*(2), 335–345. https://doi.org/10.4049/jimmunol.1900853

Connolly, K. A., Kuchroo, M., Venkat, A., Khatun, A., Wang, J., William, I., Hornick, N. I., Fitzgerald, B. L., Damo, M., Kasmani, M. Y., Cui, C., Fagerberg, E., Monroy, I., Hutchins, A., Cheung, J. F., Foster, G. G., Mariuzza, D. L., Nader, M., Zhao, H., … Joshi, N. S. (2021). A reservoir of stem-like CD8 + T cells in the tumor-draining lymph node preserves the ongoing antitumor immune response. *Sci. Immunol*, *6*, 7836. https://doi.org/10.1126/sciimmunol.abg7836

Corish, P., & Tyler-Smith, C. (1999). Attenuation of green fluorescent protein half-life in mammalian cells. *Protein Engineering, Design and Selection*, *12*(12), 1035–1040. https://doi.org/10.1093/protein/12.12.1035

Courtney, A. H., Lo, W.-L., & Weiss, A. (2018). TCR Signaling: Mechanisms of Initiation and Propagation. *Trends in Biochemical Sciences*, *43*(2), 108–123. https://doi.org/10.1016/j.tibs.2017.11.008

Courtney, A. H., Shvets, A. A., Lu, W., Griffante, G., Mollenauer, M., Horkova, V., Lo, W.-L., Yu, S., Stepanek, O., Chakraborty, A. K., & Weiss, A. (2019). CD45 functions as a signaling gatekeeper in T cells. *Science Signaling*, *12*(604). https://doi.org/10.1126/scisignal.aaw8151

Croft, M. (2009). The role of TNF superfamily members in T-cell function and diseases. *Nature Reviews Immunology*, *9*(4), 271–285. https://doi.org/10.1038/nri2526

Damasio, M. P., Marchingo, J. M., Spinelli, L., Hukelmann, J. L., Cantrell, D. A., & Howden, A. J. M. (2021). Extracellular signal-regulated kinase (ERK) pathway control of CD8+ T cell differentiation. *Biochemical Journal*, *478*(1), 79–98. https://doi.org/10.1042/BCJ20200661

Dammeijer, F., Gulijk, M. Van, Mulder, E. E., Verhoef, C., Hall, T. Van, & Aerts, J. G. (2020). The PD-1 / PD-L1-Checkpoint Restrains T cell Immunity in Tumor-Draining Lymph Nodes Article. *Cancer Cell*, *38*, 1–16. https://doi.org/10.1016/j.ccell.2020.09.001

Daniel, B., Yost, K. E., Hsiung, S., Sandor, K., Xia, Y., Qi, Y., Hiam-Galvez, K. J., Black, M., J. Raposo, C., Shi, Q., Meier, S. L., Belk, J. A., Giles, J. R., Wherry, E. J., Chang, H. Y., Egawa, T., & Satpathy, A. T. (2022). Divergent clonal differentiation trajectories of T cell exhaustion. *Nature Immunology*, *23*(11), 1614–1627. https://doi.org/10.1038/s41590-022-01337-5

Daniels, M. A., Luera, D., & Teixeiro, E. (2023). NFκB signaling in T cell memory. *Frontiers in Immunology*, *14*. https://doi.org/10.3389/fimmu.2023.1129191

Daniels, M. A., Teixeiro, E., Gill, J., Hausmann, B., Roubaty, D., Holmberg, K., Werlen, G., Holländer, G. A., Gascoigne, N. R. J., & Palmer, E. (2006). Thymic selection threshold defined by compartmentalization of Ras/MAPK signalling. *Nature*, *444*(7120), 724–729. https://doi.org/10.1038/nature05269

Das, J., Chen, C.-H., Yang, L., Cohn, L., Ray, P., & Ray, A. (2001). A critical role for NF-κB in Gata3 expression and TH2 differentiation in allergic airway inflammation. *Nature Immunology*, *2*(1), 45–50. https://doi.org/10.1038/83158

Das, J., Ho, M., Zikherman, J., Govern, C., Yang, M., Weiss, A., & Chakraborty, A. K. (2009). Theory Digital Signaling and Hysteresis Characterize Ras Activation in Lymphoid Cells. *Cell*, *136*(2), 337–351. https://doi.org/10.1016/j.cell.2008.11.051

de la Roche, M., Asano, Y., & Griffiths, G. M. (2016). Origins of the cytolytic synapse. *Nature Reviews Immunology*, *16*(7), 421–432. https://doi.org/10.1038/nri.2016.54

De Smedt, L., Lemahieu, J., Palmans, S., Govaere, O., Tousseyn, T., Van Cutsem, E., Prenen, H., Tejpar, S., Spaepen, M., Matthijs, G., Decaestecker, C., Moles Lopez, X., Demetter, P., Salmon, I., & Sagaert, X. (2015). Microsatellite instable vs stable colon carcinomas: Analysis of tumour heterogeneity, inflammation and angiogenesis. *British Journal of Cancer*, *113*(3), 500–509. https://doi.org/10.1038/bjc.2015.213

de Vries, N. L., van de Haar, J., Veninga, V., Chalabi, M., Ijsselsteijn, M. E., van der Ploeg, M., van den Bulk, J., Ruano, D., van den Berg, J. G., Haanen, J. B., Zeverijn, L. J., Geurts, B. S., de Wit, G. F., Battaglia, T. W., Gelderblom, H., Verheul, H. M. W., Schumacher, T. N., Wessels, L. F. A., Koning, F., … Voest, E. E. (2023). γδ T cells are effectors of immunotherapy in cancers with HLA class I defects. *Nature*, *613*(7945), 743–750. https://doi.org/10.1038/s41586-022-05593-1

Deaglio, S., Dwyer, K. M., Gao, W., Friedman, D., Usheva, A., Erat, A., Chen, J. F., Enjyoji, K., Linden, J., Oukka, M., Kuchroo, V. K., Strom, T. B., & Robson, S. C. (2007). Adenosine generation catalyzed by CD39 and CD73 expressed on regulatory T cells mediates immune suppression. *Journal of Experimental Medicine*, *204*(6), 1257–1265. https://doi.org/10.1084/jem.20062512

Diederichsen, A. C. P., Hjelmborg, J. V. B., Christensen, P. B., Zeuthen, J., & Fenge, C. (2003). Prognostic value of the CD4+/CD8+ ratio of tumour infiltrating lymphocytes in colorectal

cancer and HLA-DR expression on tumour cells. *Cancer Immunology, Immunotherapy*, *52*(7), 423–428. https://doi.org/10.1007/s00262-003-0388-5

Dixon, K. O., Tabaka, M., Schramm, M. A., Xiao, S., Tang, R., Dionne, D., Anderson, A. C., Rozenblatt-Rosen, O., Regev, A., & Kuchroo, V. K. (2021). TIM-3 restrains anti-tumour immunity by regulating inflammasome activation. *Nature*, *595*(7865), 101–106. https://doi.org/10.1038/s41586-021-03626-9

Dolmetsch, R. E., Lewis, R. S., Goodnow, C. C., & Healy, J. I. (1997). Differential activation of transcription factors induced by Ca2+ response amplitude and duration. *Nature*, *386*(6627), 855–858. https://doi.org/10.1038/386855a0

Duhen, T., Duhen, R., Montler, R., Moses, J., Moudgil, T., Miranda, N. F. De, Goodall, C. P., Blair, T. C., Fox, B. A., Mcdermott, J. E., Chang, S., Grunkemeier, G., Leidner, R., Bell, R. B., & Weinberg, A. D. (2018). Co-expression of CD39 and CD103 identifies tumor-reactive CD8 T cells in human solid tumors. *Nature Communications*, *9*(2724). https://doi.org/10.1038/s41467-018-05072-0

Ebinu, J. O., Bottorff, D. A., Chan, E. Y. W., Stang, S. L., Dunn, R. J., & Stone, J. C. (1998). RasGRP, a Ras Guanyl Nucleotide- Releasing Protein with Calcium- and Diacylglycerol-Binding Motifs. *Science*, *280*(5366), 1082–1086. https://doi.org/10.1126/science.280.5366.1082

Eftychi, C., Schwarzer, R., Vlantis, K., Wachsmuth, L., Basic, M., Wagle, P., Neurath, M. F., Becker, C., Bleich, A., & Pasparakis, M. (2019). Temporally Distinct Functions of the Cytokines IL-12 and IL-23 Drive Chronic Colon Inflammation in Response to Intestinal Barrier Impairment. *Immunity*, *51*(2), 367-380.e4. https://doi.org/10.1016/j.immuni.2019.06.008

Elliot, T. A. E., Jennings, E. K., Lecky, D. A. J., Rouvray, S., Mackie, G. M., Scarfe, L., Sheriff, L., Ono, M., Maslowski, K. M., & Bending, D. (2022). Nur77-Tempo mice reveal T cell steady state antigen recognition. *Discovery Immunology*, *November*, 1–9. https://doi.org/doi.org/10.1093/discim/kyac009

Elliot, T. A. E., Jennings, E. K., Lecky, D. A. J., Thawait, N., Flores-Langarica, A., Copland, A., Maslowski, K. M., Wraith, D. C., & Bending, D. (2021). Antigen and checkpoint receptor engagement recalibrates T cell receptor signal strength. *Immunity*, *54*(11), 2481-2496.e6. https://doi.org/10.1016/j.immuni.2021.08.020

Fairfax, B. P., Taylor, C. A., Watson, R. A., Nassiri, I., Danielli, S., Fang, H., Mahé, E. A., Cooper, R., Woodcock, V., Traill, Z., Al-Mossawi, M. H., Knight, J. C., Klenerman, P., Payne, M., & Middleton, M. R. (2020). Peripheral CD8+ T cell characteristics associated with durable responses to immune checkpoint blockade in patients with metastatic melanoma. *Nature Medicine*, *26*(2), 193–199. https://doi.org/10.1038/s41591-019-0734-6

Falvo, J. V., Lin, C. H., Tsytsykova, A. V., Hwang, P. K., Thanos, D., Goldfeld, A. E., & Maniatis, T. (2008). A dimer-specific function of the transcription factor NFATp. *Proceedings of the National Academy of Sciences*, *105*(50), 19637–19642. https://doi.org/10.1073/pnas.0810648105

Fathman, C. G., & Lineberry, N. B. (2007). Molecular mechanisms of CD4+ T-cell anergy. *Nature Reviews Immunology*, *7*(8), 599–609. https://doi.org/10.1038/nri2131

Fergusson, J. R., Smith, K. E., Fleming, V. M., Rajoriya, N., Newell, E. W., Simmons, R., Marchi, E., Björkander, S., Kang, Y.-H., Swadling, L., Kurioka, A., Sahgal, N., Lockstone, H., Baban, D., Freeman, G. J., Sverremark-Ekström, E., Davis, M. M., Davenport, M. P., Venturi, V., … Klenerman, P. (2014). CD161 Defines a Transcriptional and Functional Phenotype across Distinct Human T Cell Lineages. *Cell Reports*, *9*(3), 1075–1088. https://doi.org/10.1016/j.celrep.2014.09.045

Fields, P. E., Gajewski, T. F., & Fitch, F. W. (1996). Blocked Ras Activation in Anergic CD4 $^{+}$ T Cells. *Science*, *271*(5253), 1276–1278. https://doi.org/10.1126/science.271.5253.1276

Finco, T. S., Kadlecek, T., Zhang, W., Samelson, L. E., & Weiss, A. (1998). LAT Is Required for TCR-Mediated Activation of PLCγ1 and the Ras Pathway. *Immunity*, *9*(5), 617–626. https://doi.org/10.1016/S1074-7613(00)80659-7

Fischer, A. M., Katayama, C. D., Pagès, G., Pouysségur, J., & Hedrick, S. M. (2005). The Role of Erk1 and Erk2 in Multiple Stages of T Cell Development. *Immunity*, *23*(4), 431–443. https://doi.org/10.1016/j.immuni.2005.08.013

Flemer, B., Lynch, D. B., Brown, J. M. R., Jeffery, I. B., Ryan, F. J., Claesson, M. J., O'Riordain, M., Shanahan, F., & O'Toole, P. W. (2017). Tumour-associated and non-tumour-associated microbiota in colorectal cancer. *Gut*, *66*(4), 633–643. https://doi.org/10.1136/gutjnl-2015-309595

Flemer, B., Warren, R. D., Barrett, M. P., Cisek, K., Das, A., Jeffery, I. B., Hurley, E., O'Riordain, M., Shanahan, F., & O'Toole, P. W. (2018). The oral microbiota in colorectal cancer is distinctive and predictive. *Gut*, *67*(8), 1454–1463. https://doi.org/10.1136/gutjnl-2017-314814

Foletta, V. C., Segal, D. H., & Cohen, D. R. (1998). Transcriptional regulation in the immune system: all roads lead to AP-1. *Journal of Leukocyte Biology*, *63*(2), 139–152. https://doi.org/10.1002/jlb.63.2.139

Fourcade, J., Sun, Z., Benallaoua, M., Guillaume, P., Luescher, I. F., Sander, C., Kirkwood, J. M., Kuchroo, V., & Zarour, H. M. (2010). Upregulation of Tim-3 and PD-1 expression is associated with tumor antigen–specific CD8+ T cell dysfunction in melanoma patients. *Journal of Experimental Medicine*, *207*(10), 2175–2186. https://doi.org/10.1084/jem.20100637

Frazer, G. L., Gawden-Bone, C. M., Dieckmann, N. M. G., Asano, Y., & Griffiths, G. M. (2021). Signal strength controls the rate of polarization within ctls during killing. *Journal of Cell Biology*, *220*(10). https://doi.org/10.1083/jcb.202104093

Fu, G., Casas, J., Rigaud, S., Rybakin, V., Lambolez, F., Brzostek, J., Hoerter, J. A. H., Paster, W., Acuto, O., Cheroutre, H., Sauer, K., & Gascoigne, N. R. J. (2013). Themis sets the signal threshold for positive and negative selection in T-cell development. *Nature*, *504*(7480), 441–445. https://doi.org/10.1038/nature12718

Fucikova, J., Kepp, O., Kasikova, L., Petroni, G., Yamazaki, T., Liu, P., Zhao, L., Spisek, R., Kroemer, G., & Galluzzi, L. (2020). Detection of immunogenic cell death and its relevance for cancer therapy. *Cell Death and Disease*, *11*(11). https://doi.org/10.1038/s41419-020-03221-2

Gallagher, M. P., Conley, J. M., & Berg, L. J. (2018). Peptide Antigen Concentration Modulates Digital NFAT1 Activation in Primary Mouse Naive CD8+ T Cells as Measured by Flow Cytometry of Isolated Cell Nuclei. *ImmunoHorizons*, *2*(7), 208–215. https://doi.org/10.4049/immunohorizons.1800032

Gallagher, M. P., Conley, J. M., Vangala, P., Garber, M., Reboldi, A., & Berg, L. J. (2021). *Hierarchy of signaling thresholds downstream of the T cell receptor and the Tec kinase ITK*. *118*, 2025825118. https://doi.org/10.1073/pnas.2025825118/-/DCSupplemental

Galon, J., Costes, A., Sanchez-Cabo, F., Fridman, W.-H., & Pages, F. (2006). Type, Density, and Location of Immune Cells Within Human Colorectal Tumours Predict Clinical Outcome. *Science*, *313*(September), 1960–1965. https://doi.org/10.7551/mitpress/7347.003.0178

Galon, J., Mlecnik, B., Bindea, G., Angell, H. K., Berger, A., Lagorce, C., Lugli, A., Zlobec, I., Hartmann, A., Bifulco, C., Nagtegaal, I. D., Palmqvist, R., Masucci, G. V., Botti, G., Tatangelo, F., Delrio, P., Maio, M., Laghi, L., Grizzi, F., … Pagès, F. (2014). Towards the introduction of the 'Immunoscore' in the classification of malignant tumours. *Journal of Pathology*, *232*(2), 199–209. https://doi.org/10.1002/path.4287

Garcia-Diaz, A., Shin, D. S., Moreno, B. H., Saco, J., Escuin-Ordinas, H., Rodriguez, G. A., Zaretsky, J. M., Sun, L., Hugo, W., Wang, X., Parisi, G., Saus, C. P., Torrejon, D. Y., Graeber, T. G., Comin-Anduix, B., Hu-Lieskovan, S., Damoiseaux, R., Lo, R. S., & Ribas, A. (2017). Interferon Receptor Signaling Pathways Regulating PD-L1 and PD-L2 Expression. *Cell Reports*, *19*(6), 1189–1201. https://doi.org/10.1016/j.celrep.2017.04.031

Gascoigne, N. R. J., Rybakin, V., Acuto, O., & Brzostek, J. (2016). TCR Signal Strength and T Cell Development. *Annual Review of Cell and Developmental Biology*, *32*(1), 327–348. https://doi.org/10.1146/annurev-cellbio-111315-125324

Gautam, S., Fioravanti, J., Zhu, W., Le Gall, J. B., Brohawn, P., Lacey, N. E., Hu, J., Hocker, J. D., Hawk, N. V., Kapoor, V., Telford, W. G., Gurusamy, D., Yu, Z., Bhandoola, A., Xue, H.-H., Roychoudhuri, R., Higgs, B. W., Restifo, N. P., Bender, T. P., … Gattinoni, L. (2019). The transcription factor c-Myb regulates CD8+ T cell stemness and antitumor immunity. *Nature Immunology*, *20*(3), 337–349. https://doi.org/10.1038/s41590-018-0311-z

Gerondakis, S., & Siebenlist, U. (2010). Roles of the NF- B Pathway in Lymphocyte Development and Function. *Cold Spring Harbor Perspectives in Biology*, *2*(5), a000182–a000182. https://doi.org/10.1101/cshperspect.a000182

Gettinger, S., Choi, J., Hastings, K., Truini, A., Datar, I., Sowell, R., Wurtz, A., Dong, W., Cai, G., Melnick, M. A., Du, V. Y., Schlessinger, J., Goldberg, S. B., Chiang, A., Sanmamed, M. F., Melero, I., Agorreta, J., Montuenga, L. M., Lifton, R., … Politi, K. (2017). Impaired HLA class I antigen processing and presentation as a mechanism of acquired resistance to immune checkpoint inhibitors in lung cancer. *Cancer Discovery*, *7*(12), 1420–1435. https://doi.org/10.1158/2159-8290.CD-17-0593

Gigoux, M., Shang, J., Pak, Y., Xu, M., Choe, J., Mak, T. W., & Suh, W.-K. (2009). Inducible costimulator promotes helper T-cell differentiation through phosphoinositide 3-kinase. *Proceedings of the National Academy of Sciences*, *106*(48), 20371–20376. https://doi.org/10.1073/pnas.0911573106

Graydon, C. G., Mohideen, S., & Fowke, K. R. (2021). LAG3's Enigmatic Mechanism of Action. *Frontiers in Immunology*, *11*. https://doi.org/10.3389/fimmu.2020.615317

Gros, A., Robbins, P. F., Yao, X., Li, Y. F., Turcotte, S., Tran, E., Wunderlich, J. R., Mixon, A., Farid, S., Dudley, M. E., Hanada, K., Almeida, J. R., Darko, S., Douek, D. C., Yang, J. C., & Rosenberg, S. A. (2014). PD-1 identifies the patient-specific CD8+ tumor-reactive repertoire infiltrating human tumors. *Journal of Clinical Investigation*, *124*(5), 2246–2259. https://doi.org/10.1172/JCI73639

Gubin, M. M., Zhang, X., Schuster, H., Caron, E., Ward, J. P., Noguchi, T., Ivanova, Y., Hundal, J., Arthur, C. D., Krebber, W., Mulder, G. E., Toebes, M., Vesely, M. D., Lam, S. S. K., Korman, A. J., Allison, J. P., Freeman, G. J., Sharpe, A. H., & Pearce, E. L. (2014). Checkpoint blockade cancer immunotherpapy targets tumour-specific mutant antigens. *Nature*, *V*. https://doi.org/10.1038/nature13988

Guidoboni, M., Gafà, R., Viel, A., Doglioni, C., Russo, A., Santini, A., Del Tin, L., Macrì, E., Lanza, G., Boiocchi, M., & Dolcetti, R. (2001). Microsatellite instability and high content of activated cytotoxic lymphocytes identify colon cancer patients with a favorable prognosis. *American Journal of Pathology*, *159*(1), 297–304. https://doi.org/10.1016/S0002-9440(10)61695-1

Guinney, J., Dienstmann, R., Wang, X., De Reyniès, A., Schlicker, A., Soneson, C., Marisa, L., Roepman, P., Nyamundanda, G., Angelino, P., Bot, B. M., Morris, J. S., Simon, I. M., Gerster, S., Fessler, E., De Sousa .E Melo, F., Missiaglia, E., Ramay, H., Barras, D., … Tejpar, S. (2015). The consensus molecular subtypes of colorectal cancer. *Nature Medicine*, *21*(11), 1350–1356. https://doi.org/10.1038/nm.3967

Hansen, K. D., Irizarry, R. A., & WU, Z. (2012). Removing technical variability in RNA-seq data using conditional quantile normalization. *Biostatistics*, *13*(2), 204–216. https://doi.org/10.1093/biostatistics/kxr054

Hänzelmann, S., Castelo, R., & Guinney, J. (2013). GSVA: gene set variation analysis for microarray and RNA-Seq data. *BMC Bioinformatics*, *14*(1), 7. https://doi.org/10.1186/1471-2105-14-7

He, Y., Hara, H., & Núñez, G. (2016). Mechanism and Regulation of NLRP3 Inflammasome Activation. *Trends in Biochemical Sciences*, *41*(12), 1012–1021. https://doi.org/10.1016/j.tibs.2016.09.002

Hellström, I., Hellström, K. E., Pierce, G., & Yang, J. (1968). Cellular and Humoral immunity to Different Types of Human Neoplasms. *Nature*, *220*, 1352–1354.

Hendriks, J., Xiao, Y., & Borst, J. (2003). CD27 Promotes Survival of Activated T Cells and Complements CD28 in Generation and Establishment of the Effector T Cell Pool. *The*

Journal of Experimental Medicine, *198*(9), 1369–1380. https://doi.org/10.1084/jem.20030916

Heuberger, C., Pott, J., & Maloy, K. J. (2020). Why do intestinal epithelial cells express MHC class II? *Immunology*, 1–11. https://doi.org/10.1111/imm.13270

Hiwa, R., Brooks, J. F., Mueller, J. L., Nielsen, H. V., & Zikherman, J. (2022). NR4A nuclear receptors in T and B lymphocytes: Gatekeepers of immune tolerance*. *Immunological Reviews*, *307*(1), 116–133. https://doi.org/10.1111/imr.13072

Hogan, P. G. (2017). Calcium–NFAT transcriptional signalling in T cell activation and T cell exhaustion. *Cell Calcium*, *63*, 66–69. https://doi.org/10.1016/j.ceca.2017.01.014

Hogan, P. G., Chen, L., Nardone, J., & Rao, A. (2003). Transcriptional regulation by calcium, calcineurin, and NFAT. *Genes & Development*, *17*(18), 2205–2232. https://doi.org/10.1101/gad.1102703

Holler, P. D., & Kranz, D. M. (2003). Quantitative Analysis of the Contribution of TCR/pepMHC Affinity and CD8 to T Cell Activation. *Immunity*, *18*(2), 255–264. https://doi.org/10.1016/S1074-7613(03)00019-0

Houde, N., Beuret, L., Bonaud, A., Fortier-Beaulieu, S.-P., Truchon-Landry, K., Aoidi, R., Pic, É., Alouche, N., Rondeau, V., Schlecht-Louf, G., Balabanian, K., Espéli, M., & Charron, J. (2022). Fine-tuning of MEK signaling is pivotal for limiting B and T cell activation. *Cell Reports*, *38*(2), 110223. https://doi.org/10.1016/j.celrep.2021.110223

Hozumi, N., & Tonegawa, S. (1976). Evidence for somatic rearrangement of immunoglobulin genes coding for variable and constant regions. *Proceedings of the National Academy of Sciences*, *73*(10), 3628–3632. https://doi.org/10.1073/pnas.73.10.3628

Hu, H., Djuretic, I., Sundrud, M. S., & Rao, A. (2007). Transcriptional partners in regulatory T cells: Foxp3, Runx and NFAT. *Trends in Immunology*, *28*(8), 329–332. https://doi.org/10.1016/j.it.2007.06.006

Huang, D., Sun, W., Zhou, Y., Li, P., Chen, F., Chen, H., & Xia, D. (2018). Mutations of key driver genes in colorectal cancer progression and metastasis. *Cancer and Metastasis Reviews*, *37*, 173–187. https://doi.org/https://doi.org/10.1007/s10555-017-9726-5

Huang, J., Brameshuber, M., Zeng, X., Xie, J., Li, Q., Chien, Y., Valitutti, S., & Davis, M. M. (2013). A Single Peptide-Major Histocompatibility Complex Ligand Triggers Digital Cytokine Secretion in CD4+ T Cells. *Immunity*, *39*(5), 846–857. https://doi.org/10.1016/j.immuni.2013.08.036

Huang, Q., Wu, X., Wang, Z., Chen, X., Wang, L., Lu, Y., Xiong, D., Liu, Q., Tian, Y., Lin, H., Guo, J., Wen, S., Dong, W., Yang, X., Yuan, Y., Yue, Z., Lei, S., Wu, Q., Ran, L., … Ye, L. (2022). The primordial differentiation of tumor-specific memory CD8+ T cells as bona fide responders to PD-1/PD-L1 blockade in draining lymph nodes. *Cell*, *185*(22), 4049-4066.e25. https://doi.org/10.1016/j.cell.2022.09.020

Huang, X., & Yang, Y. (2006). The fate of effector CD8 T cells in vivo is controlled by the duration of antigen stimulation. *Immunology*, *118*(3), 361–371. https://doi.org/10.1111/j.1365-2567.2006.02381.x

Huang, Y.-H., Zhu, C., Kondo, Y., Anderson, A. C., Gandhi, A., Russell, A., Dougan, S. K., Petersen, B.-S., Melum, E., Pertel, T., Clayton, K. L., Raab, M., Chen, Q., Beauchemin, N., Yazaki, P. J., Pyzik, M., Ostrowski, M. A., Glickman, J. N., Rudd, C. E., … Blumberg, R. S. (2015). CEACAM1 regulates TIM-3-mediated tolerance and exhaustion. *Nature*, *517*(7534), 386–390. https://doi.org/10.1038/nature13848

Huels, D. J., & Sansom, O. J. (2015). Stem vs non-stem cell origin of colorectal cancer. *British Journal of Cancer*, *113*(1), 1–5. https://doi.org/10.1038/bjc.2015.214

Hui, E., Cheung, J., Zhu, J., Su, X., Taylor, M. J., Wallweber, H. A., Sasmal, D. K., Huang, J., Kim, J. M., Mellman, I., & Vale, R. D. (2017). T cell costimulatory receptor CD28 is a primary target for PD-1-mediated inhibition. *Science*, *355*, 1428–1433. https://doi.org/doi: 10.1126/science.aaf1292

Huse, M., Klein, L. O., Girvin, A. T., Faraj, J. M., Li, Q.-J., Kuhns, M. S., & Davis, M. M. (2007). Spatial and Temporal Dynamics of T Cell Receptor Signaling with a Photoactivatable Agonist. *Immunity*, *27*(1), 76–88. https://doi.org/10.1016/j.immuni.2007.05.017

Huuhtanen, J., Kasanen, H. H., Peltola, K., Lönnberg, T., Glumoff, V., Brück, O., Dufva, O., Peltonen, K., Vikkula, J., Jokinen, E., Ilander, M., Lee, M. H., Mäkelä, S., Nyakas, M., Li, B., Hernberg, M., Bono, P., Lähdesmäki, H., Kreutzman, A., & Mustjoki, S. (2023). Single-cell characterization of anti-LAG3+anti-PD1 treatment in melanoma patients. *The Journal of Clinical Investigation*, *113*(6). https://doi.org/10.1172/JCI164809

Im, S. J., Hashimoto, M., Gerner, M. Y., Lee, J., Kissick, H. T., Burger, M. C., Shan, Q., Hale, J. S., Lee, J., Nasti, T. H., Sharpe, A. H., Freeman, G. J., Germain, R. N., Nakaya, H. I., Xue, H. H., & Ahmed, R. (2016). Defining CD8+ T cells that provide the proliferative burst after PD-1 therapy. *Nature*, *537*(7620), 417–421. https://doi.org/10.1038/nature19330

Im, S.-H., & Rao, A. (2004). Activation and deactivation of gene expression by Ca2+/calcineurin-NFAT-mediated signaling. *Molecules and Cells*, *18*(1), 1–9.

Imbimbo, M., Hollebecque, A., Italiano, A., McKean, M., Macarulla, T., Castanon Alvarez, E., Carneiro, B. A., Mager, R., Barnhart, V., Murtomaki, E., He, Y., Cooper, Z. A., Tu, E., Linke, A., Fan, C., Zhou, D., Boyer Chammard, A., Paturel, C. L., Fraenkel, P. G., & Powderly, J. (2022). 188P IPH5201 as monotherapy or in combination with durvalumab (D) in advanced solid tumours. *Immuno-Oncology and Technology*, *16*, 100300. https://doi.org/10.1016/j.iotech.2022.100300

James, O. J., Vandereyken, M., & Swamy, M. (2020). *Isolation, Characterization, and Culture of Intestinal Intraepithelial Lymphocytes* (pp. 141–152). https://doi.org/10.1007/978-1-0716-0338-3_13

Jenkins, M. R., Tsun, A., Stinchcombe, J. C., & Griffiths, G. M. (2009). The Strength of T Cell Receptor Signal Controls the Polarization of Cytotoxic Machinery to the Immunological Synapse. *Immunity*, *31*(4), 621–631. https://doi.org/10.1016/j.immuni.2009.08.024

Jennings, E., Elliot, T. A. E., Thawait, N., Kanabar, S., Yam-Puc, J. C., Ono, M., Toellner, K. M., Wraith, D. C., Anderson, G., & Bending, D. (2020). Nr4a1 and Nr4a3 Reporter Mice Are Differentially Sensitive to T Cell Receptor Signal Strength and Duration. *Cell Reports*, *33*(5). https://doi.org/10.1016/j.celrep.2020.108328

Jeong, J., Kim, J., Hong, Y. S., Kim, D., Kim, J. E., Kim, S. Y., Kim, K.-P., & Kim, T. W. (2016). Association between HER2 amplification and cetuximab efficacy in patients with RAS wild-type metastatic colorectal cancer. *Annals of Oncology*, *27*, vi172. https://doi.org/10.1093/annonc/mdw370.69

Johnston, R. J., Comps-Agrar, L., Hackney, J., Yu, X., Huseni, M., Yang, Y., Park, S., Javinal, V., Chiu, H., Irving, B., Eaton, D. L., & Grogan, J. L. (2014). The Immunoreceptor TIGIT Regulates Antitumor and Antiviral CD8 + T Cell Effector Function. *Cancer Cell*, *26*(6), 923–937. https://doi.org/10.1016/j.ccell.2014.10.018

Joller, N., Hafler, J. P., Brynedal, B., Kassam, N., Spoerl, S., Levin, S. D., Sharpe, A. H., & Kuchroo, V. K. (2011). Cutting Edge: TIGIT Has T Cell-Intrinsic Inhibitory Functions. *The Journal of Immunology*, *186*(3), 1338–1342. https://doi.org/10.4049/jimmunol.1003081

June, C. H., Ledbetter, J. A., Gillespie, M. M., Lindsten, T., & Thompson, C. B. (1987). T-Cell Proliferation Involving the CD28 Pathway Is Associated witH Cyclosporine-Resistant Interleukin 2 Gene Expression. *Molecular and Cellular Biology*, *7*(12), 4472–4481. https://doi.org/10.1128/mcb.7.12.4472-4481.1987

Jung, I. Y., Narayan, V., McDonald, S., Rech, A. J., Bartoszek, R., Hong, G., Davis, M. M., Xu, J., Boesteanu, A. C., Barber-Rotenberg, J. S., Plesa, G., Lacey, S. F., Jadlowsky, J. K., Siegel, D. L., Hammill, D. M., Cho-Park, P. F., Berger, S. L., Haas, N. B., & Fraietta, J. A. (2022). BLIMP1 and NR4A3 transcription factors reciprocally regulate antitumor CAR T cell stemness and exhaustion. *Science Translational Medicine*, *14*(670), 1–20. https://doi.org/10.1126/scitranslmed.abn7336

Kakavand, H., Jackett, L. A., Menzies, A. M., Gide, T. N., Carlino, M. S., Saw, R. P. M., Thompson, J. F., Wilmott, J. S., Long, G. V., & Scolyer, R. A. (2017). Negative immune checkpoint regulation by VISTA: A mechanism of acquired resistance to anti-PD-1 therapy in metastatic melanoma patients. *Modern Pathology*, *30*(12), 1666–1676. https://doi.org/10.1038/modpathol.2017.89

Kalaora, S., Nagler, A., Nejman, D., Alon, M., Barbolin, C., Bussi, Y., Rotkopf, R., Levy, R., Benedek, G., Trabish, S., & Dadosh, T. (2021). Identification of bacteria-derived HLA-bound peptides in melanoma. *Nature*, *592*(7852), 138–143. https://doi.org/10.1038/s41586-021-03368-8

Kaminuma, O., Deckert, M., Elly, C., Liu, Y.-C., & Altman, A. (2001). Vav-Rac1-Mediated Activation of the c-Jun N-Terminal Kinase/c-Jun/AP-1 Pathway Plays a Major Role in Stimulation of the Distal NFAT Site in the Interleukin-2 Gene Promoter. *Molecular and Cellular Biology*, *21*(9), 3126–3136. https://doi.org/10.1128/MCB.21.9.3126-3136.2001

Kamphorst, A. O., Wieland, A., Nasti, T., Yang, S., Zhang, R., Barber, D. L., Konieczny, B. T., Daugherty, C. Z., Koenig, L., Yu, K., Sica, G. L., Sharpe, A. H., Freeman, G. J., Blazar, B. R., Turka, L. A., Owonikoko, T. K., Pillai, R. N., Ramalingam, S. S., Araki, K., & Ahmed, R. (2017).

Rescue of exhausted CD8 T cells by PD-1-targeted therapies is CD28-dependent. *Science*, *355*, 1423–1427. https://doi.org/doi: 10.1126/science.aaf0683

Kang, S., Na, Y., Joung, S. Y., Lee, S. Il, Oh, S. C., & Min, B. W. (2018). The significance of microsatellite instability in colorectal cancer after controlling for clinicopathological factors. *Medicine (United States)*, *97*(9), 1–6. https://doi.org/10.1097/MD.0000000000010019

Kauffmann, A., Gentleman, R., & Huber, W. (2009). arrayQualityMetrics—a bioconductor package for quality assessment of microarray data. *Bioinformatics*, *25*(3), 415–416. https://doi.org/10.1093/bioinformatics/btn647

Kersh, E. N., Shaw, A. S., & Allen, P. M. (1998). Fidelity of T Cell Activation Through Multistep T Cell Receptor ζ Phosphorylation. *Science*, *281*(5376), 572–575. https://doi.org/10.1126/science.281.5376.572

Khan, O., Giles, J. R., McDonald, S., Manne, S., Ngiow, S. F., Patel, K. P., Werner, M. T., Huang, A. C., Alexander, K. A., Wu, J. E., Attanasio, J., Yan, P., George, S. M., Bengsch, B., Staupe, R. P., Donahue, G., Xu, W., Amaravadi, R. K., Xu, X., … Wherry, E. J. (2019). TOX transcriptionally and epigenetically programs CD8+ T cell exhaustion. *Nature*, *571*(7764), 211–218. https://doi.org/10.1038/s41586-019-1325-x

Kim, D., Song, L., Breitwieser, F. P., & Salzberg, S. L. (2016). Centrifuge: rapid and sensitive classification of metagenomic sequences. *Genome Research*, *26*(12), 1721–1729. https://doi.org/10.1101/gr.210641.116

Kim, E. H., & Suresh, M. (2013). Role of PI3K/Akt signaling in memory CD8 T cell differentiation. *Frontiers in Immunology*, *4*. https://doi.org/10.3389/fimmu.2013.00020

Kimura, T., McKolanis, J. R., Dzubinski, L. A., Islam, K., Potter, D. M., Salazar, A. M., Schoen, R. E., & Finn, O. J. (2013). MUC1 vaccine for individuals with advanced adenoma of the colon: A cancer immunoprevention feasibility study. *Cancer Prevention Research*, *6*(1), 18–26. https://doi.org/10.1158/1940-6207.CAPR-12-0275

King, C. G., Kobayashi, T., Cejas, P. J., Kim, T., Yoon, K., Kim, G. K., Chiffoleau, E., Hickman, S. P., Walsh, P. T., Turka, L. A., & Choi, Y. (2006). TRAF6 is a T cell–intrinsic negative regulator required for the maintenance of immune homeostasis. *Nature Medicine*, *12*(9), 1088–1092. https://doi.org/10.1038/nm1449

King, C. G., Koehli, S., Hausmann, B., Schmaler, M., Zehn, D., & Palmer, E. (2012). T Cell Affinity Regulates Asymmetric Division, Effector Cell Differentiation, and Tissue Pathology. *Immunity*, *37*(4), 709–720. https://doi.org/10.1016/j.immuni.2012.06.021

Kirberg, J., Berns, A., & Boehmer, H. von. (1997). Peripheral T Cell Survival Requires Continual Ligation of the T Cell Receptor to Major Histocompatibility Complex–Encoded Molecules. *The Journal of Experimental Medicine*, *186*(8), 1269–1275. https://doi.org/10.1084/jem.186.8.1269

Klein, L., Kyewski, B., Allen, P. M., & Hogquist, K. A. (2014). Positive and negative selection of the T cell repertoire: what thymocytes see (and don't see). *Nature Reviews Immunology*, *14*(6), 377–391. https://doi.org/10.1038/nri3667

Klein-Hessling, S., Muhammad, K., Klein, M., Pusch, T., Rudolf, R., Flöter, J., Qureischi, M., Beilhack, A., Vaeth, M., Kummerow, C., Backes, C., Schoppmeyer, R., Hahn, U., Hoth, M., Bopp, T., Berberich-Siebelt, F., Patra, A., Avots, A., Müller, N., … Serfling, E. (2017). NFATc1 controls the cytotoxicity of CD8+ T cells. *Nature Communications*, *8*(1), 511. https://doi.org/10.1038/s41467-017-00612-6

Klement, J. D., Redd, P. S., Lu, C., Merting, A. D., Poschel, D. B., Yang, D., Savage, N. M., Zhou, G., Munn, D. H., Fallon, P. G., & Liu, K. (2023). Tumor PD-L1 engages myeloid PD-1 to suppress type I interferon to impair cytotoxic T lymphocyte recruitment. *Cancer Cell*, *41*(3), 620-636.e9. https://doi.org/10.1016/j.ccell.2023.02.005

Kortekaas, K. E., Santegoets, S. J., Sturm, G., Ehsan, I., van Egmond, S. L., Finotello, F., Trajanoski, Z., Welters, M. J. P., van Poelgeest, M. I. E., & van der Burg, S. H. (2020). CD39 identifies the CD4þ tumor-specific T-cell population in human cancer. *Cancer Immunology Research*, *8*(10), 1311–1321. https://doi.org/10.1158/2326-6066.CIR-20-0270

Kostic, A. D., Chun, E., Robertson, L., Glickman, J. N., Gallini, C. A., Michaud, M., Clancy, T. E., Chung, D. C., Lochhead, P., Hold, G. L., El-Omar, E. M., Brenner, D., Fuchs, C. S., Meyerson, M., & Garrett, W. S. (2013). Fusobacterium nucleatum Potentiates Intestinal Tumorigenesis and Modulates the Tumor-Immune Microenvironment. *Cell Host and Microbe*, *14*(2), 207–215. https://doi.org/10.1016/j.chom.2013.07.007

Koyama, M., Mukhopadhyay, P., Schuster, I. S., Henden, A. S., Hülsdünker, J., Varelias, A., Vetizou, M., Kuns, R. D., Robb, R. J., Zhang, P., Blazar, B. R., Thomas, R., Begun, J., Waddell, N., Trinchieri, G., Zeiser, R., Clouston, A. D., Degli-Esposti, M. A., & Hill, G. R. (2019). MHC Class II Antigen Presentation by the Intestinal Epithelium Initiates Graft-versus-Host Disease and Is Influenced by the Microbiota. *Immunity*, *51*(5), 885-898.e7. https://doi.org/10.1016/j.immuni.2019.08.011

Koyama, S., Akbay, E. A., Li, Y. Y., Herter-sprie, G. S., Buczkowski, K. A., Richards, W. G., Gandhi, L., Redig, A. J., Rodig, S. J., Asahina, H., Jones, R. E., Kulkarni, M. M., Kuraguchi, M., Palakurthi, S., Fecci, P. E., Johnson, B. E., Janne, P. A., Engelman, J. A., Gangadharan, S. P., … Hammerman, P. S. (2016). Adaptive resistance to therapeutic PD-1 blockade is associated with upregulation of alternative immune checkpoints. *Nature Communications*, *7*(10501), 1–9. https://doi.org/10.1038/ncomms10501

Krapp, C., Hotter, D., Gawanbacht, A., McLaren, P. J., Kluge, S. F., Stürzel, C. M., Mack, K., Reith, E., Engelhart, S., Ciuffi, A., Hornung, V., Sauter, D., Telenti, A., & Kirchhoff, F. (2016). Guanylate Binding Protein (GBP) 5 Is an Interferon-Inducible Inhibitor of HIV-1 Infectivity. *Cell Host & Microbe*, *19*(4), 504–514. https://doi.org/10.1016/j.chom.2016.02.019

Kreiter, S., Vormehr, M., Van De Roemer, N., Diken, M., Löwer, M., Diekmann, J., Boegel, S., Schrörs, B., Vascotto, F., Castle, J. C., Tadmor, A. D., Schoenberger, S. P., Huber, C., Türeci, O., & Sahin, U. (2015). Mutant MHC class II epitopes drive therapeutic immune responses to cancer. *Nature*, *520*(7549), 692–696. https://doi.org/10.1038/nature14426

Krummel, M. F., & Allison, J. P. (1995). CD28 and CTLA-4 have opposing effects on the response of T cells to stimulation. *The Journal of Experimental Medicine*, *182*(2), 459–465. https://doi.org/10.1084/jem.182.2.459

Kubin, M., Kamoun, M., & Trinchieri, G. (1994). Interleukin 12 synergizes with B7/CD28 interaction in inducing efficient proliferation and cytokine production of human T cells. *Journal of Experimental Medicine*, *180*(1), 211–222. https://doi.org/10.1084/jem.180.1.211

Kupiec-Weglinski, J. W. (2007). OX40 costimulation and regulatory T cells. *Blood*, *110*(7), 2217–2218. https://doi.org/10.1182/blood-2007-07-097642

Kurtulus, S., Madi, A., Escobar, G., Klapholz, M., Nyman, J., Christian, E., Pawlak, M., Dionne, D., Xia, J., Rozenblatt-Rosen, O., Kuchroo, V. K., Regev, A., & Anderson, A. C. (2019). Checkpoint Blockade Immunotherapy Induces Dynamic Changes in PD-1 – CD8 + Tumor-Infiltrating T Cells. *Immunity*, *50*(1), 181-194.e6. https://doi.org/10.1016/j.immuni.2018.11.014

Lal, N., Beggs, A. D., Willcox, B. E., & Middleton, G. W. (2015). An immunogenomic stratification of colorectal cancer : Implications for development of targeted immunotherapy. *Oncoimmunology*, *4*(3), 1–9. https://doi.org/10.4161/2162402X.2014.976052

Larkin, J., Chiarion-Sileni, V., Gonzalez, R., Grob, J. J., Cowey, C. L., Lao, C. D., Schadendorf, D., Dummer, R., Smylie, M., Rutkowski, P., Ferrucci, P. F., Hill, A., Wagstaff, J., Carlino, M. S., Haanen, J. B., Maio, M., Marquez-Rodas, I., McArthur, G. A., Ascierto, P. A., … Wolchok, J. D. (2015). Combined Nivolumab and Ipilimumab or Monotherapy in Untreated Melanoma. *New England Journal of Medicine*, *373*(1), 23–34. https://doi.org/10.1056/nejmoa1504030

Le, D. T., Uram, J. N., Wang, H., Bartlett, B. R., Kemberling, H., Eyring, A. D., Skora, A. D., Luber, B. S., Azad, N. S., Laheru, D., Biedrzycki, B., Donehower, R. C., Zaheer, A., Fisher, G. A., Crocenzi, T. S., Lee, J. J., Duffy, S. M., Goldberg, R. M., de la Chapelle, A., … Diaz, L. A. (2015). PD-1 Blockade in Tumors with Mismatch-Repair Deficiency. *New England Journal of Medicine*, *372*(26), 2509–2520. https://doi.org/10.1056/nejmoa1500596

Lee, J., Su, E. W., Zhu, C., Hainline, S., Phuah, J., Moroco, J. A., Smithgall, T. E., Kuchroo, V. K., & Kane, L. P. (2011). Phosphotyrosine-Dependent Coupling of Tim-3 to T-Cell Receptor Signaling Pathways. *Molecular and Cellular Biology*, *31*(19), 3963–3974. https://doi.org/10.1128/MCB.05297-11

Lee, Y.-T., Suarez-Ramirez, J. E., Wu, T., Redman, J. M., Bouchard, K., Hadley, G. A., & Cauley, L. S. (2011). Environmental and Antigen Receptor-Derived Signals Support Sustained Surveillance of the Lungs by Pathogen-Specific Cytotoxic T Lymphocytes. *Journal of Virology*, *85*(9), 4085–4094. https://doi.org/10.1128/JVI.02493-10

Leek, J. T., Johnson, W. E., Parker, H. S., Jaffe, A. E., & Storey, J. D. (2012). The sva package for removing batch effects and other unwanted variation in high-throughput experiments. *Bioinformatics*, *28*(6), 882–883. https://doi.org/10.1093/bioinformatics/bts034

Lenz, H.-J., Lonardi, S., Zagonel, V., Van Cutsem, E., Limon, M. L., Wong, M., Hendlisz, A., Aglietta, M., Garcia-Alfonso, P., Neyns, B., Gelsomino, F., Cardin, D. B., Dragovich, T., Shah, U., Yang, J., Ledeine, J.-M., & Overman, M. J. (2020). Nivolumab (NIVO) + low-dose ipilimumab (IPI) as first-line (1L) therapy in microsatellite instability-high/mismatch repair-deficient (MSI-H/dMMR) metastatic colorectal cancer (mCRC): Two-year clinical update. *Journal of Clinical Oncology*, *38*(15_suppl), 4040. https://doi.org/10.1200/JCO.2020.38.15_suppl.4040

Leupin, O., Zaru, R., Laroche, T., Müller, S., & Valitutti, S. (2000). Exclusion of CD45 from the T-cell receptor signaling area in antigen-stimulated T lymphocytes. *Current Biology*, *10*(5), 277–280. https://doi.org/10.1016/S0960-9822(00)00362-6

Li, W., Whaley, C. D., Mondino, A., & Mueller, D. L. (1996). Blocked Signal Transduction to the ERK and JNK Protein Kinases in Anergic CD4+ T Cells. *Science*, *271*(5253), 1272–1276. https://doi.org/10.1126/science.271.5253.1272

Liebmann, M., Hucke, S., Koch, K., Eschborn, M., Ghelman, J., Chasan, A. I., Glander, S., Schädlich, M., Kuhlencord, M., Daber, N. M., Eveslage, M., Beyer, M., Dietrich, M., Albrecht, P., Stoll, M., Busch, K. B., Wiendl, H., Roth, J., Kuhlmann, T., & Klotz, L. (2018). Nur77 serves as a molecular brake of the metabolic switch during T cell activation to restrict autoimmunity. *Proceedings of the National Academy of Sciences*, *115*(34). https://doi.org/10.1073/pnas.1721049115

Liu, S., Zhang, H., Li, M., Hu, D., Li, C., Ge, B., Jin, B., & Fan, Z. (2013). Recruitment of Grb2 and SHIP1 by the ITT-like motif of TIGIT suppresses granule polarization and cytotoxicity of NK cells. *Cell Death & Differentiation*, *20*(3), 456–464. https://doi.org/10.1038/cdd.2012.141

Liu, T., Zhang, L., Joo, D., & Sun, S.-C. (2017). NF-κB signaling in inflammation. *Signal Transduction and Targeted Therapy*, *2*(1), 17023. https://doi.org/10.1038/sigtrans.2017.23

Liu, X., Wang, Y., Lu, H., Li, J., Yan, X., Xiao, M., Hao, J., Alekseev, A., Khong, H., Chen, T., Huang, R., Wu, J., Zhao, Q., Wu, Q., Xu, S., Wang, X., Jin, W., Yu, S., Wang, Y., … Dong, C. (2019). Genome-wide analysis identifies NR4A1 as a key mediator of T cell dysfunction. *Nature*, *567*(7749), 525–529. https://doi.org/10.1038/s41586-019-0979-8

Liu, Z.-G., Smith, S. W., McLaughlin, K. A., Schwartz, L. M., & Osborne, B. A. (1994). Apoptotic signals delivered through the T-cell receptor of a T-cell hybrid require the immediate–early gene nur77. *Nature*, *367*(6460), 281–284. https://doi.org/10.1038/367281a0

Llosa, N. J., Cruise, M., Tam, A., Wick, E. C., Elizabeth, M., Taube, J. M., Blosser, L., Fan, H., Wang, H., Zhang, M., Papadopoulos, N., Kinzler, K. W., Vogelstein, B., Sears, C. L., Anders, R. A., Pardoll, D. M., & Housseau, F. (2015). The vigorous immune microenvironment of microsatellite instable colon cancer is balanced by multiple counter-inhibitory checkpoints. *Cancer Discov.*, *5*(1), 43–51. https://doi.org/10.1158/2159-8290.CD-14-0863.The

Lo, W.-L., Kuhlmann, M., Rizzuto, G., Ekiz, H. A., Kolawole, E. M., Revelo, M. P., Andargachew, R., Li, Z., Tsai, Y.-L., Marson, A., Evavold, B. D., Zehn, D., & Weiss, A. (2023). A single-amino acid substitution in the adaptor LAT accelerates TCR proofreading kinetics and alters T-cell selection, maintenance and function. *Nature Immunology*, *24*(4), 676–689. https://doi.org/10.1038/s41590-023-01444-x

Macian, F., García-Rodríguez, C., & Rao, A. (2000). Gene expression elicited by NFAT in the presence or absence of cooperative recruitment of Fos and Jun. *The EMBO Journal*, *19*(17), 4783–4795. https://doi.org/10.1093/emboj/19.17.4783

Macián, F., García-Cózar, F., Im, S.-H., Horton, H. F., Byrne, M. C., & Rao, A. (2002). Transcriptional Mechanisms Underlying Lymphocyte Tolerance. *Cell*, *109*(6), 719–731. https://doi.org/10.1016/S0092-8674(02)00767-5

Macián, F., López-Rodríguez, C., & Rao, A. (2001). Partners in transcription: NFAT and AP-1. *Oncogene*, *20*(19), 2476–2489. https://doi.org/10.1038/sj.onc.1204386

Man, S. M., Karki, R., Sasai, M., Place, D. E., Kesavardhana, S., Temirov, J., Frase, S., Zhu, Q., Malireddi, R. K. S., Kuriakose, T., Peters, J. L., Neale, G., Brown, S. A., Yamamoto, M., & Kanneganti, T. D. (2016). IRGB10 Liberates Bacterial Ligands for Sensing by the AIM2 and Caspase-11-NLRP3 Inflammasomes. *Cell*, *167*(2), 382-396.e17. https://doi.org/10.1016/j.cell.2016.09.012

Mariathasan, S., Weiss, D. S., Newton, K., McBride, J., O'Rourke, K., Roose-Girma, M., Lee, W. P., Weinrauch, Y., Monack, D. M., & Dixit, V. M. (2006). Cryopyrin activates the inflammasome in response to toxins and ATP. *Nature*, *440*(7081), 228–232. https://doi.org/10.1038/nature04515

Martinez, G. J., Pereira, R. M., Äijö, T., Kim, E. Y., Marangoni, F., Pipkin, M. E., Togher, S., Heissmeyer, V., Zhang, Y. C., Crotty, S., Lamperti, E. D., Ansel, K. M., Mempel, T. R., Lähdesmäki, H., Hogan, P. G., & Rao, A. (2015). The Transcription Factor NFAT Promotes Exhaustion of Activated CD8+ T Cells. *Immunity*, *42*(2), 265–278. https://doi.org/10.1016/j.immuni.2015.01.006

Martínez-Martín, N., Fernández-Arenas, E., Cemerski, S., Delgado, P., Turner, M., Heuser, J., Irvine, D. J., Huang, B., Bustelo, X. R., Shaw, A., & Alarcón, B. (2011). T Cell Receptor Internalization from the Immunological Synapse Is Mediated by TC21 and RhoG GTPase-Dependent Phagocytosis. *Immunity*, *35*(2), 208–222. https://doi.org/10.1016/j.immuni.2011.06.003

Maruhashi, T., Okazaki, I., Sugiura, D., Takahashi, S., Maeda, T. K., Shimizu, K., & Okazaki, T. (2018). LAG-3 inhibits the activation of CD4+ T cells that recognize stable pMHCII through its conformation-dependent recognition of pMHCII. *Nature Immunology*, *19*(12), 1415–1426. https://doi.org/10.1038/s41590-018-0217-9

Mason, D. (1998). A very high level of crossreactivity is an essential feature of the T-cell receptor. *Immunology Today*, *19*(9), 395–404. https://doi.org/10.1016/S0167-5699(98)01299-7

Maurice, N. J., Berner, J., Taber, A. K., Zehn, D., & Prlic, M. (2021). Inflammatory signals are sufficient to elicit TOX expression in mouse and human CD8+ T cells. *JCI Insight*, *6*(13). https://doi.org/10.1172/jci.insight.150744

Mazet, J. M., Mahale, J. N., Tong, O., Watson, R. A., Lechuga-Vieco, A. V., Pirgova, G., Lau, V. W. C., Attar, M., Koneva, L. A., Sansom, S. N., Fairfax, B. P., & Gérard, A. (2023). IFNγ signaling in cytotoxic T cells restricts anti-tumor responses by inhibiting the maintenance and diversity of intra-tumoral stem-like T cells. *Nature Communications*, *14*(1), 321. https://doi.org/10.1038/s41467-023-35948-9

McDonald, B. D., Jabri, B., & Bendelac, A. (2018). Diverse developmental pathways of intestinal intraepithelial lymphocytes. *Nature Reviews Immunology*, *18*(8), 514–525. https://doi.org/10.1038/s41577-018-0013-7

McGranahan, N., Furness, A., Rosenthal, R., Ramskov, S., Lyngaa, R., Saini, S. K., & Swanton, C. (2016). Clonal neoantigens elicit T cell immunoreactivity and sensitivity to immune checkpoint blockade. *Science*, *351*(6280), 1463–1470.

McKeithan, T. W. (1995). Kinetic proofreading in T-cell receptor signal transduction. *Proceedings of the National Academy of Sciences*, *92*(11), 5042–5046. https://doi.org/10.1073/pnas.92.11.5042

McMurray, J. (2021). *Investigating Novel Routes to High Intratumoural Immunity: Exploring the Immune Landscape in Low Mutation Burden Cancer*. University of Birmingham.

McNeill, L., Salmond, R. J., Cooper, J. C., Carret, C. K., Cassady-Cain, R. L., Roche-Molina, M., Tandon, P., Holmes, N., & Alexander, D. R. (2007). The Differential Regulation of Lck Kinase Phosphorylation Sites by CD45 Is Critical for T Cell Receptor Signaling Responses. *Immunity*, *27*(3), 425–437. https://doi.org/10.1016/j.immuni.2007.07.015

Meazza, R., Comes, A., Orengo, A. M., Ferrini, S., & Accolla, R. S. (2003). Tumor rejection by gene transfer of the MHC class II transactivator in murine mammary adenocarcinoma cells. *European Journal of Immunology*, *33*(5), 1183–1192. https://doi.org/10.1002/eji.200323712

Medema, J. P., & Vermeulen, L. (2011). Microenvironmental regulation of stem cells in intestinal homeostasis and cancer. *Nature*, *474*(7351), 318–326. https://doi.org/10.1038/nature10212

Meng, K. P., Majedi, F. S., Thauland, T. J., & Butte, M. J. (2020). Mechanosensing through YAP controls T cell activation and metabolism. *Journal of Experimental Medicine*, *217*(8). https://doi.org/10.1084/jem.20200053

Middleton, G., Liu, W., Savage, J., Bridgewater, J. A., Ross, P., Saunders, M. P., Plummer, R., Clive, S., Coyle, V., Thomas, A., P. Taniere, & Billingham, L. (2022). 426P Assessing nivolumab in class II expressing microsatellite stable (pMMR) colorectal cancer (CRC): Results of the ANICCA-Class II trial. *Annals of Oncology*, *33*, S729–S730. https://doi.org/10.1016/j.annonc.2022.07.564

Miller, B. C., Sen, D. R., Al Abosy, R., Bi, K., Virkud, Y. V., LaFleur, M. W., Yates, K. B., Lako, A., Felt, K., Naik, G. S., Manos, M., Gjini, E., Kuchroo, J. R., Ishizuka, J. J., Collier, J. L., Griffin, G. K., Maleri, S., Comstock, D. E., Weiss, S. A., … Haining, W. N. (2019). Subsets of exhausted CD8+ T cells differentially mediate tumor control and respond to checkpoint blockade. *Nature Immunology*, *20*(3), 326–336. https://doi.org/10.1038/s41590-019-0312-6

Mima, K., Nishihara, R., Qian, Z. R., Cao, Y., Sukawa, Y., Nowak, J. A., Yang, J., Dou, R., Masugi, Y., Song, M., Kostic, A. D., Giannakis, M., Bullman, S., Milner, D. A., Baba, H., Giovannucci, E. L., Garraway, L. A., Freeman, G. J., Dranoff, G., … Ogino, S. (2016). Fusobacterium nucleatum in colorectal carcinoma tissue and patient prognosis. *Gut*, *65*(12), 1973–1980. https://doi.org/10.1136/gutjnl-2015-310101

Miskov-Zivanov, N., Turner, M. S., Kane, L. P., Morel, P. A., & Faeder, J. R. (2013). The Duration of T Cell Stimulation Is a Critical Determinant of Cell Fate and Plasticity. *Science Signaling*, *6*(300). https://doi.org/10.1126/scisignal.2004217

Mittal, S. K., & Roche, P. A. (2015). Suppression of antigen presentation by IL-10. *Current Opinion in Immunology*, *34*, 22–27. https://doi.org/10.1016/j.coi.2014.12.009

Mizuno, R., Sugiura, D., Shimizu, K., Maruhashi, T., Watada, M., Okazaki, I. mi, & Okazaki, T. (2019). PD-1 primarily targets TCR signal in the inhibition of functional T cell activation. *Frontiers in Immunology*, *10*(MAR). https://doi.org/10.3389/fimmu.2019.00630

Mlecnik, B., Bindea, G., Angell, H. K., Maby, P., Angelova, M., Tougeron, D., Church, S. E., Lafontaine, L., Fischer, M., Fredriksen, T., Sasso, M., Bilocq, A. M., Kirilovsky, A., Obenauf, A. C., Hamieh, M., Berger, A., Bruneval, P., Tuech, J. J., Sabourin, J. C., … Galon, J. (2016). Integrative Analyses of Colorectal Cancer Show Immunoscore Is a Stronger Predictor of Patient Survival Than Microsatellite Instability. *Immunity*, *44*(3), 698–711. https://doi.org/10.1016/j.immuni.2016.02.025

Mognol, G. P., Spreafico, R., Wong, V., Scott-Browne, J. P., Togher, S., Hoffmann, A., Hogan, P. G., Rao, A., & Trifari, S. (2017). Exhaustion-associated regulatory regions in CD8+ tumor-infiltrating T cells. *Proceedings of the National Academy of Sciences*, *114*(13). https://doi.org/10.1073/pnas.1620498114

Moran, A. E., Holzapfel, K. L., Xing, Y., Cunningham, N. R., Maltzman, J. S., Punt, J., & Hogquist, K. A. (2011). T cell receptor signal strength in Treg and iNKT cell development demonstrated by a novel fluorescent reporter mouse. *Journal of Experimental Medicine*, *208*(6), 1279–1289. https://doi.org/10.1084/jem.20110308

Morath, A., & Schamel, W. W. (2020). αβ and γδ T cell receptors: Similar but different. *Journal of Leukocyte Biology*, *107*(6), 1045–1055. https://doi.org/10.1002/JLB.2MR1219-233R

Morton, D., Seymour, M., Magill, L., Handley, K., Glasbey, J., Glimelius, B., Palmer, A., Seligmann, J., Laurberg, S., Murakami, K., West, N., Quirke, P., & Gray, R. (2023). Preoperative Chemotherapy for Operable Colon Cancer: Mature Results of an International Randomized Controlled Trial. *Journal of Clinical Oncology*, *41*(8), 1541–1552. https://doi.org/10.1200/JCO.22.00046

Mueller, D. L., Jenkins, M. K., & Schwartz, R. H. (1989). Clonal Expansion Versus Functional Clonal Inactivation: A Costimulatory Signalling Pathway Determines the Outcome of T Cell Antigen Receptor Occupancy. *Annual Review of Immunology*, *7*(1), 445–480. https://doi.org/10.1146/annurev.iy.07.040189.002305

Muhlethaler-Mottet, A., Otten, L. A., Steimle, V., & Mach, B. (1997). Expression of MHC class II molecules in different cellular and functional compartments is controlled by differential usage of multiple promoters of the transactivator CIITA. *EMBO Journal*, *16*(10), 2851–2860. https://doi.org/10.1093/emboj/16.10.2851

Müller, M. R., & Rao, A. (2010). NFAT, immunity and cancer: a transcription factor comes of age. *Nature Reviews Immunology*, *10*(9), 645–656. https://doi.org/10.1038/nri2818

Myers, D. R., Zikherman, J., & Roose, J. P. (2017). Tonic Signals: Why Do Lymphocytes Bother? *Trends in Immunology*, *38*(11), 844–857. https://doi.org/10.1016/j.it.2017.06.010

Naito, Y., Saito, K., Shiiba, K., Ohuchi, A., Saigenji, K., Nagura, H., & Ohtani, H. (1998). CD8+ T cells infiltrated within cancer cell nests as a prognostic factor in human colorectal cancer. *Cancer Research*, *58*(16), 3491–3494.

Nallagatla, S. R., Hwang, J., Toroney, R., Zheng, X., Cameron, C. E., & Bevilacqua, P. C. (2007). 5'-Triphosphate-Dependent Activation of PKR by RNAs with Short Stem-Loops. *Science*, *318*(5855), 1455–1458. https://doi.org/10.1126/science.1147347

Nowarski, R., Jackson, R., Gagliani, N., de Zoete, M. R., Palm, N. W., Bailis, W., Low, J. S., Harman, C. C. D., Graham, M., Elinav, E., & Flavell, R. A. (2015). Epithelial IL-18 Equilibrium Controls Barrier Function in Colitis. *Cell*, *163*(6), 1444–1456. https://doi.org/10.1016/j.cell.2015.10.072

Odagiu, L., Boulet, S., Maurice De Sousa, D., Daudelin, J.-F., Nicolas, S., & Labrecque, N. (2020). Early programming of CD8+ T cell response by the orphan nuclear receptor NR4A3. *Proceedings of the National Academy of Sciences*, *117*(39), 24392–24402. https://doi.org/10.1073/pnas.2007224117

Okamura, H., Tsutsi, H., Komatsu, T., Yutsudo, M., Hakura, A., Tanimoto, T., Torigoe, K., Okura, T., Nukada, Y., Hattori, K., & et al. (1995). Cloning of a new cytokine that induces IFN-y production by T cells. *Nature*, *378*(6552), 88–91.

Ono, M., Tanaka, R. J., & Kano, M. (2014). Visualisation of the T cell differentiation programme by Canonical Correspondence Analysis of transcriptomes. *BMC Genomics*, *15*(1), 1028. https://doi.org/10.1186/1471-2164-15-1028

Orsetti, B., Selves, J., Bascoul-Mollevi, C., Lasorsa, L., Gordien, K., Bibeau, F., Massemin, B., Paraf, F., Soubeyran, I., Hostein, I., Dapremont, V., Guimbaud, R., Cazaux, C., Longy, M., & Theillet, C. (2014). Impact of chromosomal instability on colorectal cancer progression and outcome. *BMC Cancer*, *14*(1), 1–13. https://doi.org/10.1186/1471-2407-14-121

Overman, M. J., McDermott, R., Leach, J. L., Lonardi, S., Lenz, H. J., Morse, M. A., Desai, J., Hill, A., Axelson, M., Moss, R. A., Goldberg, M. V., Cao, Z. A., Ledeine, J. M., Maglinte, G. A., Kopetz, S., & André, T. (2017). Nivolumab in patients with metastatic DNA mismatch repair-deficient or microsatellite instability-high colorectal cancer (CheckMate 142): an open-label, multicentre, phase 2 study. *The Lancet Oncology*, *18*(9), 1182–1191. https://doi.org/10.1016/S1470-2045(17)30422-9

Pagès, F., Mlecnik, B., Marliot, F., Bindea, G., Ou, F. S., Bifulco, C., Lugli, A., Zlobec, I., Rau, T. T., Berger, M. D., Nagtegaal, I. D., Vink-Börger, E., Hartmann, A., Geppert, C., Kolwelter, J., Merkel, S., Grützmann, R., Van den Eynde, M., Jouret-Mourin, A., … Galon, J. (2018). International validation of the consensus Immunoscore for the classification of colon cancer: a prognostic and accuracy study. *The Lancet*, *391*(10135), 2128–2139. https://doi.org/10.1016/S0140-6736(18)30789-X

Paulson, J. N., Stine, O. C., Bravo, H. C., & Pop, M. (2013). Differential abundance analysis for microbial marker-gene surveys. *Nature Methods*, *10*(12), 1200–1202. https://doi.org/10.1038/nmeth.2658

Pećina-Šlaus, N., Kafka, A., Salamon, I., & Bukovac, A. (2020). Mismatch Repair Pathway, Genome Stability and Cancer. In *Frontiers in Molecular Biosciences* (Vol. 7). https://doi.org/10.3389/fmolb.2020.00122

Penna, A., Demuro, A., Yeromin, A. V., Zhang, S. L., Safrina, O., Parker, I., & Cahalan, M. D. (2008). The CRAC channel consists of a tetramer formed by Stim-induced dimerization of Orai dimers. *Nature*, *456*(7218), 116–120. https://doi.org/10.1038/nature07338

Philip, M., Fairchild, L., Sun, L., Horste, E. L., Camara, S., Shakiba, M., Scott, A. C., Viale, A., Lauer, P., Merghoub, T., Hellmann, M. D., Wolchok, J. D., Leslie, C. S., & Schietinger, A. (2017). Chromatin states define tumour-specific T cell dysfunction and reprogramming. *Nature*, *545*(7655), 452–456. https://doi.org/10.1038/nature22367

Podtschaske, M., Benary, U., Zwinger, S., Höfer, T., Radbruch, A., & Baumgrass, R. (2007). Digital NFATc2 Activation per Cell Transforms Graded T Cell Receptor Activation into an All-or-None IL-2 Expression. *PLoS ONE*, *2*(9), e935. https://doi.org/10.1371/journal.pone.0000935

Poltorak, A., He, X., Smirnova, I., Liu, M.-Y., Huffel, C. Van, Du, X., Birdwell, D., Alejos, E., Silva, M., Galanos, C., Freudenberg, M., Ricciardi-Castagnoli, P., Layton, B., & Beutler, B. (1998). Defective LPS Signaling in C3H/HeJ and C57BL/10ScCr Mice: Mutations in *Tlr4* Gene. *Science*, *282*(5396), 2085–2088. https://doi.org/10.1126/science.282.5396.2085

Prokhnevska, N., Cardenas, M. A., Valanparambil, R. M., Sobierajska, E., Barwick, B. G., Jansen, C., Reyes Moon, A., Gregorova, P., delBalzo, L., Greenwald, R., Bilen, M. A., Alemozaffar, M., Joshi, S., Cimmino, C., Larsen, C., Master, V., Sanda, M., & Kissick, H. (2023). CD8+ T cell activation in cancer comprises an initial activation phase in lymph nodes followed by effector differentiation within the tumor. *Immunity*, *56*(1), 107-124.e5. https://doi.org/10.1016/j.immuni.2022.12.002

Punt, J. A., Roberts, J. L., Kearse, K. P., & Singer, A. (1994). Stoichiometry of the T cell Antigen Receptor (TCR) Complex: Each TCR/CD3 Complex Contains One TCR ol, One TCR [3, and Two CD3e Chains. *The Journal of Experimental Medicine*, *180*, 587–593. http://rupress.org/jem/article-pdf/180/2/587/1676111/587.pdf

Qian, D. C., Xiao, X., Byun, J., Suriawinata, A. A., Her, S. C., Amos, C. I., & Barth, R. J. (2017). PI3K/Akt/mTOR signaling and plasma membrane proteins are implicated in responsiveness to adjuvant dendritic cell vaccination for metastatic colorectal cancer. *Clinical Cancer Research*, *23*(2), 399–406. https://doi.org/10.1158/1078-0432.CCR-16-0623

Qureshi, O. S., Zheng, Y., Nakamura, K., Attridge, K., Manzotti, C., Schmidt, E. M., Baker, J., Jeffery, L. E., Kaur, S., Briggs, Z., Hou, T. Z., Futter, C. E., Anderson, G., Walker, L. S. K., & Sansom, D. M. (2011). Trans-Endocytosis of CD80 and CD86: A Molecular Basis for the Cell-Extrinsic Function of CTLA-4. *Science*, *332*(6029), 600–603. https://doi.org/10.1126/science.1202947

Raab, M., Cai, Y. C., Bunnell, S. C., Heyeck, S. D., Berg, L. J., & Rudd, C. E. (1995). p56Lck and p59Fyn regulate CD28 binding to phosphatidylinositol 3-kinase, growth factor receptor-bound protein GRB-2, and T cell-specific protein-tyrosine kinase ITK: implications for T-cell costimulation. *Proceedings of the National Academy of Sciences*, *92*(19), 8891–8895. https://doi.org/10.1073/pnas.92.19.8891

Rangachari, M., Zhu, C., Sakuishi, K., Xiao, S., Karman, J., Chen, A., Angin, M., Wakeham, A., Greenfield, E. A., Sobel, R. A., Okada, H., McKinnon, P. J., Mak, T. W., Addo, M. M., Anderson, A. C., & Kuchroo, V. K. (2012). Bat3 promotes T cell responses and autoimmunity by repressing Tim-3–mediated cell death and exhaustion. *Nature Medicine*, *18*(9), 1394–1400. https://doi.org/10.1038/nm.2871

Rao, A., Luo, C., & Hogan, P. G. (1997). TRANSCRIPTION FACTORS OF THE NFAT FAMILY:Regulation and Function. *Annual Review of Immunology*, *15*(1), 707–747. https://doi.org/10.1146/annurev.immunol.15.1.707

Rawla, P., Sunkara, T., & Barsouk, A. (2019). Epidemiology of colorectal cancer: Incidence, mortality, survival, and risk factors. *Gastroentrorology Rev.*, *14*(2), 89–103. https://doi.org/10.5114/pg.2018.81072

Reya, T., & Clevers, H. (2005). Wnt signalling in stem cells and cancer. *Nature*, *434*, 843–850. www.nature.com/nature

Rhee, S. G. (2001). Regulation of Phosphoinositide-Specific Phospholipase C. *Annual Review of Biochemistry*, *70*(1), 281–312. https://doi.org/10.1146/annurev.biochem.70.1.281

Richard, A. C., Lun, A. T. L., Lau, W. W. Y., Göttgens, B., Marioni, J. C., & Griffiths, G. M. (2018). T cell cytolytic capacity is independent of initial stimulation strength. *Nature Immunology*, *19*(8), 849–858. https://doi.org/10.1038/s41590-018-0160-9

Riley, J. L. (2009). PD-1 signaling in primary T cells. *Immunological Reviews*, *229*(1), 114–125. https://doi.org/10.1111/j.1600-065X.2009.00767.x

Rosen, L. S., Jacobs, I. A., & Burkes, R. L. (2017). Bevacizumab in Colorectal Cancer: Current Role in Treatment and the Potential of Biosimilars. *Targeted Oncology*, *12*(5), 599–610. https://doi.org/10.1007/s11523-017-0518-1

Rota, G., Niogret, C., Dang, A. T., Barros, C. R., Fonta, N. P., Alfei, F., Morgado, L., Zehn, D., Birchmeier, W., Vivier, E., & Guarda, G. (2018). Shp-2 Is Dispensable for Establishing T Cell Exhaustion and for PD-1 Signaling In Vivo. *Cell Reports*, *23*(1), 39–49. https://doi.org/10.1016/j.celrep.2018.03.026

Rudd, C. E., & Schneider, H. (2003). Unifying concepts in CD28, ICOS and CTLA4 co-receptor signalling. *Nature Reviews Immunology*, *3*(7), 544–556. https://doi.org/10.1038/nri1131

Rudd, C. E., Taylor, A., & Schneider, H. (2009). CD28 and CTLA-4 coreceptor expression and signal transduction. *Immunological Reviews*, *229*(1), 12–26. https://doi.org/10.1111/j.1600-065X.2009.00770.x

Rudolph, M. G., Stanfield, R. L., & Wilson, I. A. (2006). HOW TCRS BIND MHCS, PEPTIDES, AND CORECEPTORS. *Annual Review of Immunology*, *24*(1), 419–466. https://doi.org/10.1146/annurev.immunol.23.021704.115658

Sabatos, C. A., Chakravarti, S., Cha, E., Schubart, A., Sánchez-Fueyo, A., Zheng, X. X., Coyle, A. J., Strom, T. B., Freeman, G. J., & Kuchroo, V. K. (2003). Interaction of Tim-3 and Tim-3 ligand regulates T helper type 1 responses and induction of peripheral tolerance. *Nature Immunology*, *4*(11), 1102–1110. https://doi.org/10.1038/ni988

Sade-Feldman, M., Yizhak, K., Bjorgaard, S. L., Ray, J. P., de Boer, C. G., Jenkins, R. W., Lieb, D. J., Chen, J. H., Frederick, D. T., Barzily-Rokni, M., Freeman, S. S., Reuben, A., Hoover, P. J., Villani, A. C., Ivanova, E., Portell, A., Lizotte, P. H., Aref, A. R., Eliane, J. P., … Hacohen, N. (2018). Defining T Cell States Associated with Response to Checkpoint Immunotherapy in Melanoma. *Cell*, *175*(4), 998-1013.e20. https://doi.org/10.1016/j.cell.2018.10.038

Safiri, S., Sepanlou, S. G., Ikuta, K. S., Bisignano, C., Salimzadeh, H., Delavari, A., Ansari, R., Roshandel, G., Merat, S., Fitzmaurice, C., Force, L. M., Nixon, M. R., Abbastabar, H., Abegaz, K. H., Afarideh, M., Ahmadi, A., Ahmed, M. B., Akinyemiju, T., Alahdab, F., … Malekzadeh, R. (2019). The global, regional, and national burden of colorectal cancer and its attributable risk factors in 195 countries and territories, 1990–2017: a systematic analysis for the Global Burden of Disease Study 2017. *The Lancet Gastroenterology and Hepatology*, *4*(12), 913–933. https://doi.org/10.1016/S2468-1253(19)30345-0

Saito, T., Yokosuka, T., & Hashimoto-Tane, A. (2010). Dynamic regulation of T cell activation and co-stimulation through TCR-microclusters. *FEBS Letters*, *584*(24), 4865–4871. https://doi.org/10.1016/j.febslet.2010.11.036

Sakuishi, K., Apetoh, L., Sullivan, J. M., Blazar, B. R., Kuchroo, V. K., & Anderson, A. C. (2010). Targeting Tim-3 and PD-1 pathways to reverse T cell exhaustion and restore anti-tumor immunity. *Journal of Experimental Medicine*, *207*(10), 2187–2194. https://doi.org/10.1084/jem.20100643

Santos, J. C., Boucher, D., Schneider, L. K., Demarco, B., Dilucca, M., Shkarina, K., Heilig, R., Chen, K. W., Lim, R. Y. H., & Broz, P. (2020). Human GBP1 binds LPS to initiate assembly of a caspase-4 activating platform on cytosolic bacteria. *Nature Communications*, *11*(1). https://doi.org/10.1038/s41467-020-16889-z

Schatoff, E. M., Leach, B. I., & Dow, L. E. (2017). WNT Signaling and Colorectal Cancer. *Current Colorectal Cancer Reports*, *13*(2), 101–110. https://doi.org/10.1007/s11888-017-0354-9

Schenkel, J. M., Herbst, R. H., Canner, D., Li, A., Hillman, M., Shanahan, S.-L., Gibbons, G., Smith, O. C., Kim, J. Y., Westcott, P., Hwang, W. L., Freed-Pastor, W. A., Eng, G., Cuoco, M. S., Rogers, P., Park, J. K., Burger, M. L., Rozenblatt-Rosen, O., Cong, L., … Jacks, T. (2021). Conventional type I dendritic cells maintain a reservoir of proliferative tumor-antigen specific TCF-1+ CD8+ T cells in tumor-draining lymph nodes. *Immunity*, 1–16. https://doi.org/10.1016/j.immuni.2021.08.026

Schenkel, J. M., & Masopust, D. (2014). Tissue-Resident Memory T Cells. *Immunity*, *41*(6), 886–897. https://doi.org/10.1016/j.immuni.2014.12.007

Schietinger, A., Philip, M., Krisnawan, V. E., Chiu, E. Y., Delrow, J. J., Basom, R. S., Lauer, P., Brockstedt, D. G., Knoblaugh, S. E., Hämmerling, G. J., Schell, T. D., Garbi, N., & Greenberg, P. D. (2016). Tumor-Specific T Cell Dysfunction Is a Dynamic Antigen-Driven Differentiation Program Initiated Early during Tumorigenesis. *Immunity*, *45*(2), 389–401. https://doi.org/10.1016/j.immuni.2016.07.011

Schmid, D., Pypaert, M., & Mu, C. (2007). Antigen-Loading Compartments for Major Histocompatibility Complex Class II Molecules Continuously Receive Input from Autophagosomes. *Immunity*, *January*, 79–92. https://doi.org/10.1016/j.immuni.2006.10.018

Schumacher, T. N., & Schreiber, R. D. (2015). Neoantigens in cancer immunotherapy. *Science*, *348*(6230), 69–74. https://doi.org/10.1126/science.aaa4971

Schwartz, R. H. (1990). Culture Model for Lymphocyte Clonal Anergy. *Science*, *148*(7), 1349–1356.

Scott, A. C., Dündar, F., Zumbo, P., Chandran, S. S., Klebanoff, C. A., Shakiba, M., Trivedi, P., Menocal, L., Appleby, H., Camara, S., Zamarin, D., Walther, T., Snyder, A., Femia, M. R., Comen, E. A., Wen, H. Y., Hellmann, M. D., Anandasabapathy, N., Liu, Y., … Schietinger, A. (2019). TOX is a critical regulator of tumour-specific T cell differentiation. *Nature*, *571*(7764), 270–274. https://doi.org/10.1038/s41586-019-1324-y

Sekine, T., Perez-Potti, A., Nguyen, S., Gorin, J. B., Wu, V. H., Gostick, E., Llewellyn-Lacey, S., Hammer, Q., Falck-Jones, S., Vangeti, S., Yu, M., Smed-Sörensen, A., Gaballa, A., Uhlin, M., Sandberg, J. K., Brander, C., Nowak, P., Goepfert, P. A., Price, D. A., … Buggert, M. (2020). TOX is expressed by exhausted and polyfunctional human effector memory CD8+ T cells. *Science Immunology*, *5*(49), 1–15. https://doi.org/10.1126/sciimmunol.aba7918

Sen, D. R., Kaminski, J., Barnitz, R. A., Kurachi, M., Gerdemann, U., Yates, K. B., Tsao, H. W., Godec, J., LaFleur, M. W., Brown, F. D., Tonnerre, P., Chung, R. T., Tully, D. C., Allen, T. M., Frahm, N., Lauer, G. M., Wherry, E. J., Yosef, N., & Haining, W. N. (2016). The epigenetic landscape of T cell exhaustion. *Science*, *354*(6316), 1165–1169. https://doi.org/10.1126/science.aae0491

Shakiba, M., Zumbo, P., Espinosa-Carrasco, G., Menocal, L., Dündar, F., Carson, S. E., Bruno, E. M., Sanchez-Rivera, F. J., Lowe, S. W., Camara, S., Koche, R. P., Reuter, V. P., Socci, N. D., Whitlock, B., Tamzalit, F., Huse, M., Hellmann, M. D., Wells, D. K., Defranoux, N. A., … Schietinger, A. (2021). TCR signal strength defines distinct mechanisms of T cell dysfunction and cancer evasion. *Journal of Experimental Medicine*, *219*(2). https://doi.org/10.1084/jem.20201966

Sharpe, A. H., & Pauken, K. E. (2018). The diverse functions of the PD1 inhibitory pathway. *Nature Reviews Immunology*, *18*(3), 153–167. https://doi.org/10.1038/nri.2017.108

Shenoy, A. R., Wellington, D. A., Kumar, P., Kassa, H., Booth, C. J., Cresswell, P., & MacMicking, J. D. (2012). GBP5 Promotes NLRP3 Inflammasome Assembly and Immunity in Mammals. *Science*, *April*, 481–486.

Sheppard, K.-A., Fitz, L. J., Lee, J. M., Benander, C., George, J. A., Wooters, J., Qiu, Y., Jussif, J. M., Carter, L. L., Wood, C. R., & Chaudhary, D. (2004). PD-1 inhibits T-cell receptor induced phosphorylation of the ZAP70/CD3ζ signalosome and downstream signaling to PKCθ. *FEBS Letters*, *574*(1–3), 37–41. https://doi.org/10.1016/j.febslet.2004.07.083

Shih, I. M., Wang, T. L., Traverso, G., Romans, K., Hamilton, S. R., Ben-Sasson, S., Kinzler, K. W., & Vogelstein, B. (2001). Top-down morphogenesis of colorectal tumors. *Proceedings of the National Academy of Sciences of the United States of America*, *98*(5), 2640–2645. https://doi.org/10.1073/pnas.051629398

Shimizu, K., Sugiura, D., Okazaki, I. mi, Maruhashi, T., Takegami, Y., Cheng, C., Ozaki, S., & Okazaki, T. (2020). PD-1 Imposes Qualitative Control of Cellular Transcriptomes in Response to T Cell Activation. *Molecular Cell*, *77*(5), 937-950.e6. https://doi.org/10.1016/j.molcel.2019.12.012

Shin, H., Blackburn, S. D., Blattman, J. N., & Wherry, E. J. (2007). Viral antigen and extensive division maintain virus-specific CD8 T cells during chronic infection. *Journal of Experimental Medicine*, *204*(4), 941–949. https://doi.org/10.1084/jem.20061937

Shin, H., & Wherry, E. J. (2007). CD8 T cell dysfunction during chronic viral infection. *Current Opinion in Immunology*, *19*(4), 408–415. https://doi.org/10.1016/j.coi.2007.06.004

Shiow, L. R., Rosen, D. B., Brdičková, N., Xu, Y., An, J., Lanier, L. L., Cyster, J. G., & Matloubian, M. (2006). CD69 acts downstream of interferon-α/β to inhibit S1P1 and lymphocyte egress from lymphoid organs. *Nature*, *440*(7083), 540–544. https://doi.org/10.1038/nature04606

Siddiqui, I., Schaeuble, K., Chennupati, V., Fuertes Marraco, S. A., Calderon-Copete, S., Pais Ferreira, D., Carmona, S. J., Scarpellino, L., Gfeller, D., Pradervand, S., Luther, S. A., Speiser, D. E., & Held, W. (2019). Intratumoral Tcf1 + PD-1 + CD8 + T Cells with Stem-like Properties Promote Tumor Control in Response to Vaccination and Checkpoint Blockade Immunotherapy. *Immunity*, *50*(1), 195-211.e10. https://doi.org/10.1016/j.immuni.2018.12.021

Simoni, Y., Becht, E., Fehlings, M., Loh, C. Y., Koo, S., Wei, K., Teng, W., Poh, J., Yeong, S., Nahar, R., Zhang, T., Kared, H., Duan, K., Ang, N., Poidinger, M., Lee, Y. Y., Larbi, A., Khng, A. J., Tan, E., … Daniel, S. W. (2018). Bystander CD8+ T cells are abundant and phenotypically distinct in human tumour infiltrates. *Nature*, *557*(575). https://doi.org/doi.org/10.1038/s41586-018-0130-2

Simpson, T. R., Quezada, S. A., & Allison, J. P. (2010). Regulation of CD4 T cell activation and effector function by inducible costimulator (ICOS). *Current Opinion in Immunology*, *22*(3), 326–332. https://doi.org/10.1016/j.coi.2010.01.001

Singer, M., Wang, C., Cong, L., Marjanovic, N. D., Kowalczyk, M. S., Zhang, H., Nyman, J., Sakuishi, K., Kurtulus, S., Gennert, D., Xia, J., Kwon, J. Y. H., Nevin, J., Herbst, R. H., Yanai, I., Rozenblatt-Rosen, O., Kuchroo, V. K., Regev, A., & Anderson, A. C. (2016). A Distinct Gene Module for Dysfunction Uncoupled from Activation in Tumor-Infiltrating T Cells. *Cell*, *166*(6), 1500-1511.e9. https://doi.org/10.1016/j.cell.2016.08.052

Sivan, A., Corrales, L., Hubert, N., Williams, J. B., Aquino-Michaels, K., Earley, Z. M., Benyamin, F. W., Lei, Y. M., Jabri, B., Alegre, M. L., Chang, E. B., & Gajewski, T. F. (2015). Commensal Bifidobacterium promotes antitumor immunity and facilitates anti-PD-L1 efficacy. *Science*, *350*(6264), 1084–1089. https://doi.org/10.1126/science.aac4255

Snook, J. P., Kim, C., & Williams, M. A. (2018). TCR signal strength controls the differentiation of CD4+ effector and memory T cells. *Science Immunology*, *3*(25), 1–13. https://doi.org/10.1126/sciimmunol.aas9103

Sobhani, N., Tardiel-Cyril, D. R., Davtyan, A., Generali, D., Roudi, R., & Li, Y. (2021). CTLA-4 in Regulatory T Cells for Cancer Immunotherapy. *Cancers*, *13*(6), 1440. https://doi.org/10.3390/cancers13061440

Solouki, S., Huang, W., Elmore, J., Limper, C., Huang, F., & August, A. (2020). TCR Signal Strength and Antigen Affinity Regulate CD8 + Memory T Cells . *The Journal of Immunology*, *205*(5), 1217–1227. https://doi.org/10.4049/jimmunol.1901167

Song-Zhao, G. X., Srinivasan, N., Pott, J., Baban, D., Frankel, G., & Maloy, K. J. (2014). Nlrp3 activation in the intestinal epithelium protects against a mucosal pathogen. *Mucosal Immunology*, *7*(4), 763–774. https://doi.org/10.1038/mi.2013.94

Srikanth, S., Jung, H.-J., Kim, K.-D., Souda, P., Whitelegge, J., & Gwack, Y. (2010). A novel EF-hand protein, CRACR2A, is a cytosolic Ca2+ sensor that stabilizes CRAC channels in T cells. *Nature Cell Biology*, *12*(5), 436–446. https://doi.org/10.1038/ncb2045

Steimle, V., Siegrist, C.-A., Mottet, A., Lisowska-Grospierre, B., & Mach, B. (1994). Regulation of MHC Class II Expression by Interferon-γ Mediated by the Transactivator Gene CIITA. *Science*, *265*(5168), 106–109. https://doi.org/10.1126/science.8016643

Stepanek, O., Prabhakar, A. S., Osswald, C., King, C. G., Bulek, A., Naeher, D., Beaufils-Hugot, M., Abanto, M. L., Galati, V., Hausmann, B., Lang, R., Cole, D. K., Huseby, E. S., Sewell, A. K., Chakraborty, A. K., & Palmer, E. (2014). Coreceptor Scanning by the T Cell Receptor Provides a Mechanism for T Cell Tolerance. *Cell*, *159*(2), 333–345. https://doi.org/10.1016/j.cell.2014.08.042

Stinchcombe, J. C., Asano, Y., Kaufman, C. J. G., Böhlig, K., Peddie, C. J., Collinson, L. M., Nadler, A., & Griffiths, G. M. (2023). Ectocytosis renders T cell receptor signaling self-limiting at the immune synapse. *Science*, *380*(6647), 818–823. https://doi.org/10.1126/science.abp8933

Subach, F. V, Subach, O. M., Gundorov, I. S., Morozova, K. S., Piatkevich, K. D., Cuervo, A. M., & Verkhusha, V. V. (2009). Monomeric fluorescent timers that change color from blue to red report on cellular trafficking. *Nature Chemical Biology*, *5*(2), 118–126. https://doi.org/10.1038/nchembio.138

Sun, L., & Chen, Z. J. (2004). The novel functions of ubiquitination in signaling. *Current Opinion in Cell Biology*, *16*(2), 119–126. https://doi.org/10.1016/j.ceb.2004.02.005

Sun, S.-C. (2011). Non-canonical NF-κB signaling pathway. *Cell Research*, *21*(1), 71–85. https://doi.org/10.1038/cr.2010.177

Sun, S.-C., Chang, J.-H., & Jin, J. (2013). Regulation of nuclear factor-κB in autoimmunity. *Trends in Immunology*, *34*(6), 282–289. https://doi.org/10.1016/j.it.2013.01.004

Sundrud, M., & Rao, A. (2007). New twists of T cell fate: control of T cell activation and tolerance by TGF-β and NFAT. *Current Opinion in Immunology*, *19*(3), 287–293. https://doi.org/10.1016/j.coi.2007.04.014

Sušac, L., Vuong, M. T., Thomas, C., von Bülow, S., O'Brien-Ball, C., Santos, A. M., Fernandes, R. A., Hummer, G., Tampé, R., & Davis, S. J. (2022). Structure of a fully assembled tumor-specific T cell receptor ligated by pMHC. *Cell*, *185*(17), 3201-3213.e19. https://doi.org/10.1016/j.cell.2022.07.010

Szamel, M., & Resch, K. (1995). T-Cell Antigen Receptor-Induced Signal-Transduction Pathways. Activation and Function of Protein Kinases C in T Lymphocytes. *European Journal of Biochemistry*, *228*(1), 1–15. https://doi.org/10.1111/j.1432-1033.1995.tb20221.x

Takenaka, M. C., Robson, S., & Quintana, F. J. (2016). Regulation of the T Cell Response by CD39. *Trends in Immunology*, *37*(7), 427–439. https://doi.org/10.1016/j.it.2016.04.009

Tawbi, H. A., Schadendorf, D., Lipson, E. J., Ascierto, P. A., Matamala, L., Castillo Gutiérrez, E., Rutkowski, P., Gogas, H. J., Lao, C. D., De Menezes, J. J., Dalle, S., Arance, A., Grob, J.-J., Srivastava, S., Abaskharoun, M., Hamilton, M., Keidel, S., Simonsen, K. L., Sobiesk, A. M., … Long, G. V. (2022). Relatlimab and Nivolumab versus Nivolumab in Untreated Advanced Melanoma. *New England Journal of Medicine*, *386*(1), 24–34. https://doi.org/10.1056/nejmoa2109970

Thaker, Y. R., Schneider, H., & Rudd, C. E. (2015). TCR and CD28 activate the transcription factor NF-κB in T-cells via distinct adaptor signaling complexes. *Immunology Letters*, *163*(1), 113–119. https://doi.org/10.1016/j.imlet.2014.10.020

Tian, H., Biehs, B., Warming, S., Leong, K. G., Rangell, L., Klein, O. D., & Sauvage, F. J. De. (2011). A reserve stem cell population in small intestine renders Lgr5- positive cells dispensable. *Nature*, *478*(7368), 255–259. https://doi.org/10.1038/nature10408.A

Tian, S., Maile, R., Collins, E. J., & Frelinger, J. A. (2007). CD8+ T Cell Activation Is Governed by TCR-Peptide/MHC Affinity, Not Dissociation Rate. *The Journal of Immunology*, *179*(5), 2952–2960. https://doi.org/10.4049/jimmunol.179.5.2952

Tischer, D. K., & Weiner, O. D. (2019). Light-based tuning of ligand half-life supports kinetic proofreading model of T cell signaling. *ELife*, *8*. https://doi.org/10.7554/eLife.42498

Trefzer, A., Kadam, P., Wang, S.-H., Pennavaria, S., Lober, B., Akçabozan, B., Kranich, J., Brocker, T., Nakano, N., Irmler, M., Beckers, J., Straub, T., & Obst, R. (2021). Dynamic adoption of anergy by antigen-exhausted CD4+ T cells. *Cell Reports*, *34*(6), 108748. https://doi.org/10.1016/j.celrep.2021.108748

Trombetta, E. S., & Mellman, I. (2005). Cell biology of antigen processing in vitro and in vivo. *Annual Review of Immunology*, *23*, 975–1028. https://doi.org/10.1146/annurev.immunol.22.012703.104538

Tsui, C., Kretschmer, L., Rapelius, S., Gabriel, S. S., Chisanga, D., Knöpper, K., Utzschneider, D. T., Nüssing, S., Liao, Y., Mason, T., Torres, S. V., Wilcox, S. A., Kanev, K., Jarosch, S., Leube, J., Nutt, S. L., Zehn, D., Parish, I. A., Kastenmüller, W., … Kallies, A. (2022). MYB orchestrates T cell exhaustion and response to checkpoint inhibition. *Nature*, *609*(7926), 354–360. https://doi.org/10.1038/s41586-022-05105-1

Tumeh, P. C., Harview, C. L., Yearley, J. H., Shintaku, I. P., Taylor, E. J. M., Robert, L., Chmielowski, B., Spasic, M., Henry, G., Ciobanu, V., West, A. N., Carmona, M., Kivork, C., Seja, E., Cherry, G., Gutierrez, A. J., Grogan, T. R., Mateus, C., Tomasic, G., … Ribas, A. (2014). PD-1 blockade induces responses by inhibiting adaptive immune resistance. *Nature*, *515*(7528), 568–571. https://doi.org/10.1038/nature13954

Ussher, J. E., Bilton, M., Attwod, E., Shadwell, J., Richardson, R., de Lara, C., Mettke, E., Kurioka, A., Hansen, T. H., Klenerman, P., & Willberg, C. B. (2014). <CD161++ CD8+ T cells, including the MAIT cell subset, are specifically activated by IL-12 + IL-18 in a TCR-independent manner. *European Journal of Immunology*, *44*(1), 195–203. https://doi.org/10.1002/eji.201343509

Utzschneider, D. T., Charmoy, M., Chennupati, V., Pousse, L., Ferreira, D. P., Calderon-Copete, S., Danilo, M., Alfei, F., Hofmann, M., Wieland, D., Pradervand, S., Thimme, R., Zehn, D., & Held, W. (2016). T Cell Factor 1-Expressing Memory-like CD8+ T Cells Sustain the Immune Response to Chronic Viral Infections. *Immunity*, *45*(2), 415–427. https://doi.org/10.1016/j.immuni.2016.07.021

Utzschneider, D. T., Legat, A., Fuertes Marraco, S. A., Carrié, L., Luescher, I., Speiser, D. E., & Zehn, D. (2013). T cells maintain an exhausted phenotype after antigen withdrawal and population reexpansion. *Nature Immunology*, *14*(6), 603–610. https://doi.org/10.1038/ni.2606

Van Der Kraak, L. A., Schneider, C., Dang, V., Burr, A. H. P., Weiss, E. S., Varghese, J. A., Yang, L., Hand, T. W., & Canna, S. W. (2021). Genetic and commensal induction of IL-18 drive intestinal epithelial MHCII via IFNγ. *Mucosal Immunology*, *May*. https://doi.org/10.1038/s41385-021-00419-1

van der Merwe, P. A., Bodian, D. L., Daenke, S., Linsley, P., & Davis, S. J. (1997). CD80 (B7-1) Binds Both CD28 and CTLA-4 with a Low Affinity and Very Fast Kinetics. *The Journal of Experimental Medicine*, *185*(3), 393–404. https://doi.org/10.1084/jem.185.3.393

Vandenborre, K., Van Gool, S. W., Kasran, A., Ceuppens, J. L., Boogaerts, M. A., & Vandenberghe, P. (1999). Interaction of CTLA-4 (CD152) with CD80 or CD86 inhibits human T-cell activation. *Immunology*, *98*(3), 413–421. https://doi.org/10.1046/j.1365-2567.1999.00888.x

Vandereyken, M., James, O. J., & Swamy, M. (2020). Mechanisms of activation of innate-like intraepithelial T lymphocytes. *Mucosal Immunology*, *13*(5), 721–731. https://doi.org/10.1038/s41385-020-0294-6

Veillette, A., Bookman, M. A., Horak, E. M., & Bolen, J. B. (1988). The CD4 and CD8 T cell surface antigens are associated with the internal membrane tyrosine-protein kinase p56lck. *Cell*, *55*(2), 301–308. https://doi.org/10.1016/0092-8674(88)90053-0

Vétizou, M., Pitt, J. M., Daillère, R., Lepage, P., Waldschmitt, N., Flament, C., Rusakiewicz, S., Routy, B., Roberti, M. P., Duong, C. P. M., Poirier-Colame, V., Roux, A., Becharef, S., Formenti, S., Golden, E., Cording, S., Eberl, G., Schlitzer, A., Ginhoux, F., … Zitvogel, L. (2015). Anticancer immunotherapy by CTLA-4 blockade relies on the gut microbiota. *Science*, *350*(6264), 1079–1084. https://doi.org/10.1126/science.aad1329

Viola, A., & Lanzavecchia, A. (1996). T Cell Activation Determined by T Cell Receptor Number and Tunable Thresholds. *Science*, *273*(5271), 104–106. https://doi.org/10.1126/science.273.5271.104

Voisinne, G., Locard-Paulet, M., Froment, C., Maturin, E., Menoita, M. G., Girard, L., Mellado, V., Burlet-Schiltz, O., Malissen, B., Gonzalez de Peredo, A., & Roncagalli, R. (2022). Kinetic proofreading through the multi-step activation of the ZAP70 kinase underlies early T cell ligand discrimination. *Nature Immunology*, *23*(9), 1355–1364. https://doi.org/10.1038/s41590-022-01288-x

Wagner, E. F., & Eferl, R. (2005). Fos/AP-1 proteins in bone and the immune system. *Immunological Reviews*, *208*(1), 126–140. https://doi.org/10.1111/j.0105-2896.2005.00332.x

Waldburger, J. M., Suter, T., Fontana, A., Acha-Orbea, H., & Reith, W. (2001). Selective abrogation of major histocompatibility complex class II expression on extrahematopoietic cells in mice lacking promoter IV of the class II transactivator gene. *Journal of Experimental Medicine*, *194*(4), 393–406. https://doi.org/10.1084/jem.194.4.393

Ward-Kavanagh, L. K., Lin, W. W., Šedý, J. R., & Ware, C. F. (2016). The TNF Receptor Superfamily in Co-stimulating and Co-inhibitory Responses. *Immunity*, *44*(5), 1005–1019. https://doi.org/10.1016/j.immuni.2016.04.019

Watson, R. A., Tong, O., Cooper, R., Taylor, C. A., Sharma, P. K., Verge De Los Aires, A., Mahé, E. A., Ruffieux, H., Nassiri, I., Middleton, M. R., & Fairfax, B. P. (2021). Immune checkpoint blockade sensitivity and progression-free survival associates with baseline CD8 + T cell clone size and cytotoxicity. *Sci. Immunol*, *6*, 8825. https://www.science.org

Wei, S. C., Levine, J. H., Cogdill, A. P., Zhao, Y., Anang, N. A. A. S., Andrews, M. C., Sharma, P., Wang, J., Wargo, J. A., Pe'er, D., & Allison, J. P. (2017a). Distinct Cellular Mechanisms Underlie Anti-CTLA-4 and Anti-PD-1 Checkpoint Blockade. *Cell*, *170*(6), 1120-1133.e17. https://doi.org/10.1016/j.cell.2017.07.024

Wei, S. C., Levine, J. H., Cogdill, A. P., Zhao, Y., Anang, N.-A. A. S., Andrews, M. C., Sharma, P., Wang, J., Wargo, J. A., Pe'er, D., & Allison, J. P. (2017b). Distinct Cellular Mechanisms Underlie Anti-CTLA-4 and Anti-PD-1 Checkpoint Blockade. *Cell*, *170*(6), 1120-1133.e17. https://doi.org/10.1016/j.cell.2017.07.024

Weigelin, B., den Boer, A. T., Wagena, E., Broen, K., Dolstra, H., de Boer, R. J., Figdor, C. G., Textor, J., & Friedl, P. (2021). Cytotoxic T cells are able to efficiently eliminate cancer cells by additive cytotoxicity. *Nature Communications*, *12*(1). https://doi.org/10.1038/s41467-021-25282-3

Weinreich, M. A., Takada, K., Skon, C., Reiner, S. L., Jameson, S. C., & Hogquist, K. A. (2009). KLF2 Transcription-Factor Deficiency in T Cells Results in Unrestrained Cytokine Production and Upregulation of Bystander Chemokine Receptors. *Immunity*, *31*(1), 122–130. https://doi.org/10.1016/j.immuni.2009.05.011

Wertz, I. E., O'Rourke, K. M., Zhou, H., Eby, M., Aravind, L., Seshagiri, S., Wu, P., Wiesmann, C., Baker, R., Boone, D. L., Ma, A., Koonin, E. V., & Dixit, V. M. (2004). De-ubiquitination and ubiquitin ligase domains of A20 downregulate NF-κB signalling. *Nature*, *430*(7000), 694–699. https://doi.org/10.1038/nature02794

Wherry, E. J. (2011). T cell exhaustion. *Nature Immunology*, *12*(6), 492–499. https://doi.org/10.1038/ni.2035

Wherry, E. J., Barber, D. L., Kaech, S. M., Blattman, J. N., & Ahmed, R. (2004). Antigen-independent memory CD8 T cells do not develop during chronic viral infection. *Proceedings of the National Academy of Sciences of the United States of America*, *101*(45), 16004–16009. https://doi.org/10.1073/pnas.0407192101

Wherry, E. J., & Kurachi, M. (2015). Molecular and cellular insights into T cell exhaustion. *Nature Reviews Immunology*, *15*(8), 486–499. https://doi.org/10.1038/nri3862

Williams, B. L., Schreiber, K. L., Zhang, W., Wange, R. L., Samelson, L. E., Leibson, P. J., & Abraham, R. T. (1998). Genetic Evidence for Differential Coupling of Syk Family Kinases to the T-Cell Receptor: Reconstitution Studies in a ZAP-70-Deficient Jurkat T-Cell Line. *Molecular and Cellular Biology*, *18*(3), 1388–1399. https://doi.org/10.1128/MCB.18.3.1388

Wilson, D. (2004). Specificity and degeneracy of T cells. *Molecular Immunology*, *40*(14–15), 1047–1055. https://doi.org/10.1016/j.molimm.2003.11.022

Wither, M. J., White, W. L., Pendyala, S., Leanza, P. J., Fowler, D. M., & Kueh, H. Y. (2023). Antigen perception in T cells by long-term Erk and NFAT signaling dynamics. *Proceedings of the National Academy of Sciences*, *120*(52). https://doi.org/10.1073/pnas.2308366120

Workman, C. J., & Vignali, D. A. A. (2003). The CD4-related molecule, LAG-3 (CD223), regulates the expansion of activated T cells. *European Journal of Immunology*, *33*(4), 970–979. https://doi.org/10.1002/eji.200323382

Wu, J. E., Manne, S., Ngiow, S. F., Baxter, A. E., Huang, H., Freilich, E., Clark, M. L., Lee, J. H., Chen, Z., Khan, O., Staupe, R. P., Huang, Y. J., Shi, J., Giles, J. R., & Wherry, E. J. (2023). In vitro modeling of CD8+ T cell exhaustion enables CRISPR screening to reveal a role for BHLHE40. *Science Immunology*, *8*(86). https://doi.org/10.1126/sciimmunol.ade3369

Wu, S., Rhee, K., Albesiano, E., Rabizadeh, S., Wu, X., Yen, H., Huso, D. L., Brancati, F. L., Wick, E., Mcallister, F., Housseau, F., Pardoll, D. M., & Sears, C. L. (2015). A human colonic commensal promotes colon tumorigenesis via activation of T helper type 17 T cell responses. *Nature Medicine*, *1*(July 2008), 1016–1023. https://doi.org/10.1038/nm.2015

Ye, X., Waite, J. C., Dhanik, A., Gupta, N., Zhong, M., Adler, C., Malahias, E., Ni, M., Wei, Y., Gurer, C., Zhang, W., Macdonald, L. E., Murphy, A. J., Sleeman, M. A., & Skokos, D. (2020). Endogenous retroviral proteins provide an immunodominant but not requisite antigen in a

murine immunotherapy tumor model. *Oncoimmunology*, *9*(1), 1758602. https://doi.org/10.1080/2162402X.2020.1758602

Yokosuka, T., Takamatsu, M., Kobayashi-Imanishi, W., Hashimoto-Tane, A., Azuma, M., & Saito, T. (2012). Programmed cell death 1 forms negative costimulatory microclusters that directly inhibit T cell receptor signaling by recruiting phosphatase SHP2. *Journal of Experimental Medicine*, *209*(6), 1201–1217. https://doi.org/10.1084/jem.20112741

Yost, K. E., Satpathy, A. T., Wells, D. K., Qi, Y., Wang, C., Kageyama, R., McNamara, K. L., Granja, J. M., Sarin, K. Y., Brown, R. A., Gupta, R. K., Curtis, C., Bucktrout, S. L., Davis, M. M., Chang, A. L. S., & Chang, H. Y. (2019). Clonal replacement of tumor-specific T cells following PD-1 blockade. *Nature Medicine*, *25*(8), 1251–1259. https://doi.org/10.1038/s41591-019-0522-3

Zamoyska, R. (2007). Why Is There so Much CD45 on T Cells? *Immunity*, *27*(3), 421–423. https://doi.org/10.1016/j.immuni.2007.08.009

Zhang, E., Kiely, C., Sandanayake, N., & Tattersall, S. (2021). Calcineurin inhibitors in steroid and TNF alpha refractory immune checkpoint inhibitor colitis. *JGH Open*, *5*(5), 558–562. https://doi.org/10.1002/jgh3.12531

Zhao, M., Kiernan, C. H., Stairiker, C. J., Hope, J. L., Leon, L. G., van Meurs, M., Brouwers-Haspels, I., Boers, R., Boers, J., Gribnau, J., van IJcken, W. F. J., Bindels, E. M., Hoogenboezem, R. M., Erkeland, S. J., Mueller, Y. M., & Katsikis, P. D. (2020). Rapid in vitro generation of bona fide exhausted CD8+ T cells is accompanied by Tcf7 promotor methylation. *PLoS Pathogens*, *16*(6 June), 1–27. https://doi.org/10.1371/journal.ppat.1008555

Zikherman, J., Jenne, C., Watson, S., Doan, K., Raschke, W., Goodnow, C. C., & Weiss, A. (2010). CD45-Csk Phosphatase-Kinase Titration Uncouples Basal and Inducible T Cell Receptor Signaling during Thymic Development. *Immunity*, *32*(3), 342–354. https://doi.org/10.1016/j.immuni.2010.03.006